3-17-2017 12:00 AM

Uncertainty Modeling in The Assessment of Climate Change Impacts on Water Resources Management

Sohom Mandal
The University of Western Ontario

Supervisor
Dr. Slobodan P. Simonovic
The University of Western Ontario

Graduate Program in Civil and Environmental Engineering
A thesis submitted in partial fulfillment of the requirements for the degree in Doctor of Philosophy

Abstract

Climate change has significant impacts on water resource systems. The objective of this study is to assess climate change impacts on water resource management. The methodology includes: (a) the assessment of uncertainty introduced by choice of precipitation downscaling methods; (b) uncertainty assessment and quantification of the impact of climate change on projected streamflow; and (c) uncertainty in and impact of climate change on the management of reservoirs used for hydropower production. The assessment of uncertainty is conducted for two future time periods (2036 to 2065 and 2066 to 2095). The study area, Campbell River basin, British Columbia, Canada, consists of three reservoirs (Strathcona, Ladore and John Hart). A new multisite statistical downscaling method based on beta regression (BR) is developed for generating synthetic precipitation series, which can preserve temporal and spatial dependence along with other historical statistics (e.g., mean, standard deviation). The BR-based downscaling method includes two main steps: (i) prediction of precipitation states for the study area using classification and regression trees, and (ii) generation of precipitation at different stations in the study area conditioned on the precipitation states. To account for uncertainty in sources, four global climate models (GCMs), three greenhouse gas emission scenarios (RCPs), six downscaling models (DSMs), are considered, and the differences in projected variables of interest are analyzed. For streamflow generation a hydrologic model is used. The results show that the downscaling models contribute the highest amount of uncertainty to future streamflow predictions when compared to the contributions by GCMs or RCPs. It is also observed that the summer (June, July & August) and fall (September, October & December) flows into Strathcona dam (British Columbia) will decrease, while winter (December, January & February) flows will

increase, in both future time periods. In addition, the flow magnitude becomes more uncertain for higher return period flooding events in the Campbell River system under climate change than the low return period flooding events. To assess the climate change impacts on reservoir operation, a system dynamics model is used for reservoir flow simulation. Results from the system dynamics model show that as the inflow decreases in summer and fall, reservoir release and power production are affected. It is projected that power production from downstream reservoirs (LDR & JHT) will decrease more drastically than the upstream reservoir (SCA) in both future time periods considered in this study.

Keywords

Downscaling, Climate change, Water resource, Streamflow, Reservoir operation, System Dynamics

Dedicated to My Teachers, Mentors, Parents and My Beloved Wife

Co-Authorship Statement

The work of this thesis is a collaborative effort by the present author and Mr. Patrick A. Breach, Dr. Roshan K. Srivastava, Dr. R. Arunkumar and Dr. Slobodan P. Simonovic. The content of section 3.2 has been published in the Journal of Hydrology with the present author as primary author, Dr. Roshan K. Srivastava as the second author and Dr. Slobodan P. Simonovic as the third author. For this paper, the first author did all the experiments and wrote the paper. Dr. Srivastava helped in the development of experiments, and Dr. Simonovic supervised both of the authors, provided direction for this research, and gave his valuable comments. Also, he edited the manuscript.

The content of section 3.3 has been published in the American Journal of Climate Change where the present author was the primary author and Mr. Patrick A. Breach and Dr. Slobodan P. Simonovic co-authors of the manuscript. In this work, the first author did all the experiments and wrote the manuscript. Mr. Patrick helped in designing of experiments as well as analysis of results. Dr. Simonovic supervised both of the authors, gave his expert opinions, and edited the manuscript.

Content from Chapter 4 has been accepted in the Hydrological Processes Journal with the present author as the primary author and Dr. Simonovic as co-author. Dr. Simonovic provided direction for this research, gave valuable feedback and edited the manuscript. The first author did all the experiments and wrote the manuscript.

Finally, the content of Chapter 5 will be submitted for publication in the near future with the present author as a primary author and Mr. Patrick A. Breach, Dr. R. Arunkumar and Dr. Simonovic as the co-authors. Dr. Arunkumar has developed the system dynamics simulation

model for reservoirs which is used in this study. Mr. Patrick developed a computational package which connects VENSIM and Python, which is used for the design of the experiments. Dr. Simonovic supervised all the three authors for the experiments and provided his valuable feedbacks. In this study, the first author did all the experiments and wrote the manuscript.

The content of section 3.2 was published as:

Sohom Mandal, Roshan K. Srivastava and Slobodan Simonovic (2015), "Use of beta regression for statistical downscaling of precipitation in the Campbell River basin, British Columbia, Canada" *Journal of Hydrology*, 538, 49-62. Doi:10.1016/j.jhydrol.2016.04.009

The content of section 3.3 was published as:

Sohom Mandal, Patrick Breach and Slobodan Simonovic (2016), "Uncertainty in precipitation projection under changing climate conditions: A regional case study" *American Journal of Climate Change*, 5, 116-132. Doi:10.4236/ajcc.2016.51012.

Content from chapter 4 is accepted as:

Sohom Mandal and Slobodan Simonovic (2017), "Assessment of future streamflow under changing climate condition: comparison of various sources of uncertainty" *Hydrological Processes Journal*. Doi: 10.1002/hyp.11174 (In Press).

Chapter 5 will be submitted for publication as:

Sohom Mandal, R. Arunkumar, Patrick A. Breach, Slobodan P. Simonovic, "Reservoir operation under climate change: a system dynamics approach" (under preparation).

Acknowledgments

It gives me immense pleasure to express my heartfelt gratitude to Prof. Slobodan P. Simonovic for his guidance, unwavering encouragement, thoughtful advice, mentorship, and financial support throughout my doctoral studies. His suggestions, comments, and many hours of enthusiastic discussions have been instrumental in enhancing my understanding of hydrology and water resource management. His sense of appreciation and persistence on a high level of technical knowledge chiseled my skills and driven me towards perfection. The dedication to, and belief in his students, is exceptional and a gift that I will carry with me until my last breath. I am fortunate and grateful for the opportunity that I got to work with a "Living Legend" in water resource engineering. I think there is no word in the dictionary which can describe his support towards students and his professionalism. I would also like to thank Ms. Tanja Malisic-Simonovic for her love, affection, and care over the years.

I am thankful to all the faculty members of the Department of Civil and Environmental Engineering, Western University for their teaching, encouragement, and support throughout the research program. During my stay at UWO, I have been fortunate enough to have had the opportunity to interact with Prof. Andrew D. Binns, Prof. Gordon McBean, and Prof. Ian McLeod, discussions with whom have been an enriching experience. Also, I want to acknowledge the guidance, love, and encouragement offered by Prof. Subhankar Karmakar from the Indian Institute of Technology Bombay, India. I am thankful to Ms. Leanna King from BC Hydro for providing UBC watershed model.

It is my privilege to thank the authority of The Western University (Department of Civil and Environmental Engineering) for providing necessary facilities for the completion of this thesis. I am also thankful to the office and technical staff for their cooperation.

I want to thank my friends and colleagues in FIDS (former and present members). A special thanks to Angela, Abhishek, Patrick, Sarah, Vladimir and Arunkumar for providing excellent companionship, constant encouragement, and discussions of technical and various other topics.

I am indebted to my parents, **Sri Madhusudan Mandal** and **Ms. Saheli Mandal** and my wife **Ms. Mrinmoyee Mandal** for their constant encouragement and for being extremely supportive of all my decisions. Words are not sufficient to express my gratitude for all the difficult decisions they had to make in their life on my account and for being there always whenever I needed them. I am also thankful to my little sister Ms. Amrita Mandal. Lastly and most importantly, I want to thank God for blessing me with everyone mentioned before.

Table of Contents

List of Tables

List of Figures

List of Appendices

Acronyms

AR5	= Fifth Assessment Report of IPCC
AR3	= Third Assessment Report of IPCC
AOGCM	= Atmosphere-Ocean Global Climate Model
BC	= British Columbia
BCCAQ	= Bias Correction Constructed Analogues with Quantile Mapping Reordering
BCSD	= Bias-corrected Spatial Disaggregation
BR	= Beta Regression
BRWS	= Beta Regression Not Conditioned to Precipitation States
CRS	= Campbell River System
CanESM2	= The Second Generation Canadian Earth System Model
CART	= Classification And Regression Tree
CCA	= Canonical-Correlation Analysis
CDF	= Cumulative Distribution Function
CF	= Change Factor
CO2	= Carbon Dioxide
CRF	= Conditional Random Field
CMIP5	= Coupled Model Intercomparison project 5
CMIP3	= Coupled Model Intercomparison Project 3
DS	= Dry Spell
DSM	= Downscaling Model
ENSO	= El Niño–Southern Oscillation
GCM	= Global Climate Model

GEV = Generalized Extreme Value

GHG = Greenhouse Gas

GWh = Gigawatt Hours

ha = Hectare

HRU = Hydrological Response Unit

HadCM3 = Hadley Centre Coupled Model Version 3

hus = Specific Humidity

JHT = John Hart

IDW = Inverse Distance Weighting

IPCC = Intergovernmental Panel on Climate Change

K-NN = k-Nearest Neighbors

KR = Kernel Regression

LDR = Ladore Reservoir

LU/LT = Land Use/Land Type

MEB = Maximum Entropy Bootstrap

mslp = Mean Sea Level Pressure

MLR = Multiple Linear Regression

MW = Megawatt

NCAR = National Center for Atmospheric Research

NCEP = National Centers for Environmental Prediction

NSGA-II = Non-dominated Sorting Genetic Algorithm-II

NSE = Nash–Sutcliffe Efficiency

PCA = Principal Component Analysis

Pr	= Precipitation
PCIC	= Pacific Climate Impacts Consortium
Q-Q plot	= Quantile-Quantile Plot
RCP	= Representative Concentration Pathways
RCM	= Regional Climate Model
SCA	= Strathcona
SDP	= Stochastic Dynamic Programming
SD	= Statistical Downscaling
SDM	= System Dynamics Model
SOP	= Standard Operating Policy
SWE	= Snow Water Equivalent
RSME	= Root Mean Square Error
Tmax	= Maximum Temperature
Tmin	= Minimum Temperature
UK	= United Kingdom
UBCWM	= UBC Watershed Model
USA	= United States of America
WG	= Weather Generator
WS	= Wet Spell
WD	= Wet Day

Chapter 1

1 Introduction

The present research describes a new approach to quantifying climate change related impacts on regional hydrology and reservoir operations considering different sources of uncertainties. The research results allow for an improved understanding of ongoing and projected climate change impacts on the West Coast of Canada. Further, a better understanding of the downscaling process and uncertainties in various steps of climate change impact analyses are discussed in this research.

This particular section discusses a brief introduction of climate change processes, different greenhouse gas emission (GHGs hereafter) scenarios defined by IPCC (2013), and climate change impacts on water resources of Canada followed by climate change impact assessment process and uncertainty in the climate change impact assessment process. Following these, the primary objectives of the present research and its contribution towards the state of the art of climate change impact studies are presented. A general outline of the larger thesis is given at the end of this section.

1.1 Climate Change and Greenhouse Gas Emission Scenarios

Any change caused directly or indirectly by human activity that modifies the global climate and remains over a significant time period can be referred to as climate change (IPCC, 2013). Climate change can be caused by natural Earth processes (e.g., volcanic eruptions, periodic changes in solar irradiance) or more recently due to anthropogenic greenhouse gas emissions (i.e., burning fossil fuel, changes in land-use patterns). The

consequences of climate change are reflected in global as well as regional climatic variables such as surface temperature, precipitation, atmospheric moisture, snow cover, the extent of land and sea ice, sea level, and patterns in oceanic and atmospheric circulation (IPCC, 2013). In the present study, climate change refers to the increase in the average temperature of earth's surface and change in precipitation patterns since the mid-20th century and its future projection. According to the Intergovernmental Panel on Climate Change (IPCC hereafter) (IPCC, 2007) the global surface temperature has increased 0.74 ± 0.18 °C between 1906 and 2005 while the annual average surface air temperature has increased by 1.5ºC over the Canadian landmass between 1950 and 2010 (Warren and Lemmen, 2014). It has been found that the increase in global surface temperature has a positive correlation with increasing concentrations of GHGs resulting from human activities such as deforestation and fossil fuel burning (Figure 1.1).

An increase in the Earth's surface temperature is expected to change the amount and pattern of precipitation and will cause sea levels to rise. IPCC (2013) has projected that the global surface temperature will increase in the range of 0.3ºC (low emission scenario) to 4.8ºC (high emission scenario) by the end of the 21st century compared to 1986-2005. Based on tide gauge data, the rate of global average sea level rise was 1.5 to 1.9 mm/year with a central value of 1.7 mm/year between 1901 and 2010 and 2.8 to 3.6 mm/year with a central value of 3.2 mm/year between 1993 and 2010 (IPCC, 2013). Decreasing snow cover (11.7 % per decade for June in Northern Hemisphere from 1967 to 2012) and land ice extent (globally 275 Gt/year over the period 1993 to 2009) continue to be positively correlated with increase land surface temperature (IPCC, 2013). Also, the behavior of El Nino Southern Oscillation (ENSO hereafter) has changed since the mid-1970s compared

with the last 100 years. The warm phase of ENSO is more intense and frequent compared with the cold ENSO phase. This pattern of ENSO leads to variation in temperature and precipitation in tropical and sub-tropical areas (IPCC, 2013).

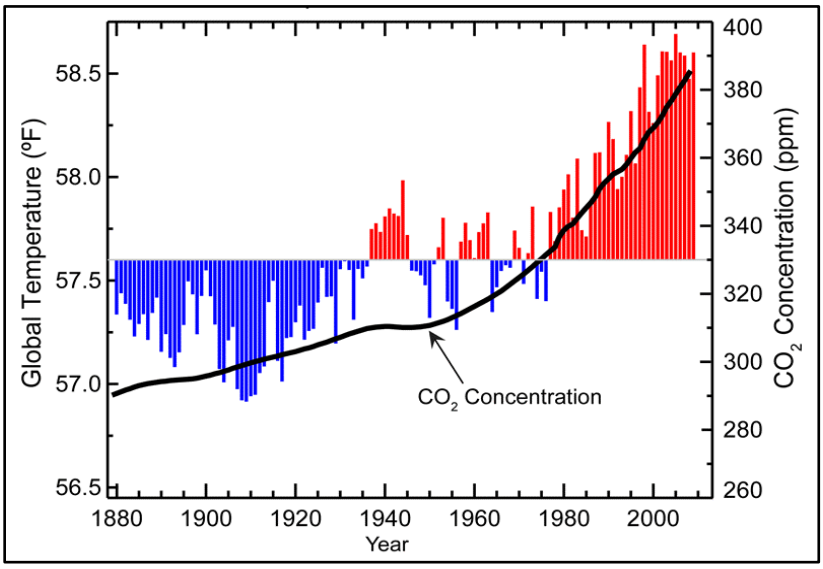

Figure 1.1 Observed change in global surface temperature with carbon dioxide concentration between 1880 and 2005 (after IPCC, 2013). Blue bars indicate temperatures that are below and red bars denote temperatures that are above the 1901-2000 average temperature. The dark black line represents the atmospheric CO_2 concentration in parts per million over time.

Precipitation in tropical areas (30°S to 30°N) increased in between 2000 to 2010 compared to mid-1970s to mid-1990s. Also in mid-latitude of the northern hemisphere (30° N to 60° N), a significant increasing trend has been found in precipitation over the last century (1901 to 2008) while in the southern hemisphere (30° S to 60° S) an abrupt declining trend in precipitation has been observed between 1979 to 2008 (IPCC, 2013).

As summarized above, significant evidence of climate change exists, especially over the last few decades. To estimate future emissions and concentrations of GHGs in the

atmosphere, IPCC Working Group-I has developed long-term emission scenarios, denoted as Representative Concentration Pathways (RCPs) (IPCC, 2013). RCPs are scenarios developed based on anthropogenic greenhouses emissions (GHGs) and do not include natural emissions such as volcanic eruption. These scenarios describe how radiative force may influence future emissions scenarios and analyze the associated uncertainties. Based on an approximate total radiative forcing in the year 2100 compared to 1750 four RCPs (2.6 W m^{-2} for RCP 2.6, 4.5 W m^{-2} for RCP 4.5, 6.0 W m^{-2} for RCP 6.0, and 8.5 W m^{-2} for RCP 8.5) are presented in the Fifth Assessment Report (AR5) of IPCC (IPCC, 2013). These four emission scenarios include one mitigation scenario (RCP 2.6), two stabilization scenarios (RCP 4.5 and RCP 6.0) and RCP 8.5 describes the maximum and unabated GHGs emission conditions. The following section describes historical and projected impacts of climate change on water resources.

1.2 Climate Change Impacts on Water Resources

Water resources are inextricably connected to climate. Therefore, the prospect of global climate change poses a serious threat to water resources across the world. Precipitation is directly impacted due to an increase in global average temperature, driving evapotranspiration rates higher and thereby increasing the concentration of water vapor in the atmosphere. Changes in precipitation is expected to differ in magnitude and frequency from region to region. Changes in precipitation will affect water resources activities including use of reservoir storage, flood control, water supply, irrigation, hydropower production, navigation, and recreation. It has also been found that the annual runoff increases in higher latitude regions (Finland, China and coterminous USA) where a decreasing pattern can be found in lower latitude regions such as parts of West Africa,

southern Latin America and southern Europe (IPCC, 2013). Labat *et al.*,(2004) observed a direct relationship between global annual temperature rise and global runoffs for the last century. It is estimated that global runoff increases by 4% per 1ºC increase in global temperature. Meanwhile a stronger warming trend has been found in the western and northern parts of Canada (Yukon, British Columbia and Northwest Territories) as compared to eastern parts during 1950-2010 (Eamer *et al.,* 2010). Change in surface temperature affects evaporation and atmospheric circulation patterns which influence rain and snowfall.

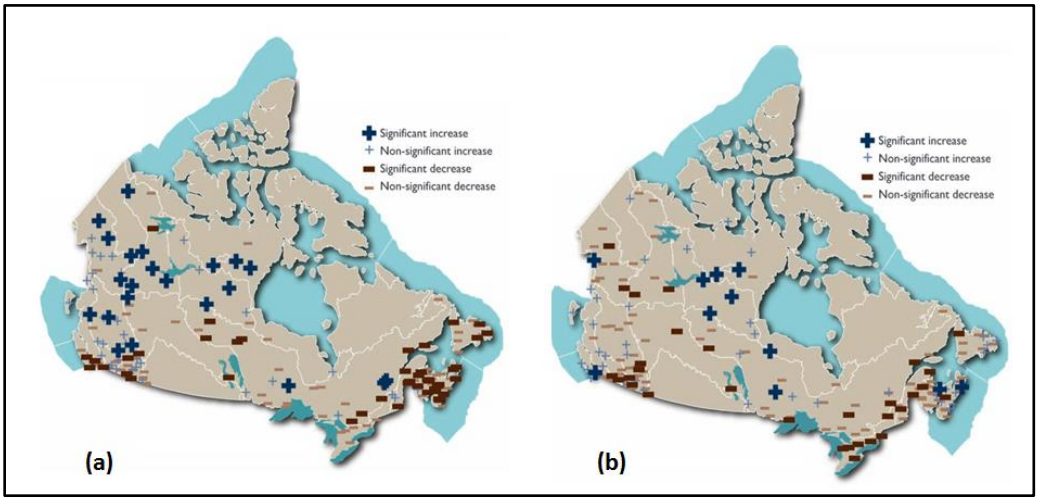

Figure 1.2(a) Minimum and (b) Maximum natural river flow trends in Canada in between 1975 to 2005 (after Eamer *et al.*, 2010).

Mekis and Vincent (2011) reported that in Canada, especially on the west coast, the total precipitation has increased in the fall and spring seasons, while it has decreased in the winter season during the period of 1950-2010. Winter precipitation decreases because of winter snowfall decreased due to warm air temperature. Seasonal variations in flows can be found in most of Canadian rivers. Annual minimum flow occurs in late winter when precipitation is mixed with ice and snow, and in late summer when evaporation is high

and rainfall is low. In a study of 172 streamflow gauging stations, in naturally flowing rivers across Canada it has been found that the annual minimum flow decreased in southern and southwestern parts of the country, whereas minimum flow has increased in the northwestern and western parts between 1970 to 2005 (Eamer *et al.*, 2010) (Figure 1.2). Maximum annual flow generally occurs in late spring and in early summer due to snow melt and seasonal rainstorms. Seventeen percent of the 172 sites indicated a significant decreasing trend of maximum annual flow across Canada, especially in the southern and southeastern parts (Eamer *et al.*, 2010) (Figure 1.2b). Most Canadian river flow is significantly influenced by snow accumulation and melting patterns. In the west coast of Canada especially coastal British Columbia (BC) and the Great Lakes- St Lawrence area, the maximum snow water equivalent (SWE) is projected to decline while increasing patterns were predicted for the Arctic coast of Nunavut (Brown and Mote, 2009). Glacier retreat has been found in Alberta and BC (Stahl *et al.*, 2008; Marshall *et al.*, 2011) and it is projected to continue in the future as the earth surface temperature warms. For watersheds that contain glaciers, it is expected that melting ice will affect runoff, especially during summer. Marshall *et al.*, (2011) compared glacier runoff for historical (2000 to 2007) and future scenarios (2000 to 2100) (using Special Report on Emissions Scenarios B1 and A1B) for the Rocky Mountain area (Bow, Red Deer, North Saskatchewan, Athabasca, and Peace Rivers). In third assessment report, IPCC (IPCC, 2000) a group of forty Special Report on Emission Scenarios (SRES) scenarios were developed from six scenario groups (A1F1, A1T, A1B, A2, B1 and B2) where A1B represents a rapid technological and demographic growth till mid-21st century after which global population decreases using energy efficient systems are introduced. B1 represents

a rapid demographic growth till mid-21st century after which it decreases due to usage of sustainable technologies, however, without any additional climate initiatives. Results showed that the glacier runoff will change -75% for the Peace River, -60% for the Athabasca River, -100% for the Bow and Red Deer Rivers and -80% for the North Saskatchewan River for the A1B scenario between 2000 and 2050. Also, Schnorbus *et al.*, (2011) projected that the glacier area will shrink in the Upper Columbia River basin (approximately 50%) and the Campbell River basin (35% approximately) for B1, A2, and A1B emission scenarios by the end of 2050. Changes to glaciers will affect runoff which will subsequently affect water resources activities including the use of dam storage, flood control, water supply, irrigation, energy production, navigation, and recreation. Payne *et al.*, (2004) observed that hydrologic changes due to climate change increased competition between reservoir storage for hydropower production and downstream streamflow targets in Columbia River basin, USA. Christensen *et al.*, (2004) projected that annual hydropower production from Glen Canyon Dam, Colorado River basin, USA will be reduced in future (2010 to 2098) compared to historical (1950 to 1999) due to changes in seasonal streamflow patterns. These impacts may require that water resources planners and managers adopt alternative water management strategies in the future. Before making any adoption strategy, an assessment of climate change impacts on water resources is essential. Details of the climate change impact assessment process are discussed in the following sub-section.

1.3 Climate Change Impact Assessment Process

Impacts of climate change on regional water resources are assessed for future climate scenarios obtained from Global Climate Model (GCM) simulations. GCMs represent

state of the art modeling with respect to the simulation of global climate variables in response to greenhouse gas emission scenarios. These models are developed based on the numerical representation of the climate system which includes biological, chemical and physical properties of climate variables and feedback relationships between these variables. GCM outputs are coarsely gridded (>100 km^2) and often fail to capture non-smooth fields such as precipitation (Hughes and Guttorp, 1994). Downscaling methods are well-known and used for transferring coarse-scale climate information to local scale.

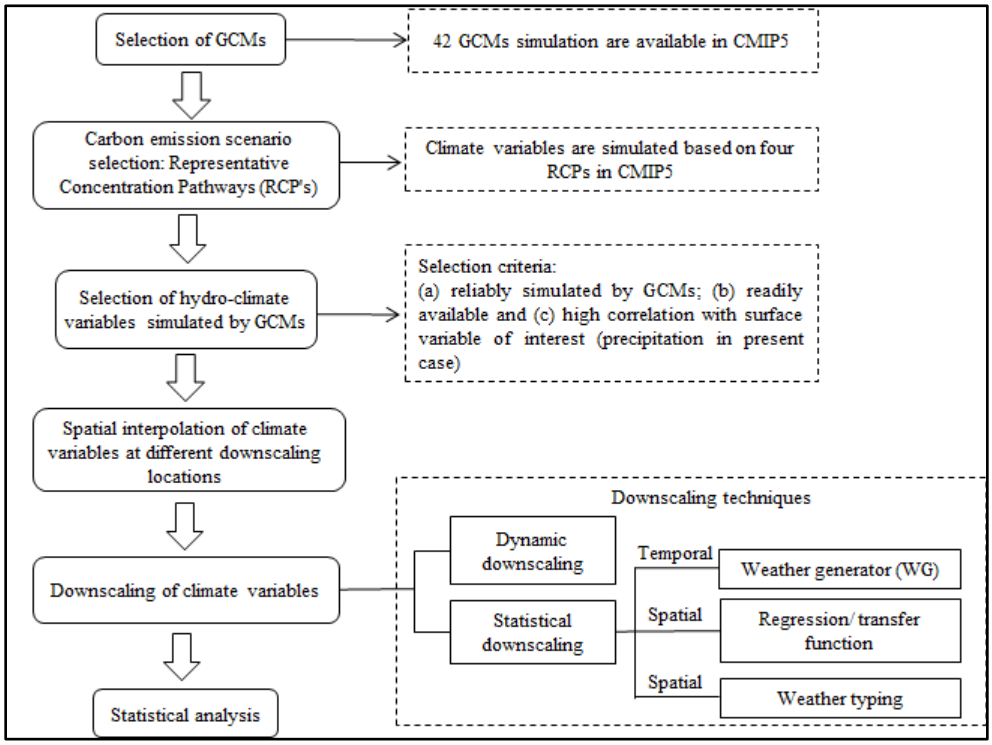

Figure 1.3 Generalized framework for downscaling climate variables under changing climate conditions.

A generalized framework for downscaling climate variables under changing climate conditions is outlined in Figure 1.3. Downscaling approaches are classified into two categories: (i) dynamic downscaling and (ii) statistical downscaling. Dynamic downscaling uses complex algorithms to describe atmospheric processes at finer

resolutions (typically 50 km x 50 km), nested within coarse resolution GCMs to derive boundary conditions. These models are known as regional climate models (RCMs).

Statistical downscaling (SD) derives an empirical or statistical relationship between large-scale climate variables and hydrological variables (such as precipitation). SD methods can be classified into three groups: (i) classification/ weather typing methods (Hay *et al.*, 1991; Hughes and Guttorp, 1994; Hughes *et al.*, 1999; Mehrotra and Sharma, 2005); (ii) regression/transfer function methods (Von Storch *et al.*, 1993; Wilby *et al.*, 1999, 2002; Hashmi *et al.*, 2009; Ghosh, 2010; Goyal and Ojha, 2010; Kannan and Ghosh, 2013; Chen *et al.*, 2014); and (iii) weather generators (WG) (Wilks, 1999; Wilks and Wilby, 1999; Sharif and Burn, 2006; Eum and Simonovic, 2012; Lee *et al.*, 2012; Srivastav and Simonovic, 2014; King *et al.*, 2015). Details about these methods are provided in the Literature Review of this document. The following sub-section describes the various sources of uncertainty during the downscaling process.

1.4 Process Uncertainty in Climate Change Impact Assessment

Since the GCM output is coarsely gridded, the first step in the climate change impact assessment on hydrology is downscaling the hydro-climate variables (e.g., precipitation, temperature) to a local scale based on the large scale climate variables (e.g. specific humidity, mean sea level pressure) simulated by the GCMs. At the regional scale, the projection of hydro-climatic variables under changing climatic conditions is burdened with a considerable amount of uncertainty originating from several sources. These sources include: (i) inter-model variability due to different model structures between GCMs (Kay *et al.*, 2009); (ii) inter-scenario variability due to different types of emission

scenarios; (iii) intra-model variability due to the model parameter selection; and (iv) the choice of downscaling models (Figure 1.3). From past studies, it has been found that GCMs contribute the largest source of uncertainty in regional applications that only consider single downscaling models (Prudhomme and Davies, 2008a; Najafi *et al.*, 2011). Also, when the downscaling relationship is assumed to be stationary, it is subject to uncertainty, which impacts future hydrologic projections.

Quantification of uncertainties is therefore part of the downscaling process, and it is very relevant to the climate change impact assessment process. Generally, hydro-climatic variables are used as input for the hydrologic models. Therefore if we want to project future streamflow rates using downscaled GCMs climate variables, the projected streamflow rates will carry uncertainties from the downscaling process because "*any individual source of uncertainty, if quantified in some way, can be propagated through to give an uncertainty in the end result*" (Kay *et al.*, 2009). Also, multiple hydrological models are available and each one of these uses different parameters which could be another source of uncertainty (Dibike and Coulibaly, 2005). Therefore, uncertainty assessment in the climate change impacts assessment process is an important aspect of this study. The primary objectives of the present work are presented in following sub-section.

1.5 Research Objectives

The primary objective of this research to build a framework for assessing probable future impacts of climate change on hydro-climatic variables and energy variables (e.g. precipitation, temperature, flow, and generated hydropower). To obtain higher resolution climate projections for a catchment (under study) from low-resolution GCMs data, a

robust and efficient downscaling model is required. Therefore, development of a robust downscaling model is another objective of this study. Uncertainties are inherent in each step of the climate change impact assessment process. Hence, quantification of different sources of uncertainty in projected climate and hydrologic variables is another objective of this study. The main objectives of this research are summarized below:

1. Develop a reliable, efficient, and robust multisite multivariate statistical downscaling technique for predicting higher resolution future precipitation from low-resolution GCM data.

2. Quantify climate change effects on the hydro-climatic variables (i.e., precipitation and temperature) and streamflow.

3. Quantify uncertainty associated with the projected hydro-climatic variables (e.g., precipitation, temperature, streamflow).

4. Study climate change impacts on reservoir operation under uncertainty in hydrologic impacts of climate change.

5. Assess future hydropower generation under changing climate conditions using a system dynamics simulation model (SDM).

The detailed steps of this study are illustrated in Figure 1.4. The first objective involves the development of a new statistical downscaling (SD) model which will be able to capture spatial and temporal correlation in addition to other statistical characteristics (i.e. mean, standard deviation). Further, the performance of the proposed SD model will be compared to existing downscaling models. The second objective deals with the future

projection of hydro-climatic variables under different greenhouse gas emission scenarios reported by IPCC (2013) and the generation of streamflow considering these hydro-climatic variables as an input to a hydrologic model. The third objective analyzes and quantifies uncertainties associated with the climate change impact assessment process in managing water resources. This objective includes uncertainty in temperature, precipitation and streamflow projection under climate change conditions.

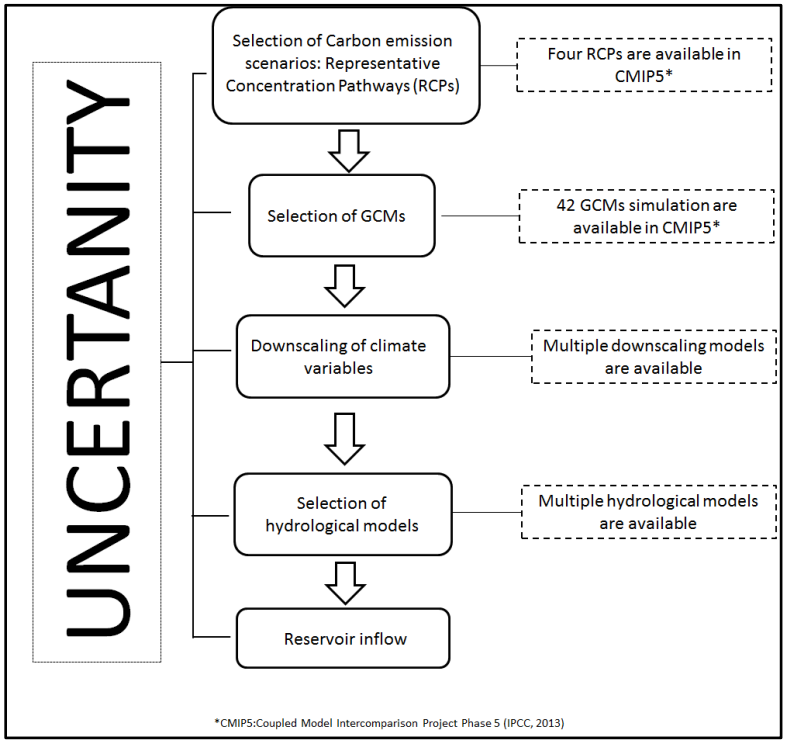

Figure 1.4 Generalized framework of the present study.

The fourth objective deals with addressing different sources of uncertainties in reservoir operation under different climate change scenarios (Figure 1.4). To address these uncertainties, six downscaling models, four GCMs, three GHGs emission scenarios and a hydrologic model (UBC watershed model) are used. Finally, the last objective deals with hydropower production from reservoirs under changing climate conditions. Since the

projected streamflow of a river is burden with a considerable amount of uncertainties stemming from several sources of the climate change impact analysis process, it will affect reservoir (if existed in the basin) storage and release curves. If storage and release changes, it will modify the existing reservoir operation policy. Now the question is how much will present reservoir operation policies be affected in future climate conditions especially in terms of hydropower production. A system dynamics model (SDM) is used to simulate reservoir operations under different climate change conditions. This methodology is applied to the Campbell River basin in British Columbia, Canada. Three reservoirs (Upper Campbell, Lower Campbell and John Hart) are present in this river system and they are connected in a series. If the upstream reservoir is affected by climate change, it will affect the downstream reservoirs too and the quantification of this effect is the one objective of this study. The assessment process we followed in this study is given in Figure 1.5.

In the present work, an attempt is made to capture uncertainty in the climate change impacts assessment process. Primary objectives of this study are to address different sources of uncertainties in the climate change impact assessment process and assess the relative contribution of sources of uncertainty towards the total uncertainty. In this study we used RCP 2.6, RCP 4.5 and RCP 8.5 as emission scenarios where we downscaled data from CanESM2, CCSM4, CSIRO-Mk3-6-0 and GFDL-ESM2G. To execute the present work we developed a beta regression based downscaling model. Along with the beta regression model, another five downscaling models (bias corrected spatial disaggregation (BCSD); bias correction constructed analogues with quantile mapping reordering (BCCAQ); delta change method coupled with a non-parametric K-nearest neighbor

weather generator; delta change method coupled with maximum entropy based weather generator and non-parametric statistical downscaling model based on the kernel regression) are used in this study.

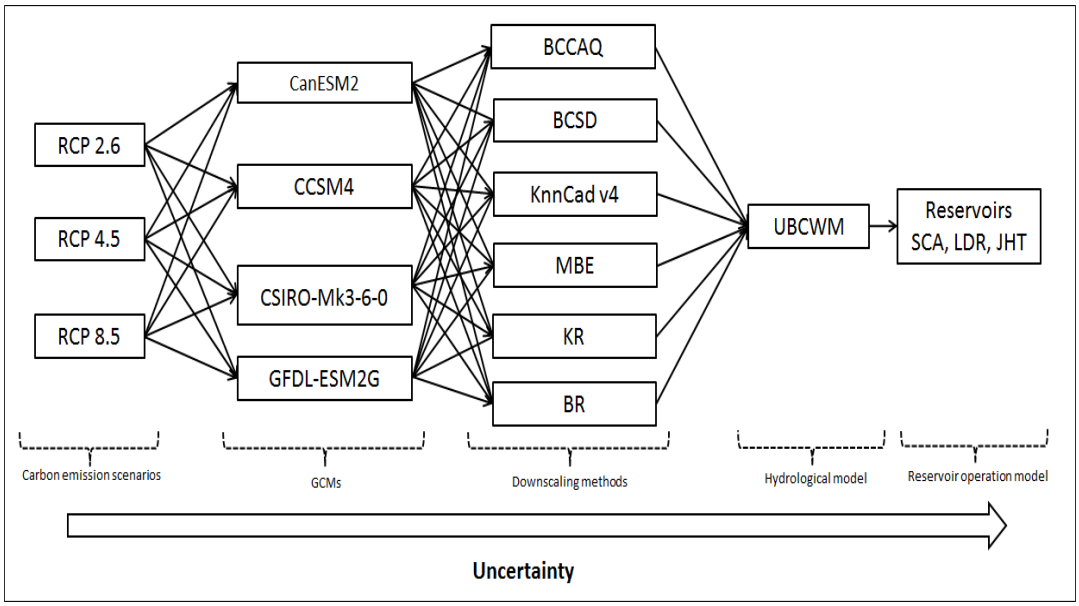

Figure 1.5 Framework presenting the climate change impact assessment process followed in this study (after Mandal *et al.*, 2016a).

1.6 Research Contributions

Contributions from the present research are given below:

1. Downscaling models often fail to capture extreme behavior in generated precipitation sequences, and also fail to simulate multisite sequences with realistic spatial and temporal dependence. Therefore, using beta regression, a multisite, statistical downscaling model is developed and used in this study to downscale GCM based precipitation projection.

2. Another contribution of this study is uncertainty assessment on hydro-climatic variables with the use of multiple downscaling models, GCMs and future greenhouse gas scenarios.

3. The assessment of the impacts of climate change on reservoir operation is another novel aspect of this study.

4. Quantification of climate change impact analysis process uncertainties in projected hydro-climatic variables (e.g., precipitation, temperature, and streamflow) and analyze the propagation of these uncertainties in reservoir operation are addressed in the present study. This is an another novel contribution of this study.

Previously, most of the studies stated that the choice of GCMs contributes the largest source of uncertainty when only one or two downscaling models are considered. An important aspect of this study is to understand the variation in hydro-climate variables projections due to the choice of different downscaling models. Therefore, multiple downscaling models are considered in this study. We started with an assumption is that the choice of GCMs is not the highest source of uncertainty; downscaling models can be dominating too. GCMs are mathematical models which simulate climate variables considering multiple assumptions where downscaling models are statistical models, also subject to multiple assumptions. Therefore, making a conclusion without assessing results from multiple downscaling models might not be valid. This task has been treated as a significant contribution of this study.

Due to significant changes in climate for decades, stakeholders or decision-makers are motivated in acquiring information about climate change risk. More specifically, planners and managers are expressing interest in information regarding adaptive and risk-based planning approaches for management of water resources systems. They need appropriate management procedures based on the projected hydrological change. Therefore, this study could give them an overview, how regional water resources can be affected by climate change and they could make risk-based planning approach for water resource system based on the present work.

1.7 Outline of the Thesis

Chapter 2 provides a review of the literature related to the development of downscaling models for assessment of climate change impact on hydrology/water resources. The details about different sources of uncertainties in climate change impacts assessment process are presented in the second section of this chapter. The last part of this chapter reviews climate change impacts on reservoir operation and management.

Chapter 3 describes methodology related to future precipitation projection under changing climate condition and quantifies uncertainties in downscaling process. The details about data and study area are provided in second and third section in this chapter respectively. Development of a new downscaling technique based on CART, PCA and beta regression and its validation are provided in next section. Quantification of the major source of uncertainties is discussed in second last section of this chapter followed by a summary.

Chapter 4 provides an assessment of future projected streamflow under changing climate conditions. The second part of this chapter describes the hydrological model (UBCWM) and its validation. Quantification of different sources of uncertainties in future streamflow projections due to climate change is given in third part of this chapter followed by a summary.

Chapter 5 presents operation details of multiple reservoirs under climate change scenarios. The first section provides a brief introduction to reservoir operation in changing climate condition while the second section describes the study area (Campbell River system) and three reservoirs (Upper Campbell, Lower Campbell and John Hart) situated in this basin. The third part of this section provides details about a system dynamics simulation model (SDM) developed by Arunkumar and Simonovic (2017) which connects the three reservoirs together. This section also provides information about simulated inflow (historical and future) by the system dynamics model for all three reservoirs. The fourth section presents future storage, release and hydropower production for three reservoirs in the Campbell River basin followed by a summary section.

A detail discussion about uncertainty propagation in future simulated results is provided in Chapter 6 where Chapter 7 presents a summary, conclusions, and future scopes of the present study.

Chapter 2

2 Literature Review

Literature related to impacts assessment of climate change on water resources which use downscaling methods and uncertainties in such assessment processes are reviewed in this present chapter. The following section describes different downscaling models. Literature related to different sources of uncertainty in climate change impact assessment process is reviewed subsequently.

2.1 Downscaling Climate Variables

Global Climate Models (GCMs) are credible and reliable tools for global scale climate analyses. These models are developed based on numerical representations of climate system which includes biological, chemical and physical properties of climate variables and feedback relationships between these variables. GCMs simulate the present climate and predict future climate change with forcing by aerosols and GHGs. Since GCMs provide information on the global scale, tools are required for regional studies to convert this information to the local scale. Downscaling tools are widely used for transferring coarse-scale climate information to regional scales. Downscaling method includes two different approaches: (i) dynamic downscaling approach and (ii) statistical downscaling approach. The details about these two approaches are presented in the following sub-section.

2.1.1 Dynamic Downscaling

Dynamic downscaling is based upon nesting a finer scale regional climate model (RCM) (up to 10 km x 10 km horizontal resolution) within GCMs(Wood *et al.*, 2004). Dynamic

downscaling has thus far been attempted with three approaches: (i) simulate a regional scale model with GCM data as geographical boundary conditions; (ii) run a global scale experiment with high resolution atmospheric GCMs, with coarse GCM data as initial and partial boundary conditions; and (iii) a variable-resolution global model. The major drawbacks of dynamic downscaling are model complications, high computational requirements, their dependence on boundary conditions obtained from GCMs and lack of transferability to different regions.

2.1.2 Statistical Downscaling

The statistical downscaling method uses an empirical relationship between large-scale GCMs simulated climate variables (predictors) and regional scale variables (predictands) such as precipitation. There are three assumptions made when using this downscaling technique (Hewitson and Crane, 1996): (i) predictor variables are realistically modeled by GCMs; (ii) the empirical relationship is valid for any climatic conditions (stationary and non-stationary) and (iii) the predictors fully represent the climate change signal. Statistical downscaling is more adaptable, flexible and popular because of low computational requirements, simple modeling structure and easy modifications for use at various locations. SD methods developed so far can be classified into three groups: (a) classification/ weather typing methods; (b) regression/transfer function methods and (c) weather generators (WG).

2.1.2.1 Weather Generator

Weather generators are statistical models that stochastically simulate random sequences of synthetic climate variables that preserve statistical properties of observed climate data (Mehrotra and Sharma, 2005; King *et al.*, 2014; Srivastav and Simonovic, 2014).

Mehrotra and Sharma (2005) developed a K-nearest-neighbor (K-NN) based nonparametric nonhomogeneous hidden Markov model (NHMM) for downscaling multisite rainfall over a network of 30 different locations near Sydney, Australia. This model generates rainfall based on average rainfall occurrence over the previous day and conditional to a continuous weather state. This model was successful in capturing day-to-day rainfall characteristics compared to discrete state NHMM.

Another non-parametric multisite weather generator named KnnCAD V4 was developed by King *et al.,* (2014). The KnnCAD V4 is the updated version of KnnCAD V3 (Eum *et al.,* 2010) which includes block resampling and perturbation. This model was used for downscaling daily temperature and precipitation data in the Upper Thames River basin, Ontario, Canada. This model can adequately reproduce statistical characteristics of historical climate variables as well as extrapolate historical extremes.

Most recently, Srivastava and Simonovic (2014) developed a non-parametric multisite, multivariate maximum entropy based weather generator (MEBWG) for generating daily precipitation and minimum and maximum temperature values. The three main steps involved in MEB are (i) orthogonal transformation of daily climate variables at multiple sites to remove spatial correlation; (ii) use of maximum entropy bootstrap (MEB) to generate synthetic replicates of climate variables and (iii) inverse orthogonal transformation of synthetic climate variables to re-established spatial correlation. Principal component analysis is used for orthogonal transformation. This method can capture temporal and spatial dependency structures along with other historical statistics (e.g. mean, standard deviation) in downscaled climate variables. The performance of MEBWG is free of modeling parameters, and it is computationally inexpensive.

2.1.2.2 Weather Typing

Weather typing approaches develop the relationship between local climate and atmospheric circulation variables based on a given weather classification scheme. The observed local climate variables are related to weather classes which include principal component analysis (PCA) (Schoof and Pryor, 2001; Wetterhall *et al.*, 2005), fuzzy rules (Bardossy *et al.*, 1995), canonical correlation analysis (CCA) (Gyalistras *et al.*, 1994), analogues procedure(Martin *et al.*, 1997) or other pattern recognition methods based on correlation (Wilby and Wigley, 1997). The major drawbacks of this approach are the stationary relationships between local climate variables and different types of atmospheric circulation and the additional effort needed for weather classification. Non-stationarities are inherent traits of the climate system and can be observed in different spatiotemporal scales (Hertig and Jacobeit, 2013). Hence, ignoring the nonstationary relationships between climate variables may mislead the downscaling process.

2.1.2.3 Transfer Function

Transfer function based models usually build a statistical relationship between GCM or RCM outputs (large-scale predictor) and local-scale climate variables (predictands). Generally multivariate linear or nonlinear regression (Vrac *et al.*, 2007; Chen *et al.*, 2014), non-parametric regression (Sharma and O'Neill, 2002; Kannan and Ghosh, 2013) and support vector machine (SVM) approach (Tripathi *et al.*, 2006; Ghosh, 2010) are used for deriving those relationships. These approaches are widely used and known as 'perfect-prognosis' downscaling methods.

Raje and Mujumdar (2009) developed a conditional random field (CRF) downscaling method which does not require the assumption of independence for climate variables and

their distribution. In this method, four surface flux variables (precipitation flux, surface temperature, maximum and minimum surface temperature) and four surface/pressure variables (specific humidity, sea level pressure, U wind and V wind) are needed to maintain spatial and temporal dependence which makes this method computationally demanding. Also, the CRF method moderately captures spatial correlation and also overestimates the mean value of the predictand (precipitation). Individually downscaling at multiple stations may be the reason for poor spatial correlations and discretization of historical rainfall data into different classes. Without confirming an exact number of rainfall classes when using the clusters validity test it may produce bias toward over-prediction of mean precipitation values at different stations. For this reason non-parametric statistical methods like K-nearest neighbors (K-NN)(Young, 1994; Brandsma and Buishand, 1998; Sharif and Burn, 2006; Eum and Simonovic, 2012; King *et al.*, 2014) or Kernel density estimator are referred in the literature as plausible approaches for the downscaling purposes (Mehrotra and Sharma, 2010; Kannan and Ghosh, 2013). Although non-parametric methods can successfully capture the spatial dependence of observed data, they often fail to capture extreme events in the case of precipitation. Markov based downscaling models (Hughes and Guttorp, 1994; Mehrotra and Sharma, 2005, 2007) perform satisfactorily in capturing spatial variability of daily precipitation but they fail to reproduce the variability of a non-stationary climate as exogenous climate predictors are not considered. Coulibaly *et al.*, (2005) developed a downscaling model based on a time-lagged feed-forward neural network (TLFN) method. The major assumption of the model is that the local weather variables (i.e. precipitation and temperature) depend on present and past large-scale atmospheric states. The performance

of this model compared with SDSM (Wilby *et al.*, 2002) and found TLFM model performs well in downscaling temperature and precipitation data compare to SDSM. However, TLFN overestimates wet-spell length and no spatial correlation assessment was mentioned in the study.

It seems that despite progress made in the development and application of downscaling models for climate impact assessments in the past, all of them have limitations. The weather typing method considered a stationary relationship between local climate variables and different types of atmospheric circulation which is not true. Transfer functions provide ease of use but only explain a fraction of observed variability. Parametric weather generators have limitations due to a large number of parameters, representation of temporal and spatial variability in the generated sequences (Wilby *et al.*, 2004), accurate generation of extremes (maximum and minimum) (Pour *et al.*, 2014) and generation of multisite sequences with spatial dependence. Most of the downscaling models developed in the past have failed to capture spatial dependence in rainfall occurrence, and they assume that the probability distributions of observed and future climate variables will remain the same, which can be a limiting assumption.

In spite of considerable progress in the development of downscaling methods, in particular for the simulation of precipitation, challenges still exist in accurately capturing extreme behavior in generated precipitation sequences and simulating multisite sequences with realistic spatial and temporal dependence (Raje and Mujumdar, 2009). Moreover, the downscaling method should be efficient and computationally inexpensive to simulate the underlying processes present in the observed data. Recently, Kannan and Ghosh (2013) developed a multisite statistical downscaling model using a non-parametric kernel

density function. Exogenous climate predictors were used in this method for generating multisite precipitation. This method encouraged the development of a statistical downscaling model based on a new regression approach. This downscaling model is divided into two phases. In the first phase, the model predicts precipitation states using classification and regression trees (CART) wherein the second phase, daily precipitation is simulated at a particular station using multivariate beta regression.

In addition, the water resources of a river basin are sensitive to projected climate change. The following sub-section describes state of the art regarding streamflow projection under climate change.

2.2 Streamflow Projection under Climate Change

Climate change has serious impacts on water resource across the world. The magnitude and frequency of river flows are affected by climate change and will continue to be in future. Changes to the river flow are not uniform across the world but regionally specific. Variation in magnitude and frequency of streamflow increases the vulnerability of water infrastructure. A study by the Canadian Institute of Actuaries (2014) found that water-related insured damage and losses could increase by about 20% to 30% in the next few decades across Canada. Simonovic (2008) also suggested that water resource's infrastructure planning, design, and operations should be revised to accommodate the expected changes in magnitude and frequency of streamflows. Therefore quantification of the impacts of climate change on streamflow is essential.

Maurer (2007) studied climate change impacts on streamflow in the Sierra Nevada region, California, USA under two emission scenarios (SRES A2 & B1). The results

show that winter streamflow will increase, while streamflow during late spring and summer will decrease between 2071-2100. This study also projected that the average temperature would increase by 2.4 °C to 3.7 °C in that timeframe which causes less snow in the winter time and will thus affect late spring streamflow.

Spring snowmelt is a significant contribution to the streamflow of many rivers in north - western America. Stewart *et al.*,(2004) conducted an assessment to study shifts in the timing of future spring runoff due to climate change in northwestern American rivers, especially the Pacific Northwest, Sierra Nevada, and Rocky Mountain regions. Results stated that spring snowmelt could be expected 30-40 days earlier in the future (1995 to 2099) compared to 1948 to 2000 due to temperature change.

Minville *et al.*, (2008) conducted a study to assess climate change impacts on streamflow in the Chute-du-Diable watershed, Quebec, Canada. They compared historical runoff (1961 to 1990) with three future time periods centered on the years 2020, 2050 and 2080. Results projected that future spring runoff would appear 1-5 weeks earlier than usual with a variation of -40% to 25%. In addition, future summer runoff will decrease while runoff during the winter, spring and fall will increase in the Chute-du-Diable watershed. However these future projections contain several sources of uncertainty during the climate change impact assessment process. The details about these uncertainties discussed below.

2.2.1 Sources of Uncertainties

The assessment of climate change impacts on water resource systems is subject to a range of uncertainties due to either “incomplete” or “unknowable” knowledge. “Incomplete”

knowledge arises from a lack of information or understanding about biological, chemical and physical properties of climate variables and feedback relationships between these variables or due to inadequate analytical resources. “Unknowable” knowledge originates from the inability to predict future socio-economic and human behavior in a definitive manner or from the inherent unpredictability of the Earth’s systems. These cascades of uncertainty in any climate change impact study are interdependent but not necessarily additive or multiplicative way. Further, uncertainty due to future greenhouse gas emission scenarios is compounded when emission scenarios translate into atmospheric concentration because of inadequate knowledge regarding source, sink and recycling rates of GHGs in the Earth system. Additional uncertainty in the climate change impact assessment process arises from the structural, conceptual, and computational limitation of the GCMs (Gates *et al.*, 1999). Finally, the outputs from assessment models (downscaling) are subject to uncertainties resulting from downscaling model structures and assumptions. Another source of uncertainty is added to the result if we simulate future streamflow using the downscaled climate variables as input to a hydrological model. There are multiple hydrologic models available and its parameterization has significant effects on projected stormflow (Najafi *et al.*, 2011). Since uncertainties accumulate at various levels of climate change impact assessment process, their propagation at the regional or local level leads to large uncertainty ranges (Wilby, 2005; Minville *et al.*, 2008).

A number of studies have been conducted to address and quantify uncertainties in climate change impact assessments. Prudhomme and Davies (2009) examined uncertainties in climate change impact analyses in four different catchments of the UK. In this study, they

downscaled precipitation using either the statistical or dynamic downscaling model from an ensemble of GCMs and scenarios and used this result to forecast river flow through a lumped hydrological model. The results show that the choice of downscaling method is a significant source of uncertainty, as is the choice of GCM. Kay *et al.,* (2009) compared six different sources of uncertainty (GCMs structure; downscaling from GCMs including Regional Climate Model structure; hydrological model structure; hydrological model parameters and the internal variability of the climate system) with respect to climate change impact on flood frequency in England. This study concludes that the largest source of uncertainty is GCM structure, however if GCMs are omitted, other sources of uncertainty become more significant.

Seiller and Anctil (2014) studied climate change impacts on the Haut-Saint-François catchment in Quebec, Canada. They compared streamflow data using twenty different lumped hydrological models, twenty-four potential evapotranspiration formulations, and seven snowmelt modules but used a Single GCM (CGCM version 3) and a single emission scenario (A2 scenario from SRES). Results indicated that natural climate variations are the primary source of uncertainty followed by potential evapotranspiration formulations and hydrological models. However, they did not assess uncertainty due to GCMs or emission scenarios.

Minville *et al.,* (2008) conducted another study that examined the impact of climate change on the hydrology of the Chute-du-Diable watershed in Canada. Minville *et al.,* (2008) observed that projection of precipitation is most sensitive to the choice of GCM where Wilby and Harris (2006) found that GHG emission scenarios also caused uncertainty in precipitation projections under changing climatic conditions. Najafi *et al.,*

(2011) conducted a study to compare uncertainties in predicted future flow stemming from different GCMs, emission scenarios, and hydrological models. This study concludes that uncertainty in streamflow due to GCM structure is higher than the uncertainty due to the choice of hydrologic model. However, this study also suggests that hydrologic model selection is important when assessing hydrologic impacts under changing climate conditions. Some other studies reported that a systematic bias is present in future projections and must be considered when interpreting results (Piani *et al.*, 2010). Many studies have also found that understanding current and future natural variability is important in assessing hydrologic impacts under changing climate conditions (Wilby, 2005; Kay *et al.*, 2009). Rupp *et al.*, (2013) and Kay *et al.*, (2009) also suggested that multiple catchments, or different locations, should be analyzed in order to obtain a comprehensive understanding of different sources of uncertainty. However, in most previous climate change impact assessment studies it has been found that GCMs contribute the largest uncertainty in the modeling of regional impacts (Wilby and Harris, 2006; Chen *et al.*, 2011).

Studies presented in this section reported that climate change impacts on regional water resource are burdened with a considerable amount of uncertainty that originates from several sources. Uncertainties may arise from (i) inter-scenario variability of emission scenarios; (ii) inter-model variability of GCMs; (iii) choice of downscaling model and (iv) intra-model variability due to hydrological model parameter selection or hydrologic model selection. Many studies have been conducted to quantify the significance of different sources of climate change process uncertainty in relation to the total uncertainty. However, it has been found that different studies came to different conclusions, and all

sources of process uncertainty were not accounted for the climate change impact assessment. The work presented in this thesis considers all major sources of process uncertainty in climate change impact assessment process. The following sub-section describes climate change impacts on reservoir operations.

2.3 Reservoir Operation under Changing Climate Conditions

Most climate studies can be classified into three groups: (i) mechanism and reasons behind climate change; (ii) impacts of climate change and (iii) mitigation and adoption of climate change policy. Studies related to the mechanism and reasons behind climate change are discussed in the first chapter. The impact of climate change on reservoir operation is addressed in this section.

Simonovic and Burn (1996) examined impacts of climate change on the Shellmouth reservoir in Manitoba, Canada. They studied the operational performance of this reservoir using two different "cool" and "warm" sets of climate condition. The results from this study indicated that reservoir performance varies with inflow and that climate change has significant effects on reservoir operation. Li *et al.,* (2010) studied the variation of streamflow and reservoir performance under changing climate conditions in the prairie region of North America. They found that the frequency and magnitude of high peak streamflow will increase in the future due to climate change. Eum *et al.,* (2009) developed an integrated reservoir management system for the Upper Thames River basin in Ontario, Canada. This management system was applied with two downscaling models, two GCMs and two climate scenarios. This study concluded that streamflow is sensitive to climate scenarios which in turn affects reservoir system operations.

Raje and Mujumdar (2010) developed a stochastic dynamic programming (SDP) model to capture uncertainty associated with inflow due to climate change and derived a standard operating policy (SOP) for a multipurpose reservoir system in Orissa, India. This study analyzed two different sources of uncertainties resulting from different GCM structure and choices of greenhouse gas emission scenarios. The result of this study indicates that due to the hydrologic impact of climate change, performance and hydropower generation of the reservoir will decrease in the future. A major limitation of this study is that the reservoir optimization model (SDP) is based on transition probability. Therefore, this model assumes an "*unconditional steady state probability distribution*" for monthly streamflows which will not change from one year to the next. This assumption of steady-state transition probability is practically not acceptable because the variation in the streamflows changes with time, especially under the influence of climate change.

Ahmadi *et al.,* (2014) developed adaptive rules based on a non-dominated sorting genetic algorithm (NSGA-II) for reservoir management with regard to climate change. They applied this model in the Karron-4 reservoir, Iran. Results showed that new adaptive rules are better in terms of reliability in hydropower generation. However, they only considered a single GCM (HadCM3), a single GHG emission scenario (A2) and a single hydrologic model. Therefore uncertainties in the climate change assessment process were not included in this study.

Pina *et al.,*(2017) conducted a study to assess future climate change impacts on water resource system of the Gatineau River Basin in Quebec, Canada using the vertical and the horizontal approaches. They examined weekly and annual hydropower generation from

the Gatineau River Basin. Structural hydrologic uncertainty and natural variability were addressed in this study. However they used a single GCM (CGCM3) under a single emission scenario (A2). Climate data from CGCM3 were downscaled using dynamical downscaling method. Hence, uncertainties stem from GCMs, downscaling models or emission scenario were not explored in this study.

Minville *et al.*, (2009) investigated the impacts of climate change on the Peribonka River Basin, Quebec, Canada which consists of two large reservoirs (Marouane Lake reservoir and Passes-Dangereuses reservoir) that are used for hydropower generation. The objectives of this study were to evaluate climate change impacts on hydropower, power plant efficiency, and reliability of the reservoir under changing climate conditions. They developed a stochastic and a dynamic optimization model to adopt new reservoir operation rules according to the evolution of the climate. The results described that due to climate change the reliability of a reservoir would decrease where vulnerability will increase. However, they did not address uncertainties in the climate change assessment process.

Climate change is expected to have significant impacts on regional hydrology and reservoir inflow. A comprehensive assessment of future reservoir operation under climate change condition considering different sources of uncertainty is incessant in the present context. In addition assessment of future hydropower production under different climate change conditions also addressed in the present study. The following chapters present the development of a new robust downscaling model, uncertainty combination, and assessment of future reservoir operation under climate change.

Chapter 3

3 Precipitation Projections under Changing Climate Conditions

Based on: Sohom Mandal, Roshan K. Srivastava and Slobodan Simonovic (2015), "Use of beta regression for statistical downscaling of precipitation in the Campbell River basin, British Columbia, Canada" Journal of Hydrology, 538, 49-62.DOI: 10.1016/j.jhydrol.2016.04.009

Impacts of climate change on regional water resources are assessed for future climate scenarios obtained from Global Climate Model (GCM) simulations. GCMs represent state of the art with respect to the simulation of global climate variables in response to emission scenarios of greenhouse gasses. GCMs can satisfactorily model smoothly varying fields such as mean sea level pressure, but often fail to capture non-smooth fields such as precipitation (Hughes and Guttorp, 1994). In addition, the spatial scale of GCM output is very coarse (>100 km^2). Therefore, on a regional scale, capturing the impacts of climate change on hydro-meteorological variables (e.g. temperature, precipitation, soil moisture) is more difficult and uncertain. At the catchment level (<50 km^2), downscaling of coarsely gridded GCM data is necessary for a better understanding and assessment of future hydrologic conditions in response to climate change. As discussed before, existing downscaling models have many limitations i.e. capturing extreme behavior in generated precipitation sequences, simulating multisite sequences with realistic spatial and temporal dependence and computational burden. Therefore, in this study, a new statistical downscaling approach is proposed.

This downscaling model considers the historical effect of exogenous climate variables for the generation of multisite precipitation amounts. Precipitation states of the basin are obtained from large-scale circulation patterns to capture the spatial patterns within the basin. We also use a multivariate beta regression model to downscale multisite precipitation amounts conditioned on precipitation states of the catchment. Based on the precipitation states, beta regression is used to generate precipitation at each individual location within the catchment. This regression method based on the beta distribution has proven to be very versatile and flexible to model exogenous variables (Ferrari and Cribari-Neto, 2004) and is novel in its application as a statistical downscaling technique. For model performance evaluation, the results obtained from the proposed method are compared with those obtained from a recently developed model based on Kernel density estimation (Kannan and Ghosh, 2013). The primary objective of the comparison is to analyze the advantages and disadvantages of the proposed beta regression based downscaling method.

The methodology is developed in two steps. First, precipitation states are predicted using the CART algorithm. Second, we generate time series of multisite daily precipitation by downscaling outputs of CanESM2 for a historical time period (1983–2005) and a future time period (2036–2065). The proposed downscaling method is applied to a case study in the Campbell River basin, British Columbia, Canada (Figure 3.1). Information regarding case study area and datasets used for this study are given in the next section.

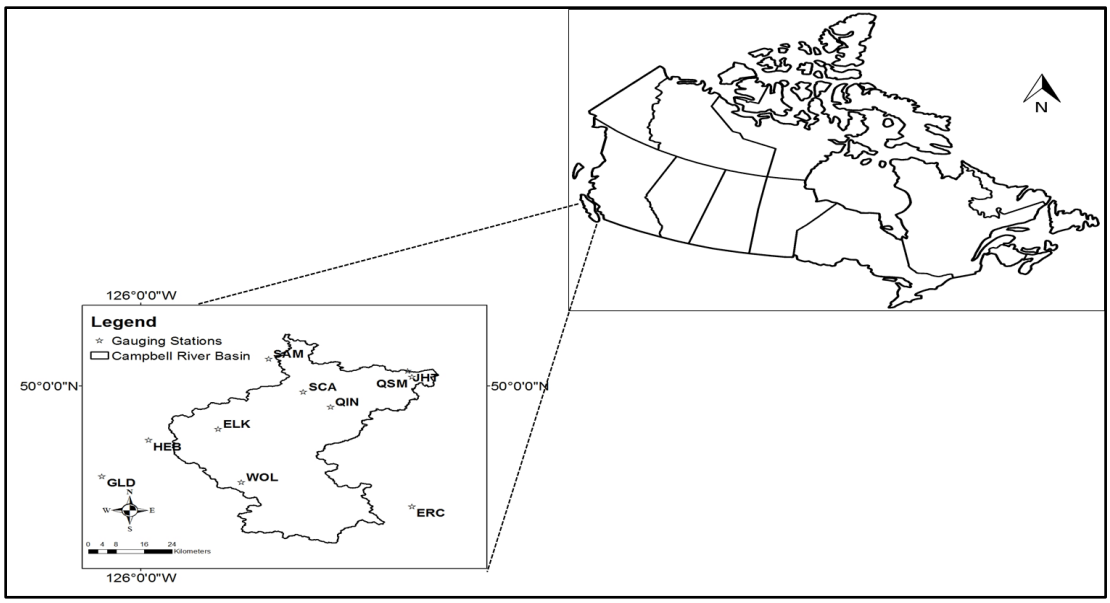

Figure 3.1 The Campbell River basin with the location of gauging stations (after Mandal *et al.*, 2016c).

3.1 Study Area and Data Extraction

Campbell River is situated in between the dry east coast and wet west coast climate on Vancouver Island, Canada. The total drainage area of this basin is approximately 1856 km^2 with a length of 33 km from the origin (Strathcona provincial park). The Campbell River basin consists of three lakes namely Buttle Lake and Upper Campbell Lake, Lower Campbell Lake and John Hart Lake. Campbell River system produces 2.5% of BC Hydro's total hydroelectric power which is equivalent to 11% of Vancouver Island's annual energy demand (BC Hydro Generation Resource Management, 2012). In this river basin, streamflow is a mixture of melting snow and rainfall. Generally, the streamflow is high during fall and spring and low during the summer season. The salient features (longitude, latitude, elevation) of the gauging stations in the basin are given in Table 3.1.

Table 3.1 Salient features of precipitation stations in the Campbell River Basin, BC, Canada (after Mandal *et al.*, 2016c).

Station	Elevation(m)	Latitude (° N)	Longitude (° W)	Station Abbreviation
Elk R ab Campbell Lk	270	49.85	125.8	ELK
Eric Creek	280	49.6	125.3	ERC
Gold R below Ucona R	10	49.7	126.1	GLD
Heber River near Gold River	215	49.82	125.98	HEB
John Hart Substation	15	50.05	125.31	JHT
Quinsam R at Argonaut Br	280	49.93	125.51	QIN
Quinsam R nr Campbell R	15	50.03	125.3	QSM
Salmon R ab Campbell Div	215	50.09	125.67	SAM
Strathcona Dam	249	49.98	125.58	SCA
Wolf River Upper	1490	49.68	125.74	WOL

Historical daily precipitation data (0.1° latitude x 0.1° longitudes) for a 40 years span (1961–2013) have been obtained from the ANUSPLIN Data Set, Environment Canada (Hutchinson and Xu, 2013). ANUSPLIN data is developed using ‘‘thin plate smoothing splines” algorithm. This technique interpolates climate variables as a function of latitude, longitude, and elevation. For this study, the daily precipitation data is used at ten locations covering the entire Campbell River basin. Details about ANUSPLIN data sets are provided in Appendix A.

Large-scale climate circulation patterns govern the regional climate. Therefore, selection of the predictors is necessary for the downscaling process (Wilby *et al.*, 2004; Wetterhall *et al.*, 2005). According to Wilby *et al.*, (1999), predictors used for downscaling need to

be: (a) easily available, (b) reliably simulated and (c) strongly correlated with response variable (precipitation in this case). Considering those conditions, daily maximum and minimum air surface temperature (Tmax and Tmin), mean sea level pressure (mslp), specific humidity (hus) at 500 hPa, zonal (u-wind) and meridional (v-wind) wind are used as predictors.

Due to inadequate historical climate data for a longer period, predictor data is extracted from the NCEP/NCAR (National Centers for Environmental Prediction/National Center for Atmospheric Research) reanalysis dataset (Kalnay *et al.*, 1996) for 53 years spanning 1961–2013. NCEP/NCAR data set is a combination of physical process and model forecast gridded data at the 2.5° x 2.5° spatial resolution. More details about NCEP/NCAR data are provided in Appendix A. In the context of GCM outputs downscaling, historical data from CanESM2 (1983–2013) is used for proposed model performance evaluation. CanESM2 (2.813° latitude x 2.79° longitude) is a second generation earth system model from the Coupled Model Inter-comparison Project (CMIP5) developed by the Canadian Centre for Climate Modeling and Analysis.

ANUSPLIN, NCEP/NCAR and GCM (CanESM2) data have a different spatial resolution. Therefore, all the data sets are spatially interpolated to a location of interest (gauging station) using inverse distance square method (Shepard, 1968). Six climate variables (Tmax, Tmin, mslp, hus, u-wind and v-wind) at ten locations in the basin are used as model predictors where precipitation is the model predictand.

Standardization procedure (Wilby *et al.*, 2004) is applied to the predictors data to reduce the systematic bias among the variable means and standard deviations. Standardization is

carried out by subtracting the mean and dividing by standard deviation from all respective variables. A 30 years span (1961–1990) is considered as a model training period, where 23 years (1991–2013) daily data is used for model validation. Predictors for a particular station are expected to have a high correlation with other nearby stations which may lead to the multicollinearity problem (Ghosh, 2010). Multicollinearity is a statistical phenomenon which refers to highly correlated predictors in multiple regression analyses. It occurs when predictors are not only correlated with response variable but also to each other. Multicollinearity may lead to larger changes in the regression model estimation for small changes in the data. Therefore, it is necessary to remove multicollinearity from the predictor variables (Salvi *et al.*, 2013). Apart from this, the model is expected to be computationally inexpensive for its multiple dimensions. Now if the dimensions are reduced without considering the internal variability and patterns of the data, it may lead us to an erroneous model result. Hence, to reduce the multicollinearity and dimensionality, the principal component analysis (PCA) is used. PCA is a powerful statistical tool which can identify patterns in multidimensional data. On the other hand, it can reduce dimensions without reducing the internal variability of the original data. There are no clear rules for choosing a number of principal components that explains the maximum percentage of variance. Srivastav and Simonovic (2014) investigated the performance of a multisite weather generator with different principal components and considered first principal component for their study. Kannan and Ghosh (2013) adopted Kasier's rule for selecting principal components that explain more than the average amount of total variance. In this study, we considered first five principal components that explain 97% variability of the original data (Figure 3.2).

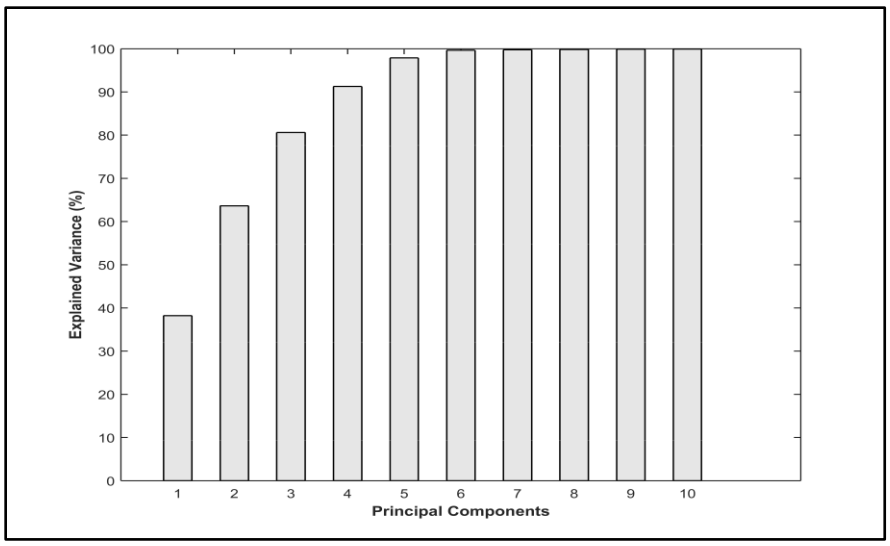

Figure 3.2 Cumulative percent of variance explained by principal components (after Mandal *et al.*, 2016c).

3.2 Statistical Downscaling of GCM Simulations with Beta Regression

The details of beta regression-based statistical downscaling technique conditioned to the precipitation states are outlined in this section. The proposed modeling framework is shown in Figure 3.3. This framework is divided into two parts. In the first part (Figure 3.3 (a)), the daily precipitation states are generated using a supervised classification technique, namely CART (classification and regression trees) wherein the second part (Figure 3.3 (b)), the daily precipitation sequences are generated for a particular location using multivariate beta regression. CART classifies predictor variables or builds relationship in terms of explanatory power and variance using an ‘‘acyclic tree”. The following subsections describe in details procedures for generation of precipitation states (part 1) and daily precipitation generation (part 2).

3.2.1 Generation of Daily Precipitation States

The daily precipitation state is a qualitative representation of precipitation status for a given day in a particular region where multiple sites of interest belong. For predicting daily precipitation states in the river basin, CART algorithm coupled with an unsupervised classification method (K-means clustering) is used following Kannan and Ghosh (2013). K-means clustering helps to identify daily precipitation states in the river basin. CART is a classification and regression algorithm based on 'if-then' logic. The advantages of using CART are: (1) it does not follow a prior statistical distribution of predictors; (2) it is flexible and efficient with high dimensional data; and (3) it can effectively deal with a mixture of categorical, discrete and continuous predictor variables (James *et al.*, 2013). The procedure for daily precipitation states estimation is explained in Figure 3.3(a). It includes few steps as follows:

Step-I: Use K-means clustering technique for identifying precipitation states from the observed ANUSPIN precipitation data (1961–1990). For an optimum number of clusters, cluster validity index e.g. Silhouette Index, Davis–Bouldin index, Dunn Index and Connectivity measures (Brock *et al.*, 2008) are used.

Step-II: Standardize the NCEP/NCAR predictor variables by subtracting mean and dividing the data by standard deviation. After standardization, PCA is used to reduce the dimension and remove multicollinearity from the standardized predictor variables. Preserve the principal component/scores and eigenvectors/factors for the next step.

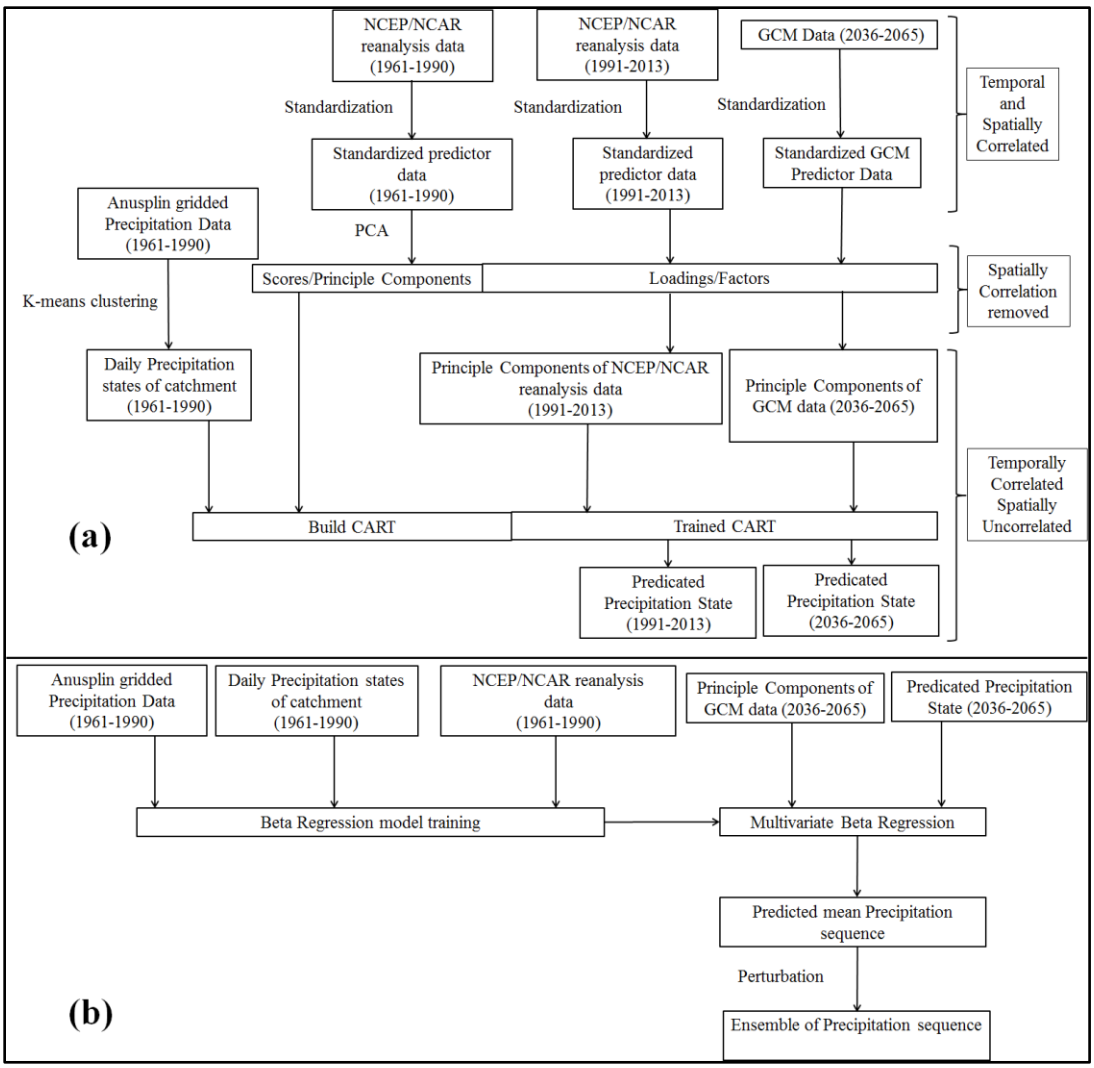

Figure 3.3 The schematic of proposed downscaling framework. (a) prediction of precipitation state using CART. (b) multivariate beta regression model for synthetic precipitation generation (after Mandal *et al.*, 2016c).

Step-III: Apply the standardization procedure and PCA to historical NCEP/NCAR predictor data and historical GCM predictor data (CanESM2) for a different time period.

Step-IV: Build the CART with the help of principal components obtained from NCEP/NCAR predictor data and precipitation states obtained from K-means.

Step-V: Apply the CART model to GCM historical data (1983 to 2005) and historical NCEP/NCAR data (1991 to 2013) to derive rainfall states for a different time period and compare statistics with observed historical data for the same time period. These two different historical time periods are used for validating the proposed the downscaling model with GCM and NCEP/NCAR data set.

Step-VI: For calculating future precipitation states under different climate change scenarios the CART model is applied to standardized future GCM (CanESM2) predictor data (2036–2065).

Preserving the spatial correlation and capturing the variability of predictand are the important aspects of the statistical downscaling. Hence, it will be more acceptable if the procedure provides for derivation of precipitation states first and then generate precipitation amount. Precipitation states of the river basin combined with data driven regression approach (beta regression) preserve the spatial dependence in the precipitation fields. This combined procedure retains the marginal and joint density structure of historical precipitation series which includes nonlinearity and state dependence.

3.2.2 Multisite Precipitation Generation

For multisite precipitation generation, a relationship between predictors and predictand climate variables has to be developed.

$$P_t = F_R(X_t / S_t) \tag{3.1}$$

The generalized relationship between predictors and predictand is described by Eq. (3.1) where P_t is the precipitation at a certain station at time t, X_t is predictor variables at time t and S_t is precipitation state of the river basin at time t.

Generally this kind of relationship is developed using regression (parametric/non-parametric) or probabilistic approach (Wilby and Harris, 2006; Mehrotra and Sharma, 2007; Srivastav and Simonovic, 2014). In this study, beta regression is applied to model the above-mentioned relationship. The predictors used to build the regression model are current day principal components of reanalysis predictor data and current day precipitation states from CART where predictand is present day precipitation at different stations (generated separately).

3.2.2.1 Beta Regression

Regression analysis builds a relationship between independent variables (x) and dependent variable (y). In this study, large-scale global climate variables are independent variables or predictors and precipitation is dependent variable or predictand. The relationship between them can be formalized as follows:

$$y_i = f(x_i) + \varepsilon_i, \qquad i = 1, 2, ...n \tag{3.2}$$

where ε_i is a normally distributed non-zero error term. If the relationship is linear then the expression (3.2) is modified as follows:

$$y = x^T \beta + \varepsilon_i = \beta_0 + x_1\beta_1 + x_2\beta_2 + ...x_d\beta_d + \varepsilon_i \tag{3.3}$$

where x is a vector of predictor variables with dimension d and β is a coefficient vector. The relationship in Eq. (3.3) is developed using beta regression (BR). This regression approach follows the beta distribution. The beta distribution is very flexible for modeling dependent variables since its density can assume a number of different shapes based on its parameters. Apart from this, the beta distribution is heteroskedastic and can successfully accommodate asymmetric data (Ferrari and Cribari-Neto, 2004; Schmid *et al.*, 2013). Another advantage of using beta distribution is that it can model nonlinear relationship (Simas *et al.*, 2010). The beta density function of the predictand can be written as:

$$f(y;\mu,\phi)=\frac{\Gamma(\phi)}{\Gamma(\mu\phi)\Gamma((1-\mu)\phi)}y^{\mu\phi-1}(1-y)^{(1-\mu)\phi-1},\quad 0<y<1,0<\mu<1,\phi>0 \tag{3.4}$$

μ is the mean of predictand, ϕ is a precision parameter, y is dependent variable and Γ(.) is gamma function. The beta distribution includes gamma function. In the past, gamma function was successfully implemented to model precipitation (Stern and Coe, 1984; Groisman *et al.*, 1999; Wilks and Wilby, 1999). The shape of beta density function can change depending on the values of μ and ϕ which help to estimate and model underlying structure of the data without assuming any functional form of estimators (Schmid *et al.*, 2013). If $\mu=1/2$ then the model is symmetric and if $\mu\neq 1/2$ then the model becomes asymmetric.

The proposed regression model assumed that the dependent variable or predictand is beta distributed and constrained to the unit interval (0, 1). Therefore any dependent variable bounded in an interval (a, b) where a and b are known scalar values (a < b) need to be

scaled to (0, 1) interval. For this case y (predictand) is scaled into (0, 1) interval using the following two steps:

Step (i): $$y' = \left(y - a\right) / \left(b - a\right) \tag{3.5}$$

Step (ii): $$\mathrm{Pr}_{scaled} = (y'(n-1) + 0.5) / n\,; \tag{3.6}$$

where y is precipitation data, a is minimum value of y, b is maximum value of y, n is sample size and Pr_{scaled} has scaled precipitation data into (0,1).

To relate the conditional expectation function $E(y / x)$ for multivariate predictors, beta regression assumes a predictor-predictand relationship given by

$$g(\mu_t) = \sum_{i=1}^{k} x_{ti}\beta_i \tag{3.7}$$

$$x_{ti} = (x_{t1}, ..., x_{tk}); t = 1, ..., n \tag{3.8}$$

$$\beta_i = (\beta_1, ...\beta_k)^T (\beta \in \square^k) \tag{3.9}$$

where β_i is a vector of unknown regression parameters and x_{ti} are observations of k covariates (k < n). g (.) is strictly monotonic and invertible link function that maps (0, 1) into $\square$. Many types of link functions are possible here (e.g. probit, logit, log-log). Logit transformation is used for this work following Ferrari and Cribari-Neto (2004). Maximum likelihood estimation (MLE) is used to estimate β.

One of the major challenges of downscaling methods is generation of precipitation data outside of the observed range. A perturbation technique is used with stochastic

precipitation simulations and enhances the generation of extreme precipitation following King *et al.,* (2015). The following equation is used for perturbation:

$$y^{j}_{ppt,t+i} = \lambda_{ppt} x^{j}_{ppt,t+i} + \left(1-\lambda_{ppt}\right) z_{t+i} \; ; t = 1,2,....n \tag{3.10}$$

where $y^{j}_{ppt,t+i}$ is the perturbed precipitation value for $t+i$ th day in jth location, $x^{j}_{ppt,t+i}$ is precipitation value for $t+i$ th day in jth location and t is number of days and z_{t+i} comes from two parameters log-normal distribution (King *et al.,* 2015). λ_{ppt} value varies in between 0 to 1 (0 means data series are totally perturbed and 1 means no perturbation in the results) and larger value of λ_{ppt} is reasonable to preserve spatial correlation. It has been found that λ_{ppt}=0.9 can adequately preserve spatial correlation and other statistics (i.e. mean, variance) while it can still produce precipitation values outside of the observed range (King *et al.*, 2015).

KNN algorithm is used to resample a block of days and ranks them. A cumulative probability distribution is calculated based on a day's rank. The next day precipitation is selected based on this probability distribution and a random number u (0, 1) which selects the closest day. For instance, precipitation of a day which is similar to present day precipitation has a higher probability of being selected and that helps to preserve temporal correlation of climate variables. After the resampling, the perturbation is used to reshuffle the precipitation values. This process can be repeated several times for generating alternative precipitation realizations.

3.2.3 Model Application

An unsupervised K-means clustering method is used to identify historical daily precipitation states (1961–1990) in the river basin. The optimum numbers of clusters or precipitation states are obtained from cluster internal validity tests e.g. Connectivity measure, Silhouette index and Dunn index and Davis–Bouldin index (Brock *et al.*, 2008). Each validity index has different criteria for identification of an optimum number of clusters. For an optimum number of clusters, connectivity index value should be minimized where Silhouette index, Davis–Bouldin index and Dunn index value should be maximized. All four indices are tested for a number of clusters varying from 2 to 10 (Figure 3.4)**.** Apart from cluster validity index there is a hydrological aspect in selecting number of precipitation states or optimum number of clusters (Kannan and Ghosh, 2010). Table 3.2 shows cluster centroids calculated using k-means clustering technique for clusters varying from 2 to 4. It is found that the dry condition states (low cluster centroid value) are well separated from the other states in all clusters (Table 3.2). To preserve the daily temporal correlational among predictor (large scale global climate variable) and predictand (precipitation) dry state condition need to be identified. Hence, the number of clusters exceeding 2 is considered following Kannan and Ghosh (2010). Cluster validity indices show that the optimal number of clusters should be greater than 2 where Davis–Bouldin index indicates 3 clusters as the optimal number. After the cluster validity measure analysis and consideration of other hydrologic issues, 3 clusters are selected to be used in this study. These clusters divide precipitation states into ‘‘almost dry”, ‘‘medium” and ‘‘high,” based on precipitation amount stored in the cluster centroid.

Daily precipitation amount divided into different clusters provides more realistic prediction of precipitation states (Kannan and Ghosh, 2010).

CART model is constructed to predict precipitation states in the river basin using principal components derived from NCEP/NCAR predictor data and historical daily precipitation states obtained from the K-means clustering. CART prunes a classification tree conditioned to daily precipitation states. Principal components of NCEP/NCAR predictor variables for 30 years period (1961–1990) are used to prune the tree where the remaining 23 years of data (1991–2013) is used for validation of the model. It has been reported that the performance of classification tree was acceptable using NCEP/NCAR data with a lag-1 precipitation state (Kannan and Ghosh, 2010). The following relationship is used for building the CART model:

$$s_t = f\{p_t, p_{t-1}, s_{t-1}\} \tag{3.11}$$

where s_t is precipitation state, p_t is set of climate variables on t^{th} day and p_{t-1} / s_{t-1} is precipitation state/ set of climate variables on $(t\text{-}1)^{\text{th}}$ day.

Therefore, CART model build in this study used principal components of NCEP/NCAR predictor variables of the current day and the previous day with lag-1 precipitation state. BR model constructs a featured linear space based on identified daily precipitation states for the daily multisite precipitation generation. The linear space contains standardized and dimensionally reduced NCEP/NCAR predictors and corresponding daily observed precipitation data for 30 years period (1961–1990). For BR model validation, the

remaining 23 years (1991 to 2013) of standardized and dimensionally reduced NCEP/NCAR predictors are used conditioned to the precipitation states.

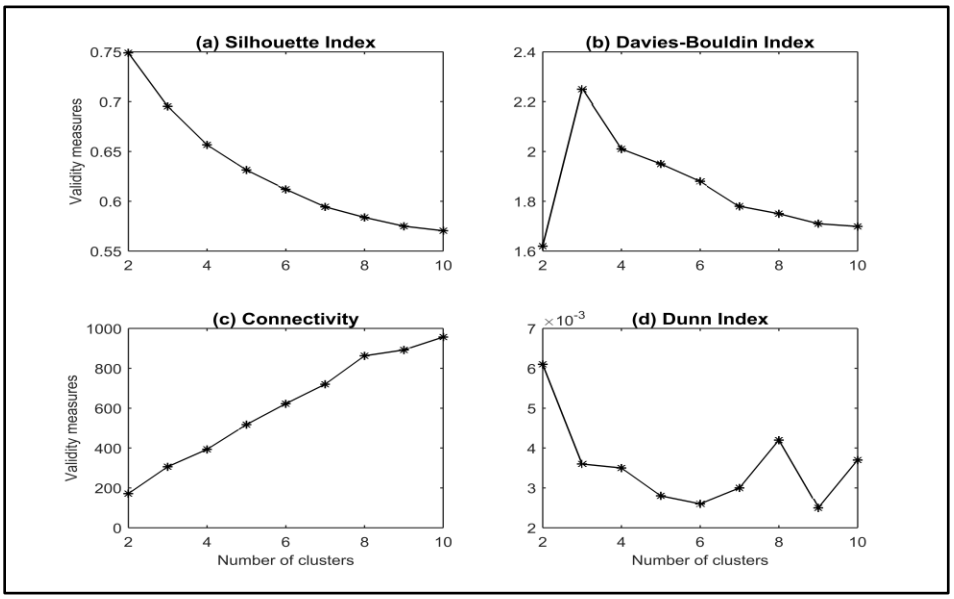

Figure 3.4 Cluster validity measures (after Mandal *et al.*, 2016c).

Table 3.2 Cluster centroid calculated from K-means clustering (after Mandal *et al.*, 2016c).

No. of clusters	Cluster centroids									
2	3.08	3.04	3.47	3.20	2.12	2.47	2.09	2.60	2.45	3.21
	27.71	27.82	33.43	31.83	20.06	25.36	20.05	24.96	24.96	29.57
3	1.92	1.87	2.10	1.94	1.31	1.48	1.29	1.60	1.48	1.97
	16.40	16.56	19.33	18.07	11.77	14.24	11.69	14.30	14.04	17.49
	41.43	41.19	50.64	48.80	29.58	39.00	29.66	38.09	38.29	44.08
4	1.19	1.14	1.29	1.19	0.79	0.88	0.77	0.98	0.89	1.21
	10.61	10.64	12.18	11.28	7.472	8.86	7.38	9.09	8.71	11.22
	24.3	24.57	29.11	27.53	17.62	21.84	17.58	21.57	21.50	26.02
	48.02	47.55	59.07	57.29	34.66	46.06	34.76	44.84	45.28	50.99

In the context of GCM data downscaling and model performance test using GCM outputs, standardized and dimensionally reduced historical (1983–2005) predictors from the CanESM2 are downscaled and compared with daily observed data for the same period. The proposed BR model simulated output is compared with the multisite non-parametric kernel regression (KR) model (Kannan and Ghosh, 2013). The kernel regression model has been used for generating multisite precipitation in the Mahanadi river basin, India. This model combines K-means, bias-correction, PCA, CART and kernel regression to generate synthetic precipitation. Simulation results from the BR model without rainfall state conditioning (BRWS) is also compared with the proposed BR model results in order to better understand the role of rainfall state in the down-scaling process. The comparison details and advantage of the BR model are discussed in the next section. A brief description of models used in this study with their acronyms is listed in Table 3.3.

The objective is to demonstrate the efficacy of the proposed multisite BR model. Using BR model, 30 independent realizations are generated for the validation period (1991–2013). The present downscaling method is also applied to GCM (CanESM2) simulated standardized predictor data for a future time (2036–2065) periods.

Proposed BR model performance evaluation is based on the reproduction of historical statistics such as (1) temporal mean and standard deviation, (2) seasonal total precipitation (3) temporal and spatial cross correlation, and (4) preservation of quantiles. Results from different downscaling approaches such as BR, BRWS and KR are evaluated for spatial and temporal variation of precipitation over the river basin.

Table 3.3 Brief description of models used for comparison (after Mandal *et al.*, 2016c).

Acronym	Description
BR	Beta regression conditioned to precipitation states
BRWS	Beta regression not conditioned to precipitation states
KR	Kernel regression conditioned to precipitation states

3.2.3.1 Model Validation

3.2.3.1.1 Comparison of Statistical Characteristics

The statistical characteristics (such as mean and standard deviation) from BR, BRWS and KR model applications are shown in Table 3.4 and they are compared with observed precipitation for the validation period (1991–2013) at ten downscaling locations. Student t-test is conducted to check if the means of model simulated precipitation series at different stations similar to those of the observed data. The hypothesis is stated as ‘‘H_0: means of two series are the same” at 5% significance level. Results from the t-test are presented in

Table 3.5. It can be seen that the BR model can generate precipitation time series similar to observed precipitation at different stations except for two locations: GLD and WOL. The BRWS and KR model results show mixed outcomes at a 5% significance level.

3.2.3.1.2 Basin Average Annual and Monthly Precipitation

Streamflow of the Campbell River is affected by snowmelt and rain. Peak streamflow is observed in spring and fall while the low flows are usually experienced during the

summer and winter (Zwiers *et al.*, 2011). Hence, annual or seasonal changes in precipitation (snow/rain) will affect streamflow in the river. A comparison of the annual and monthly variability of basin average precipitation (50^{th} percentile estimates) simulated from different models for the validation period are presented in this section. Figure 3.5 (a) and (b) compares annual and mean monthly precipitation generated by BR, BRWS and KR models in the river basin for a 23 year time period (1991–2013). Figure 3.5 (c) and (d) presents the correlation coefficient between basin average annual and monthly precipitation simulated by different downscaling models and observed precipitation for the validation time period (1991 to 2013).

Table 3.4 Mean and standard deviation for observed and simulated precipitation (mm) series (after Mandal *et al.*, 2016c).

	Downscaling Location									
	ELK	ERC	GLD	HEB	JHT	QIN	QSM	SAM	SCA	WOL
	Mean									
Observed	6.01	5.91	7.29	7	4.56	5.45	4.53	5.5	5.47	6.31
BR	5.4	7.2	7.37	6.65	3.95	3.49	3.94	4.27	4.	7.16
BRWS	3.2	5.52	6.49	9.79	6.23	6.58	6.33	6.51	6.96	5.97
KR	9.00	9.08	10.50	9.77	6.02	7.71	6.00	7.69	7.49	9.61
	Standard Deviation									
Observed	10.22	10.22	12.7	12.4	8.19	9.84	8.20	9.63	9.79	10.81
BR	10.58	11.65	10.5	12.8	7.89	9.62	7.63	10.02	8.8	9.8
BRWS	8.40	7.28	9.02	9.36	4.94	8.77	7.94	8.75	9.26	7.99
KR	12.9	13.02	15.76	14.93	9.26	11.67	9.25	11.47	11.45	13.87

Table 3.5 Hypothesis test results for testing mean of observed and simulated precipitation series (after Mandal *et al.*, 2016c).

	Student's t-test result for acceptance/ rejection of the null hypothesis at 5% confidence		
Station	KR	BRWS	BR
ELK	Reject	Do not Reject	Do not Reject
ERC	Reject	Do not Reject	Do not Reject
GLD	Reject	Do not Reject	Reject
HEB	Do not Reject	Do not Reject	Do not Reject
JHT	Do not Reject	Do not Reject	Do not Reject
QIN	Do not Reject	Reject	Do not Reject
QSM	Do not Reject	Reject	Do not Reject
SAM	Do not Reject	Reject	Do not Reject
SCA	Do not Reject	Reject	Do not Reject
WOL	Reject	Do not Reject	Reject

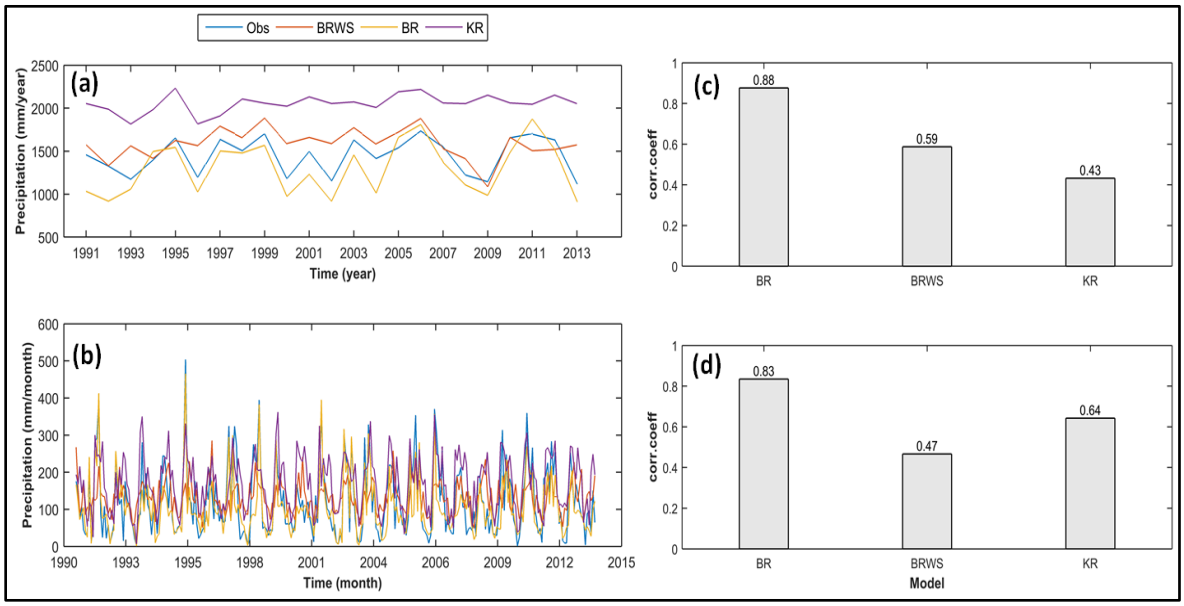

Figure 3.5 (a) Annual and (b) monthly mean precipitation, spatially averaged over the Campbell River basin. The corresponding temporal correlation coefficients for different downscaling approaches are shown in (c and d) (after Mandal *et al.*, 2016c).

BR model is simulated mean annual precipitation (basin average) series shows a high correlation (correlation coefficient of 0.88) with the observed precipitation, which means that the BR model can capture annual variability fairly well over the basin. For monthly basin average precipitation BR shows a satisfactory match with the observed series and obtained correlation coefficients is 0.83, where KR performs moderately well with a monthly correlation coefficient of 0.64. Overall beta regression based method outperforms all other models in terms of capturing annual and monthly variability.

Figure 3.6 (a)–(c) compares cumulative distribution function (CDF) of basin-average simulated precipitation series generated from different downscaling methods with those obtained using observed rainfall series. Compare to KR and BRWS, the CDF computed from BR model simulated data shows minimum deviation from the CDF obtained using observed precipitation. CDF of basin average precipitation obtained from BR model using historical CanESM2 GCM predictors (1983–2005) data is shown in Figure 3.6 (d) together with CDF of the observed precipitation. It seems BR model fairly well represents basin average precipitation using GCM (CanESM2) predictors data (Tmax, Tmin, mslp, hus, u-wind and v-wind). Another important observation is that the BR model is capable of capturing the percent of dry days (precipitation $\leq$ 1 mm/day) adequately. Using the BR, percent of dry days in the river basin calculated from simulated precipitation data is 42% for validation period, almost equal to actual observed dry day percent (Figure 3.6 (a)). Although, KR performs well in capturing percent of dry day (42%) but it has an upward shift which refers a decreased frequency of precipitation events from actual. Percent of dry days calculated from the CanESM2 (48%) is also

acceptable when compared to observed dry day percent (Figure 3.6 (d)). However, BR model ability to capture extreme precipitation (maximum) is very poor.

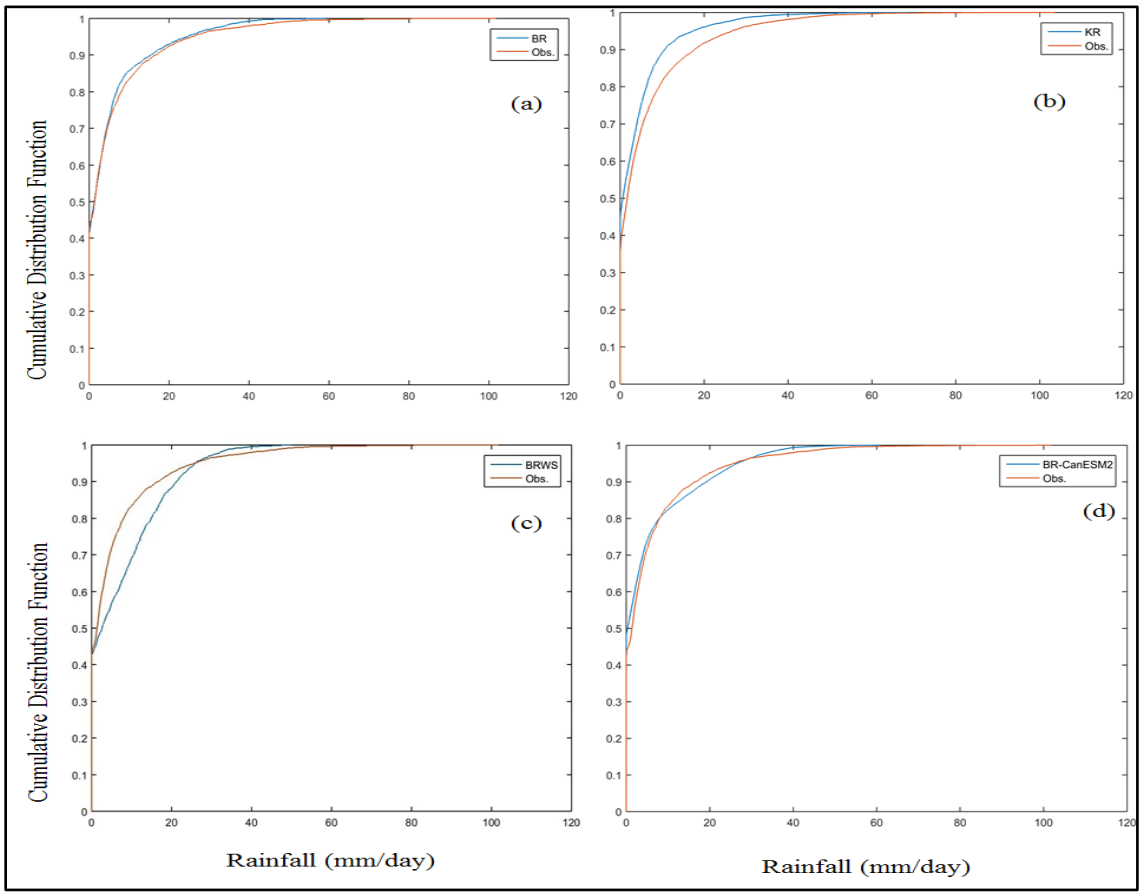

Figure 3.6 (a–c) CDF of basin average precipitation obtained from different downscaling methods using reanalysis data (1991–2013). (d) CDF of basin average precipitation obtained from BR model using CanESM2 data (1983–2005) (after Mandal *et al.*, 2016c).

3.2.3.1.3 Basin Average Wet/Dry Spell Length and Seasonal Precipitation Amounts

Wet and dry spell lengths are very important in water resource planning and management especially where the reservoir needs a certain water storage level for hydropower generation. Hence, reproduction of wet/dry spell lengths along with seasonal precipitation is a very important aspect of the downscaling process. Although there are many

definitions presented in the literature for wet/dry spell (WS/DS) length, the following definition for WS/DS from WCRP (2009) is used for this study. A WS (DS) defined as a maximum number of consecutive days with precipitation greater than (less or equal to) 1 mm.

Table 3.6 shows the annual average total seasonal precipitation and compares 5^{th}, 50^{th} and 95^{th} percentile for both observed and downscaled precipitation. It is found that overall performance of BR model is better compared to KR in terms of capturing total seasonal precipitation. KR performs well in spring and summer period. However, KR simulates the high amount of precipitation in winter and fall compare to historical precipitation which is not acceptable for water resource planning and management.

Table 3.7 describes annual average wet and dry spell lengths from simulated precipitation. BR and KR perform similar in reproducing dry spell length, but BR performs well in capturing wet spell length. It seems from both Table (Table 3.6 and 3.7), BR model also performs satisfactorily in capturing seasonal precipitation (except fall) and WS/DS length using CanESM2 predictors data.

3.2.3.1.4 Temporal variability and spatial dependence

Assessment of temporal and spatial variability of precipitation is high importance for water resource management (municipal water supply, irrigation scheduling, hydropower generation, *etc.*). A better understanding of rainfall variability (temporal and spatial) is needed to better manage impacts of natural disasters (e.g. floods, droughts) in a changing climate. Therefore, the downscaling model should capture the temporal and spatial variability of precipitation accurately. Hence, the performance of all downscaling

methods in capturing temporal and spatial dependence of simulated precipitation series is examined.

Table 3.6 Observed and downscaled annual average seasonal total precipitation (5^{th}, 50^{th} (median) and 95^{th} percentile) for testing period (1991-2013) (after Mandal *et al.*, 2016c).

	Rainfall amount (mm)				
		Simulated percentile estimate			Percentage change in median value
Season	Observed	5^{th} percentile	Median	95^{th} Percentile	Rainfall amount
Model using Reanalysis data for 1991-2013 Model: BR					
Winter	253.61	240.32	284.92	310.25	12.34
Spring	409.33	354.23	376.86	404.21	-7
Summer	263.10	224.5	267.06	289.36	1.5
Fall	188.39	180.5	217.37	266.52	15.3
Model: BRWS					
Winter	253.61	358.23	410.55	425.36	61.8
Spring	409.33	554.23	605.11	630.23	47.8
Summer	263.10	359.36	404.73	456.32	53.4
Fall	188.39	219.32	237.31	265.36	25.9
Model: KR					
Winter	253.61	290.32	355.63	420.32	40.22
Spring	409.33	410.35	494.11	550.35	20.71
Summer	263.10	265.36	290.90	310.85	10.56
Fall	188.39	289.36	308.43	340.25	63.72
Downscaled precipitation data using current climate data of GCM (CanESM2) for 1983 - 2005 Model : BR					
Winter	204.65	178.36	195.62	230.23	-4.41
Spring	304.21	256.36	290.23	331.65	-4.59
Summer	257.99	240.36	278.36	339.36	7.89
Fall	129.99	155.36	160.36	225.36	23.35

Table 3.7 Annual averaged dry spell length and wet spell length of observed and downscaled precipitation (after Mandal *et al.*, 2016c).

Obs	BR	BRWS	KR
Model: using Reanalysis data for 1991-2013			
Dry spell length			
21	19	10	18
Wet spell length			
23	20	14	37

Obs	BR
Model: using current climate data of GCM (CanESM2) for 1983-2005	
Dry spell length	
26	23
Wet spell length	
28	26

Table 3.8 provides the correlation coefficient between model simulated precipitation time series and observed precipitation at all ten downscaling locations for the validation period. From the results, it can be concluded that the overall performance of BR model conditioned to precipitation states is moderately better when compared to other methods. Figure 3.7 shows the scatter plot of interstation correlation coefficients computed from model-simulated daily precipitation series and observed precipitation for all station pairs using different modeling approaches. From the plot in Figure 3.7, it can be concluded that the BR model captures spatial correlation better than the KR. Artificial correlation has been added during the simulation by the conditioned rainfall states which can lead the BR model to overestimation of precipitation. Hence, the rainfall states should be used

cautiously when the spatial correlation is of primary interest. The BRWS model fails to preserve the spatial correlation between data series.

Table 3.8 Correlation coefficients obtained for observed and simulated precipitation series at different stations in the Campbell River basin, BC, Canada (Validation period: 1991– 2013) (after Mandal *et al.*, 2016c).

	Correlation coefficient from Model generated precipitation series		
Stations	BR	BRWS	KR
ELK	0.6999	0.6160	0.5697
ERC	0.6804	0.5984	0.4737
GLD	0.7086	0.6321	0.5389
HEB	0.6925	0.6301	0.5674
JHT	0.6312	0.5788	0.5282
QIN	0.6842	0.6058	0.5678
QSM	0.6299	0.5831	0.4685
SAM	0.6997	0.6155	0.6075
SCA	0.6858	0.6107	0.4480
WOL	0.6906	0.6131	0.3938

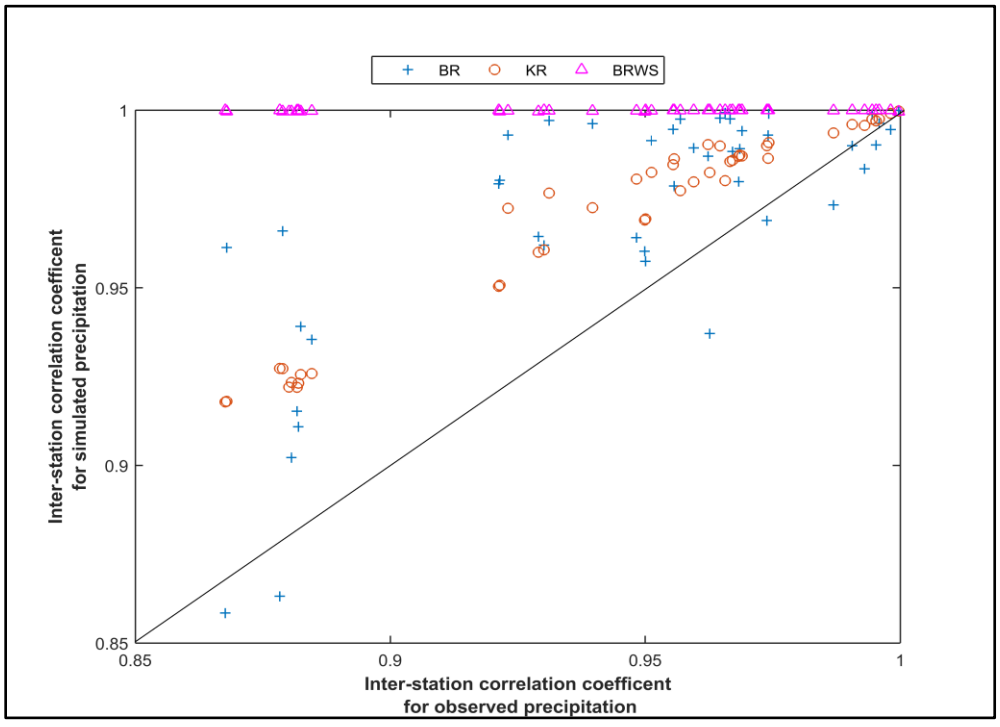

Figure 3.7 Interstation correlation coefficients for different downscaling approaches (after Mandal *et al.*, 2016c).

3.2.3.1.5 Seasonal Wet Days Characteristics

Changes in wet day precipitation may lead to extreme hydrological events such as floods and droughts. Investigation of wet day characteristics is important for water resource planning and management. Accurate reproduction of wet days is one of the important aspects of statistical downscaling. Although there are different criteria used in the literature to assess the wet days (WD), this work follows the definition of WD from Gaur and Simonovic (2013).

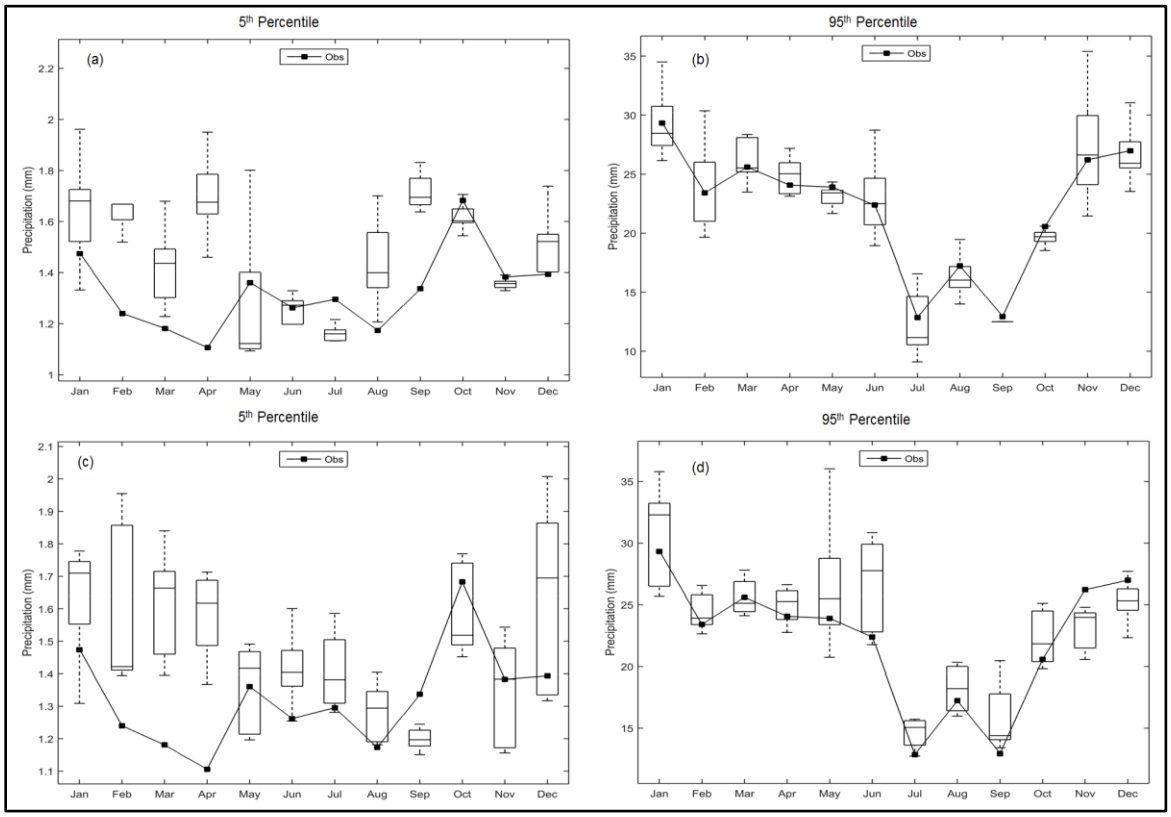

Figure 3.8 Characteristics of monthly wet day extremes for observed and simulated precipitation at the JHT station. (a and b) Obtained from NCEP/NCAR (time period: 1991– 2013). (c and d) Obtained from CanESM2 (time period: 1983–2005) (after Mandal *et al.*, 2016c).

According to Gaur and Simonovic (2013) if the amount of precipitation in a day is greater than 1 mm, then it is considerd as a wet day. Figure 3.8 represents 5^{th} and 95^{th} percentile estimates of downscaled monthly wet days for JHT station (considered as the only location to shorten the manuscript length). Figure 3.8 (a) and (b) shows WD characteristics obtained from the simulated reanalysis monthly precipitation data where Figure 3.8 (c) and (d) shows WD characteristics of downscaled data obtained using the historical CanESM2 (1983–2005) monthly data. From Figure 3.8 it can be observed that the BR model can generate values beyond extremes, but sometimes it underestimates extremes precipitation. This may be caused by scaling the response variable (precipitation) to (0, 1) interval.

3.2.3.1.6 Adding Value to GCM Projections

Future climate change projections using GCMs simulation are very sensitive due to the existence of historical climate bias (Liang *et al.*, 2008). If a GCM reasonably simulates present and historical climate then the credibility of future climate projection using the same GCM simulation will be higher. This can be possible if a downscaling model adds value to historical and present GCM climate variables. An experiment is conducted to explore whether BR model adds value to GCMs historical climate change following Racherla *et al.*,(2012). The steps we followed for this experiment are:

Step-I: First CanESM2 simulated historical precipitation data divided into two-time slices e.g. 1983–1994 (T1 hereafter) and 1995–2005 (T2 hereafter).

Step-II: ANUSPLIN and BR simulated precipitation data also divided into same time slices following step-I.

Step-III: Precipitation biases are calculated by subtracting daily historical precipitation data (ANUSPLIN) from CanESM2/BR simulated precipitation data. These biases are calculated for T1 and T2 time period and converted to seasonal mean precipitation biases shown in Figure 3.9.

Step-IV: Historical climate change (T2 minus T1) is calculated using above mentioned three data sets (ANUSPLIN, CanESM2 and BR simulated precipitation) and presented in Figure 3.10. DJF, MAM, JJA and SON represent winter, spring, summer and fall season respectively.

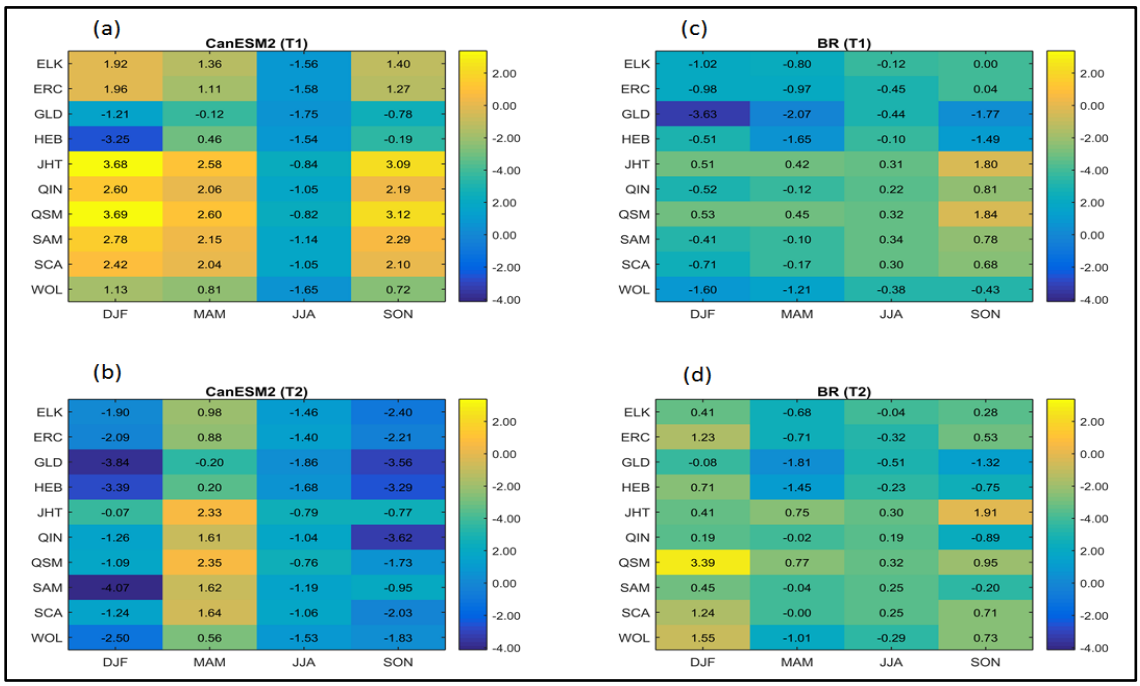

Figure 3.9 Seasonal mean (T1/T2 time periods) biases of daily averaged precipitation (mm/day; CanESM2/BR simulated precipitation minus ANUSPLIN precipitation) at different downscaling locations (after Mandal *et al.*, 2016c).

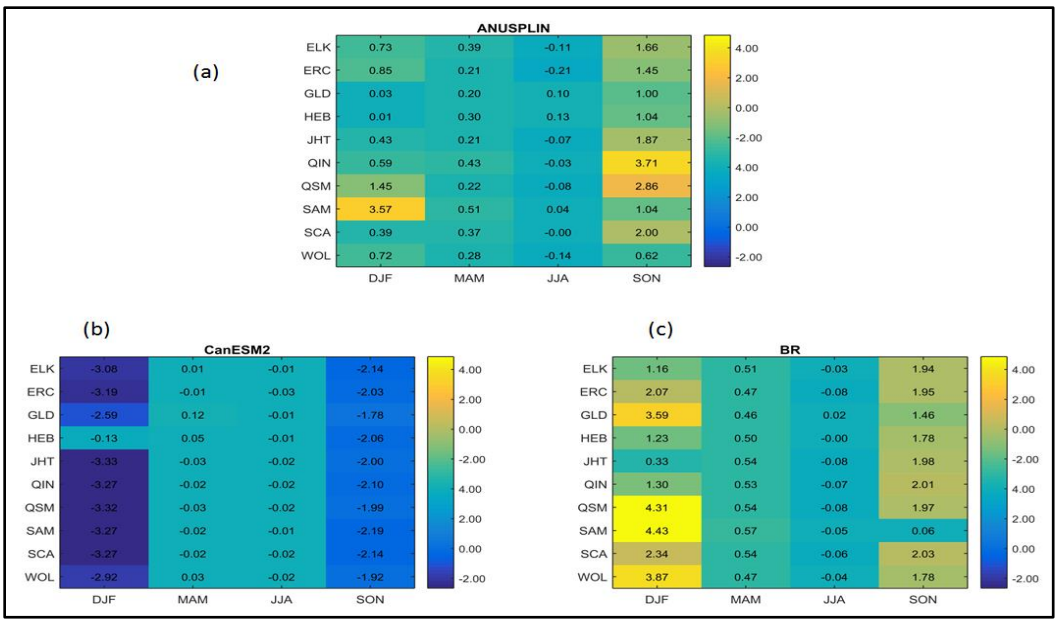

Figure 3.10 Seasonal mean daily average precipitation changes (mm/day; T2 minus T1 time periods) (after Mandal *et al.*, 2016c).

It has been found that a wet bias is present in CanESM2 T1 time period (Figure 3.9 (a)) especially in fall and winter season where a dry bias has been found in T2 time period except spring season (Figure 3.9 (b)). The biases are reduced in BR simulated precipitation in both time periods except GLD station (Figure 3.9 (c) and (d)). Downscaled changes in seasonal precipitation between T1 and T2 time periods are presented in Figure 3.10. The most visible observed positive changes in precipitation have found in fall and winter, where a small decreasing trend found in summer time (Figure 3.10(a)). Evidently observed changes are not reproduced well in CanESM2 except summer (Figure 3.10 (b)). However, BR model fairly reproduces observed changes except for winter season (Figure 3.10 (c)). From this experiment, it can be concluded that GCMs historical bias can be reduced using BR model but not for all seasons and all stations. This limitation may be overcome if we consider different GCMs for the same experiment.

3.2.4 Future Precipitation Projection using GCM Simulation

The BR model applied with standardized predictor data pertaining to RCP 2.6, RCP 4.5 and RCP 8.5 scenarios of CanESM2 where RCP 2.6 represents low carbon emission scenario; RCP 4.5 referred as intermediate carbon emission scenario and RCP 8.5 is high emission scenario. To investigate the impact of future climate change on precipitation under different emission scenarios, a future time slice (2036–2065) is selected.

Figure 3.11 represents CDF of daily precipitation at four downscaling locations. These four downscaling stations are selected based on their geographical location. JHT located near John hart dam where QIN and SCA are located near Strathcona dam. All of these three stations are located in downstream of the Campbell River basin where WOL is in upstream of the river. The CDFs obtained for three scenarios are similar to each other and almost match with the CDF of observed precipitation (1991–2013). However, a downward shift pertaining to all three scenarios can be observed for JHT which indicates an increased frequency of high precipitation events during 2036–2065 compared to 1991– 2013 (Figure 3.11 (a)). JHT station is located in downstream of the Campbell River and surrounded by forest. According to Sheil and Murdiyarso (2009) winds travel through forests can produce more than twice times precipitation compare to when they travel over the land which can be the reason of increased precipitation events at JHT. Although the results obtained from a single GCM output using BR are compared here. More variation can be expected if the present analysis is performed with multiple GCMs (Werner, 2011).

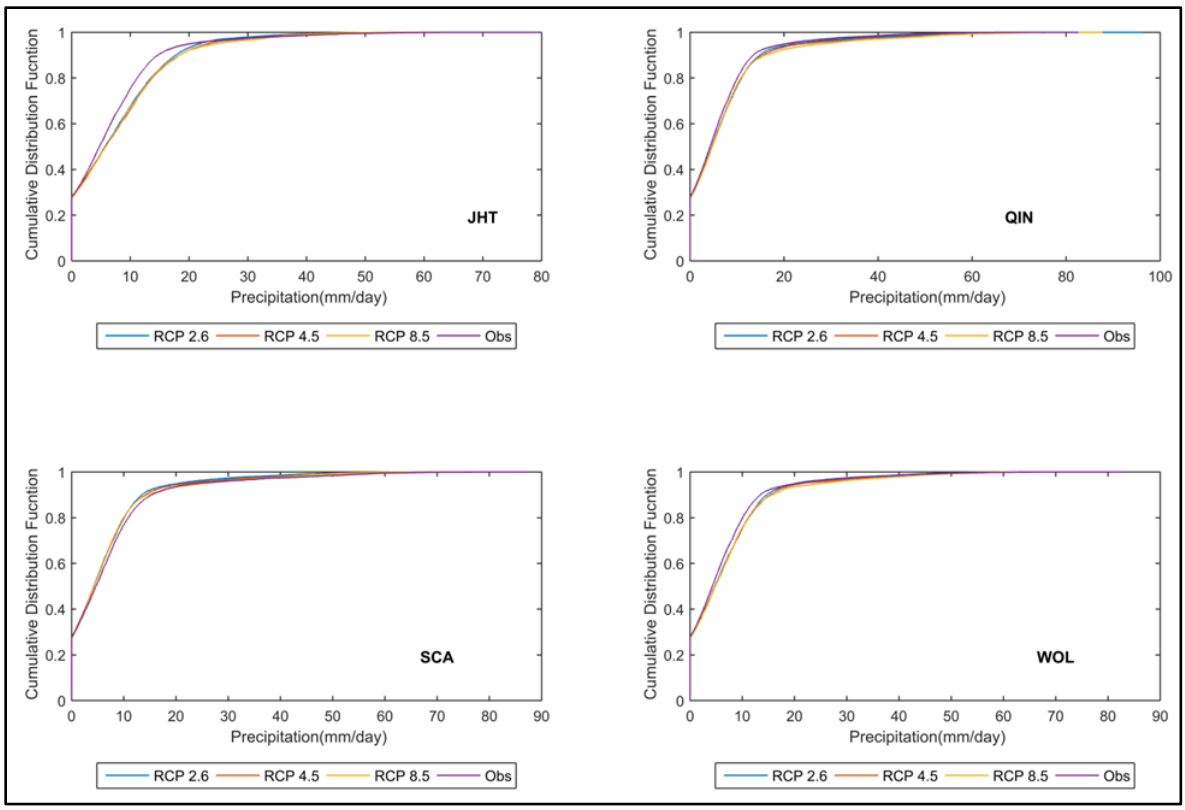

Figure 3.11 CDF of simulated future (2036–2065) daily precipitation using CanESM2 predictor data under three emission scenarios (RCP 2.6, RCP 4.5 and RCP8.5) at different locations compare with observed precipitation (1991–2013) (after Mandal *et al.*, 2016c).

3.2.4.1 Projected Future Seasonal Precipitation Changes during 2036– 2065

Table 3.9 and Table 3.10 provide information on estimated changes in number of wet days and seasonal precipitation amounts during 2036–2065. Percentage change in the median of any scenario is estimated with respect to observed data (1991–2013). For all three scenarios, summer precipitation amounts are going to decrease along with wet days. Maximum 58% can be decreased in summer precipitation amount where wet days can be reduced up to 18%. The changes detected for all three scenarios show precipitation amount in the fall is going to increase with wet days. For RCP 8.5, the increase is 22% in

precipitation and 13% in wet days during winter time. For RCP 2.6 and RCP 4.5 both project a small amount of precipitation increase in spring time but the wet day increases 26% and 21% respectively.

Table 3.9 Seasonal changes in numbers of wet days during 2036-2065 (after Mandal *et al.*, 2016c).

		Scenario					
	Observed (1991-2013)	RCP 2.6		RCP 4.5		RCP 8.5	
Season	Median estimate of number of wet days	Median estimate of number of wet days	Percentage change in median estimate	Median estimate of number of wet days	Percentage change in median estimate	Median estimate of number of wet days	Percentage change in median estimate
Winter	23	22	-4	26	13	26	13
Spring	19	24	26	23	21	24	26
Summer	16	15	-6	13	-18	15	-6
Fall	15	18	20	24	60	23	53

The description and validation of a new downscaling method based on beta regression are discussed in the section 3.2.3. As discussed before there are multiple significant sources of uncertainty exists in the downscaling process, it is essential to quantify all primary sources of uncertainty. The following section provides a method to quantify different sources uncertainty in precipitation projection under climate change.

Table 3.10 Seasonal changes in precipitation amount during 2036-2065 (after Mandal *et al.*, 2016c).

	Scenario						
	Observed (1991-2013)	RCP 2.6		RCP 4.5		RCP 8.5	
Season	Median estimate of mean precipitation (mm)	Median estimate of mean precipitation (mm)	Percentage change in median estimate	Median estimate of mean precipitation (mm)	Percentage change in median estimate	Median estimate of mean precipitation (mm)	Percentage change in median estimate
Winter	253	260	2	289	13	311	22
Spring	409	425	3	437	6	485	18
Summer	263	116	-55	110	-58	108	-58
Fall	188	236	25	252	33	267	41

3.3 Uncertainty in Precipitation Projections

Based on: Sohom Mandal, Patrick Breach and Slobodan Simonovic (2016), "Uncertainty in precipitation projection under changing climate conditions: A regional case study", American Journal of Climate Change, 5, 116-132. DOI: 10.4236/ajcc.2016.51012

It is necessary to quantify the uncertainty involved in the hydrologic impact assessment analysis, in order to provide useful results for decision-making, to account for climate change. Spatial downscaling translates large scale climate variables simulated by GCMs to a regional scale. A generalized climate change impact assessment process framework is outlined in Figure 3.12 (a). At the regional scale, the projection of hydro-climatic variables under changing climatic conditions is burdened with a considerable amount of uncertainty originating from several sources. Uncertainty may arise from: (a) inter-model variability due to different model structure between GCMs; (b) inter-scenario variability due to different type of emission scenarios; (c) intra-model variability due to the model parameter selection; and (d) the choice of downscaling model (Figure 3.12(a)). Minville *et al.,* (2008) observed that projection of precipitation is most sensitive to the choice of GCM where Wilby and Harris (2006) found out that GHG emission scenarios also caused uncertainty in precipitation projections under changing climatic conditions. However, according to Prudhomme and Davies (2008a) downscaling is a significant source of uncertainty along with the uncertainty due to the choice of GCM. There are several climate impact studies conducted on the west coast of Canada (Werner, 2011; Bürger *et al.,* 2012) but future precipitation projections considering the propagation of uncertainty

(GCMs uncertainty, GHG emission scenarios uncertainty and downscaling uncertainty) are rarely performed.

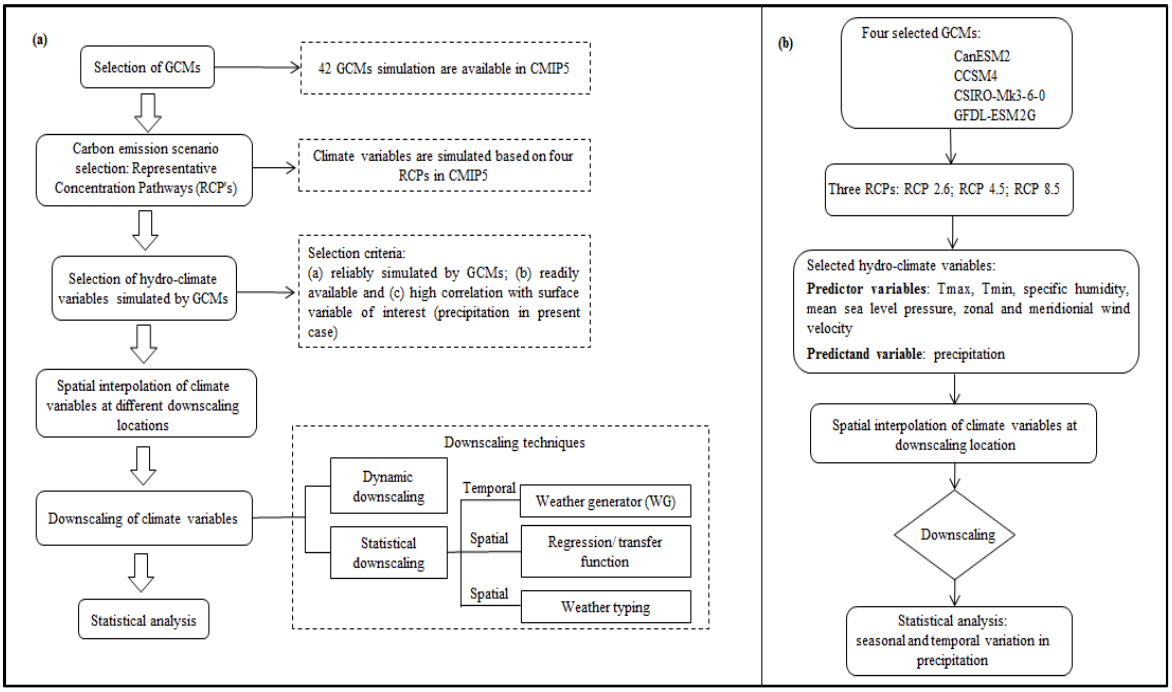

Figure 3.12 (a) Generalized framework of climate change impact assessment process; (b) flow chart presenting the assessment process followed in this study (after Mandal *et al.*, 2016b).

Werner (2011) conducted a study to project future monthly precipitation in three BC watersheds (Peace, Campbell and Upper Columbia) with eight GCMs under three emission scenarios (B1, A1B and A2). This study found that the uncertainty in precipitation projection due to the choice of GCM to be larger than that due to the choice of emission scenarios for different temporal scales. However, this study did not assess the uncertainty due to the choice of downscaling method. Bürger *et al.*, (2012) looked at changes in precipitation extremes in various climatic zones in British Columbia with six GCMs from the Coupled Model Inter-comparison Project (CMIP3) under three emission scenarios (B1, A1B and A2). Eight downscaling methods were used to compare

downscaling uncertainty. This investigation concludes that the results are more sensitive to the choice of downscaling methods followed by choice of GCM where the emission scenarios have a minor influence. Although this study addressed different sources of uncertainty, GCM data is now available from the CMIP5 and the conclusion is conflicting with other regional climate impact studies (Wilby and Harris, 2006; Wilby *et al.*, 2006). From the past studies, it has been found (a) inconsistency in the conclusions and (b) that sometimes all sources of uncertainty are not included in the climate change impact analyses. Ensuring that all sources of uncertainty are included during quantification of climate change impacts on the regional hydrology is essential (Kay *et al.*, 2009).

It this section, an investigation is carried out to address the three primary sources of uncertainty attributed to the selection of GCM, emission scenario, and downscaling model for the assessment of the climate change impacts on total monthly precipitation in the Campbell River basin, BC, Canada (Figure 3.1). This investigation includes four GCMs, three emission scenarios, and six downscaling methods. GCM simulations from Coupled Model Inter-Comparison Phase 5 (CMIP5) are used in this study (IPCC, 2013). The list of GCMs is shown in Table 3.11. These four GCMs are selected based on data availability for the six downscaling methods (described in section 3.3.1). Four Representative Concentration Pathway (RCP) emission scenarios are recommended by the Fifth Assessment Report (AR5) of Intergovernmental Panel on Climate Change (IPCC) (IPCC, 2013). Three of these are used in this research (RCP 2.6, RCP 4.5 and RCP 8.5) that cover the range of emission scenarios. RCP 2.6 represents lower carbon emission scenario, RCP 4.5 and RCP 6.0 represent intermediate carbon emission

scenarios and RCP 8.5 assumes high and unabated carbon emission by the end of 2100. Six Downscaling methods applied in this study are as follows: (i) bias-corrected spatial disaggregation (BCSD) (Wood *et al.*, 2004; Bürger *et al.*, 2012), (ii) bias correction constructed analogues with quantile mapping reordering (BCCAQ) (Werner and Cannon, 2015), (iii) delta change method coupled with a non-parametric K-nearest neighbor weather generator (King *et al.*, 2014), (iv) delta change method coupled with maximum entropy bootstrap based weather generator (Srivastav and Simonovic, 2014), (v) non-parametric statistical downscaling model based on the kernel regression (Kannan and Ghosh, 2013), and (vi) beta regression based statistical downscaling model (disused above). BCSD and BCAAQ were successfully applied across Canada in the past, however these methods cannot explicitly capture changes in daily extremes (Werner and Cannon, 2015) where the other four downscaling methods can capture changes in daily extremes and can produce extreme values outside of the historical boundaries (Kannan and Ghosh, 2013; King *et al.*, 2014; Srivastav and Simonovic, 2014; Mandal *et al.*, 2016d). The above mentioned six downscaling methods are used to quantify the amount of uncertainty arising from different types of statistical downscaling methods and compare it with other sources of uncertainties. The steps followed for this study are shown in Figure 3.12(b).

For this assessment, historical daily precipitation (prep) data for a 25 year span (1976 to 2005) was extracted from the ANUSPLIN data set on a 0.1 º x 0.1 º grid (Hutchinson and Xu, 2013). The ANUSPLIN data set is developed by applying a “thin-plate smoothing spline” algorithm to observed data from Environment Canada. Historical precipitation data is extracted for ten locations covering the entire Campbell River basin (Table 3.1).

Daily maximum and minimum air surface temperature (Tmax and Tmin), mean sea level pressure (mslp), specific humidity (hus) at 500 hPa, zonal (u-wind) and meridional (v-wind) wind are considered as predictor variables in this study following Kannan and Ghosh (2013). These climate variables are extracted from four GCMs (

Table 3.11) for a period of 25 years spanning 1976-2005, as well as for a near future period (2036 to 2065) and a far future period (2066 to 2095) under RCP 2.6, RCP 4.5 and RCP 8.5 emission scenarios. Details with regards to the use of these climate variables for the regression-based statistical downscaling models are given in next section.

The ANUSPLIN and GCM data sets used in this study have different spatial resolutions. For climate change impact assessment at the catchment scale, all the data sets are spatially interpolated to the ten locations of interest (Table 3.1) using the inverse distance square method (Shepard, 1968).

Table 3.11 List of GCMs (after Mandal *et al.*, 2016b)

GCM model	Centre Name	GCM resolution (Lon. Vs Lat.)
CanESM2	Canadian Centre for Climate Modeling and Analysis	2.8 x 2.8
CCSM4	National Center of Atmospheric Research, USA	1.25 x 0.94
CSIRO-Mk3-6-0	Australian Commonwealth Scientific and Industrial Research Organization in collaboration with the Queensland Climate Change Centre of Excellence	1.8 x 1.8
GFDL-ESM2G	National Oceanic and Atmospheric Administration's Geophysical Fluid Dynamic Laboratory, USA	2.5 x 2.0

3.3.1 Precipitation Projections using Multiple Downscaling Techniques

Two gridded statistical downscaling methods from the Pacific Climate Impacts Consortium (PCIC) (Pacific Climate Impacts Consortium, 2014), two weather generators (based on K-nearest neighbor and maximum entropy bootstrap) and two regression based statistical downscaling methods (kernel regression and beta regression) are used for future precipitation projection. The details of these methods are given below.

3.3.1.1 Gridded downscaling methods

Bias-corrected spatial disaggregation (BCSD) (Wood *et al.*, 2004; Bürger *et al.*, 2012) and bias correction constructed analogues with quantile mapping reordering (BCCAQ) (Werner and Cannon, 2015) are gridded statistical downscaling methods that can effectively produce plausible hydro-climate variables from the GCM output with computational efficiency. The BCSD downscaling method is performed in three steps. First, monthly GCM simulated precipitation data is corrected for bias using quantile mapping. Next, bias corrected monthly precipitation is downscaled by interpolating "monthly anomalies" from the historical time period at each station. This step is called "local scaling" because simulated coarse gridded monthly precipitation data is multiplied by a monthly scaled factor at each local station. This step helps to remove long term bias between large-scale simulated precipitation and observed precipitation at a regional scale. The mathematical description of the "local scaling" process is as follows:

$$P_{ds}(x,t) = P_{\mathrm{mod}}(x,t)\frac{\left\langle P_{obs}\right\rangle_{mon}}{\left\langle P_{\mathrm{mod}}\right\rangle_{mon}} \tag{3.12}$$

where $P_{\mathrm{mod}}(x,t)$ is simulated large scaled mean monthly precipitation from station x at time t in months 'mon'; $P_{\mathrm{mod}}(x,t)$ is observed mean monthly precipitation; $P_{ds}(x,t)$ is the monthly downscaled mean precipitation and $\langle ... \rangle_{mon}$ is the monthly mean precipitation calculated from gridded observed and historical GCM datasets.

Finally, the daily time series is generated by temporal downscaling of monthly mean precipitation to daily using a stochastic resampling technique following Wood *et al.*, (2002). BCCAQ is a hybrid method that combines bias correction constructed analogues (BCCA) and bias-corrected climate imprint (BCCI) where BCCI is referred as "inverse BCSD". BCCA follows the same spatial aggregation and bias correction (quantile mapping) steps as BCSD but it includes spatial information from daily GCM anomalies (Werner and Cannon, 2015). Simulated daily future precipitation datasets using BCSD and BCCAQ downscaling techniques are extracted from the PCIC database (Ahmed *et al.*, 2013).

3.3.1.2 Weather Generators

Development of future precipitation projections using a weather generator is divided into two steps: (i) scaling of future scaled climate variables and (ii) generation of synthetic future climate time series (Gaur and Simonovic, 2013). The delta change, or change factor methodology is used in this study for scaling climate variables to account for GCM simulated climate change. In the delta change method, change factors are calculated from historical and future GCM data. This change is then applied to the observed historical climate data to scale the historically observed climate variables to account for the projected changed between the historical and future GCM condition. Several types of

change factors (CF) can be applied at different temporal scales (monthly, seasonal or annual). They can use different mathematical formulations (additive or multiplicative) or can be applied based on number of change factors (single or multiple). Using only a single CF will not capture changes in event frequency calculation and antecedent conditions in the case of hydrologic modeling due to the importance of temporal sequencing of dry and wet days which remains unchanged (Anandhi *et al.*, 2011). In the present study, we used 25 evenly spaced additive CFs across the precipitation distribution for scaling the precipitation data following Anandhi *et al.*, (2011).

After scaling the climate data, weather generators (WGs) are used for generating a synthetic time series. WGs can preserve statistical characteristics of input data as well as capture temporal and spatial correlation between climate variables at multiple sites. The two different WGs: (i) K-nearest neighbor (K-nn CAD V4) and (ii) maximum entropy bootstrap (MBE), are used in this investigation.

3.3.1.2.1 KnnCAD V4

A non-parametric multisite weather generator named KnnCAD V4 (King *et al.*, 2015) based on K-nearest neighbors (K-NN) is used in this study. The KnnCAD V4 is the updated version of KnnCAD V3 (Eum *et al.*, 2010) which includes block resampling and perturbation. A detailed description of block resampling can be found in King *et al*., (2015). For perturbation the following equation is used:

$$y^{j}_{ppt,t+i} = \lambda_{ppt} x^{j}_{ppt,t+i} + \left(1-\lambda_{ppt}\right) z_{t+i} \; ; \; i = 1, 2, ...n \tag{3.13}$$

where z_{t+i} comes from two parameters log-normal distribution; $x^{j}_{ppt,t+i}$ is reshuffled non-zero precipitation value for *t+i* th day in *j*th location; $y^{j}_{ppt,t+i}$ is the perturbed precipitation value for *t+i* th day in *j*th location and t is current day. λ_{ppt} value varies in between 0 to 1 (0 means data series are totally perturbed and 1 means no perturbation in the results) (King *et al.,* 2015). This model can adequately reproduce statistical characteristic of historical climate variables as well as extrapolate historical extremes.

3.3.1.2.2 Maximum Entropy Based Weather Generator (MEBWG)

Srivastav and Simonovic (2014) developed a non-parametric multisite, multivariate maximum entropy based weather generator (MEBWG) for generating daily precipitation and minimum and maximum temperature. The three main steps involved in MBE are: (i) orthogonal transformation of daily climate variables at multiple sites to remove spatial correlation; (ii) use of maximum entropy bootstrap (MEB) to generate synthetic replicates of climate variables and (iii) inverse orthogonal transformation of synthetic climate variables to re-established spatial correlation. Principal component analysis is used for orthogonal transformation. The maximum entropy density is constructed using the following equations to satisfy ergodic theorem (mean preserving):

$$m_1 = 0.75O_1 + 0.25O_2 \tag{3.14}$$

$$m_k = 0.25O_{k-1} + 0.5O_k + 0.25O_{k+1} \; ; \forall k = 2,3,....,t-1 \tag{3.15}$$

$$m_t = 0.25O_{t-1} + 0.75O_t \tag{3.16}$$

where O_t is a rank matrix derived from first principal component and t is time step. This method can capture temporal and spatial dependency structures along with

other historical statistics (e.g. mean, standard deviation) in downscaled climate variables. The performance of MBEWG is free of modeling parameters, and it is computationally inexpensive.

3.3.1.3 Regression Based Downscaling Methods

Regression based methods are most commonly used for statistical downscaling. In this method a statistical relationship (linear or non-linear) is established between large scale climate variables simulated by GCMs (predictors) with observed local surface variable (predictand) which is then applied to future climate. For this assessment, two multivariate regression methods (based on kernel regression and beta regression) are used in this study.

3.3.1.3.1 Multivariate Kernel Regression Model

A multisite multivariate non-parametric kernel regression (KR) based statistical downscaling method was proposed by Kannan and Ghosh (2013). This model projects precipitation conditioned on precipitation states. A non-parametric regression is a smoothing technique that projects the predictand using a set of predictor variables. Multiple sites can be included by applying weights to the other neighboring region predictand of the one desired. Multivariate kernel regression is used for calculating the conditional expectation of a random variable. In this study, kernel regression is used to capture a non-linear relationship between daily precipitation and other predictor variables. The conditional expectation of the kernel regression can be expressed as follows:

$$E(Y / X) = m(X) = \frac{\int yf(y / x)}{f_x(x)} \tag{3.17}$$

where Y is the predictand; X is principal component of the predictor variable; $f(y/x)$ is conditional probability density function (pdf) of Y given X=x and $f_x(x)$ is marginal pdf of X.

The multivariate pdf in Eq. (3.17) is replaced by kernel density estimator and formulated as follows:

$$m_h(x) = \frac{\sum_{i=1}^{n} K_h(x - X_i) Y_i}{\sum_{i=1}^{n} K_h(x - X_i)} \tag{3.18}$$

where $m_h(x)$ the expected is value Y for a condition of $X_i = x$; and K_h is the kernel with bandwidth h. The method can efficiently capture extreme precipitation events as well as autocorrelations and spatial cross-correlation among downscaling sites.

The multisite multivariate downscaling method based on beta regression (discussed in Section 3.2) also used in this assessment to study uncertainty in projected precipitation. The main objective of this study is to quantify sources of uncertainty and assess which one has a major influence on precipitation projections. Daily precipitation is projected using different downscaling models (BCSD, BCCAQ, KnnCad V4, MEBWG, KR and BR) at different locations over the river basin and results are compared at different temporal and spatial scales. The details are given below.

3.3.2 Comparison and Quantification of Uncertainties

The annual average total monthly precipitation is used to compare the different sources of uncertainty amongst the selection of GCM, DSM, and RCP scenario for the near (2036-

2065) and the far future (2066-2095) time slices (Figure 3.13). Results for the three stations; JHT, SCA and WOL are shown in Figure 3.13(a-f).

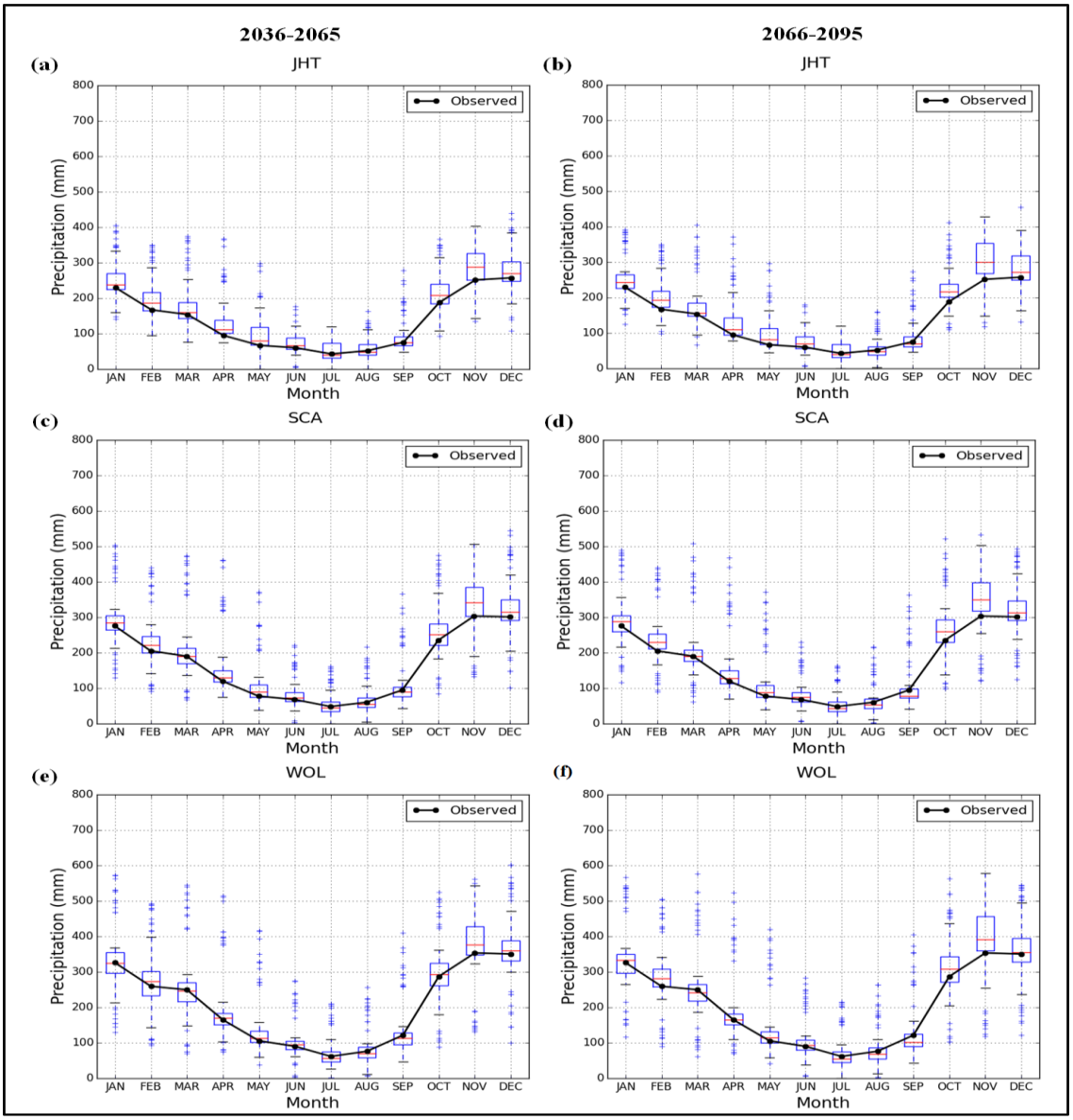

Figure 3.13 Boxplots showing projected annual average total monthly precipitation at three different stations in the Campbell River basin with historical (1976-2005) observed precipitation - comparison between two future time periods (after Mandal *et al.*, 2016b).

WOL are located upstream of the river where SCA and JHT are located downstream near Strathcona dam and John hart reservoir respectively. On the contrary, these three stations have different elevation levels (Table 3.1) which may have an influence on the result. The dark black line in this figure represents historical annual average total monthly precipitation. To calculate historical annual average total monthly precipitation, we used 30 years (1976 to 2005) of daily ANUSPLIN data. Figure 3.13 shows that the summer months (June, July and August) are typically drier in comparison to the other seasons (Fall, winter and spring) for all three stations. However, there is a potential for more extreme events in the spring (March, April and May) for all three stations. Although the median total monthly precipitation is higher for the winter months, there is still a potential for larger amounts of precipitation in the early spring, as indicated by the outliers in Figure 3.13. Figure 3.13 shows a significant variation in precipitation projections without clear identification of the sources of uncertainty.

3.3.2.1 Quantification of Uncertainty

To identify and quantify the sources of uncertainty, an uncertainty metric is calculated. This metric was chosen as it will allow for uncertainty to be disaggregated across the seasons. The uncertainty metric is used to gauge the amount of uncertainty associated with each step of the statistical downscaling process (i.e. choice of GCMs, RCP scenario and downscaling model). The calculation for each weather station and calendar month can be summarized by the following steps:

Step- I: Calculate the total monthly precipitation by summing the precipitation into monthly bins, and taking the average for each calendar month, m across all years

for the future downscaled precipitation ($F_{i,j,k,l,m}$) for each GCM (i), DSM (j) , RCP scenario (k), and weather station (l).

Step-II: Follow the same procedure as described in previous step for observed historical precipitation to calculate monthly total historical precipitation ($H_{l,m}$) where m is month and l is weather station

Step-III: Take the ratio of the future downscaling to observed total monthly precipitation values

$$A_{i,j,k,l,m} = \frac{F_{i,j,k,l,m}}{H_{l,m}} \qquad \begin{matrix} \forall i = 1,2..,4;\ j = 1,2..,6;\ k = 1,2,3 \\ \forall l = 1,2...10;\ m = 1,2...12 \end{matrix} \tag{3.19}$$

Step-IV: Calculate the range across the dimensions representing a selection step in the downscaling process:

$$GCM_{uncertainty} = \max\left(A_{i,j,k,l,m}\right)_i - \min\left(A_{i,j,k,l,m}\right)_i \tag{3.20}$$

$$DSM_{uncertainty} = \max\left(A_{i,j,k,l,m}\right)_j - \min\left(A_{i,j,k,l,m}\right)_j \tag{3.21}$$

$$RCP_{uncertainty} = \max\left(A_{i,j,k,l,m}\right)_k - \min\left(A_{i,j,k,l,m}\right)_k \tag{3.22}$$

The resulting ranges in total monthly precipitation represent the uncertainty in results associated with the downscaling process due to the choice of a particular GCM, DSM, or RCP scenario. This method uses the range in total monthly precipitation as a metric for the amount of uncertainty and does not consider the distribution of total monthly precipitation attributed to the selection made in a level of the downscaling process.

In Figure 3.14 uncertainty is aggregated for each step of the downscaling process for each month in different future time periods. It can be observed that uncertainty in precipitation projections can mainly be attributed to the choice of DSMs compared to GCMs and RCPs throughout the year. A larger amount of uncertainty has been found in the late spring (May) and summer months (June, July and August) using different DSMs. Further disaggregation can show the level of uncertainty associated with a single choice of GCMs and DSMs for different RCPs and future time periods (Figure 3.15). From this, it is shown that the two regression based statistical downscaling methods (KR and BR) are attributed a larger portion of uncertainty in precipitation projections than the other methods. KR and BR model used six predictor climate variables which may influence the uncertain precipitation projection.

The combined spatial and seasonal variations of uncertainty in the precipitation projections across the ten stations in the river basin are analyzed (Figure 3.16 - Figure 3.18). GCMs were shown to be associated with larger amounts of uncertainty in summer precipitation for both time periods (Figure 3.16 (e-f)) along with spring precipitation for the near future (Figure 3.16 (c)). The choice of RCP was only associated with a small amount of uncertainty in the far future (2066 to 2095) summer months (Figure 3.17(f)).

Another important observation is that the uncertainty in downstream precipitation is higher than that of the stations upstream except for the winter period (Figure 3.16). This may be caused because of basin topography because stations located in the upstream have higher elevation compare to downstream stations and three reservoirs (Strathcona, Ladore and John Hart) are located in the downstream of the Campbell River. Compared to GCMs

and RCPs, the choice of DSM shows maximum uncertainty in precipitation projections across all seasons in the basin (Figure 3.18**)**.

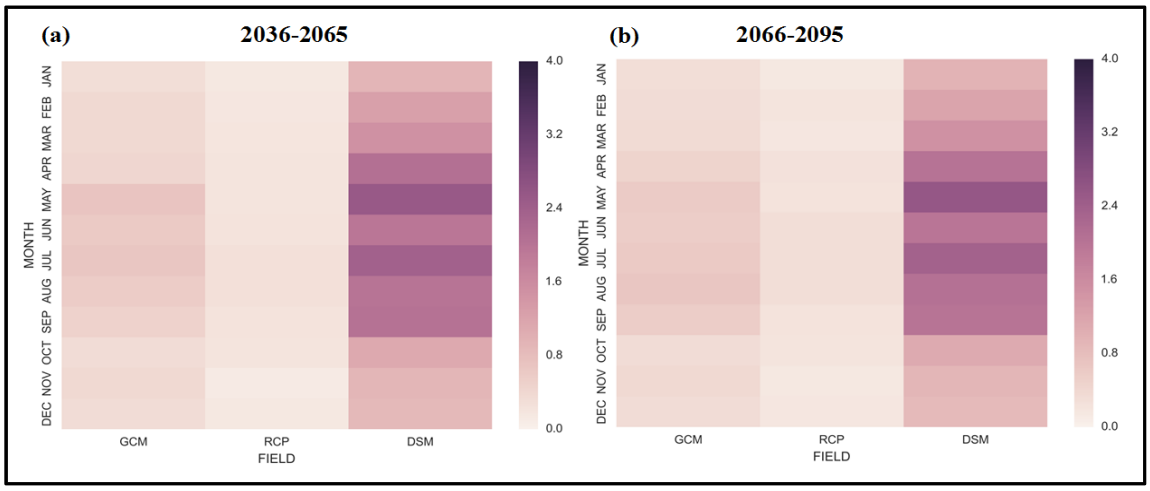

Figure 3.14 Heat maps showing comparison of different sources of uncertainty metrics for two future time periods (after Mandal *et al.*, 2016b).

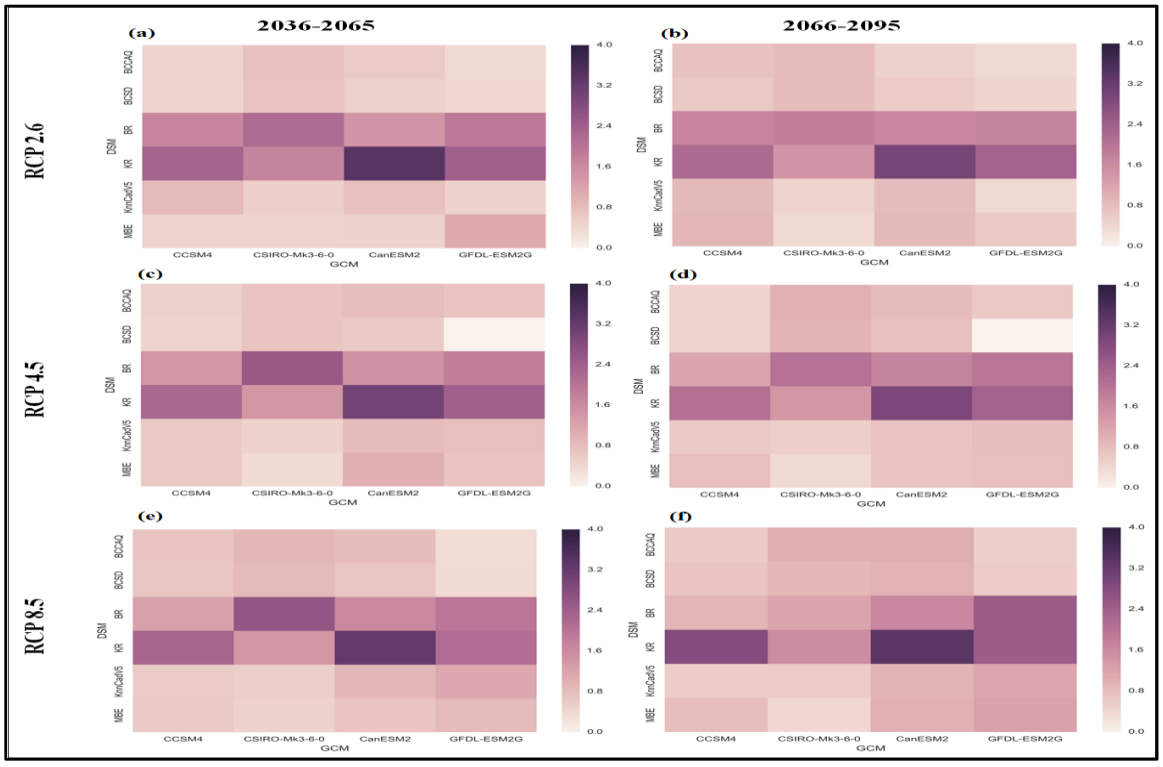

Figure 3.15 Heat maps showing GCMs and DSMs uncertainty metrics for different emission scenarios - comparison between two future time periods (after Mandal *et al.*, 2016b).

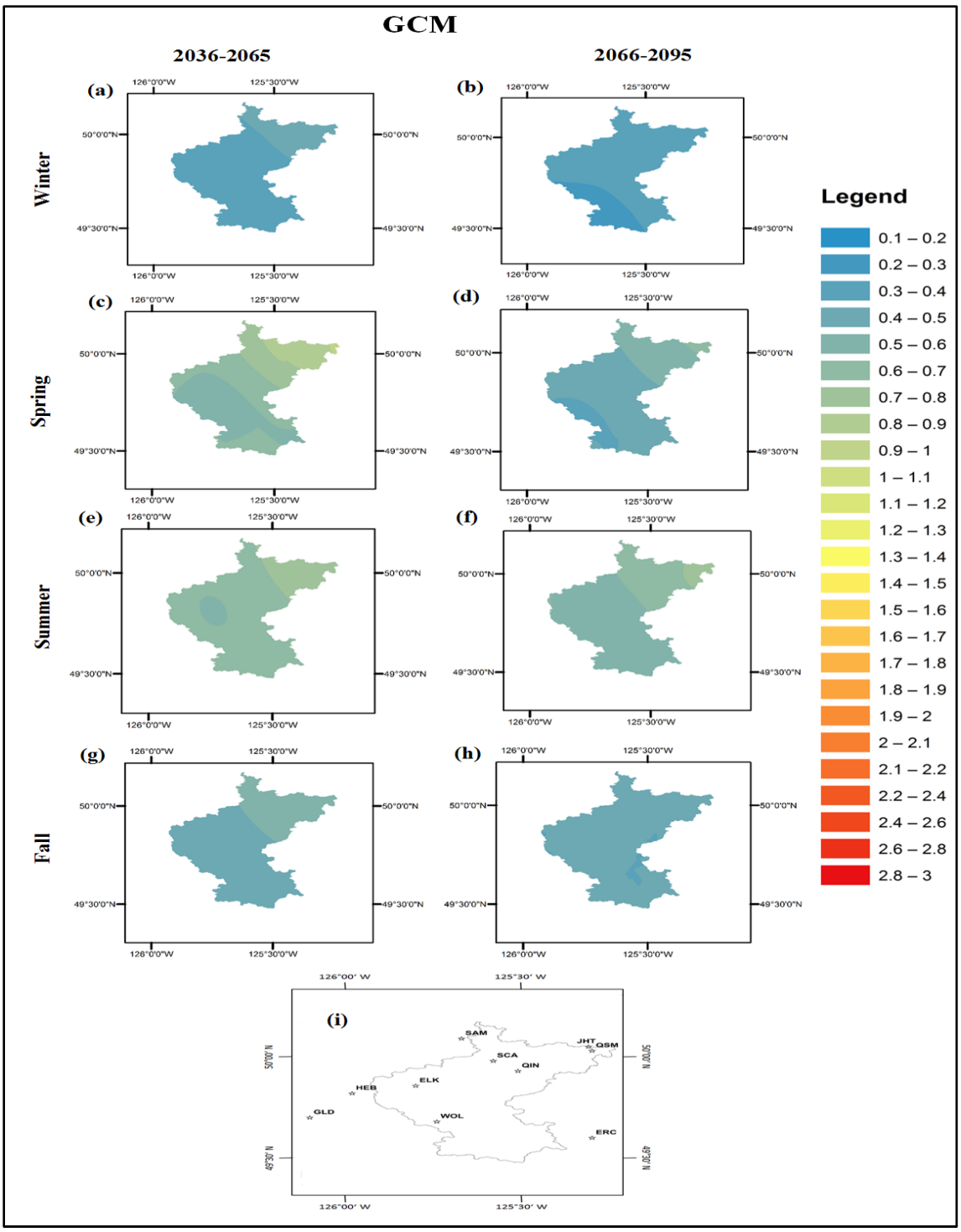

Figure 3.16 Seasonal variation of GCMs uncertainty metric in the Campbell River basin for two future time periods (a-h). (i) Location of the downscaling stations (after Mandal *et al.*, 2016b).

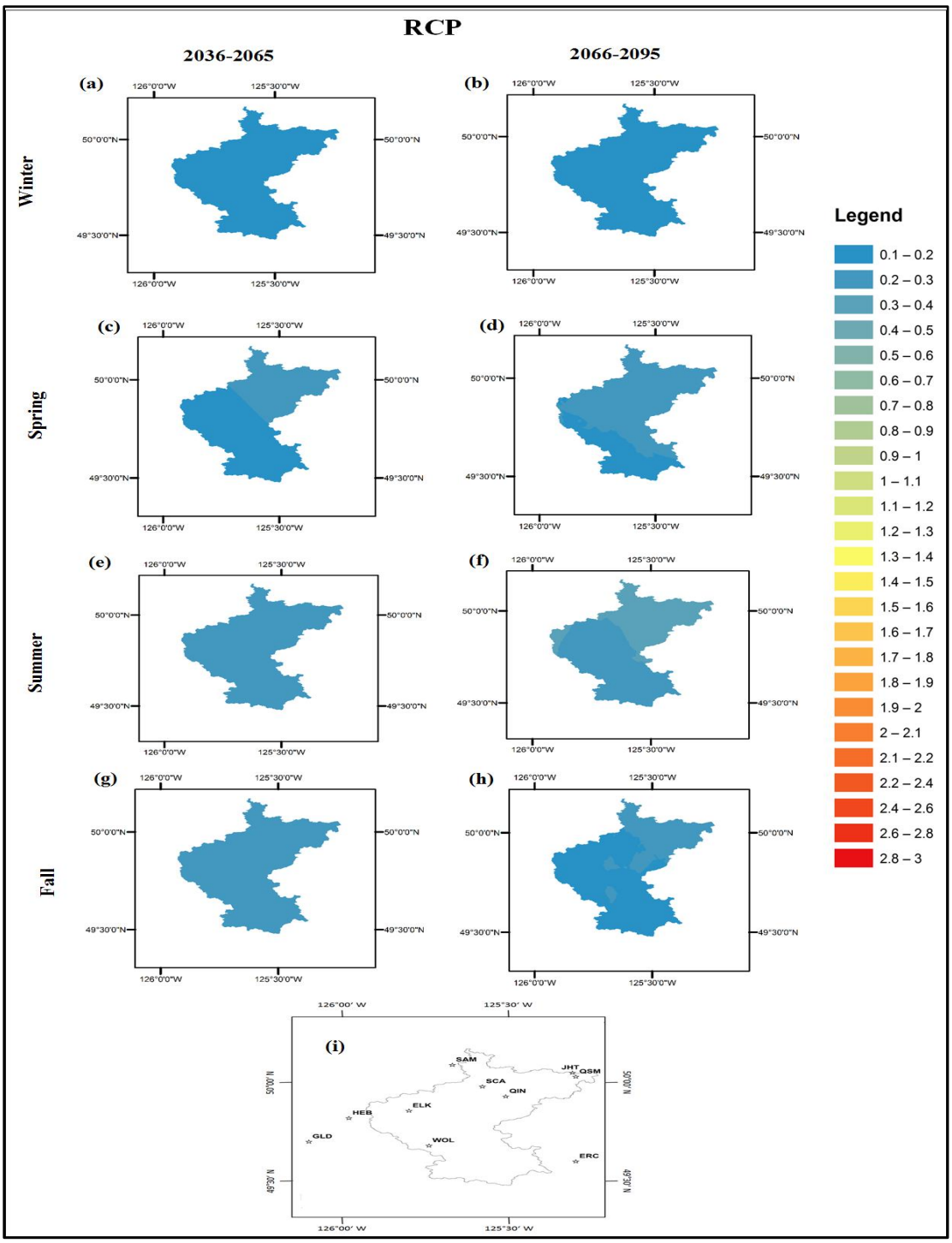

Figure 3.17 Seasonal variation of RCPs uncertainty metric in the Campbell River basin for two future time periods (a-h). (i) Location of the downscaling stations (after Mandal *et al.*, 2016b).

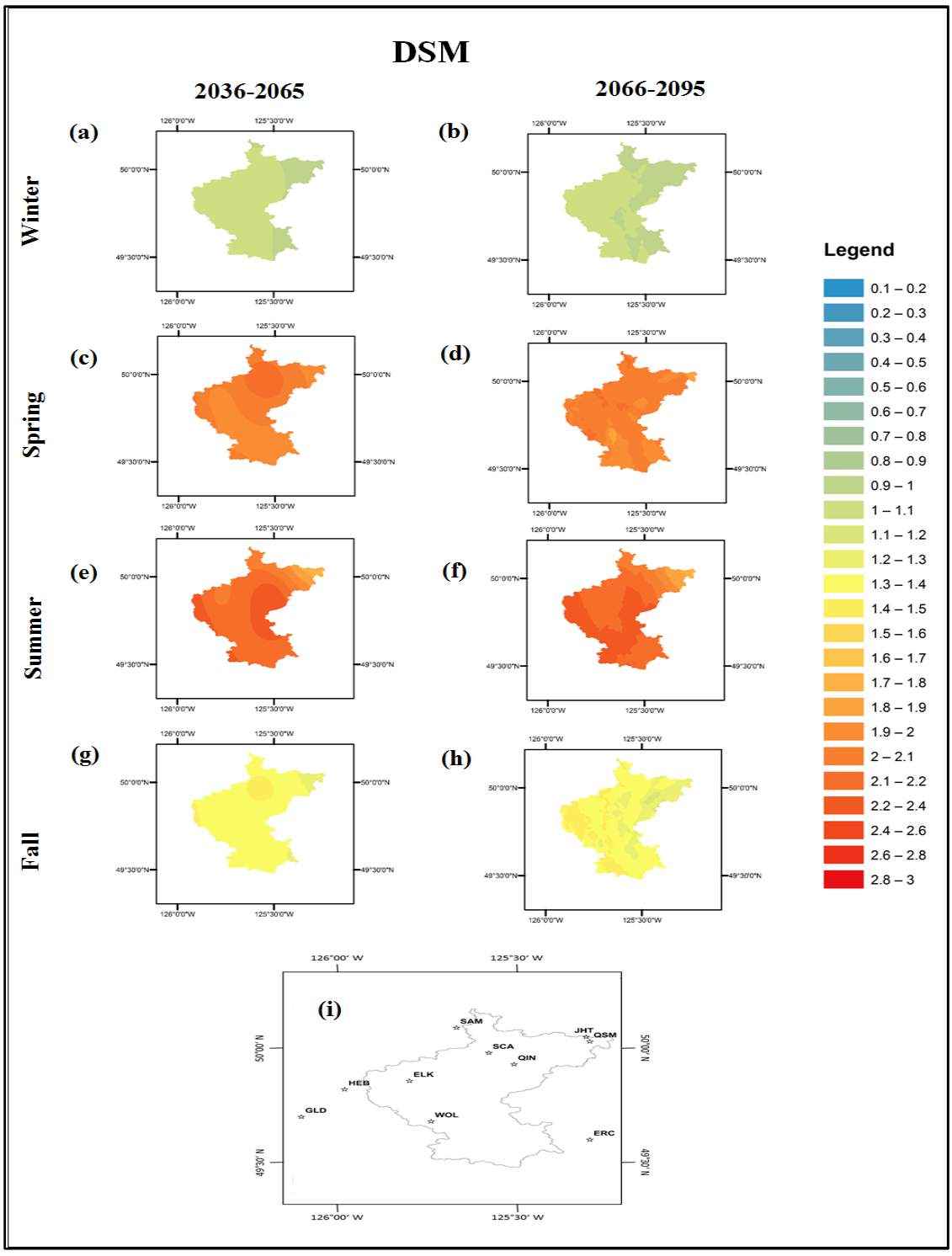

Figure 3.18 Seasonal variation of DSMs uncertainty metric in the Campbell River basin for two future time periods (a-h). (i) Location of the downscaling stations (after Mandal *et al.*, 2016b).

3.4 Summary

In this chapter, a new multisite statistical downscaling model is proposed for generating precipitation for a river basin using large scale climate variables conditioned to daily rainfall states. The proposed downscaling approach can reproduce the spatiotemporal structure of the historical data at daily time scale, in addition to other statistics (i.e. mean and standard deviation). The proposed downscaling method involves two main steps: (1) rainfall state generation using CART; and (2) generation of multisite precipitation amounts using multivariate BR model. To capture multicollinearity and reduce dimensionality we combine principal components analysis (PCA) with the BR. First, five principal components are selected for this study which explains 97% variability of the original data.

CART constructs a classification tree based on the categorical and continuous predictors to generate precipitation state of the river basin. Lag-1 precipitation is used to prune the classification tree. The multisite precipitation sequences in the Campbell River basin are generated using beta regression conditioned to precipitation states in the river basin. As BR model estimates mean precipitation values, perturbation method is added to the model for stochastic generation of precipitation outside the observed range following King *et al.*,(2015). The model performs well in terms of preserving temporal and spatial dependence. However, BR overestimates spatial interstation cross-correlation.

Since there is no clear guidance for determining the optimal number of principal components, we considered a number of components which represent a large fraction of the variability (here 97%) contained in the original data. However, with the availability of large data set obtained from the GCM simulated climate variables we may follow the step

wise procedure described by Srivastav and Simonovic (2014). BR method is a data driven method which builds a relationship between climate variables and daily precipitation. It is considered a stationary relationship among predictand and predictors variable (precipitation) which may not always be true. The basic relationships between climate variables controlled by conservation laws are not going to alter because of climate change. However, if the downscaling model is calibrated under stationary conditions and regional warming (e.g. El Nino-Southern Oscillation) influences the convective precipitation fraction then the stationary relationship in the downscaling process may indeed change. Salvi *et al.,* (2013) observed that the kernel regression (KR) based statistical downscaling model failed to capture the changes in mean precipitation under non-stationary climate. They also identified that the assumption of stationarity was violated during the model testing period. It may be the reason for the changes in climate pattern occurring at large-scale or interference by some local factors e.g. urbanization. The urban areas have different climatology (Kishtawal *et al.*, 2010; Shastri *et al.*, 2015) and the effect of urbanization is not included in the BR model. Therefore the same outcomes might be possible from BR if we test the BR model under non-stationary condition. Hence, identifying the exact reason of non-stationary behavior and validating the proposed model under non-stationary climate condition may be considered as a future scope of the present work.

Another important factor is the link function in the beta regression model. Several link functions are available such as logit, probit and log–log link. In this study, we used only logit link function. Different outcomes may be expected if other link functions are used. In the present study, we used only one GCM output for downscaling. Future precipitation

estimation may be different for the use of other GCMs. Uncertainty modeling of downscaled precipitation from different GCMs is a potential research area under consideration.

The main advantage of using BR based downscaling model is multisite rainfall sequence generation which captures the temporal and spatial variability of the predictand at each downscaled location which makes this model reliable and robust. The proposed model is computationally inexpensive and ideal for practical engineering application. It can use any number of predictor variables which may be considered the scope of future work and it makes this model efficient.

Further, different sources of uncertainty in the projection of total monthly precipitation were assessed and compared for two future time periods in the Campbell River basin. Previous studies found that the choice of GCM is the largest source of uncertainty in the downscaling process (Minville *et al.*, 2008; Prudhomme and Davies, 2008a). However, this study concludes that the choice of DSMs dominates other sources of uncertainty, particularly in the case of the regression based models. Downscaling methods used in this study have significant difference in formulation. Every statistical downscaling model is subject to constraints imposed by different sets of predictor variables, and they all assume a stationary relationship between predictor and predictand. This can be the reason why DSMs show the largest source of uncertainty.

Uncertainty metric for different sources of uncertainty is very simple to calculate, and it is computationally inexpensive. It can be used at any temporal and spatial scale. This study represents the analyses on a regional scale, however if applied to continental or

global scales the spatial component of uncertainty in downscaled precipitation projections can be studied more in depth. The following chapter discusses future streamflow variation under changing climate condition.

Chapter 4

4 Assessment of Future Streamflow under Changing Climate Conditions

Based on: Sohom Mandal and Slobodan Simonovic (2017), “Assessment of future streamflow under changing climate condition: comparison of various sources of uncertainty”. Hydrological Processes Journal. DOI: 10.1002/hyp.11174 (In press).

Impacts of climate change possess a significant threat to the water resources for all continents in the world. Changing climate will magnify the existing risks and increase the future risks associated with management of water resources systems. The frequency and magnitude of streamflow are affected by climate change, and there is a clear indication that changes in streamflow will continue in the future because of continuous increase in the concentration of greenhouse gasses in the atmosphere (IPCC, 2013). The streamflow variation is not uniform across the world, but it is hydrologic regime specific. For example, a decreasing trend in maximum flows is identified for the maritime provinces of Canada (east coast) and the St Lawrence River basin (Leclerc and Ouarda, 2007) in the last two decades. On the contrary, in the northwest and west parts of Canada, an increasing trend in minimum annual flow has been observed for the period of 1970-2005 (Warren and Lemmen, 2014). Variation in magnitude and frequency of streamflow increases the vulnerability of the water infrastructure. According to the Public Infrastructure Engineering Vulnerability Committee of Engineers Canada (Canadian Council of Professional Engineers, 2008), failure of water resource’s infrastructures due to extreme hydrological events (droughts and floods) will increase across Canada due to

climate change. A study by the Canadian Institute of Actuaries (2014) found that water-related insured damage and losses could increase by about 20% to 30% in the next few decades across Canada. Simonovic (2008) also suggested that water resource infrastructure planning, design, and operations should be revised to accommodate the expected changes in magnitude and frequency of streamflows.

According to Prudhomme and Davies (2008), selection of GCMs creates more uncertainty in the downscaling process compared to the choice of emission scenarios or model parameterization. However, its also found that downscaling methods might be a significant source of uncertainty in hydrologic projections compared to the choice of climate models and emission scenarios that are a much less significant source of uncertainty (Bürger *et al.*, 2012). Most past studies investigated only changes in climatic variables e.g. temperature or precipitation. Najafi *et al.*, (2011) conducted a study to compare uncertainties in predicted future flow stemming from different GCMs, emission scenarios, and hydrological models. They considered eight GCMs, two emission scenarios from CMIP3 (Coupled Model Intercomparison Project 3) and four hydrologic models. The Tualatin River basin, Oregan, USA was used as a study area. The study concludes that uncertainty in streamflow due to the GCMs structure is higher than the uncertainty due to the choice of the hydrologic model. However, Najafi *et al.*, (2011) also suggested that hydrologic model selection is important when assessing hydrologic impacts under changing climate condition. The structural difference in hydrological models and uncertainties in parameter estimation can affect the spatial and temporal distribution of runoff. Reccntly, Surfleet and Tullos (2012) have conducted another study to explore uncertainties in predicted hydrologic response due to the choices of GCMs and

a hydrological model. They selected the Santiam River basin in Oregon, USA for case study purpose and found that GCM structure and parameterization contribute more to the uncertainties in predicted flow, compared to the contribution of hydrologic models. However, limited literature is available, which investigates all sources of uncertainty in streamflow projections under climate change. Schnorbus et al.,(2011) assessed the hydrologic impacts of climate change in three different watersheds (Peace, Campbell and Columbia River) of British Columbia (BC), Canada. This investigation is conducted using a suite of eight Global Climate Models (GCMs) with three emission scenarios. Climate variables from GCMs were downscaled using Bias Corrected Spatial Disaggregation (BCSD) method. This assessment concludes that GCMs are indeed a significant source of uncertainty when only a single downscaling model is used. Another study has been conducted by Das and Simonovic (2012) to assess uncertainty due to climate change in extreme flood flows for the Upper Thames River Basin, Ontario, Canada. In this study, three carbon emission scenarios and six GCMs with a single weather generator based on the K-Nearest Neighbour (K-NN) used for downscaling the climate variables. This study also found that different GCMs introduce more uncertainty compared to others sources. Dibike and Coulibaly (2005) assessed impacts of climate change on streamflow in the Saguenay watershed, Quebec, Canada. They used two downscaling models and two hydrological models for this study. The results of their work show that the variation in river flow due to the choice of downscaling model is more significant than the variation introduced by choice of hydrological model. However, they did not consider variation due to the choice of emission scenario and/or GCMs.

Previously, most of the climate change assessment studies conducted in Canada were based on a single downscaling method except Dibike and Coulibaly (2005) who compared two downscaling tools and two hydrologic models. The main objective of this chapter is to characterize the primary sources of uncertainty in simulated streamflow under changing climate conditions. The case study area is Campbell River basin, BC, Canada. The Campbell River is a coastal watershed in the central part of Vancouver Island. It consists of three reservoirs: Upper Campbell, Lower Campbell, and John Hart. From this river catchment, 1,230 GWh (gigawatt hours) of electricity is generated, which is equal to 11% of Vancouver Island's annual energy demand (BC Hydro Generation Resource Management, 2012). Hence the variation in inflow into Campbell River reservoirs may have very significant economic and environmental consequences.

Total drainage area of this watershed is approximately 1,856 km^2 (BC Hydro Generation Resource Management, 2012). Annual average precipitation during the last 20 years (1994 to 2013) in the catchment is 2,960 mm. The magnitude of precipitation is high in the upstream section of the basin compared to downstream (Figure 4.1b). As the river originates from the west-facing mountains, orographic lifting of warm moist air from the Pacific Ocean causes heavy precipitation in the upstream part of the basin. Campbell River includes three dams, Strathcona, Ladore and John Hart (Figure 4.1a). Strathcona dam is located in the upstream section of the river, where other two are in the downstream section. Three reservoirs created by the dams are Upper Campbell Lake reservoir, Lower Campbell Lake reservoir and John Hart Lake reservoir. The UBCWM hydrologic model used in this study simulates inflow into the Upper Campbell Lake reservoir, and the inflow into other two reservoirs is regulated by release from the

Strathcona dam. The focus of this chapter is to assess the inflow variations into the Strathcona dam due to climate change. UBCWM is calibrated for the area upstream of Strathcona dam (1,176 km^2) excluding the Heber and Crest Diversions.

The detailed objectives of this study include quantification of the magnitude and frequency of streamflow in Campbell River basin considering three main sources of uncertainty introduced by the selection of downscaling methods, GCMs, and GHGs (greenhouse gasses) emission scenarios. Four GCMs, three emission scenarios, and six downscaling models are used for this purpose. The UBC Watershed model (UBCWM) (Quick and Pipes, 1977) is used for hydrologic flow simulation.

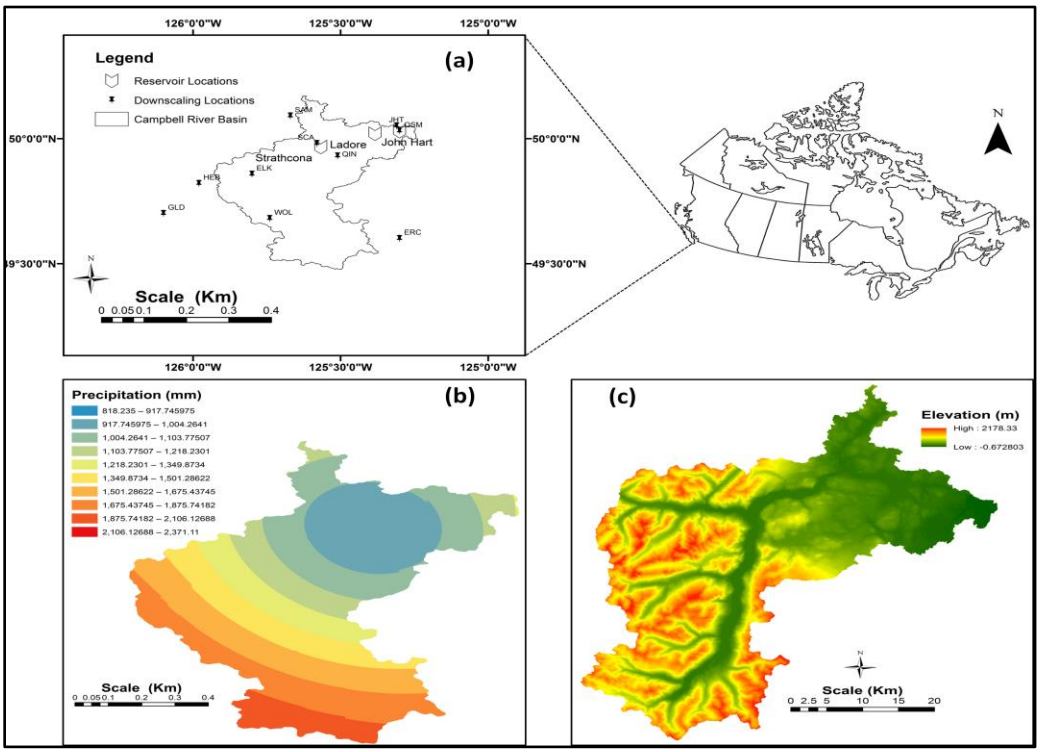

Figure 4.1 (a) Campbell River basin, British Columbia, Canada, with different downscaling locations and reservoirs location; (b) Spatial representation of annual average precipitation (1994-2013); (c) Digital elevation model (DEM) of the Campbell River basin (after Mandal and Simonovic, 2017).

Daily time series of climate variables (e.g. precipitation (Pr), maximum temperature (Tmax) and minimum temperature (Tmin)) are required for simulating flow using UBCWM. For two of downscaling methods, BCSD (bias-corrected spatial disaggregation) and BCCAQ (bias correction constructed analogues with quantile mapping reordering), climate variables (Pr, Tmax, and Tmin) are extracted from the Pacific Climate Impacts Consortium (PCIC) database (Pacific Climate Impacts Consortium, 2014). For K-NN CAD v4 (K-nearest neighbor weather generator) and MEB (maximum entropy bootstrap weather generator), climate variables (Pr, Tmax, and Tmin) are obtained from CMIP5 database (IPCC, 2013). In addition to these variables, mean sea level pressure (mslp), specific humidity (hus) at 500 hPa, zonal (u-wind) and meridional (v-wind) wind are extracted from the CMIP5 repository for BR (beta regression) and KR (kernel regression) downscaling method. All the climate variables extracted for the corresponding GCMs shown in Table 3.11. For the hydrologic model validation, historical daily inflow data (1984 to 2013) for the Strathcona dam has been obtained from the BC Hydro repository. The following sub-section provides details about hydrological model (UBCWM) structure and its validation.

4.1 UBC Watershed Model

In this study, the UBCWM is used to simulate streamflow in the Campbell River basin. This is a continuous hydrological model and only need precipitation, maximum and minimum temperature to simulate flow. As the UBCWM was designed from minimum meteorological parameters, it is very useful in the mountainous watershed e.g. Campbell River watershed where meteorological and flows data are often spare (Micovic and Quick, 2009). Since the hydrologic response of a mountainous watershed depends on

elevation, UBCWM adapted the "area-elevation band" concept. This concept includes orographic gradients of temperature and precipitation which are assumed as dominate gradients of hydrological behavior in the mountainous catchment and act similarly for each storm. The UBCWM not only estimates streamflow in a catchment but also provides information about groundwater storage, soil moisture, surface and sub-surface components of runoff, energy available for snowmelt, snowpack water equivalent, the area of the snow cover, evapotranspiration and interception losses (Quick and Pipes, 1977). The UBCWM integrates multiple meteorological sub-models as described in (Micovic and Quick, 1999). A schematic of UBC watershed model is given in Figure 4.2.

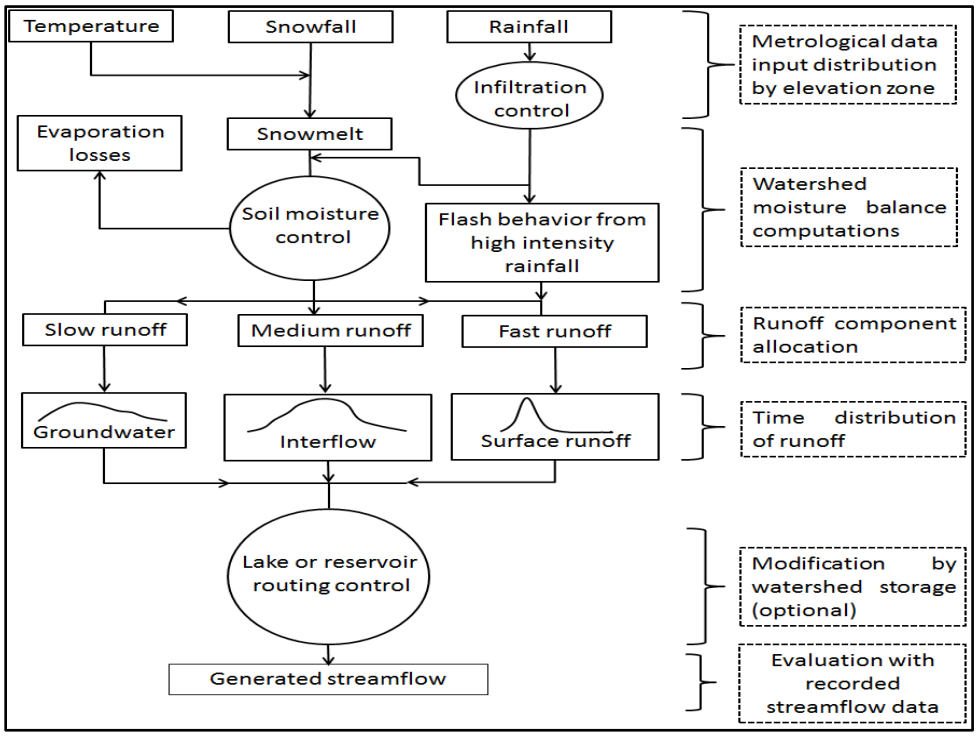

Figure 4.2 Generalized flow chart of UBC watershed model (after Quick and Pipes, 1977)

The hydrologic model UBCWM is calibrated by British Columbia Hydro (BC Hydro) for Campbell River system and used in this study. UBCWM is available as a hydrological modeling framework under the name "Raven"(Craig and Snowdon, 2010). Raven considers a catchment as the integration of multiple subbasins where a number of non-contiguous and contiguous hydrological response units (HRUs) are assembled. Each HRU setup is based on a single combination of vegetation cover, terrain type and land use/land type (LU/LT). Also, each HRU has a defined soil profile and stratified aquifer. Raven has a large number of user-customized subroutines which can be used to develop a number of existing hydrologic models. UBCWM is emulated successfully in Raven by BC Hydro. Details about RAVEN are presented in Appendix – B.

4.1.1 Validation of UBC Watershed Model

For this assessment purpose, the model is validated using observed data. Due to an inadequate amount of historical observed climate data, daily precipitation (Pr), maximum and minimum temperature (Tmax and Tmin) have been extracted from ANUSPLIN data set (0.1º latitude x 0.1º longitude), Environment Canada (Hutchinson and Xu, 2013). These data sets are extracted for a 20-year time period (1984 to 2013). ANUSPLIN data set is generated using "thin-plate smoothing spline" algorithm and broadly used in climate studies (Irwin *et al.*, 2016; Mandal *et al.*, 2016c). As the ANUSPLIN data set has a different spatial resolution from GCMs, all the variables are spatially interpolated using IDW to downscaling locations (Table 3.1) and used as input to the UBCWM. Multiple statistical indices, Nash–Sutcliffe Efficiency (*NSE*) index, Pearson correlation coefficient (R^2), Root Mean square error (*RSME*), and relative bias are used to compare UBCWM simulated flow with the observed historical flow (1984 to 2013) (Table 4.1) at different

temporal scales. Nash–Sutcliffe Efficiency (*NSE*) index is a goodness-of-fit index which is used to compare model simulated data with observed data. NSE is calculated as:

$$NSE = 1 - \frac{\sum_{t=1}^{T}(Q_m^t - Q_o^t)^2}{\sum_{t=1}^{T}(Q_0^t - \overline{Q}_o)^2} \tag{4.1}$$

where Q_o^t is observed flow at time t, Q_m is model simulated flow and $\overline{Q_o}$ mean observed flow. For accurate model prediction which means simulated flow (Q_m^t) value is equal to observed flow (Q_o^t), NSE will be 0. However, in this study, the value of NSE is high for all four temporal scales.

Table 4.1 Hydrological model performance statistics (1984-2013) in the Campbell River basin, British Columbia, Canada (after Mandal and Simonovic, 2017).

Time period	Nash–Sutcliffe Efficiency (*NSE*)	Pearson correlation coefficient (R^2)	Root mean square error (RSME in mm)	Relative bias (% *Bias*)
Total Daily flow	0.35	0.83	46.78	-13.69
Total Monthly flow	0.39	0.88	296.33	-13.72
Total Quarterly flow	0.36	0.89	563.20	-13.72
Total Annual flow	0.60	0.85	6540.60	-11.32

For total annual flow, the NSE reaches 0.6, which is not acceptable. Dimensionless statistical index e.g. R^2 plays an important role in the assessment of both, the hydrologic and statistical significance during a hydrologic model validation (McCuen, 2016). For example, if R^2 between predicted and measured values is high, that means the model outputs have quite similar pattern with measured values. R^2 varies between 0 to 1. High R^2 indicates a good correlation between observed and simulated data, which is desired. The results are showing R^2 values between 0.83 to 0.89 for different temporal scales. These values can be improved. RSME is a dimensioned statistical index, and low RSME is desired in hydrologic model validation. However, the results obtained in this study show a very high value of RSME, 6540.6 for total annual flow, which is not acceptable. Relative bias is used for comparing different data sets. Relative bias lower than 5% is usually recommended as the threshold value in hydrologic model validation (McCuen, 2016). However, the results obtained in the present study show relative bias higher than 5%, which is again not satisfactory. Figure 4.3 (a-d) presents time series comparison of simulated and observed flow at different temporal scales (daily, monthly, quarterly and yearly). It shows that the UBCWM often fails to capture the extreme flow events. Figure 4.3 (e-g), represents the Q-Q plot between model generated and historical daily, monthly and quarterly flows, respectively. The Q-Q plots also show that for higher quantiles, simulated flow is not matching the observed data. However, if we review Figure 4.3(d) after 2010, the simulated streamflow matches with observed streamflow very well. BC Hydro (BC Hydro Generation Resource Management, 2012) reported that the Herber dam used to release water into the Campbell River system until 2012 when it was decommissioned. The Herber River is located approximately 70 km west of the City of

Campbell river. It naturally flows southwest for approximately 14 km before joining the Elk river which later joins Strathcona reservoir. During this 14 km stretch, the Herber river connects Crest lake, Mud lake, Upper and Lower Drum lakes before joining the Elk river. The Herber river connects with Crest lake through a wood stave and diverts water, when available. The Herber diversion used to divert on average 1.1 m^3/s into Elk river where annual mean inflow to Strathcona reservoir is 77.5 m^3/s. Although the diverted flow from Herber diversion is much smaller than the inflow into Strathcona reservoir, the total annual amount of 35 Mm^3/year represents a significant contribution to the Strathcona reservoir volume. The Herber diversion has been decommissioned in 2010 (BC Hydro Generation Resource Management, 2012).

The hydrologic model (UBCWM) was calibrated in 2014 by BC Hydro. Therefore UBCWM does not consider additional flow from the Herber dam before 2010 and that is the possible explanation for unsatisfactory validation results. For further investigation, the new validation period has been selected, 2012-2013, for daily and monthly streamflow analyses. For yearly flow validation, we considered a three-year time span (2010 to 2013). The validation results for a new period are shown in Table 4.2. Due to inadequate data set after 2013, we selected three years (2010-2013) for new validation period. There are studies (Refsgaard, 1997; Asokan and Dutta, 2008) conducted in the past using less than five years of data for hydrological model validation. For the new validation period (2010 to 2013), the NSE value is improved compared to the validation using 1984-2013 period. The NSE value for total annual flow is 0.08. An improvement is also observed for other three indexes. Relative bias is lower than 5% for all four temporal scales.

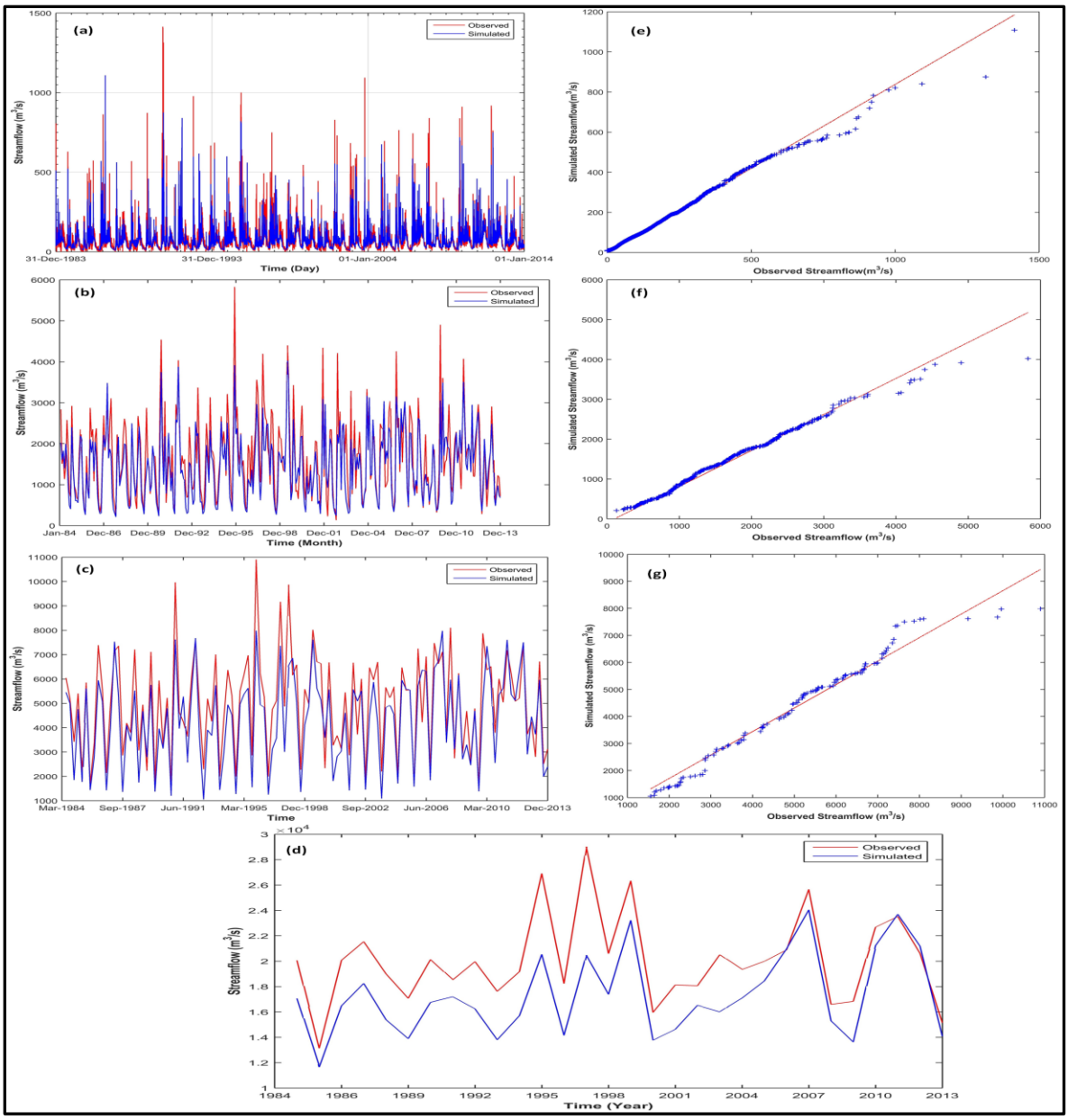

Figure 4.3 (a-d): Daily, Monthly, Quarterly and Yearly simulated and observed total inflow into the Strathcona reservoir, British Columbia, Canada respectively (1984 - 2013); (e-g): Daily, Monthly and Quarterly Q-Q plot of simulated and observed total inflow into the Strathcona reservoir (1984 - 2013) respectively (after Mandal and Simonovic, 2017).

Table 4.2 Hydrological model performance statistics for (2012-2013) in the Campbell River basin, British Columbia, Canada (after Mandal and Simonovic, 2017).

Period	Nash–Sutcliffe Efficiency (*NSE*)	Pearson correlation coefficient (R^2)	Root mean square error (RSME)	Relative bias (%*Bias*)
Total Daily flow	0.27	0.87	30.61	-2.28
Total Monthly flow	0.18	0.91	210.67	-1.40
Total Quarterly flow	0.15	0.92	421.56	-1.40
Total Annual flow (2010-2013)	0.08	0.97	952.51	-2.16

Simulated daily, monthly, quarterly and yearly streamflow for new validation period are shown in Figure 4.4 (a-d), respectively. These plots confirm that the UBCWM generated flow is quite similar to the observed flow. Figure 4.4 (f) shows a Q-Q plot between model generated and historical flows. It also certifies that the UBCWM model generated streamflow matches historical flow. Therefore, from the validation analyses, it can be concluded that the UBCWM performs well in capturing historical flow.

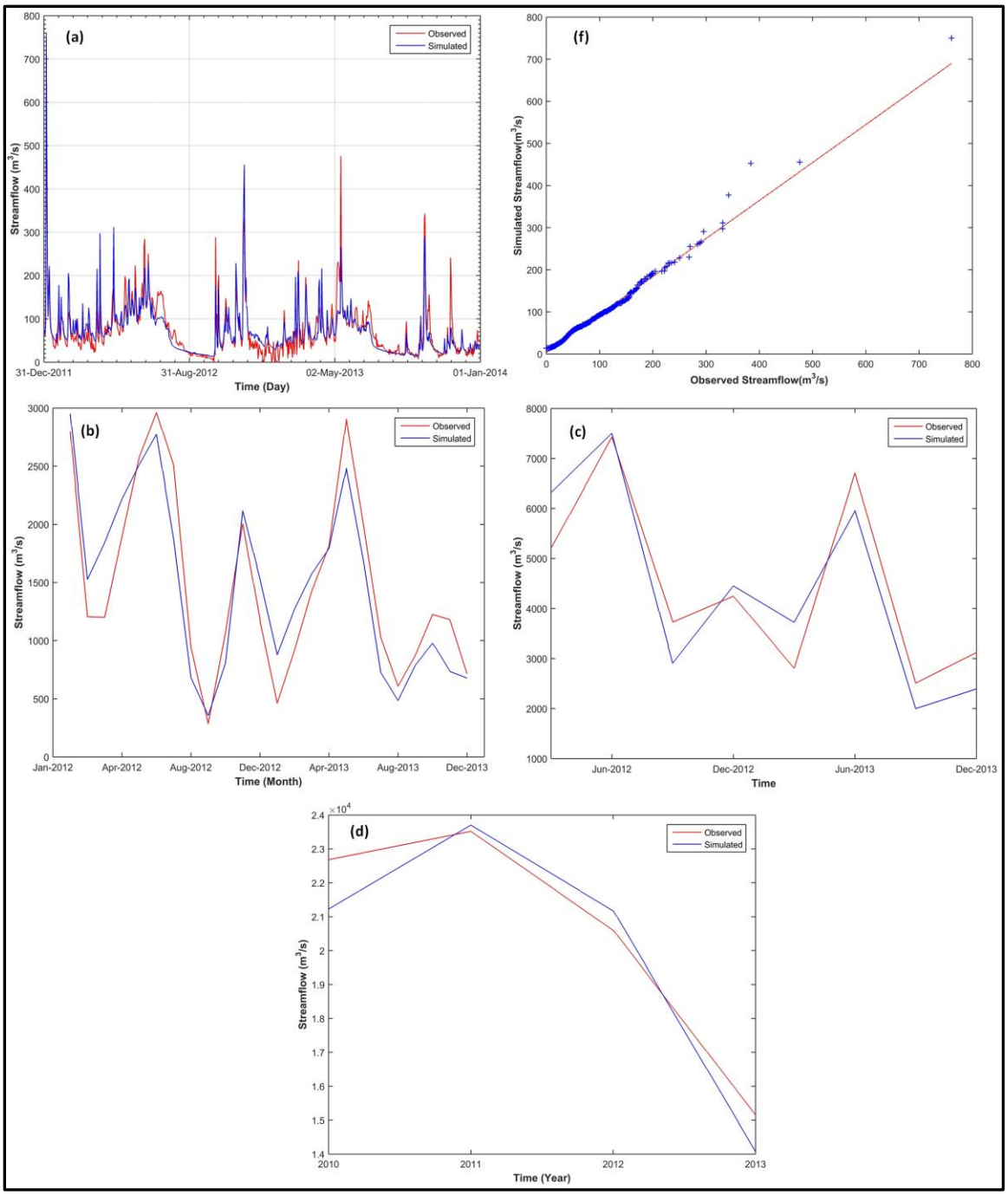

Figure 4.4 (a-d): Daily (2012-2013), Monthly (2012-2013), Quarterly (2012-2013) and Yearly (2010-2013) simulated and observed total inflow of the Strathcona reservoir respectively; (f) Daily Q-Q plot of simulated and observed total inflow of the Strathcona reservoir (2012-2013) (after Mandal and Simonovic, 2017).

4.2 Streamflow Projection using UBCWM

In this section details regarding streamflow projection using UBC watershed model are discussed.

4.2.1 Uncertainty in the Streamflow Predictions

Downscaled climate variables (Pr, Tmax and Tmin) are used with the hydrologic model for future flow generation. The simulated flow is generated and analyzed for two future time periods (2036-2065 and 2066-2095). Figure 4.5 - Figure 4.7 present cumulative distribution function (CDF) of simulated flow for different emission scenarios, GCMs and DSMs respectively. The CDF is a useful tool for assessing the intensity of the occurrence of high/low flow in the catchment. It has found that CDFs obtained from different emission scenarios are quite similar (Figure 4.5). A similar pattern can be found in Figure 4.6 and Figure 4.7. However, RCP 4.5 and RCP 8.5 show the high intensity of flow compared to historical flow in the near future (2036-2065) (Figure 4.5 c and e). In far future (2066-2095) a high-intensity flow is found for RCP 2.6 and RCP 8.5 (Figure 4.5 b and f). Another observation is that flow intensity in higher quantiles is subject to higher uncertainty for different RCPs and GCMs (Figure 4.5 and Figure 4.6). However, Figure 4.7 shows that in higher quantile CDFs are less flattered compare to Figure 4.5 and Figure 4.6. Results in Figure 4.5 and 4.6 are generated for fixed choice of DSMs (BCSD, BCAAQ, BR, KR, K-NN CAD v4 and MEB), wherein Figure 4.7, the resulting CDFs are obtained for different DSMs. Different DSMs are developed using different statistical methods and assumption and therefore the downscaled values may show variation in flow intensity. For further investigation, comparison of a single combination of RCP, GCM and DSM is included in Figure 4.8. Results in Figure 4.8 confirm that

variations in streamflow due to the choice of DSMs are higher compared to the variations due to the selection of RCPs or GCMs.

Table 4.3 Historical (1984-2013) and future mean seasonal flows (m^3/s) (5^{th}, median - 50^{th}, and 95^{th} percentile estimates) for different emission scenarios in Upper Campbell Lake reservoir, British Columbia, Canada (after Mandal and Simonovic, 2017).

		2036-2065				2066-2095			
	Historical	5^{th}	50^{th}	95^{th}	Change in median value (%)	5^{th}	50^{th}	95^{th}	Change in median value (%)
					RCP 2.6				
Winter	7602	4553	8591	15397	13	4586	8744	15233	15
Spring	7763	4202	6772	16726	-12	4115	6750	16459	-13
Summer	6661	1726	3254	7282	-51	1518	3393	6650	-49
Fall	6924	3245	5714	12990	-17	2729	5821	12853	-15
					RCP 4.5				
Winter	7602	4758	9094	16221	19	4763	9306	16897	22
Spring	7763	4085	6681	15319	-13	3346	6568	14821	-15
Summer	6661	1745	3232	7110	-51	1608	2697	6062	-59
Fall	6924	3142	5895	13382	-14	3021	6260	13312	-9
					RCP 8.5				
Winter	7602	4896	8884	16962	16	4663	9802	17312	29
Spring	7763	3925	6528	15558	-16	2922	6111	13857	-21
Summer	6661	1631	2694	6235	-59	1276	2265	5686	-66
Fall	6924	2645	5612	13342	-19	3341	5912	12930	-14

Average historical and future seasonal flow statistics for different RCPs, GCMs and DSMs are shown in Table 4.3 to Table 4.5, respectively. Table 4.3 indicates that mean winter flow will increase, with estimated range between 13% to 19% in the near future (2036 to 2065) and 15% to 29% in the far future (2066 to 2095) for different emission scenarios. However, summer mean streamflow will decrease by at least 51% in the near future and 66 % in the far future (Table 4.3). A Similar kind of trend is found in Table 4.4 and Table 4.5.

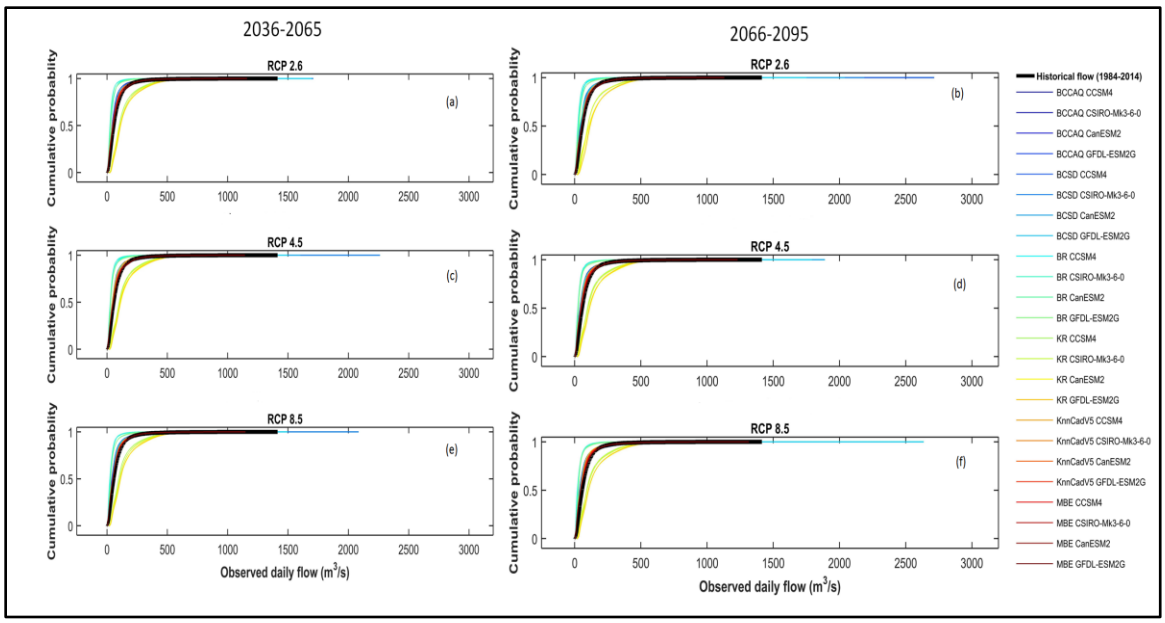

Figure 4.5 Cumulative probability distribution (CDF) of simulated (2036-2065 and 2066-2095) and historical (1984-2013) daily streamflow into the Strathcona reservoir, BC, Canada for different emission scenarios (after Mandal and Simonovic, 2017).

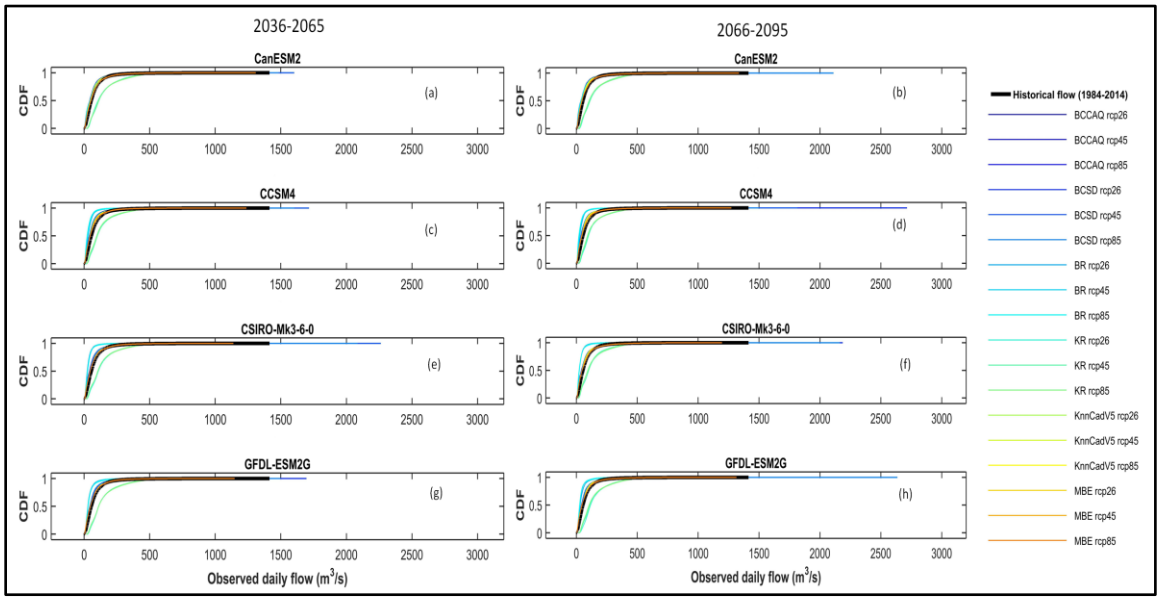

Figure 4.6 Cumulative probability distribution (CDF) of simulated (2036-2065 and 2066-2095) and historical (1984-2013) daily streamflow into the Strathcona reservoir, BC, Canada for different GCMs (after Mandal and Simonovic, 2017).

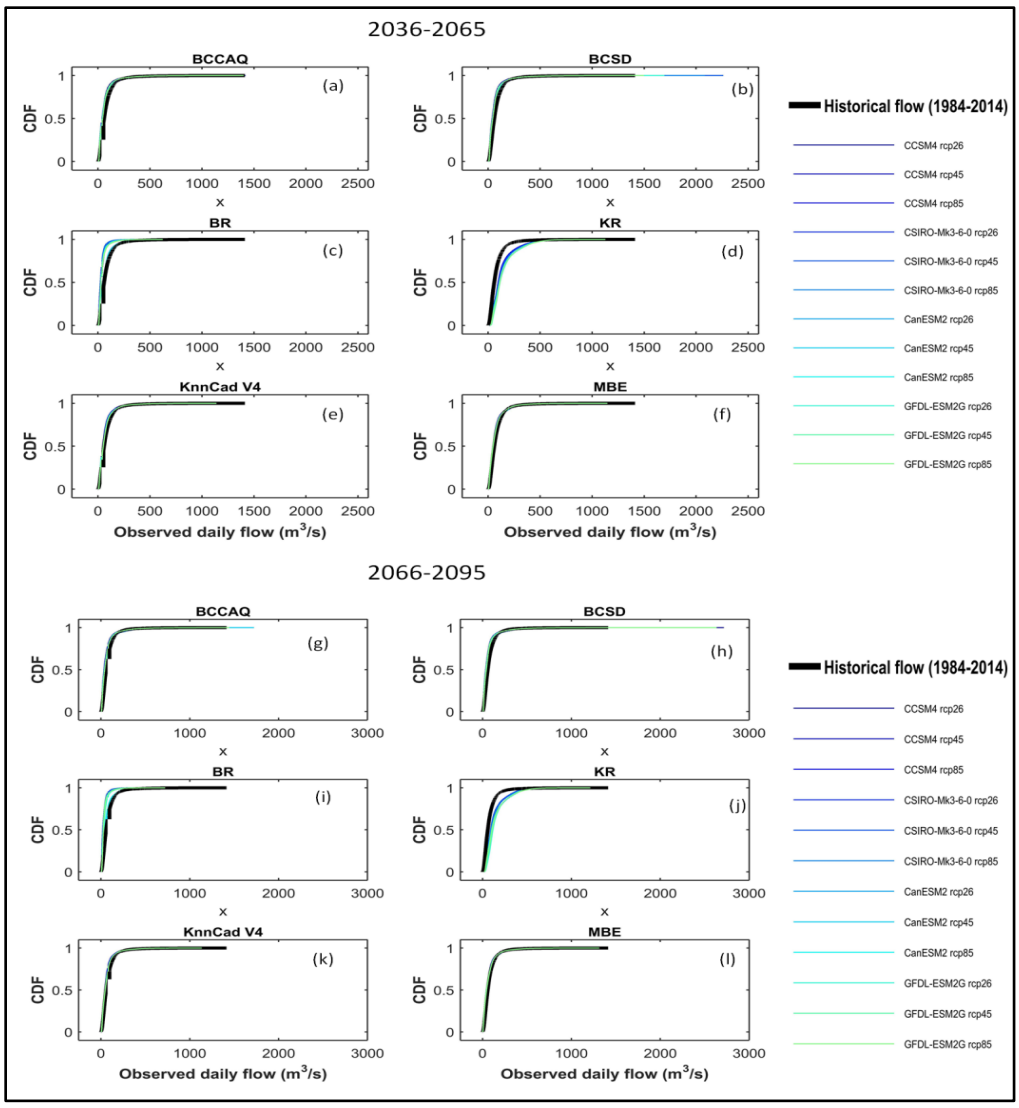

Figure 4.7 **C**umulative probability distribution (CDF) of simulated (2036-2065 and 2066-2095) and historical (1984-2013) daily streamflow of the Strathcona dam, BC, Canada for different downscaling methods. BCAAQ: Bias correction constructed analogues with quantile mapping reordering; BCSD: Bias-corrected spatial disaggregation; BR:Beta regression based statistical downscaling model; KR: non-parametric statistical downscaling model based on the kernel regression; KnnCAD v4:Delta change method coupled with a non-parametric K-nearest neighbor weather generator; MBE: Delta change method coupled with maximum entropy weather generator (MBE) (after Mandal and Simonovic, 2017).

Table 4.4 Historical (1984-2013) and future mean seasonal flows (m^3/s) (5th, median - 50th, and 95th percentile estimates) for different GCMs in Upper Campbell Lake reservoir, British Columbia, Canada (after Mandal and Simonovic, 2017).

		2036-2065				2066-2095			
	Historical	5th	50th	95th	Change in median value (%)	5th	50th	95th	Change in median value (%)
				CCSM4					
Winter	7602	5324	7999	14413	5	5320	8620	15422	13
Spring	7762	3814	6229	15238	-19	3137	6436	14369	-17
Summer	6661	1455	3000	6441	-54	1241	2506	5924	-62
Fall	6923	2812	5302	13040	-23	2481	5498	12706	-20
				CSIRO-Mk3-6-0					
Winter	7602	4186	9053	16274	19	4524	10023	16261	31
Spring	7762	3877	7021	15699	-9	3223	6567	14184	-15
Summer	6661	1802	3332	6103	-49	1473	2373	5440	-64
Fall	6923	2375	6371	12974	-7	2539	6727	12945	-2
				CanESM2					
Winter	7602	8569	9368	16284	23	8446	10054	17810	32
Spring	7762	6272	6942	18321	-10	5168	6604	16728	-14
Summer	6661	1605	2855	7172	-57	1422	2242	6207	-66
Fall	6923	5294	5985	13105	-13	5165	6048	12729	-12
				GFDL-ESM2G					
Winter	7602	4561	8925	16994	17	4357	9426	17082	24
Spring	7762	4682	6694	15561	-13	3621	6682	15175	-13
Summer	6661	1771	3358	7569	-49	1771	2771	7242	-58
Fall	6923	3883	5580	14911	-19	4025	5768	15531	-16

Table 4.5 Historical (1984-2013) and future mean seasonal flows (m^3/s) (5th, median - 50th, and 95th percentile estimates) for different downscaling methods in Upper Campbell Lake reservoir, British Columbia, Canada (after Mandal and Simonovic, 2017).

Downscaling method		Historical	5th	Median	95th	Change in median value (%)	5th	Median	95th	Change in median value (%)
BCCAQ	Winter	7602	8382	9493	10884	24	8846	10284	11313	35
	Spring	7762	5807	6260	6877	-19	5466	5878	6403	-24
	Summer	6661	1791	2019	2324	-69	1587	1886	2403	-71
	Fall	6923	5361	5935	7098	-14	5419	6094	7686	-11
BR	Winter	7602	6601	7479	12394	-1	4175	4927	10806	-35
	Spring	7762	6111	6782	8840	-12	2829	3651	5830	-52
	Summer	6661	3903	4251	4562	-36	1179	1530	2038	-77
	Fall	6923	4752	5850	8945	-15	2373	3523	5783	-49
KR	Winter	7602	9995	12077	13866	58	10426	12499	13846	64
	Spring	7762	11003	11756	14867	51	8810	10688	12997	37
	Summer	6661	1577	2813	4195	-57	3905	4893	6890	-26
	Fall	6923	8307	9138	11452	31	8289	8917	11578	28
BCSD	Winter	7602	8150	9170	9918	20	8627	9636	10918	26
	Spring	7762	6098	6358	7237	-18	5378	5830	6749	-25
	Summer	6661	1889	2156	2520	-67	1618	1879	2530	-71
	Fall	6923	4889	5602	6374	-19	5351	6075	6897	-12
KnnCADV4	Winter	7602	7218	8334	8942	9	7786	8502	9517	12
	Spring	7762	6663	7003	7553	-9	6304	6752	7412	-13
	Summer	6661	3601	4259	4960	-36	2423	3629	5121	-45
	Fall	6923	4946	5459	6450	-21	4864	5497	6353	-20
MBE	Winter	7602	7589	8257	9223	8	7858	8796	9998	15
	Spring	7762	6386	6942	7624	-10	6594	6818	7344	-12
	Summer	6661	4560	5243	5724	-21	3070	4488	6087	-32
	Fall	6923	5194	5846	6468	-15	5246	5911	6722	-14

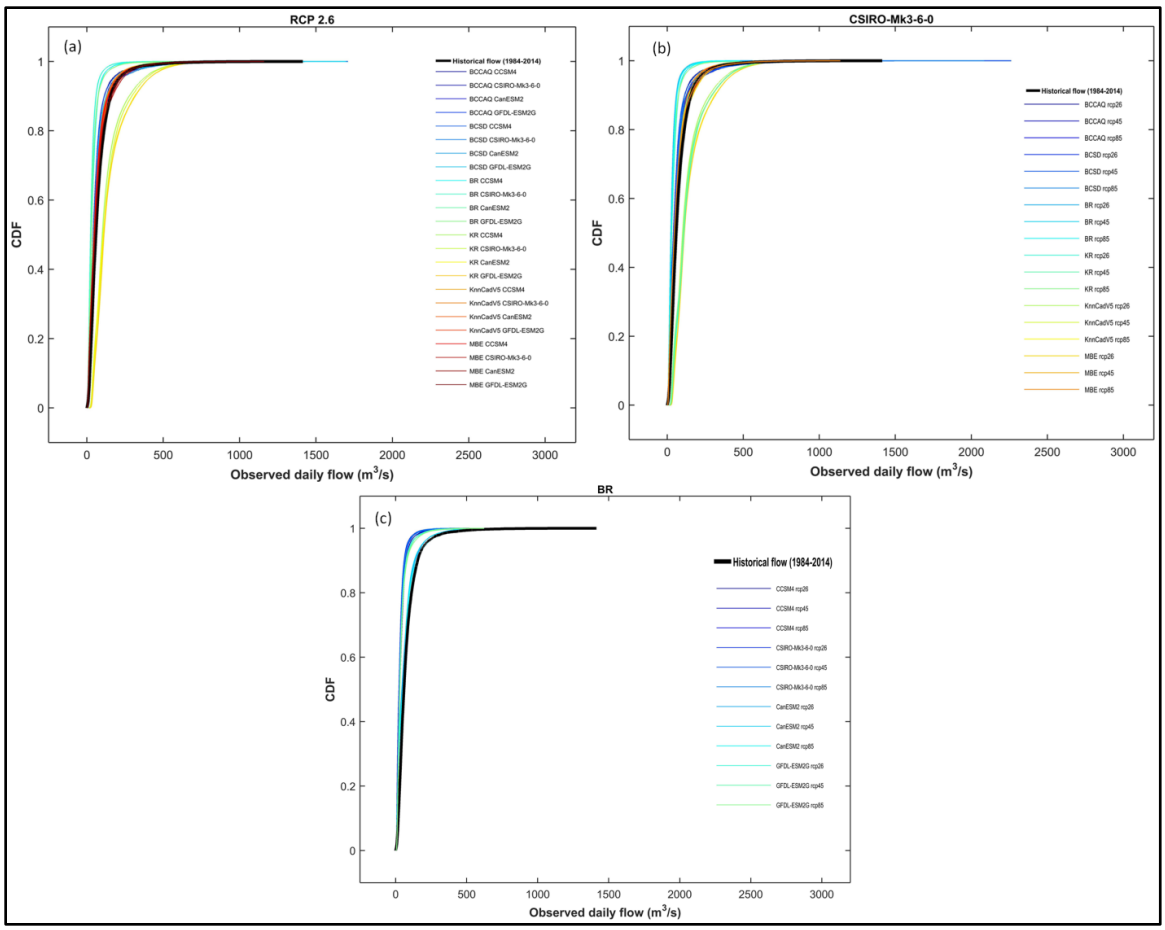

Figure 4.8 Cumulative probability distribution (CDF) of simulated (2036-2065) and historical (1984-2013) daily streamflow of the Strathcona dam, BC, Canada for (a) RCP 2.6; (b) CSIRO-Mk-3-6-0 and (c) Beta Regression based statistical downscaling model (BR) (after Mandal and Simonovic, 2017).

The results indicated that the winter flow will increase where other seasonal flow will decrease, in both future time periods (Table 4.4 & Table 4.5). Summer flow will decrease from 49 % to 57 % in near future and 58 % to 66 % in the far future where winter flow will increase 5% to 23% and 13% to 32% in near and far future respectively for different GCMs (Table 4.4). Results from Table 4.5 indicate that the summer flow in the near future will be reduced up to a maximum of 69% compared to the historical flow where the highest decrease in the flow of 71% may be experienced in the far future. Only the

KR model provides different results (Table 4.5). To summarize, the summer flow in the Campbell River basin (British Columbia, Canada) will be highly affected by the changing climate conditions. Spring flow will range from -9% to -19 % and -12% to -52% for near and far future respectively except for KR model results. Streamflow during fall will decrease in the range from -7% to -23% and -2% to -49% for near and far future respectively except KR model results.

Figure 4.9 to Figure 4.11 present box plots of projected mean monthly simulated streamflow with the historical flow for different emission scenarios, GCMs, and downscaling models respectively. It is clearly visible that the mean monthly flow in Figure 4.9 and Figure 4.10 are quite different when compared to the flows in Figure 4.11. In Figure 4.11 for summer months, (May, June and July) future flows for both time periods are less than historical summer mean flows. However, in Figure 4.11, variation in mean monthly flows is less compared to Figure 4.9 and Figure 4.10. These results support the hypothesis that the choice of DSMs introduces a higher level of uncertainty in streamflow prediction compared to the choice of RCPs and GCMs. In addition, the results in Figure 4.10confirm that future summers will be drier and future winters will be wetter compared to the historical time period (1984-2013). Schnorbus *et al.,* (2011) investigated hydrologic impacts of climate change in the Campbell River basin where they found that decreasing trend (-14% for A1B scenario) in future precipitation (2041 to 2070) for June, July and August and increasing trend (5% to 11%) in October through December. This study also found that monthly mean temperature would have a significant and strong signal of shifting to warmer temperature throughout the year and particularly higher for July, August, and September in future (2041 to 2070). Streamflow

in the Campbell River is fed by a mix of rain and snowmelt. As the temperature is increasing, it has been predicted that snowfall will decrease throughout the fall and winter where rainfall will increase (Schnorbus *et al.*, 2011) in this river basin. This leads to a conclusion that the streamflow in this river basin will be rainfall dominated compare to the hybrid mix (snow and rain). Due to projected higher temperature in mid-winter and early spring (Schnorbus *et al.*, 2011), snow will melt faster than before, whereas less snow will be available for melt because of significant reduction of historical spring freshet. This evidence is the possible reason behind the increasing flow in winter, and less flow in summer (Figure 4.10). From this study it can be concluded that the Campbell River basin will become a pluvial regime (rainfall dominated) in future from the hybrid nival-pluvial regime (snow influenced). Schnorbus *et al.*, (2011) also provided similar conclusion in their study. The details about flow frequency analysis are given in the following section.

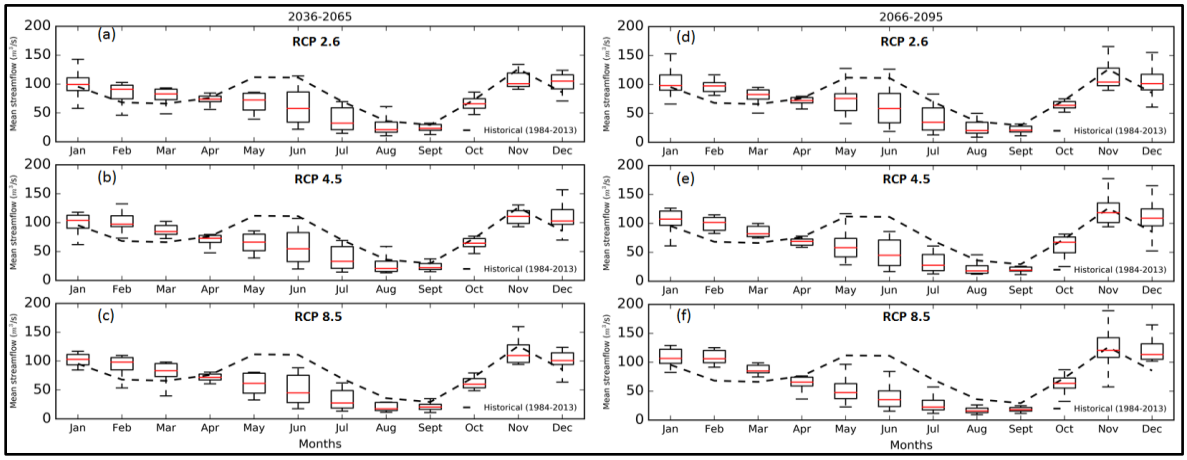

Figure 4.9 Boxplots showing projected mean monthly simulated streamflow for the near future (2036-2065) and the far future (2066-2095) with historical (1984-2013) observed flow into the Strathcona dam, BC, Canada for different emission scenarios (after Mandal and Simonovic, 2017).

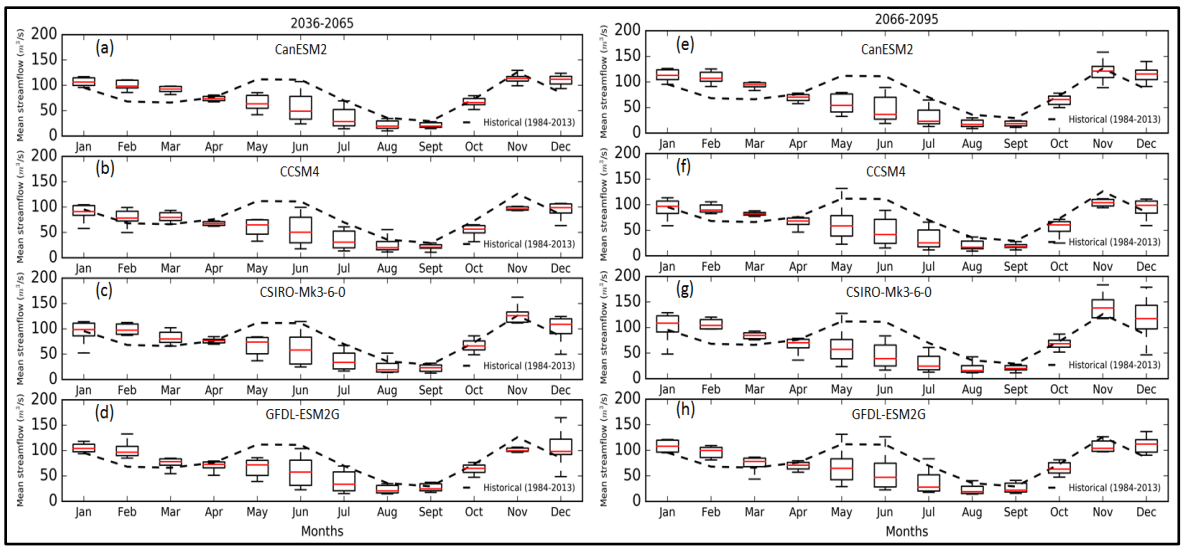

Figure 4.10 Boxplots showing projected mean monthly simulated streamflow for the near future (2036-2065) and the far future (2066-2095) with historical (1984-2013) observed flow into the Strathcona dam, BC, Canada for different GCMs (after Mandal and Simonovic, 2017).

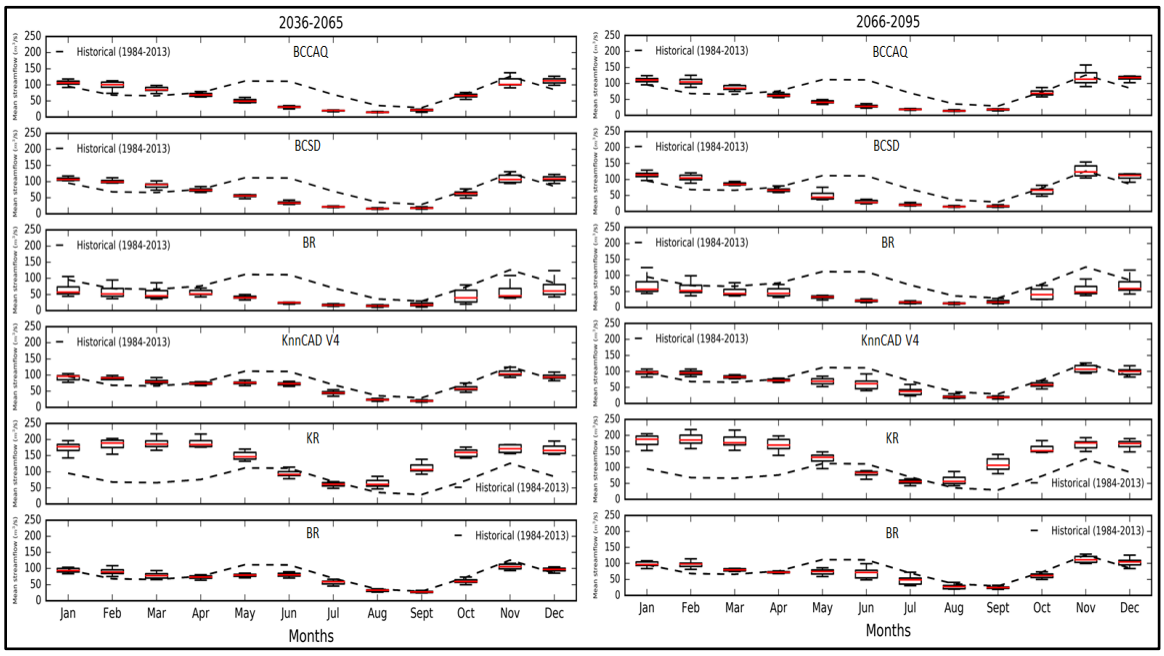

Figure 4.11 Boxplots showing projected mean monthly simulated streamflow for the near future (2036-2065) and the far future (2066-2095) with historical (1984-2013) observed flow into the Strathcona dam, BC, Canada for different downscaling models (after Mandal and Simonovic, 2017).

4.2.2 Flow Frequency Analysis

The Generalized Extreme Value (GEV) distribution is used for flow frequency analysis. GEV is an integration of continuous probability distributions which combines the Gumbel (EV1), Frechet and Weibull distributions and is widely used in flow frequency analysis (Fowler and Wilby, 2010; Das and Simonovic, 2012; Das *et al.*, 2013). The GEV has three parameterse.g. location, shape and scale. The shift in the distribution is described by the location parameter where the scale parameter describes the spread of the distribution and the shape parameter describes the skewness. If the shape parameter (k) =0, GEV becomes Gumbel distribution, and when k<0 it is transformed in Weibull distribution. If k>0, then the GEV is converted into the Frechet distribution. Cumulative distribution (CDF) and probability distribution (PDF) function of GEV are defined as follows (Hosking and Wallis, 1997):

$$F\left(x;\alpha,\kappa,\xi\right)=\exp\left\{-\left(y\right)^{-\frac{1}{\kappa}}\right\} \quad \text{when } y\rangle 0 \ \& \ \kappa\neq 0 \qquad (4.2)$$

$$=\exp\left(-\exp\left(\frac{x-\xi}{\alpha}\right)\right) \quad \text{when } \kappa=0 \qquad (4.3)$$

$$f\left(x;\alpha,\kappa,\xi\right)=\alpha^{-1}\left[y\right]^{\left(-1-\frac{1}{\kappa}\right)}\exp\left(-y^{-\frac{1}{k}}\right) \quad \text{when } \kappa\neq 0 \qquad (4.4)$$

$$=\alpha^{-1}\exp\left[-\left(\frac{x-\xi}{\alpha}\right)\right]\exp\left\{-\exp\left[-\left(\frac{x-\xi}{\alpha}\right)\right]\right\} \text{ when } \kappa=0 \qquad (4.5)$$

where $y=\left[1+\kappa\left(\frac{x-\xi}{\alpha}\right)\right]$; ξ is the location parameter; α is the scale parameter and κ is the shape parameter.

The flow frequency analysis is conducted using 'ismev' package (Heffernan, 2016) in R-studio combined with python environment. The flow frequency curves are shown in Figure 4.12. The flow frequency curve derived from the observed historical data is also shown in Figure 4.12. The results are presented for various return periods from 2 to 200 years. The figure summarizes the impact of choosing different GCMs and DSMs on the flows corresponding to different return periods. It is found that the uncertainty increases with the increase in the return period where CDFs become flattered. It is also found that in the far future, CDFs are flatter compared to the near future time period. The average percentage changes in flow magnitudes are shown in Table 4.6. The maximum average percentage changes of the 50-year flow magnitude between future climate (2036-2065 and 2065-2095), and the historical (1984-2013) are respectively -20.2% and -5.7%. In the near future, for RCP 8.5, a decreasing trend is observed with the increase in the return period. On the contrary, in the far future for RCP 8.5 an increasing trend is observed with the increase in the return period. RCP 8.5 considers maximum amount of GHGs emission

in the atmosphere which is approximately three times of today's carbon emission by the end of this century (Vuuren *et al.*, 2011). GHGs emissions have a positive correlation with atmospheric temperature (IPCC, 2013). Therefore, the precipitation pattern can be changed significantly. This can be a possible reason for decreasing trend of flow magnitude for near future.

Table 4.7 shows a comparison between historical and future flow return periods for different emission scenarios. For all emission scenarios, the return period of higher flow event will increase in both future time periods. For example, 1250 m^3/s flow had a return period of 11 years but it will change to 20 years (2036-2065) and 21 years (2066-2095)

for RCP 2.6 emission scenarios (almost doubled). A similar trend could be found for other emission scenarios too.

Table 4.6 Average percentage changes in streamflow magnitude between baseline period (1984-2013) and future time periods in Upper Campbell Lake reservoir, British Columbia, Canada (after Mandal and Simonovic, 2017).

Return period (year)	2036-2065			2066-2095		
	RCP 2.6	RCP 4.5	RCP 8.5	RCP 2.6	RCP 4.5	RCP 8.5
5	-14.0	-13.2	-16.1	-13.8	-12.5	-6.6
10	-14.1	-14.4	-17.8	-15.0	-13.6	-6.8
50	-13.0	-16.1	-20.2	-16.0	-14.4	-5.7
100	-11.8	-16.4	-21.0	-16.0	-14.0	-4.6
150	-11.0	-16.5	-21.1	-15.6	-13.4	-3.9
200	-10.3	-16.6	-21.3	-15.2	-13.0	-3.2

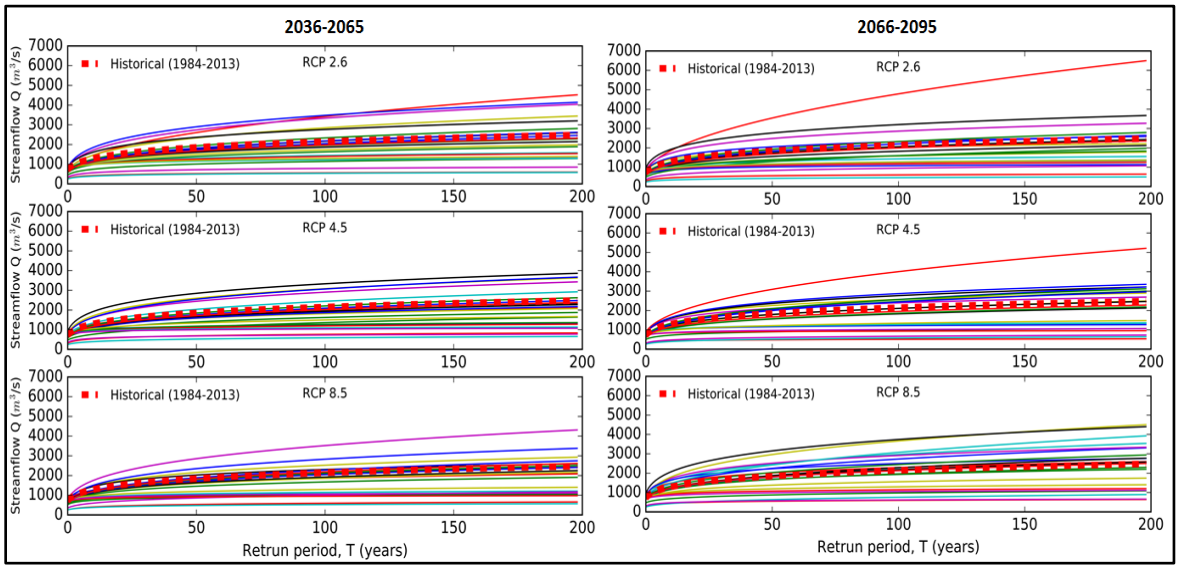

Figure 4.12 Simulated flow frequency results of the Strathcona dam, BC, Canada using GEV for different emission scenarios between two future time periods (after Mandal and Simonovic, 2017).

Table 4.7 Comparison of historical (1984-2013) and projected flow return periods for two future time periods (2036-2065 and 2066-2095) in Upper Campbell Lake reservoir, British Columbia, Canada (after Mandal and Simonovic, 2017).

		Return period (Year)					
		2036-2065			2066-2095		
Flow (m^3/s)	Historical	RCP 2.6	RCP 4.5	RCP 8.5	RCP 2.6	RCP 4.5	RCP 8.5
800	3	4	4	4	4	4	3
1000	5	8	8	10	8	8	6
1250	11	20	21	26	21	20	14
1500	22	40	45	57	45	42	28
1900	60	105	135	178	130	117	75

4.3 Summary

This study used multiple RCPs, GCMs and DSMs to assess the uncertainty in streamflow due to climate change. The analyses are performed for the case study of Campbell River basin in British Columbia, Canada, with the focus on Strathcona dam location. Most of the previous regional studies in Canada found that the choice of GCMs is the biggest source of uncertainty in downscaling processes. The analyses in the Campbell River basin performed with different RCPs, GCMs and DSMs show that the choice of DSMs has a higher influence on streamflow variation compared to the choice of GCMs or RCPs. Downscaling models (DSMs) are developed based on a statistical relationship between climate variables. DSMs includes multiple assumptions, selections of statistical parameters (e.g. scale, shape, skewness) and climate variables (predictand and predictors) which make a DSM different from other DSMs. Therefore structure and procedure

followed in a DSM could be possible reasons for significant streamflow variation for various DSMs. Hence, it is important to use multiple DSMs during climate change impact assessment. In section 3.3 we reached a similar conclusion in the study of precipitation projection under changing climatic conditions. It is to be expected that if the precipitation pattern is affected then the streamflow will change too. However, the previous section (section 3.3) does not quantify the amount of precipitation or future streamflow changes. According to Warren and Lemmen (2014) increasing trend in average annual precipitation can be found on the west coast of Canada where snowfall has decreased in last 61 years (1950 to 2010). Therefore quantifying changes in streamflow due to climate change is an important contribution of this study that makes it different from the previous work. Another important difference of this study is the analysis of propagation of sources of uncertainty in the projected streamflow, which is discussed in the results section.

From the Table 4.5, it can be found that all the DSMs show similar pattern e.g. increasing trend in streamflow for winter and a decreasing trend for other seasons except KR and BR. However, KR agrees with summer and winter flow trend with other DSMs where BR captures streamflow pattern for all seasons except winter. BR and KR models are regression based, and multiple predictors variables (Tmax, Tmin, mslp, hus at 500 hPa, u-wind and v-wind) are used for build a relationship between predictors and predictand (here precipitation). These predictor variables are correlated with each other (positively/negatively) which could be the reason for disagreement between KR and BR results when compared with other DSMs.

For the purpose of this present study, a single hydrologic model (UBCWM) is used which is a limitation of this study at this stage. Hydrologic models should be selected based on the study region, available data, basin characteristics, and study purposes but often the model is selected which is readily available. In this case, BC Hydro provided the calibrated model (UBCWM). In addition, Kay *et al.,* (2009) investigated the role of different hydrologic models and found that the choice of the hydrologic model also contributes to the uncertainty in projected streamflow. Also projected streamflow is highly sensitive to hydrologic model parameterization (Jiang *et al.*, 2007; Poulin *et al.*, 2011). However, it has been found that uncertainty due to the hydrological model structure is more significant compared to model parameter uncertainty. Therefore, streamflow generation using multiple hydrological models with multiple RCPs, GCMs and DSMs may be advised for the continuation of the presented work. There are two other dams in the basin (Ladore and John Hart) which are connected with the Strathcona dam. Hence, quantifying stream flow uncertainty due to climate change at all three dam locations could be another area of future research. Another limitation of the study is the use of a single river catchment. The consistency of GCMs varies substantially from one region to another. Rupp *et al.*,(2013) and Kay *et al.*,(2009) also suggested that multiple catchments, or different locations, should be analyzed in order to obtain a more comprehensive understanding of different sources of uncertainty. Focus of the present work is in the development of the uncertainty assessment methodology that can be used with multiple catchments for more thorough analyses of uncertainty. This work is considered as a potential future research topic. In this study, only four GCMs are used due to data availability for all downscaling models. GCMs use mathematical relationships

to simulate global climate system in three spatial dimensions with respect to time. GCMs simulate different atmospheric components (e.g. temperature, sea-ice, humidity) at various scales (horizontal spacing and grid size) and include many complexities (parameterization schemes). Some GCMs are based on the same analytical procedures and even share the same mathematical equations. Therefore, future climate predictions using an arbitrary number of GCMs may be very precise and consistent for a particular region, but it may be inaccurate as the outcome can be consistently biased. For example, Rupp *et al.*, (2013) found that two GCMs, MIROC-ESM- CHEM and MIROC-ESM, to perform poorly in Europe and Southeast Asia. However, these two models perform well in Africa. Therefore selection of GCMs is crucial for uncertainty analysis and may be a potential future research area.

Another main observation of the presented study is that the winter flow will be increasing in both future time periods considered (2036-2065 and 2065-2095), where the summer flow will be decreasing by atleast 21%. These findings can have a serious effect on the management of water resources infrastructure in the basin, which is one of the main components of the British Columbia hydropower generation system. However, a major weakness of river flow forecast under climate change is limited validation. There is a prospect for testing the primary flow patterns relative to recent empirical trends which provide an opportunity for future work. The recommendations of the study presented in this chapter are: (a) new water resources infrastructure planning and design guidelines should be developed in order to include the changing climatic conditions in the future; and (b) the serious review of the current operational rules for the water resources infrastructure in the basin should be conducted in with the main goal of finding the best

adaptation strategies to changing future conditions. The next chapter gives an assessment of reservoir operation under changing climate conditions.

Chapter 5

5 Reservoir Operation under Changing Climate Condition

Based on: Sohom Mandal, R. Arunkumar, Patrick A. Breach, Slobodan P. Simonovic, "Reservoir operation under climate change: a system dynamics approach" (under preparation).

In the previous chapter (Chapter 4), it is presented how streamflow in the Campbell river is projected to change under the influence of climate change. The projected changes are also found to be uncertain depending on the choice of GCMs, downscaling methods and emission scenarios for analysis. Changes in streamflow, in turn, will require changes in reservoir operation rules to better manage water resources in Campbell river basin. A methodology to assess the climate change impacts on future reservoir operation rules is discussed in this chapter.

Reservoir operation is a complex problem that involves a significant number of decision variables, objective functions and constraints (Yeh, 1985; Simonovic, 1992). It contains an inherent uncertainty due to inflow variability. There are two reasons behind inflow variability: (a) natural seasonal variability; and (b) long-term variability due to climate change (Raje and Mujumdar, 2010). Inflow variation due to climate change and analysis of operating rules under uncertain inflows are the primary focus of this chapter.

The majority of studies performed in the past focused on climate change impacts on hydro-climate variables, such as precipitation, temperature, streamflow, etc. (Ghosh and Mujumdar, 2006; Mehrotra and Sharma, 2006; Ghosh, 2010; Das and Simonovic, 2012; Gaur and Simonovic, 2013; Kannan and Ghosh, 2013) or anticipated future water

demand under hydrologic impact of climate change (Asokan and Dutta, 2008; Li *et al.*, 2010). Particularly, analysis of reservoir operating rules considering primary sources of uncertainty in streamflow caused by climate change is rarely addressed in climate change impact studies. Li *et al.*,(2010) studied the variation of streamflow and reservoir performance under changing climate conditions in the North American prairie region. They found that the frequency and magnitude of peak streamflow will increase in future due to climate change. However, they did not use multiple downscaling models to address uncertainties. Ahmadi *et al.*, (2014) used adaptive rules based on non-dominated sorting genetic algorithm (NSGA-II) for reservoir management considering climate change. They applied this model in Karron-4 reservoir, Iran. The result showed that new adaptive rules are better in terms of reliability in hydropower generation. However, they only considered a single GCM (HadCM3), single GHG emission scenario (A2) and a single hydrologic model. Therefore uncertainties in climate change assessment process were not included in this study. Minville *et al.*, (2009) studied climate change impacts on the Peribonka River Basin, Quebec, Canada which consists of two large reservoirs (Marouane lake reservoir and Passes-Dangereuses reservoir) for hydropower generation. The objectives of this study were to evaluate climate change impacts on hydropower, power plant efficiency, and reliability of the reservoir under changing climate condition. However, they did not address uncertainties in the climate change assessment process.

In summary, past uncertainty modeling studies of reservoir operation due to climate change are limited only to the impact of choosing GCMs and emission scenarios. However, there are no studies especially in Canada, which address the cascade of uncertainty due to (i) choice of GCMs; (ii) selection of emission scenarios (iii) choice of

downscaling models. Therefore to assess the impact of climate change on reservoir operation, primary sources of uncertainties need to be addressed. For case study purpose, Campbell river system is used. Campbell river system includes: Buttle lake and Upper Campbell lake reservoir (Strathcona dam, Strathcona generating station and Crest diversion); Lower Campbell lake reservoir (Ladore dam, Ladore generating station, Salmon diversion dam, Quinsam diversion dam and Quinsam storage dam) and John Hart lake reservoir (John Hart dam and generating station). The details of this river system and reservoirs are discussed in the following section.

5.1 Campbell River System and Reservoirs

Campbell river system is located on Central Vancouver island, western part of Canada. It originates from Strathcona Provincial Park and connects Buttle Lake and Upper Campbell lake reservoir, Lower Campbell lake reservoir and John Hart lake reservoir, before drains into Strait of Georgia. The Buttle lake and Upper Campbell lake flow is regulated by Strathcona dam, Lower Campbell lake by Ladore dam and John Hart lake reservoir is regulated by John Hart dam. Campbell river system has three diversion namely Crest (and formally Heber), Salmon and Quinsam. At full supply level (220.98 m water storage height), Buttle and Upper Campbell lake reservoir has a surface area of 6,870 ha with 2,459 million m^3 (approximately) of water storage. In 212 m elevation level both lakes (Buttle and Upper Campbell) becomes a single reservoir. However, in between 212 m and 208 m they separated into two lakes. Strathcona Dam is an earthfill dam located northeast arm of Upper Campbell lake. This dam is 53 m in height and 550 m in length, has two 42,000 hp (2x 31.3 MW) turbines for power generation. Maximum turbine discharge from Strathcona varies from 175.0 to 197.4 m^3/s. Figure 5.1 shows the

water use plan for Upper Campbell lake reservoir. Upper Campbell river has a maximum (220.5 m) and minimum (212 m) operating levels to meet recreation, shoreline, fisheries and flood mitigation interest (Figure 5.1). It also has a preferred maximum (220.5 m) and preferred minimum (217 m) operating levels for summer recreation (Figure 5.1).

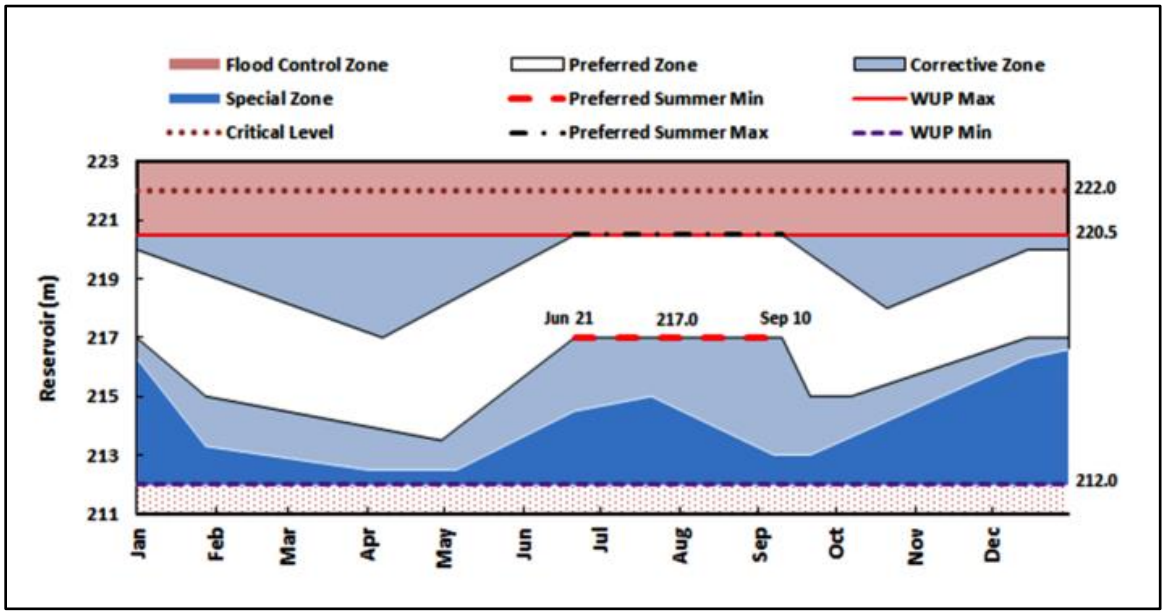

Figure 5.1 Upper Campbell Reservoir Operation Zones (after BC Hydro Generation Resource Management, 2012).

Lower Campbell reservoir has a surface area of 2,650 ha and a total storage of 316 million m^3 (approximately). Ladore dam controlls flow from Lower Campbell reservoir. Ladore is a concrete gravity dam situated 15km west from the City of Campbell river. This dam has two 35,000 hp (2x 26.1 MW) turbines for hydropower generation. Maximum turbine discharge from Ladore varies from 160.0 to 167.9 m^3/s. Operation policy of Lower Campbell reservoir is shown in Figure 5.2. The maximum and minimum operating level is 178.3 m and 174.0 m respectively (Figure 5.2). However, the preferred

maximum and preferred minimum operation level is 177.5 m and 176.5 m respectively (Figure 5.2).

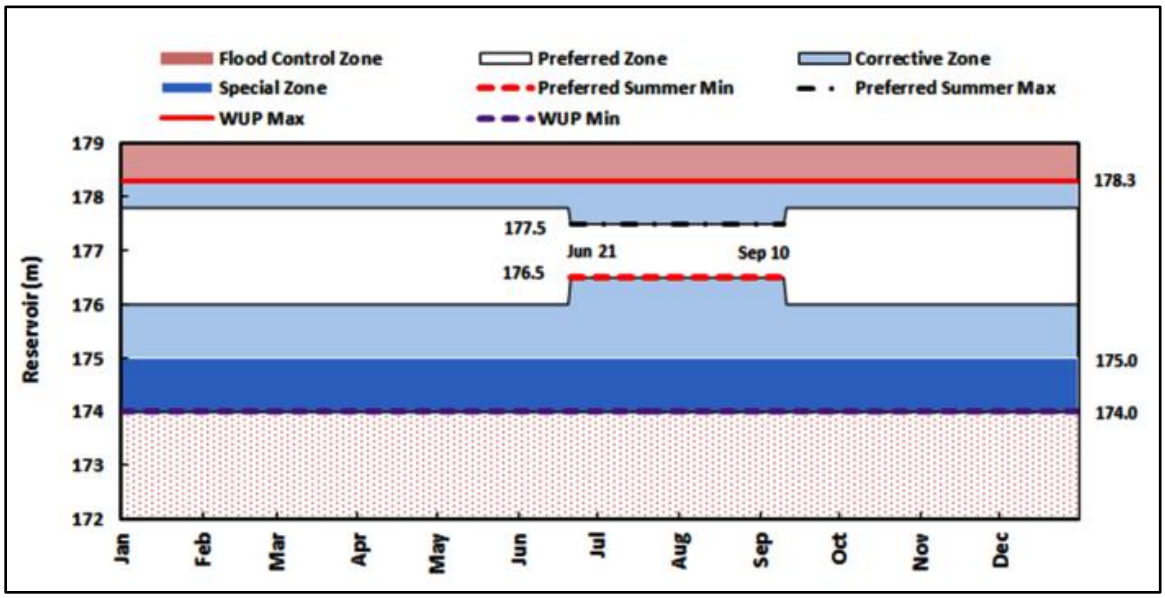

Figure 5.2 Lower Campbell Reservoir Operation Zones (after BC Hydro Generation Resource Management, 2012).

The last reservoir of the Campbell river system is John Hart lake reservoir which includes another hydropower generating station into the river system. John Hart has an earthfill dam and six generation units (6x 20.9 MW). Maximum turbine discharge from John Hart varies from 122.0 to 124.0 m^3/s. John Hart has a preferred operation range of 139.60 m (maximum) to 139.0 m (minimum). The details about Campbell River system and reservoir storage are shown in Figure 5.3. All the information described in this sub-section is extracted from Campbell river water use plan developed by BC Hydro (BC Hydro Generation Resource Management, 2012).

Typically, for coastal reservoirs like reservoirs in Campbell River system peak inflow occur between October and March. During this time of the year, peak flow results from

seasonal rainstorms and spring snowmelt (Figure 5.4). It is typical for winter months when snowpack increases, followed by large short-term Pacific disturbances with warmer temperatures which help to melt a portion of the snowpack.

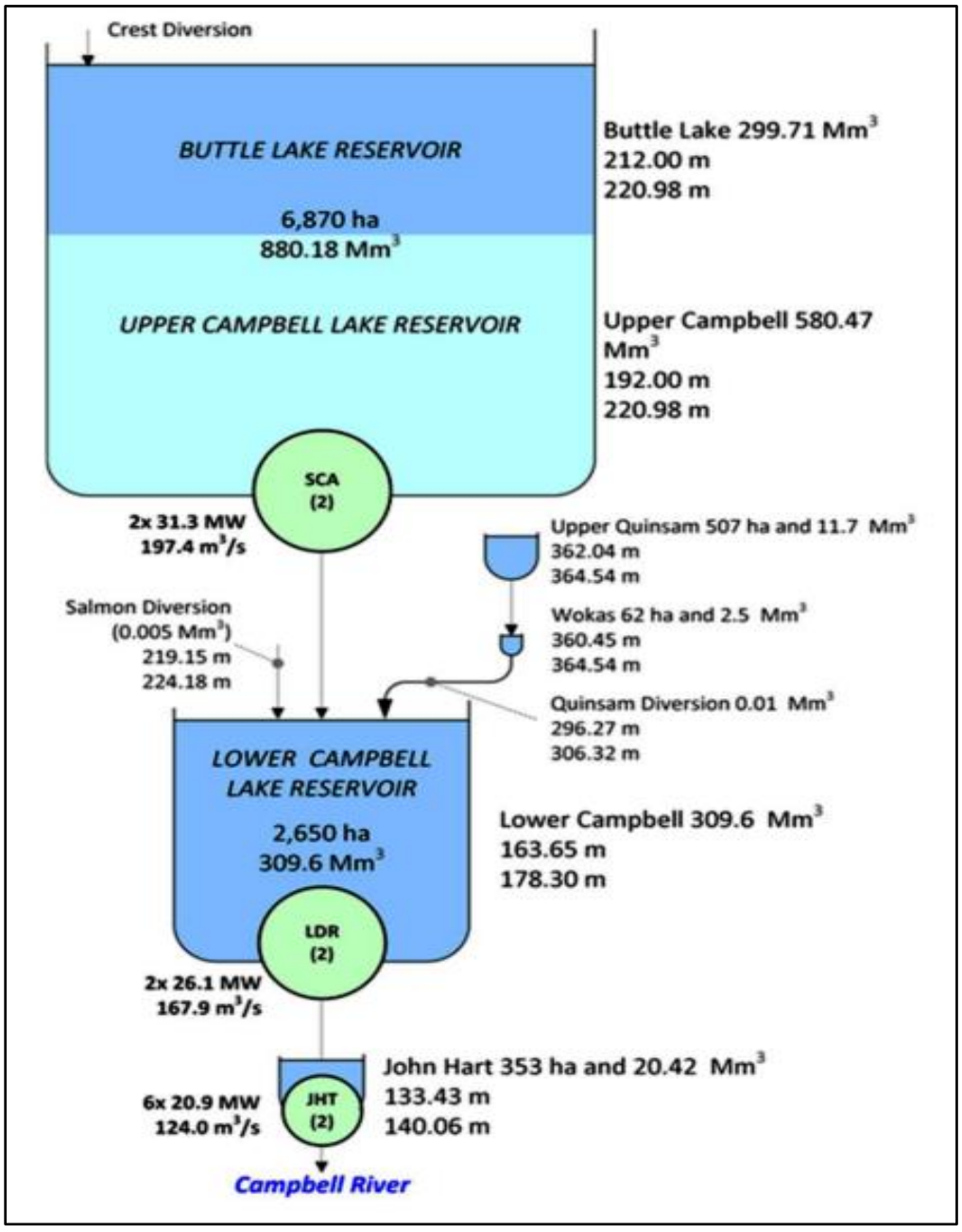

Figure 5.3 Campbell river system: relative storage volume (after BC Hydro Generation Resource Management, 2012).

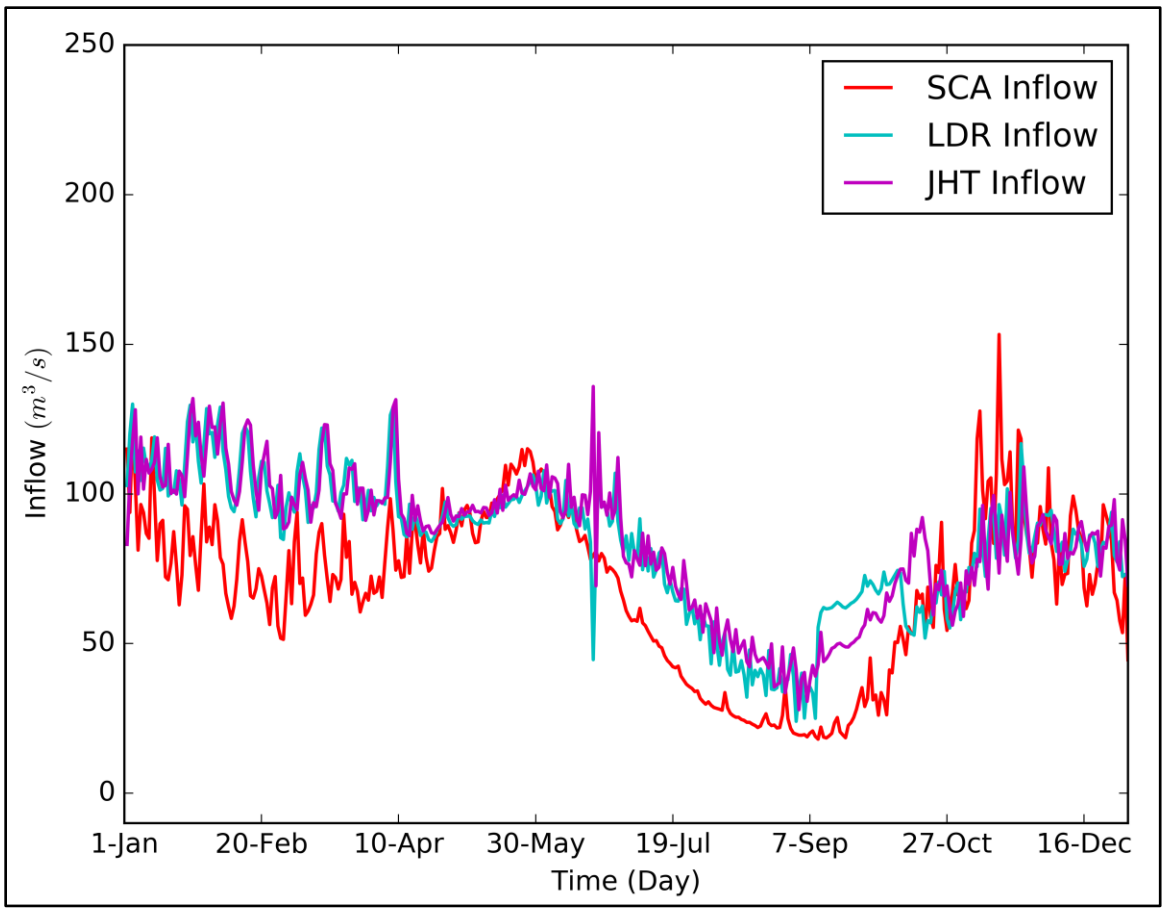

Figure 5.4 Historical (1984 - 2013) mean daily inflows of Upper Campbell reservoir (SCA inflow), Lower Campbell reservoir (LDR inflow) and John Hart reservoir (JHT inflow) (after Mandal *et al.*, 2016a).

As discussed in Chapter 4, streamflow of the Campbell river could be affected due to climate change. Therefore an assessment which includes future operation details of all three reservoirs in the Campbell rivers system under climate change scenarios is conducted in this chapter. As there are three reservoirs in the river system and connected in a series, Arunkumar and Simonovic (2017) developed a system dynamics simulation model to connect these reservoirs. The details about this model are discussed in the following section.

5.2 System Dynamics Simulation Model of Reservoir System

System dynamics simulation was first developed in the 1960s on the basis of control theory and has evolved into a widespread approach for modeling dynamic non-linear systems. It is a rigorous object-oriented simulation approach, which can be used in the analysis of dynamic systems (Simonovic, 2009). The strength of the system dynamics approach is in modeling complex non-linear feedback systems over time, where the change in the system state or in the variables due a decision is internalized within a feedback loop. Thus, system dynamics simulation allows the modeler to observe the behavior of a system and its response to any disturbance over time. Also, the transparency of system dynamics simulation allows the modeler to understand the links between the system structure and its dynamic behavior through interaction and relationships among the different variables (Simonovic and Fahmy, 1999). Water resources systems have many interrelated components and their interactions and dynamic behavior make them complex. System dynamics simulation is a suitable tool for effective analysis of water resources systems that address the dynamic behavior and complex interactions of various components in a realistic way, where the stakeholder can be involved in the modeling process.

Application of system dynamics simulation technique has been an important focus of research in water resources engineering, and numerous models have been reported, for example long-term water resources planning and policy analysis (Simonovic *et al.*, 1997), flood management studies (Ahmad and Simonovic, 2000; Simonovic and Li, 2003), water shortage mitigation studies (Yang *et al.*, 2008; Qin *et al.*, 2012), design a multi-

purpose reservoir (Chu *et al.*, 2010), weather forecasting system (Rajasekaram *et al.*, 2010), hydrological impact studies (Sharifi *et al.*, 2013) and many more. Wei *et al.*, (2012) studied the interactions between water resources, environmental flow and socio-economy of the water resources system using a system dynamics model (SDM). In this work, the SDM was used to assess socio-economic impacts for different levels of environmental flow allocation in the Weihe River Basin of China. Felfelani *et al.*, (2013) developed a comprehensive SDM simulation model to study the operations of multi-purpose Dez Reservoir in southwestern Iran. The reservoir operations were simulated using forecasted monthly inflow and water release demand for hydropower, irrigation, and urban water supply. A goal-seeking hedging policy was proposed to avoid severe deficits. It is reported that the reservoir operations improved significantly after applying the hedging rule and reached the most stable condition during the simulation process. Teegavarapu and Simonovic (2014) assessed the behavior of a hydraulically coupled multiple reservoir systems using system dynamics approach. The developed model was applied to a real-life hydropower reservoir system in the Province of Manitoba, Canada. The hydraulic coupling between the reservoirs in the system was represented using the tailwater curves. It was reported that system dynamics approach helped in understanding the dynamics of the operation of a hydraulically coupled multiple reservoir systems.

Jahandideh-Tehrani *et al.*, (2014) simulated the operations of a hydropower system using SDM approach to study the effects of the operation of upstream reservoirs on a downstream reservoir. Multi-reservoir operations were simulated for eight scenarios over 44 years and the performance of the reservoirs was evaluated using reliability, resilience and vulnerability. It was reported that construction of additional reservoir increased the

power production without affecting the performance of other reservoirs in the system. Abadi *et al.,* (2015) used the SDM approach to simulate the water resources system for different scenarios and different policy packages. The SDM model was developed with various sub-systems and the policies were ranked using analytical hierarchy method. Recently, Morrison and Stone (2015) developed a SDM model to assess the environmental flow alternatives on reservoir storage, releases, hydropower production and revenue in Rio Chama basin, Mexico. It was concluded that SDM simulation was a promising approach, especially for reservoir operation studies. Thus, system dynamics modeling approach provides considerable flexibility and is an appropriate tool to address the dynamic water resources systems for prospectively enhancing its resilience (Winz *et al.*, 2009). Most of the reported studies (discussed above) are focused on reservoir operations using SDM approach. A climate change impact assessment on multi-reservoirs using SDM approach is not done in the past. Another important aspect of this study is the introduction of all primary sources of uncertainty in climate change impacts assessment process which could address the impacts future climate change on reservoir operation.

5.2.1 System Dynamics Model of the Campbell River System

The operation of the multi-reservoirs of Campbell River System (CRS) is simulated through system dynamics (SDM) approach. In the present study, the SDM simulation model is developed in Vensim software (Vensim, 2014). In Vensim, the reservoir components are modeled using stocks, flows, arrows and auxiliary variables. Stocks are used to represent state variables that accumulate over time. An example of stock variable could be reservoir storage. Flows represent the actions that change the stocks. Reservoir inflow and releases are examples of flows, since they change the amount of water stored

in the reservoir over time. Auxiliaries are dynamic variables that are computed from other variables during the simulation. Arrows are used to establish the relationship among variables in the model and they carry information from one variable to another variable. The direction of the arrow describes the dependency relationship between the connected variables. A positive sign indicates that an increase in the independent variable causes an increase in the dependent variable and vice versa. A negative sign indicates that an increase in the independent variable causes a decrease in the dependent variable and vice versa.

The stock and flow representation of CRS is shown in Figure 5.5. All the three reservoirs are represented as stocks and their inflows and outflows are modelled as flows. The three reservoirs namely, Strathcona (SCA), Ladore (LDR) and John Hart (JHT), are in series. The Strathcona is the upstream and largest reservoir in the basin and regulates the flow to the downstream reservoirs. The outflow, both the power releases and spill from the Strathcona reservoir is the major inflow to the Ladore. Similarly, the outflow from the Ladore dam is the major inflow to the John Hart reservoir. During average conditions, all the reservoirs in the system are operated with the intent to maintain the reservoir water level within the specified preferred storage zones. Thus, releases from the upstream reservoir adjusted such that the downstream conditions are met. The SDM simulation model is developed with the objective of maintaining the reservoir storage level within the preferred storage zones. The storage in the reservoir at time t is computed using the continuity equation. In general, the continuity equation is expressed as:

$$Storage_{n,t} = Storage_{n,t-1} + Inflow_{n,t} - Outflow_{n,t} \quad (5.1)$$

where $Storage_{n,t}$ is the storage at the end of time '*t*' of reservoir '*n*'; $Storage_{n,t-1}$ is the storage at the beginning of time 't'; $Inflow_{n,t}$ is the inflow during the time '*t*'; $Outflow_{n,t}$ is the total releases from the reservoir, which includes power releases and spill during the time period '*t*'. It is to be noted that the outflow from the upstream reservoir is the addition inflow to the downstream reservoir apart from its natural inflow. The system constraints, reservoir operating rules and the release decisions are captured using IF-THEN-ELSE statements in the simulation model.

According to the water use plan (BC Hydro Generation Resource Management, 2012), the reservoir levels need to be maintained within the preferred operating zones of each reservoir (discussed in section 5.1). The preferred operating zones also vary for each reservoir for different time periods. Therefore, SDM simulation model is developed in such a way that the reservoir levels are maintained within the preferred operating zones and the releases are made accordingly. This is achieved by developing separate release rules for each reservoir as a function of its inflow, storage and downstream conditions. The downstream conditions may be the storage level of the downstream reservoir or the water level in the downstream river reach. These rules are developed using multiple linear regression (MLR) technique and three years of historical data from 2012. The present water use plan is operational from the year 2012 and hence data from 2012 is only used for developing the release rules. In addition to these rules, the deviation from the preferred zones is deducted or added. At the starting of the simulation, the deviations are set as zero and the releases are computed. Then the final storage and reservoir water levels for that time period are estimated. If the water levels are outside the preferred storage zones, the deviations are estimated. The water level above the maximum level of

the preferred zone will have positive deviation and below the minimum level of preferred zone will have negative deviation. These releases equations are solved simultaneously until the downstream condition is satisfied. Thus, the iteration is continued within the simulation time step unit the upstream and downstream conditions are met. The final equations for the releases from each reservoir are given below:

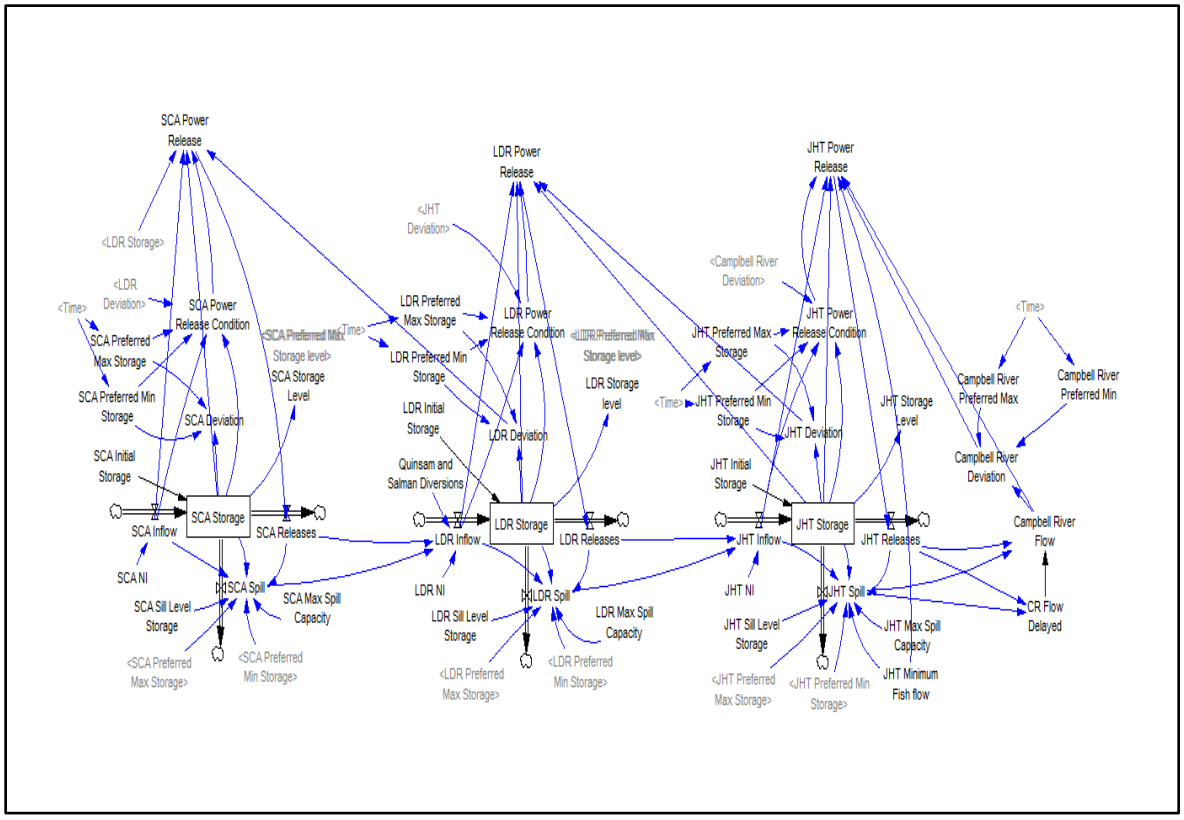

Figure 5.5 System Dynamics simulation model of Campbell River system (after Arunkumar and Simonovic, 2017).

For Strathcona reservoir:

$$SCA\_Release = ((SCA\ Inflow * 0.14832) + (SCA\ Storage * 0.00508) + (0.01486 * LDR\ Storage) - 122.676 - LDR\ Deviation) \quad (5.2)$$

For Ladore reservoir:

$$LDR\_Release = \begin{pmatrix} (LDR\ Inflow * 0.33505) + (LDR\ Storage * 0.00593) \\ + (JHT\ Storage * (-1.10655)) + 555.218 - JHT\ Deviation \end{pmatrix} \quad (5.3)$$

For John Hart reservoir:

$$JHT\_Release = \begin{pmatrix} (JHT\ Inflow * 0.07369) + (JHT\ Storage * 0.07855) + \\ (Campbell\ River\ Flow * 0.77581) - 32.4619 - \\ Camplbell\ River\ Deviation - JHT\ Minimum\ Fish\ flow \end{pmatrix} \quad (5.4)$$

For hydropower calculation the following equation is used in this study:

$$MW_t = \frac{9.81 * 10^6 R_t H_t \eta}{3600 * 1000} = 2.725 R_t H_t \eta \quad (5.5)$$

where MW is megawatts power is produced in time t, R_t is total release in Mm^3 in time period t, H_t is the net head of water available for power generation in meters during t time period and η is turbine efficiency. Here turbine efficiency (η) is taken as 0.80, 0.90 and 0.90 for Strathcona, Ladore and John Hart power station respectively. Gross water head for all three reservoirs can be calculated from SDM outputs and tail water head elevation (174.35 m for Strathcona, 144.1 m for Ladore and 15.03 m for John Hart) is provided by BC Hydro. Subtracting tail water head elevation from gross head gives us the net head (H_t). The following sub-section provides projected reservoirs operation details using SDM model under different climate change emission scenarios.

5.2.2 Future Flow Generation

As discussed above the SDM model connects all three reservoirs in a series where inflow data is needed for the first reservoir (Strathcona) to start the model simulation. Streamflow data from UBC watershed model (discussed in section 4.2) is used as input to the SDM model. We simulated the SDM model for both time periods i.e. historical (1984-2013) and future (2036-2065 & 2066-2095). The SDM model gives inflow, storage and release information for all three reservoirs (SCA, LDR & JHT). The SDM model tried to keep the storage level in between maximum level of preferred zone (WUP_{max}) and minimum level of preferred zone (WUP_{min}) specified by BC Hydro (BC Hydro Generation Resource Management, 2012). From release and storage information, we calculated power (plug into Eq. (5.5)). The SDM model simulated and observed historical (1984 to 2013) daily mean inflow (m^3/s), storage (m) and release (m^3/s) information of Strathcona reservoir are shown in Figure 5.6. From the Figure 5.6 (b), it can be conclude that the SDM model performance is satisfactory in terms of keeping simulated storage level in between WUP_{max} and WUP_{min} zone. The following subsection discussed simulated results for future time period (2036-2065) from the SDM model.

5.2.2.1 Results

Projected mean daily future simulated inflow (m^3/s), storage (m) and release (m^3/s) for near future (2036-2065) with historical (1984-2013) observed inflow (m^3/s), storage (m) and release (m^3/s) information from Strathcona dam under different emission scenarios are shown in Figure 5.7. The dark black line represents historical information in all subplots of Figure 5.7. Figure 5.8 and Figure 5.9 provide the same information as Figure 5.7 but for LDR and JHT reservoir. As the inflow of SCA is decreasing in summer time

(Figure 5.7 (a-c)) and SDM model tries to keep the same operational strategies (storage level in between

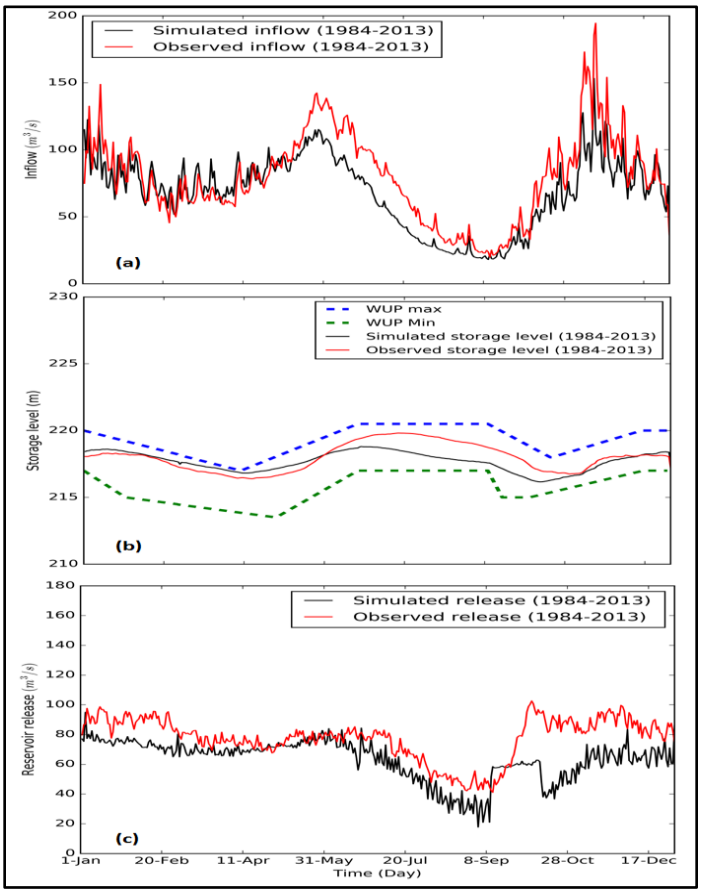

Figure 5.6 SDM model simulated and observed historical (1984-2013) daily mean (a) inflow (m^3/s), (b) storage (m) and (c) release (m^3/s) information of Strathcona reservoir, British Columbia, Canada (after Mandal *et al.*, 2016a).

WUP_{max} and WUP_{min}) specified by BC Hydro, the release from the SCA reservoir will be greatly affected in near future (2036-2065) (Figure 5.7 (g-i)). Simulated future releases (2036-2065) (Figure 5.7 (g-i)) for almost all scenarios are smaller than the observed historical (1984-2013). Similar kind of pattern can be found for other two downstream reservoirs i.e. LDR and JHT (Figure 5.8 and Figure 5.9). As it is found that due to climate change, inflow into the SCA reservoir is going to decrease for all seasons except winter

(Table 4.3), the release will also follow the similar decreasing trend. As the hydropower is directly proportional to reservoir storage level and release, it will also decrease. Figure 5.10 to Figure 5.12 describe projected future (2036-2065) with historical (1984-2013) hydropower production from SCA, LDR and JHT under different emission scenarios, respectively. As the release from SCA decreases from late spring to beginning of fall, the power production also decreases. This similar pattern can be found for LDR and JHT too (Figure 5.11 and Figure 5.12). A comparison of mean seasonal future (2036-2065 & 2066-2095) power production and historical power production is given in Table 5.1 to Table 5.3 for SCA, JHT and LDR under different emission scenarios, respectively. The results show that power production from all three reservoirs is going to decrease in both future time periods when compared to historical (1984-2013). In the near future (2036-2065), -7% (RCP 4.5, winter) to -67% (RCP 8.5, summer) change and in the far future (2065-2066), -6% (RCP 4.5 RCP 8.5, winter) to -72% (RCP 8.5, summer) changes in power production are projected for SCA reservoir (Table 5.1). For LDR, -26% (RCP 2.6 & RCP 4.5, spring) to -70% (RCP 8.5, summer) change in between 2036 to 2065 and -27% (RCP 2.6, spring) to -74% (RCP 8.5, summer) change in between 2066 to 2095 are projected (Table 5.2). Power production change from -11 % (RCP 4.5, spring) to -60% (RCP 8.5, summer) in between 2036-2065 and changes from -11% (RCP 2.6, spring) -66% (RCP 8.5, summer) are predicted for JHT reservoir (Table 5.3). The negative changes in power production during summer and fall time are larger compared to winter and spring seasons for all three reservoirs in both future time periods. As discussed in Section 4.2, streamflow of the Campbell river will decrease during summer and fall, which has direct influence on the reservoir release as reflected in the present results.

Another important observation is that change in power production of the upstream reservoir (SCA) is smaller when compared to the downstream reservoirs (LDR & JHT). As the upstream reservoir gets lower inflow, maintaining the reservoir water level at certain position requires reduction of release (compared to historical release) which directly affects power production. In addition, these three reservoirs are connected in series, therefore if the first reservoir release deviate from target, the deviation will propagate through other two reservoirs - the reason behind higher percentage change in downstream reservoir power production. Projected mean daily future simulated inflow (m^3/s), storage (m) and release (m^3/s) for the far future (2066-2095) and with historical (1984-2013) observed inflow (m^3/s), storage (m) and release (m^3/s) information under different emission scenarios are given in Appendix-C. A similar trend can be found for the far future (2066 to 2095) as found for the near future (2036 to 2065).

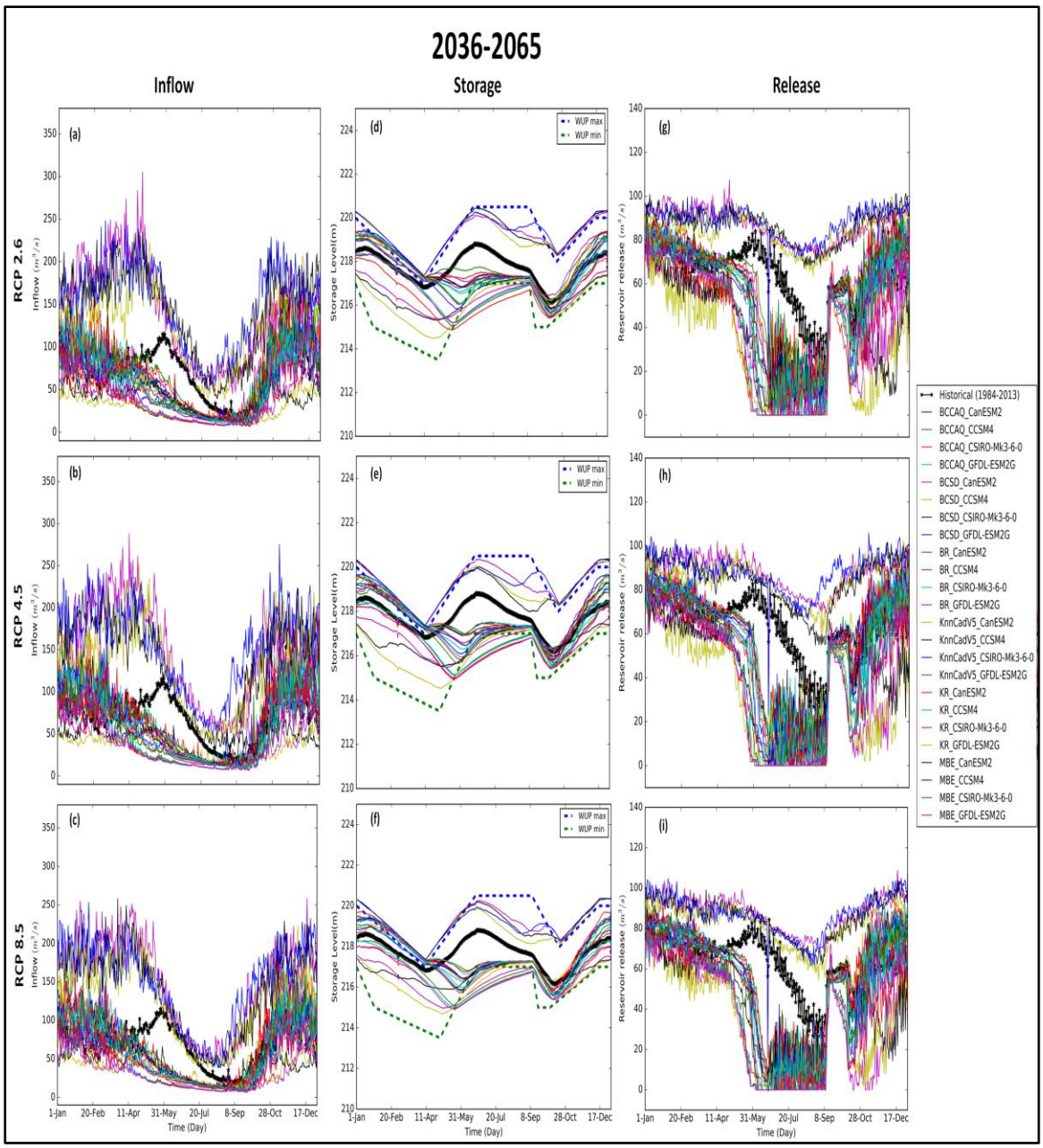

Figure 5.7 Projected mean daily simulated inflow (m^3/s) (a-c), storage level (m) (d-f) and release (m^3/s) (g-i) for near future (2036-2065) with historical (1984-2013) observed inflow (m^3/s), storage level (m) and release (m^3/s) from Strathcona Dam, BC, Canada for different emission scenarios (after Mandal *et al.*, 2016a).

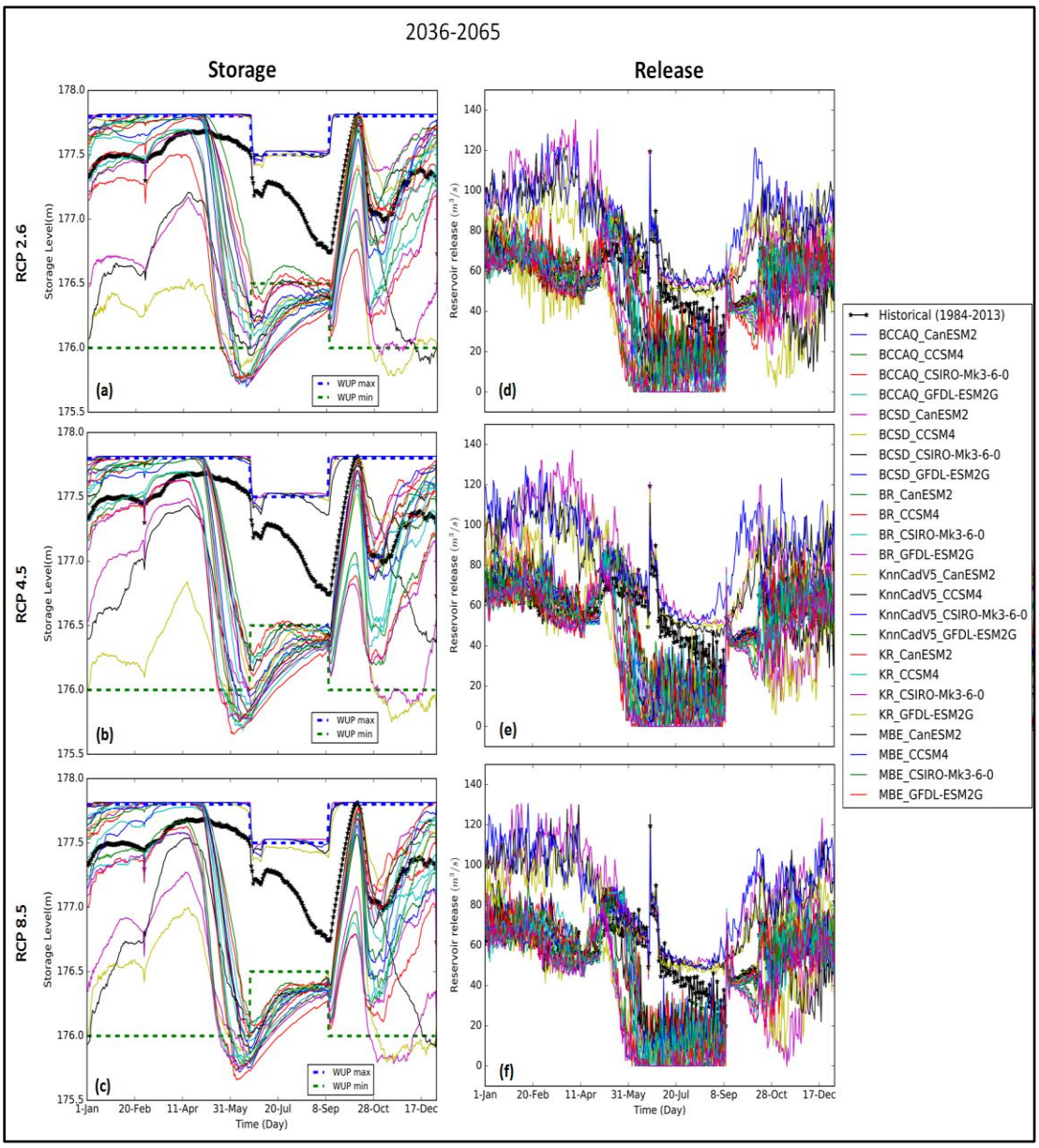

Figure 5.8 Projected mean daily simulated storage level (m) (a-c) and release (m^3/s) (d-f) for near future (2036-2065) with historical (1984-2013) observed storage level (m) and release (m^3/s) from Ladore Dam, BC, Canada for different emission scenarios (after Mandal *et al.*, 2016a).

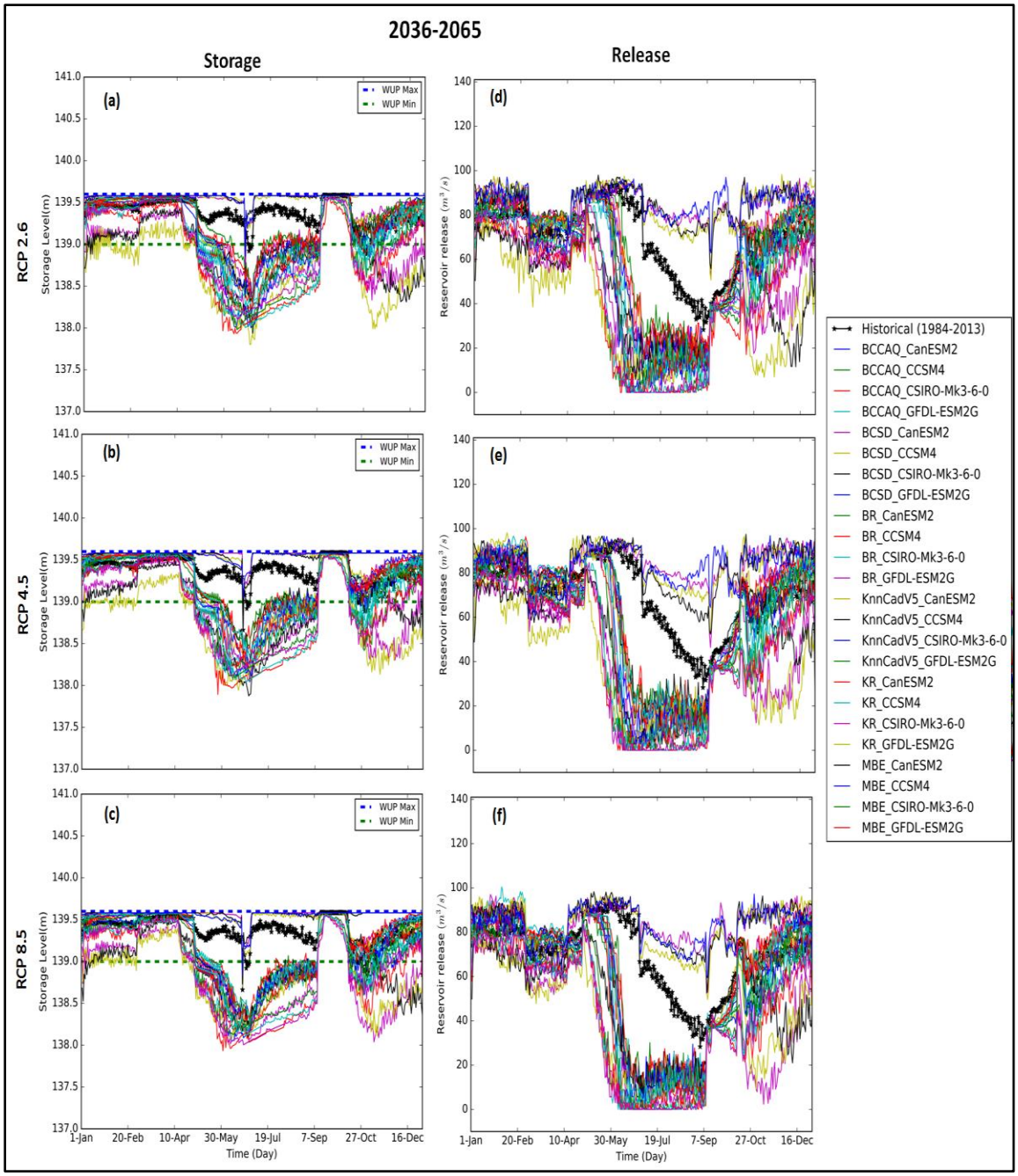

Figure 5.9 Projected mean daily simulated storage level (m) (a-c) and release (m^3/s) (d-f) for near future (2036-2065) with historical (1984-2013) observed storage level (m) and release (m^3/s) from John Hart Dam, BC, Canada for different emission scenarios (after Mandal *et al.*, 2016a).

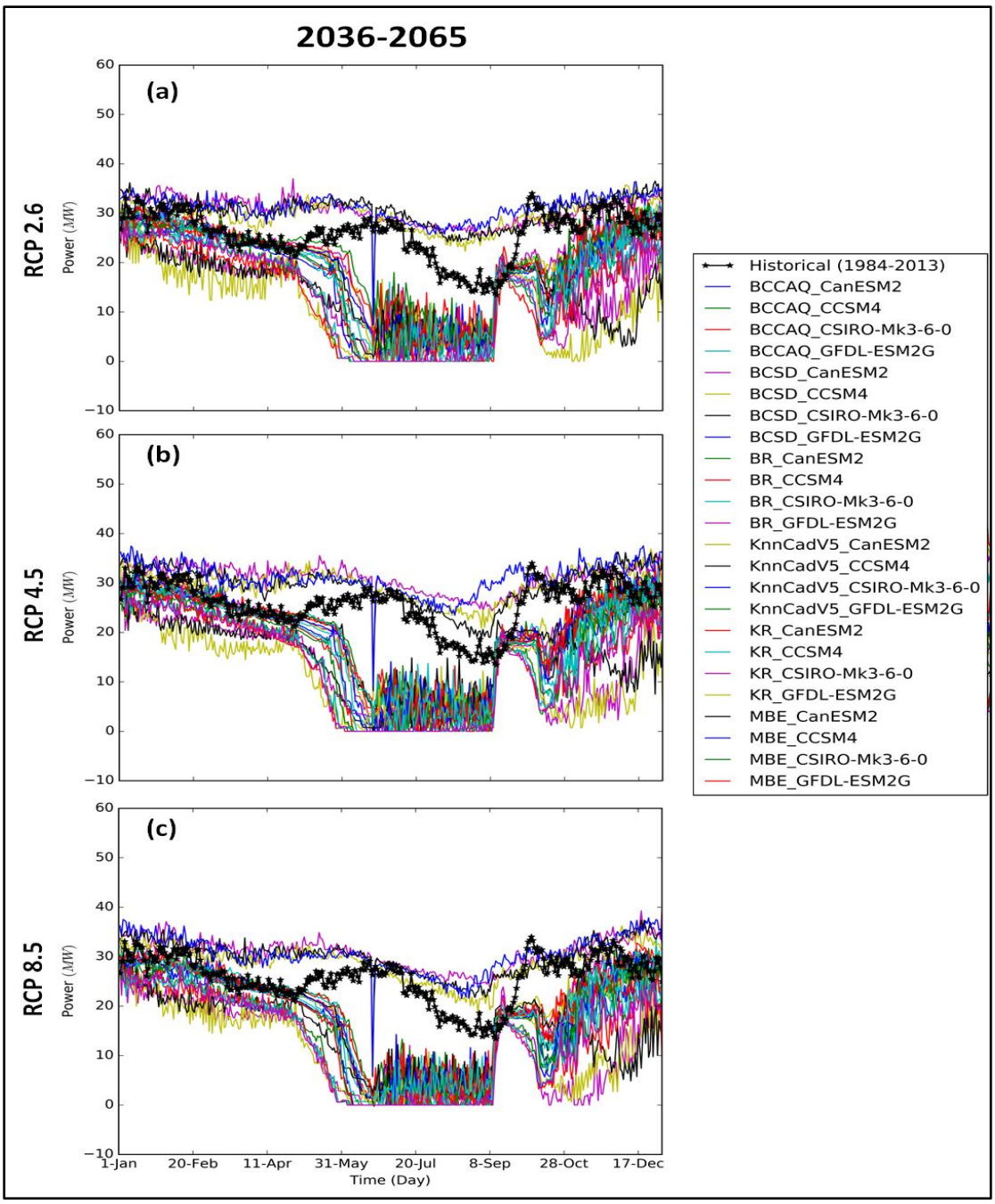

Figure 5.10 Projected mean daily power production (megawatt) for near future (2036-2065) with historical (1984-2013) power production (megawatt) from Strathcona Dam, BC, Canada for different emission scenarios (after Mandal *et al.*, 2016a).

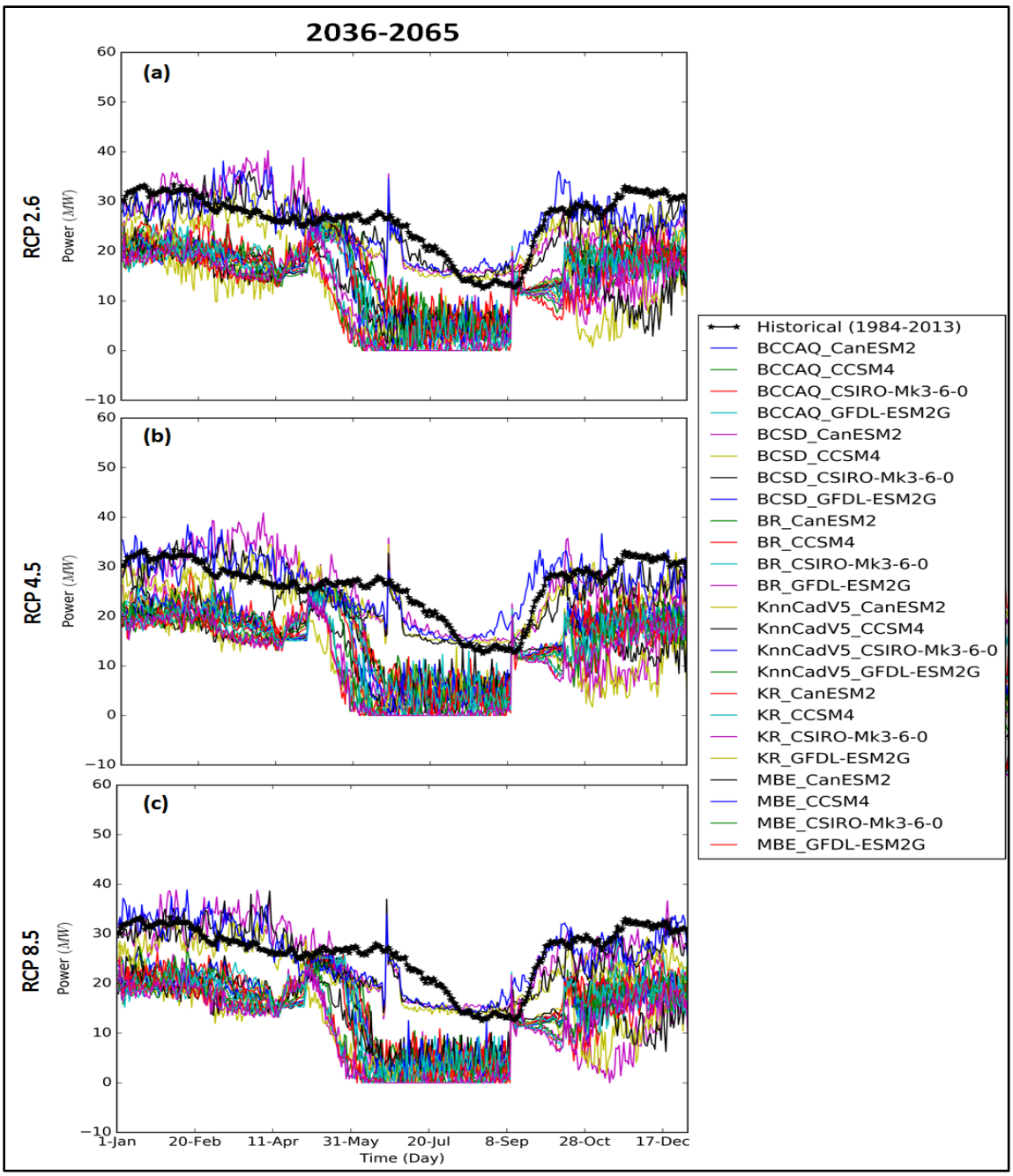

Figure 5.11 Projected mean daily power production (megawatt) for near future (2036-2065) with historical (1984-2013) power production (megawatt) from Ladore Dam, BC, Canada for different emission scenarios (after Mandal *et al.*, 2016a).

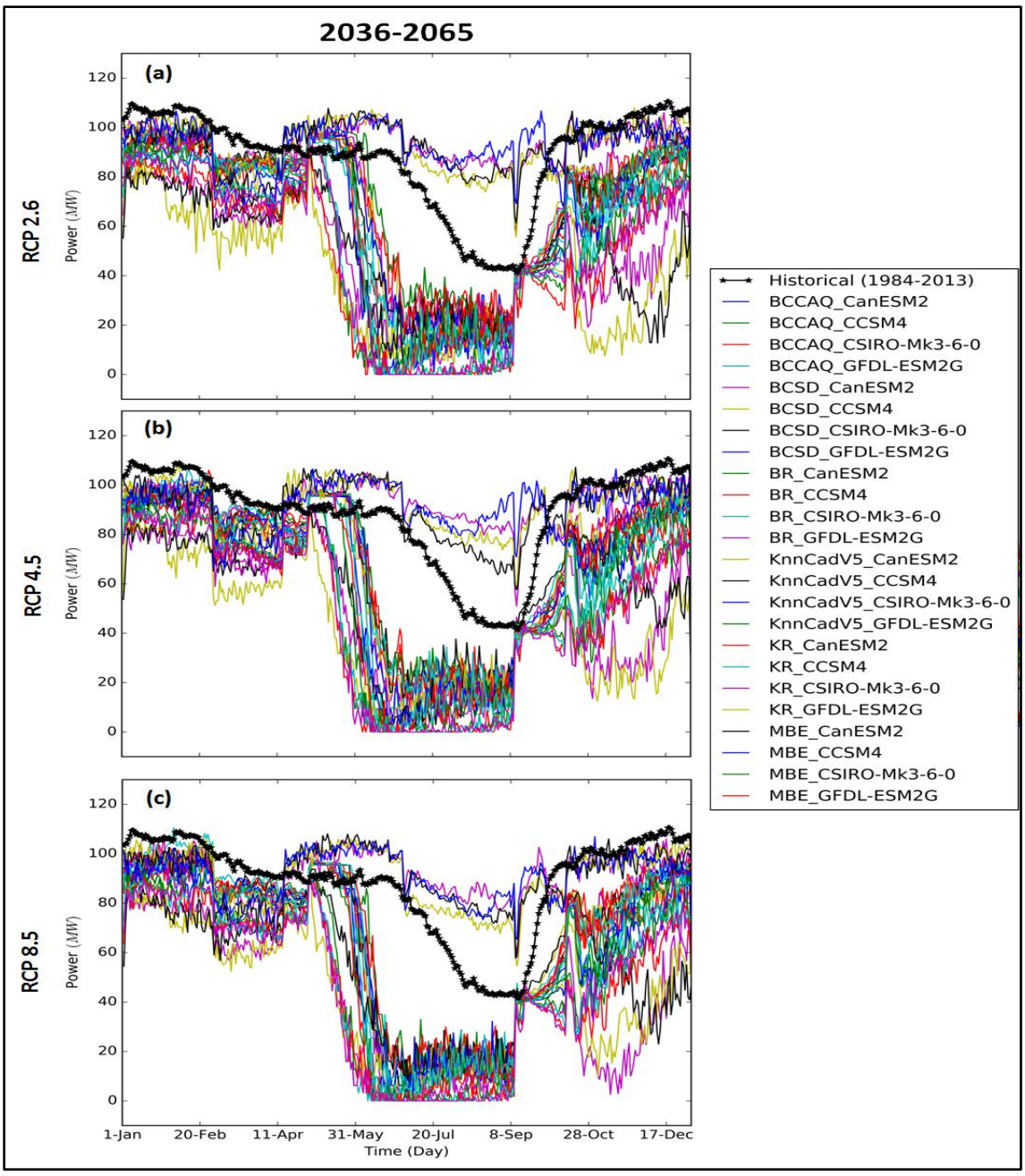

Figure 5.12 Projected mean daily power production (megawatt) for near future (2036-2065) with historical (1984-2013) power production (megawatt) from John Hart Dam, BC, Canada for different emission scenarios (after Mandal *et al.*, 2016a).

Table 5.1 Comparison of Historical (1984-2013) and future mean seasonal power production (megawatt) for different emission scenarios in Strathcona Dam, Campbell River System, BC, Canada (after Mandal *et al.*, 2016a).

	2036-2065						
	Historical	RCP 2.6		RCP 4.5		RCP 8.5	
	mean	mean	Change in mean value (%)	mean	Change in mean value (%)	mean	Change in mean value (%)
Winter	29.46	26.82	-9	27.30	-7	27.09	-8
Spring	24.53	22.44	-8	22.50	-8	22.12	-9
Summer	22.66	8.50	-61	7.85	-65	7.14	-67
Fall	25.93	18.22	-27	18.37	-27	17.70	-30
	2066-2095						
Winter	29.46	27.04	-8	27.50	-6	27.48	-6
Spring	24.53	22.42	-8	21.73	-11	21.32	-12
Summer	22.66	8.25	-62	6.70	-70	5.97	-72
Fall	25.93	18.07	-28	18.11	-28	17.88	-29

Table 5.2 Comparison of Historical (1984-2013) and future mean seasonal power production (megawatt) for different emission scenarios in Ladore Dam, Campbell River System, British Columbia, Canada (after Mandal *et al.*, 2016a).

	2036-2065						
	Historical	RCP 2.6		RCP 4.5		RCP 8.5	
	mean	mean	Change in mean value (%)	mean	Change in mean value (%)	mean	Change in mean value (%)
Winter	31.56	20.90	-33	21.45	-32	21.35	-32
Spring	27.00	19.79	-26	19.97	-26	19.65	-27
Summer	20.76	7.02	-65	6.55	-68	5.94	-70
Fall	25.13	15.24	-38	15.38	-37	14.90	-40
	2066-2095						
Winter	31.56	21.22	-32	21.76	-31	21.87	-30
Spring	27.00	19.66	-27	19.45	-28	19.06	-29
Summer	20.76	6.87	-65	5.56	-73	5.01	-74
Fall	25.13	15.20	-38	15.22	-38	15.00	-40

Table 5.3 Comparison of Historical (1984-2013) and future mean seasonal power production (megawatt) for different emission scenarios in John Hart Dam, Campbell River System, British Columbia, Canada (after Mandal *et al.*, 2016a).

	2036-2065						
	Historical	RCP 2.6		RCP 4.5		RCP 8.5	
	mean	mean	Change in mean value (%)	mean	Change in mean value (%)	mean	Change in mean value (%)
Winter	106.42	87.82	-17	88.63	-16	87.92	-17
Spring	92.05	80.94	-12	81.53	-11	80.54	-12
Summer	68.73	30.51	-54	28.36	-58	25.94	-60
Fall	84.56	59.32	-28	59.51	-28	57.40	-31
	2066-2095						
Winter	106.42	87.88	-17	88.62	-16	88.20	-17
Spring	92.05	81.47	-11	79.55	-13	78.47	-14
Summer	68.72	29.93	-55	24.23	-64	21.87	-66
Fall	84.56	58.51	-29	58.31	-30	57.38	-31

5.3 Summary

In this Chapter, a system dynamics simulation (SDM) model is used to assess climate change impacts on multiple reservoirs in the Campbell River System. Results are analyzed under different GHG emission scenarios. The output from UBC watershed model is used as an input to the SDM model. The SDM model provides historical and future inflow, storage and release information for all three reservoirs (SCA, LDR, JHT) in the CRS. Using this information, we calculated hydropower and compared with historical hydropower produced by reservoirs.

The results show that the release from all three reservoirs is projected to decrease; consequently power production is also projected to decrease. Power production during summer and fall will be more drastically effected due to climate change as compared to winter and spring seasons. Deviation of hydropower production from target in the upstream reservoir (SCA) is smaller when compared to downstream reservoirs (LDR & JHT). It should be noted that we have only discussed the variation of hydropower production under different emission scenarios. The uncertainty analysis of hydropower production under different GCMs and DSMs can be considered for future work. The summary and conclusions are presented in the following chapter.

Chapter 6

6 Summary and Conclusions

The research reported in this thesis contributes towards the general methodology for the analyses of uncertainties within the climate change impact assessment process in managing water resources. This process includes selecting GCMs, selecting emission scenarios, downscaling hydro-climatic variables (e.g. precipitation, temperature), streamflow analysis and reservoir storage-release analyses. The following paragraphs provide a summary and the conclusions of the study presented in this thesis:

The first research question was related to the development of an efficient and robust multisite and multivariate statistical downscaling model for predicting precipitation at local scales. In this study a new beta regression based multisite and multivariate statistical downscaling method is developed for generating synthetic precipitation time series. This model can capture the temporal and spatial variability of the predictand at each downscaled location. The proposed model was compared with existing downscaling models and was found to be computationally inexpensive and ideal for practical engineering application.

The second objective was the quantification of climate change impacts on projected hydro-climatic variables and streamflow. This study investigated climate change impacts on precipitation in the Campbell River System, BC, Canada and also projected streamflow of the Campbell River under different climate change emission scenarios. This work is conducted for two different future time periods (2036 to 2065 and 2066 to 2095). Results show that the summer months (June, July and August) are typically drier

in comparison to the other seasons in the Campbell river basin. However, there is a potential for more extreme events in the spring (March, April and May). The median total monthly precipitation is higher for the winter months and there is potential for larger amounts of precipitation in the early spring in the future. Apart from these results we also found that climate change has a significant influence on streamflow variation. It is projected that the summer flow in the Campbell River will decrease and winter flows will increase in both future time periods. The generalized extreme value (GEV) distribution is used for the streamflow frequency analysis. Flow frequency analysis shows that the changes in the flow magnitude become more significant for higher return periods under climate change.

The third objective was the quantification of uncertainties in climate change impact assessment process. For this purpose, four global climate models (GCMs), three greenhouse gas emission scenarios (RCPs), six downscaling models (DSMs) and a hydrologic model (UBCWM) were used. Using these downscaling models, hydro-climatic variables (precipitation, maximum, and minimum temperature) are downscaled for different emission scenarios. The streamflow is generated using a hydrologic model (UBC watershed model) where downscaled hydro-climatic variables are used as an input into the hydrologic model. As we used three emission scenarios, four GCMs and six downscaling models for streamflow generation, the assessment process resulted in 72 different experiments (Figure 1.5). The 72 different streamflow time series are all considered as possible extreme scenarios for the assessment of three sources of uncertainty (choice of RCPs, GCMs and downscaling models). We analyzed uncertainty in projected precipitation, streamflow, and reservoir operation. Results were analyzed

temporally (monthly and quarterly) and spatially for two future time periods (2036 to 2065 and 2066 to 2095). An uncertainty metric was calculated using the variation in simulated precipitation due to choice of GCMs, emission scenarios and downscaling models. The results show that the selection of a downscaling method provides the largest amount of uncertainty when compared to the choice of GCM and/or emission scenario. However, the choice of GCM provides a significant amount of uncertainty if the choice of downscaling method is not considered. Similar conclusions have been found for future streamflow projections.

The fourth objective was to study climate change impacts on reservoir operation under uncertainty in hydrologic impacts of climate change. To address this objective we used a system dynamics simulation model (SDM) to connect all three reservoirs in the river basin. In this model, the reservoir components were modeled using stocks, flows, arrows, and auxiliary variables. The SDM model provides inflow, storage and release information for all three reservoirs (SCA, LDR & JHT). Streamflow predicted using UBC watershed model was used as an input to the SDM. The SDM model attempted to keep reservoirs storage levels within certain specified (WUP_{max} and WUP_{min}) zone established by BC Hydro (BC Hydro Generation Resource Management, 2012). The Campbell river flow originates from the mix of snow and rain. As the temperature increases, the snow and ice start melting faster and that affects the temporal distribution of contributing sources of streamflow. As the projected streamflow carries all different scenarios of climate change, the SDM model outputs also showed wide variations due to climate change. Since the future inflow of SCA varies seasonally and SDM model attempted to keep storage levels within the fixed range (WUP_{max} and WUP_{min}), release of SCA decreases compared to

historical (1984-2013). This situation creates inflow deficit in the LDR because LDR inflow is directly related to the release from SCA. It has been found that LDR and JHT release have a decreasing trend similar to SCA. The three reservoirs (SCA, LDR, and JHT) connect in a series. Therefore, it is obvious if one's release is affected due to low inflow others will be face the same fate. Results show that during late spring and summer seasons future release (2036 to 2065 and 2066 to 2095) will be lower compared to fall or winter seasons for all three reservoirs. Based on the results of this study re-evaluation of reservoir level targets and operating rules is suggested in order to address the potential impacts of changing climatic conditions.

The final objective of the study was to assess hydropower generation under changing climate conditions. The system dynamics simulation model used in this study provides storage and release information for all three reservoirs in the Campbell River System. From this information, future hydropower production rates are projected and compared with the historically obtained hydropower from the three reservoirs. Results show that in all season future hydropower production will be lower when compared to present production (1984-2013). The lower predicted future flows result in the decreases of reservoir releases and they result in lower power production. Another important observation is that the downstream reservoirs (LDR & JHT) are affected more in terms of power production compared to the upstream one (SCA).

As presented in Figure 1.5, the whole climate change impacts assessment process has multiple steps. Each step contributes some amount of uncertainty that propagates towards the final results. The careful observation points to the fact that the climate variables have uncertainty possess from different emission scenarios. However this uncertainty is larger

when GCMs simulated climate data is used because GCMs simulate climate variables mathematically considering multiple assumptions (Dobler *et al.*, 2012). Another source of variation results from downscaling the climate information to the regional scale. To quantify these uncertainties in climate variables, a simple relative matrix is calculated in this study (section 3.3.2). Based on this matrix, propagated uncertainties showed in different temporal and spatial scale (section 3.3.2). Later on we calculated uncertainty in streamflow using cdf and seasonal mean changes. Propagated uncertainty in reservoir storage and release is calculated using mean daily statistics. As discussed before, all three relative sources of uncertainty (RCPs, GCMs & DSMs) contribute towards the total uncertainty associated with the climate change impact assessment process. But one question still remains, what is the highest source of uncertainty? To answer this question, variations in streamflow for different GHGs emission scenarios, GCMs and downscaling models (Table 4.3 to Table 4.5) are analyzed. The results show that that largest source of uncertainty is from the choice of downscaling model, while emission scenarios contribute less uncertainty to the final results. However, all of these relative uncertainties accumulate and cause a significant variation in the end result which is reflected here in reservoirs release or power production. For example, in the near future (2036-2065) power production of SCA for RCP 2.6, varies from -9% to -61% (Table 5.1).

The results presented in this research considered consistency, not "certainty". This relates to the key analytical characters of "precision" versus "accuracy". A method may be very precise, in always providing the same outcome, but in fact, it may be inaccurate as the outcome is consistently biased. Thus, downscaling may result in more variable results, but the emission scenarios may be too conservative and/or the four GCMs may be highly

consistent, not because they are correct, but because they are based on the same analytical sequence and even often share the same equations. So these GCMs may be consistent, but all four may be quite incorrect. Therefore selection of GCMs is crucial for uncertainty analysis.

An extensive study is presented in this thesis to capture uncertainties in climate change impact assessment process. In a nutshell, adequate knowledge is needed regarding future climate impacts. Without adequate information, it is very difficult to connect climate impacts with adaptation actions. Water resource planners and managers are interested in information regarding adaptive and risk-based planning approaches for management of water resources systems. Appropriate management procedures are needed for projecting hydrological change. This present study could be used as a stepping stone for the management of water resource system under climate change. In addition, this work has also opened up several potential research areas that can be considered as the future scope of the present work. Details of potential future research areas are described in the following section.

6.1 Scope of Future Studies

The beta regression downscaling model developed here is a data-driven method which builds a stationary relationship between climate variables and daily precipitation which may not always be accurate. Salvi *et al.*,(2015) observed that a regression (kernel regression) based statistical downscaling models fail to capture the changes in mean precipitation under non-stationary climate. Therefore testing the present beta regression based downscaling model under non-stationary climate conditions can be considered as a future research topic.

Another limitation of this study is “link” function in the beta regression model. Here only the logit link function is used. Several link functions are available such as probit, log–log link *etc*. Hence, testing the model using different link functions can improve model robustness.

The present study includes a single river system, and we do not really know if the consistency, especially across GCMs is typical. It will be appropriate for the comparison to be undertaken with other river systems and particularly in other hydro-geographical regions. The literature that the consistency of GCMs varies substantially across regions (Rupp *et al.*, 2013).

Use of a single hydrologic model (UBCWM) in this work is a limitation at this stage. Streamflow generation using multiple hydrological models with multiple emission scenarios, GCMs and downscaling models should be considered for the continuation of the presented work.

The final suggestion is related to the use of a system dynamics simulation model for reservoirs operation analysis. The model provides future storage release information under climate change. Results show that future release will be lower if the present reservoir operation policy is followed in the future. Release and storage reservoir targets are dependent on the functional requirements of the reservoir system. In order to adapt to the effects of climate change on stream flows and meet various reservoir water demands and flood control requirements, an optimization analysis is suggested to derive operating rules that will be better adapted to changing climate conditions.

The programming code of the beta regression model is given in Appendix-D and Appendix-E provides flow frequency analysis code.

References

Abadi LSK, Shamsai A, Goharnejad H. 2015. An Analysis of the Sustainability of Basin Water Resources using Vensim Model. *KSCE Journal of Civil Engineering* **19** (6): 1941–1949 DOI: 10.1007/s12205-014-0570-7

Ahmad S, Simonovic SP. 2000. System Dynamics Modeling of Reservoir Operations for Flood Management. *Journal of Computing in Civil Engineering* **14** (3): 190–198 DOI: 10.1061/(ASCE)0887-3801(2000)14:3(190)

Ahmadi M, Haddad OB, Loáiciga HA. 2014. Adaptive Reservoir Operation Rules Under Climatic Change. *Water Resources Management* **29** (4): 1247–1266 DOI: 10.1007/s11269-014-0871-0

Ahmed KF, Wang G, Silander J, Wilson AM, Allen JM, Horton R, Anyah R. 2013. Statistical Downscaling and Bias Correction of Climate Model Outputs for Climate Change Impact Assessment in The U.S. Northeast. *Global and Planetary Change* **100**: 320–332 DOI: 10.1016/j.gloplacha.2012.11.003

Anandhi A, Frei A, Pierson DC, Schneiderman EM, Zion MS, Lounsbury D, Matonse AH. 2011. Examination of Change Factor Methodologies for Climate Change Impact Assessment. *Water Resources Research* **47**: 1–10 DOI: 10.1029/2010WR009104

Arunkumar R, Simonovic SP. 2017. Dynamic resilience of a multi-reservoir system for various failure events (manuscript under preparation)

Asokan SM, Dutta D. 2008. Analysis of Water Resources in the Mahanadi River Basin, India Under Projected Climate Conditions. *Hydrological Processes* **22**: 3589–3603 DOI: 10.1002/hyp

Bardossy A, Duckstein L, Bogardi I. 1995. Fuzzy Rule-Based Classification of Atmospheric Circulation Patterns. *International Journal of Climatology* **15** (10): 1087–1097 DOI: 10.1002/joc.3370151003

BC Hydro Generation Resource Management. 2012. Campbell River System Water Use Plan Available at: http://www.bchydro.com/content/dam/hydro/medialib/internet/documents/planning_regulatory/wup/vancouver_island/2012q4/campbell_river_WUP_accept_2012_11_21.pdf

Brandsma T, Buishand TA. 1998. Simulation of Extreme Precipitation in the Rhine Basin by Nearest-Neighbour Resampling. *Hydrology and Earth System Sciences* **2** (2–3): 195–209 DOI: 10.5194/hess-2-195-1998

Brock G, Pihur V, Datta S, Datta S. 2008. clValid , an R Package for Cluster Validation. *Journal of Statistical Software* **25(4)** (4)

Brown RD, Mote PW. 2009. The Response of Northern Hemisphere Snow Cover to a Changing Climate. *Journal of Climate* **22** (8): 2124–2145 DOI: 10.1175/2008JCLI2665.1

Bürger G, Sobie SR, Cannon AJ, Werner AT, Murdock TQ. 2012. Downscaling Extremes: An Intercomparison of Multiple Methods for Future Climate. *Journal of Climate* **26**: 3429–3449 DOI: 10.1175/JCLI-D-12-00249.1

Burn DH, Simonovic SP. 1996. Sensitivity of Reservoir Operation Performance to Climatic Change. *Water Resources Management* **10**: 463–478

Canadian Council of Professional Engineers. 2008. Adapting to Climate Change: Canada's First national Engineering Vulnerability Assessment of Public Infrastructure Available at: http://www.pievc.ca/e/Adapting_to_climate_Change_Report_Final.pdf

Canadian Institute of Actuaries. 2014. Water Damage Risk and Canadian Property Insurance Pricing Available at: http://www.cia-ica.ca/docs/default-source/2014/214020e.pdf

Carven P, Wahba G. 1979. Smoothing Noisy Data with Spline Functions. *Numerische Mathematik*: 377–403

Chen J, Brissette FP, Leconte R. 2014. Assessing Regression-Based Statistical Approaches for Downscaling Precipitation over North America. *Hydrological Processes* **28** (9): 3482–3504 DOI: 10.1002/hyp.9889

Chen J, Brissette FP, Poulin A, Leconte R. 2011. Overall Uncertainty Study of the Hydrological Impacts of Climate Change for a Canadian Watershed. *Water Resources Research* **47**: W12509 DOI: 10.1029/2011WR010602

Christensen NS, Wood AW, Voisin N, Lettenmaier DP, Palmer RN. 2004. The Effects of Climate Change on the Hydrology and Water Resources of the Colorado River Basin. *Climate Change* **62**: 337–363 DOI: 10.1023/B:CLIM.0000013684.13621.1f

Chu H-J, Chang L-C, Lin Y-P, Wang Y-C, Chen Y-W. 2010. Application of System Dynamics on Shallow Multipurpose Artificial Lakes: A Case Study of Detention Pond at Tainan, Taiwan. *Environmental Modeling & Assessment* **15** (3): 211–221 DOI: 10.1007/s10666-009-9196-4

Coulibaly P, Dibike YB, Anctil F. 2005. Downscaling Precipitation and Temperature with Temporal Neural Networks. *Journal of Hydrometeorology* **6** (4): 483–496 DOI: 10.1175/JHM409.1

Craig JR, Snowdon AP. 2010. Raven: A Rigorously Formalized Modular Hydrological Model. *Environmental Modeling and Software* **2** (20) Available at: http://www.civil.uwaterloo.ca/jrcraig/Raven/files/RavenManual_v2.6.pdf

Das S, Simonovic SP. 2012. Assessment of Uncertainty in Flood Flows Under Cliamte Change: The Upper Thames River Basin (Ontario, Canada). Department of Civil and Environmental Engineering, University of Western Ontario, London, Ontario. Available at: http://www.eng.uwo.ca/research/iclr/fids/publications/products/79.pdf

Das S, Millington N, Simonovic SP. 2013. Distribution Choice for the Assessment of Design Rainfall for the City of London (Ontario, Canada) Under Climate Change. *Canadian Journal of Civil Engineering* **40** (2): 121–129 DOI: 10.1139/cjce-2011-0548

Dibike YB, Coulibaly P. 2005. Hydrologic Impact of Climate Change in the Saguenay Watershed: Comparison of Downscaling Methods and Hydrologic Models. *Journal of Hydrology* **307** (1–4): 145–163 DOI: 10.1016/j.jhydrol.2004.10.012

Dobler C, Hagemann S, Wilby RL, StÃtter J. 2012. Quantifying different sources of uncertainty in hydrological projections in an Alpine watershed. *Hydrology and Earth System Sciences* **16** (11): 4343–4360 DOI: 10.5194/hess-16-4343-2012

Eamer J, Hayes T, Simth R. 2010. Canadian Biodiversity: Ecosystem Status and Trends 2010 Available at: http://www.biodivcanada.ca/A519F000-8427-4F8C-9521-8A95AE287753/EN_CanadianBiodiversity_FULL.pdf

Eum H, Simonovic SP, Kim Y. 2010. Climate Change Impact Assessment Using K-Nearest Neighbor Weather Generator: Case Study of the Nakdong River Basin in Korea. *Journal of Hydrologic Engineering* **15** (10): 772–785 DOI: 10.1061/(ASCE)HE.1943-5584.0000251

Eum H-I, Simonovic SP. 2012. Assessment on Variability of Extreme Climate Events for the Upper Thames River Basin in Canada. *Hydrological Processes* **26** (4): 485–499 DOI: 10.1002/hyp.8145

Eum H-I, Arunachalam V, Simonovic SP. 2009. Integrated Reservoir Management System for Adaptation to Climate Change Impacts in the Upper Thames River Basin Available at: http://citeseerx.ist.psu.edu/viewdoc/download?doi=10.1.1.668.3450&rep=rep1&type=pdf

Felfelani F, Movahed AJ, Zarghami M. 2013. Simulating Hedging Rules for Effective Reservoir Operation by using System Dynamics: A Case Study of Dez Reservoir, Iran. *Lake and Reservoir Management* **29** (2): 126–140 DOI: 10.1080/10402381.2013.801542

Ferrari SLP, Cribari-Neto F. 2004. Beta Regression for Modelling Rates and Proportions. *Journal of Applied Statistics* **31**: 799–815 DOI: 10.1080/0266476042000214501

Fowler HJ, Wilby RL. 2010. Detecting Changes in Seasonal Precipitation Extremes using Regional Climate Model Projections: Implications for Managing Fluvial Flood Risk. *Water Resources Research* **46** (3): 1–17 DOI: 10.1029/2008WR007636

Gates WL, Boyle JS, Covey C, Dease CG, Doutriaux CM, Drach RS, Fiorino M, Gleckler PJ, Hnilo JJ, Marlais SM, et al. 1999. An Overview of the Results of the Atmospheric Model Intercomparison Project (AMIP I). *Bulletin of the American Meteorological Society* **80** (1): 29–55 DOI: 10.1175/1520-0477(1999)080<0029:AOOTRO>2.0.CO;2

Gaur A, Simonovic PS. 2013. Climate Change Impact on Flood Hazard in the Grand River Basin, Ontario, Canada Available at: http://ir.lib.uwo.ca/cgi/viewcontent.cgi?article=2592&context=etd

Ghosh S. 2010. SVM-PGSL Coupled Approach for Statistical Downscaling to Predict Rainfall from GCM Output. *Journal of Geophysical Research* **115** (D22): D22102 DOI: 10.1029/2009JD013548

Ghosh S, Mujumdar PP. 2006. Future Rainfall Scenario over Orissa with GCM Projections by statistical Downscaling. *Current Science* **90** (3)

Goyal MK, Ojha CSP. 2010. Evaluation of Various Linear Regression Methods for Downscaling of Mean Monthly Precipitation in Arid Pichola Watershed. *Natural Resources* **1** (1): 11–18 DOI: 10.4236/nr.2010.11002

Groisman PY, Karl TR, Easterling DR, Knight RW, Jamason PF, Hennessy KJ, Suppiah R, Page CM, Wibig J, Krzysztof, Fortuniak Vyacheslav RN, et al. 1999. Changes in the Probability of Heavy Precipitation. Important Indicators of Climate Change. *Climate Change* **42**: 243–283

Gyalistras D, Storch H Von, Fischlin A, Beniston M. 1994. Linking GCM-Simulated Climatic Changes to Ecosystem Models: Case Studies of Statistical Downscaling in the Alps. *Climate Res.* **4**: 167–189

Hashmi MZ, Shamseldin AY, Melville BW. 2009. Statistical Downscaling of

Precipitation: State-of-the-Art and Application of Bayesian Multi-model Approach for Uncertainty Assessment. *Hydrology and Earth System Sciences* **6**: 6535–6579 DOI: 10.5194/hessd-6-6535-2009

Hay LE, McCabe GJ, Wolock DM, Ayers MA. 1991. Simulation of Precipitation by Weather Type Analysis. *Water Resources Research* **27** (4): 493–501 DOI: 10.1029/90WR02650

Heffernan JE. 2016. An Introduction to Statistical Modeling of Extreme Values: 1–33 Available at: http://www.ral.ucar.edu/~ericg/softextreme.php

Hertig E, Jacobeit J. 2013. A Novel Approach to Statistical Downscaling Considering Nonstationarities: Application to Daily Precipitation in the Mediterranean Area. *Journal of Geophysical Research: Atmospheres* **118** (2): 520–533 DOI: 10.1002/jgrd.50112

Hewitson BC, Crane RG. 1996. Climate Downscaling : Techniques and Application. *Climate Research* **7**: 85–95

Hosking JRM, Wallis JR. 1997. *Regional Frequency Analysis: An approach based on L-moments.* United States of America by Cambridge University Press, New York. Available at: https://books.google.com.pe/books?hl=es&lr=&id=gurAnfB4nvUC&oi=fnd&pg=PP1&dq=Regional+frequency+analysis+an+approach+based+on+l-moments&ots=7Re17uu4PZ&sig=cQloBXfu6O-1BS3wGAj_pUvSJYI#v=onepage&q&f=false

Hughes JP, Guttorp P. 1994. A Class of Stochastic Models for Relating Synoptic Atmospheric Patterns to Regional Hydrologic Phenomena. *Water Resources Research* **30** (5): 1535–1546 DOI: 10.1029/93WR02983

Hughes JP, Guttorp P, Charles SP. 1999. A Non-homogeneous Hidden Markov Model for Precipitation Occurrence. *Applied Statistics* **48(1)** (1): 15–30 Available at: http://doi.wiley.com/10.1111/1467-9876.00136

Hutchinson MF, de Hoog FR. 1985. Smoothing noisy data with spline functions. *Numerische Mathematik* **47** (1): 99–106 DOI: 10.1007/BF01389878

Hutchinson MF, Xu T. 2013. Anusplin Version 4.4 User Guide. (August) Available at: http://fennerschool.anu.edu.au/files/anusplin44.pdf

IPCC. 2000. Summary for Policymakers Emissions Scenarios

IPCC. 2007. Climate change 2007: The Physical Science Basis.Basis. Contribution of Working Group I to the Fourth Assesment Report of the Intergovernmental Panel on Climate Change DOI: 10.1038/446727a

IPCC. 2013. *Climate Change 2013: The Physical Science Basis. Contribution of Working Group I to the Fifth Assessment Report of the Intergovernmental Panel on Climate Change*. Cambridge University Press, Cambridge, United Kingdom and New York, NY, USA, 1535 pp.

Irwin S, Srivastav RK, Simonovic SP, Burn DH. 2016. Delineation of Precipitation Regions using Location and Atmospheric Variables : The Role of Attribute Selection. *Hydrological Sciences Journal* **62** (2) DOI: 10.1080/02626667.2016.1183776

Jahandideh-Tehrani M, Bozorg Haddad O, Mariño MA. 2014. Power Generation Simulation of a Hydropower Reservoir System Using System Dynamics: Case Study of Karoon Reservoir System. *Journal of Energy Engineering* **140** (4): 4014003 DOI: 10.1061/(ASCE)EY.1943-7897.0000179

James G, Witten D, Hastie T, Tibshirani R. 2013. *An Introduction to Statistical Learning with Applications in R*. DOI: 10.1007/978-1-4614-7138-7

Jiang T, Chen YD, Xu C yu, Chen X, Chen X, Singh VP. 2007. Comparison of Hydrological Impacts of Climate Change Simulated by Six Hydrological Models in the Dongjiang Basin, South China. *Journal of Hydrology* **336** (3–4): 316–333 DOI: 10.1016/j.jhydrol.2007.01.010

Kalnay E, Kanamitsu M, Kistler R, Collins W, Deaven D, Gandin L, Iredell M, Saha S, White G, Woollen J, et al. 1996. The NCEP/NCAR 40-year reanalysis project. *Bulletin of the American Meteorological Society* **77** (3): 437–471 DOI: 10.1175/1520-0477(1996)077<0437:TNYRP>2.0.CO;2

Kannan S, Ghosh S. 2010. Prediction of Daily Rainfall State in a River Basin using Statistical Downscaling from GCM Output. *Stochastic Environmental Research and Risk Assessment* **25** (4): 457–474 DOI: 10.1007/s00477-010-0415-y

Kannan S, Ghosh S. 2013. A Nonparametric Kernel Regression Model for Downscaling Multisite Daily Precipitation in The Mahanadi Basin. *Water Resources Research* **49**: 1360–1385 DOI: 10.1002/wrcr.20118

Kay AL, Davies HN, Bell VA, Jones RG. 2009. Comparison of Uncertainty Sources for Climate Change Impacts: Flood Frequency in England. *Climatic Change* **92**: 41–63 DOI: 10.1007/s10584-008-9471-4

King LM, Mcleod IA, Simonovic SP. 2014. Simulation of Historical Temperatures Using A Multi-site, Multivariate Block Resampling Algorithm with Perturbation. *Hydrological Processes* **28**: 905–912 DOI: 10.1002/hyp.9596

King LM, Mcleod IA, Simonovic SP. 2015. Improved Weather Generator Algorithm for Multisite Simulation of Precipitation and Temperature. *Journal of the American Water Resources Association* **7**: 1–16 DOI: 10.1111/1752-1688.12307

Kishtawal CM, Niyogi D, Tewari M, Pielke RA, Shepherd JM. 2010. Urbanization Signature in the Observed Heavy Rainfall Climatology over India. *International Journal of Climatology* **30** (13): 1908–1916 DOI: 10.1002/joc.2044

Labat D, Goddéris Y, Probst JL, Guyot JL. 2004. Evidence for Global Runoff Increase Related to Climate Warming. *Advances in Water Resources* **27** (6): 631–642 DOI: 10.1016/j.advwatres.2004.02.020

Leclerc M, Ouarda TBMJ. 2007. Non-Stationary Regional Flood Frequency Analysis at Ungauged Sites. *Journal of Hydrology* **343** (3–4): 254–265 DOI:

10.1016/j.jhydrol.2007.06.021

Lee T, Ouarda TBMJ, Jeong C. 2012. Nonparametric Multivariate Weather Generator and an Extreme Value Theory for Bandwidth Selection. *Journal of Hydrology* **452**–**453**: 161–171 DOI: 10.1016/j.jhydrol.2012.05.047

Li L, Xu H, Chen X, Simonovic SP. 2010. Streamflow Forecast and Reservoir Operation Performance Assessment under Climate Change. *Water Resources Management* **24**: 83–104 DOI: 10.1007/s11269-009-9438-x

Liang XZ, Kunkel KE, Meehl GA, Jones RG, Wang JXL. 2008. Regional Climate Models Downscaling Analysis of General Circulation Models Present Climate Biases Propagation into Future Change Projections. *Geophysical Research Letters* **35** (8): 1–5 DOI: 10.1029/2007GL032849

Mandal S, Simonovic SP. 2017. Quantification of Uncertainty in the Assessment of Future Streamflow under Changing Climate Conditions. *Hydrological Processes (in press)* DOI: 10.1002/hyp.11174

Mandal S, Arunkumar R, Breach PA, Simonovic SP. 2016a. Reservoir operation under climate change : a system dynamics approach. *(manuscript under preparation)*

Mandal S, Breach PA, Simonovic SP. 2016b. Uncertainty in Precipitation Projection under Changing Climate Conditions: A Regional Case Study. *American Journal of Climate Change* **5** (1): 116–132 DOI: 10.4236/ajcc.2016.51012

Mandal S, Srivastav RK, Simonovic SP. 2016c. Use of Beta Regression for Statistical Downscaling of Precipitation in the Campbell River Basin, Brithish Columbia, Canada. *Journal of Hydrology* **538**: 49–62

Mandal S, Srivastav RK, Simonovic SP. 2016d. Use of beta regression for statistical downscaling of precipitation in the Campbell River basin, British Columbia, Canada. *Journal of Hydrology* **538**: 49–62 DOI: 10.1016/j.jhydrol.2016.04.009

Marshall SJ, White EC, Demuth MN, Bolch T, Wheate R, Menounos B, Beedle MJ, Shea

JM. 2011. Glacier Water Resources on the Eastern Slopes of the Canadian Rocky Mountains. *Canadian Water Resources Journal* **36** (March 2010): 109–134 DOI: 10.4296/cwrj3602823

Martin E, Timbal B, Brun E. 1997. Downscaling of General Circulation model Outputs: Simulation of the Snow Climatology of the French Alps and Sensitivity to Climate Change. *Climate Dynamics* **13** (1): 45–56 DOI: 10.1007/s003820050152

Maurer EP. 2007. Uncertainty in Hydrologic Impacts of Climate Change in the Sierra Nevada, California, Under Two Emissions Scenarios. *Climatic Change* **82** (3–4): 309–325 DOI: 10.1007/s10584-006-9180-9

McCuen RH. 2016. Assessment of Hydrological and Statistical Significance. *Journal of Hydrologic Engineering* **21** (4): 2516001 DOI: 10.1061/(ASCE)HE.1943-5584.0001340

Mehrotra R, Sharma A. 2005. A Nonparametric Nonhomogeneous Hidden Markov Model for Downscaling of Multisite Daily Rainfall Occurrences. *Journal of Geophysical Research* **110** (16): 1–13 DOI: 10.1029/2004JD005677

Mehrotra R, Sharma A. 2006. Conditional Resampling of Hydrologic Time Series using Multiple Predictor Variables: A K-nearest Neighbour Approach. *Advances in Water Resources* **29** (7): 987–999 DOI: 10.1016/j.advwatres.2005.08.007

Mehrotra R, Sharma A. 2007. A Semi-Parametric Model for Stochastic Generation of Multi-site Daily Rainfall Exhibiting Low-Frequency Variability. *Journal of Hydrology* **335**: 180–193 DOI: 10.1016/j.jhydrol.2006.11.011

Mehrotra R, Sharma A. 2010. Development and Application of a Multisite Rainfall Stochastic Downscaling Framework for Climate Change Impact Assessment. *Water Resources Research* **46**: 1–17 DOI: 10.1029/2009WR008423

Mekis É, Vincent LA. 2011. An overview of the second generation adjusted daily precipitation dataset for trend analysis in Canada. *Atmosphere-Ocean* **49(2)** (2): 163–177 DOI: 10.1080/07055900.2011.583910

Micovic Z, Quick MC. 1999. A rainfall and snowmelt runoff modelling approach to flow estimation at ungauged sites in British Columbia. *Journal of Hydrology* **226** (1–2): 101–120 DOI: 10.1016/S0022-1694(99)00172-9

Micovic Z, Quick MC. 2009. Investigation of the model complexity required in runoff simulation at different time scales / Etude de la complexité de modélisation requise pour la simulation d'écoulement à différentes échelles temporelles. *Hydrological Sciences Journal* **54** (5): 872–885 DOI: 10.1623/hysj.54.5.872

Minville M, Brissette F, Krau S, Leconte R. 2009. Adaptation to climate change in the management of a Canadian water-resources system exploited for hydropower. *Water Resources Management* **23** (14): 2965–2986 DOI: 10.1007/s11269-009-9418-1

Minville M, Brissette F, Leconte R. 2008. Uncertainty of The Impact of Climate Change on The Hydrology of A Nordic Watershed. *Journal of Hydrology* **358**: 70–83 DOI: 10.1016/j.jhydrol.2008.05.033

Morrison RR, Stone MC. 2015. Evaluating the Impacts of Environmental Flow Alternatives on Reservoir and Recreational Operations Using System Dynamics Modeling. *JAWRA Journal of the American Water Resources Association* **51** (1): 33–46 DOI: 10.1111/jawr.12231

Najafi MR, Moradkhani H, Jung IW. 2011. Assessing the uncertainties of hydrologic model selection in climate change impact studies. *Hydrological Processes* **25** (18): 2814–2826 DOI: 10.1002/hyp.8043

Pacific Climate Impacts Consortium U of V. 2014. Statistically Downscaled Climate Scenarios Available at: https://pacificclimate.org/data/statistically-downscaled-climate-scenarios [Accessed 23 July 2015]

Payne J, Wood A, Hamlet A. 2004. Mitigating the effects of climate change on the water resources of the Columbia River basin. *Climatic Change* **62** (1–3): 233–256 DOI: 10.1023/B:CLIM.0000013694.18154.d6

Piani C, Weedon GP, Best M, Gomes SM, Viterbo P, Hagemann S, Haerter JO. 2010.

Statistical bias correction of global simulated daily precipitation and temperature for the application of hydrological models. *Journal of Hydrology* **395** (3–4): 199–215 DOI: 10.1016/j.jhydrol.2010.10.024

Pina J, Tilmant A, Ph D, Anctil F, Ph D. 2017. Horizontal Approach to Assess the Impact of Climate Change on Water Resources Systems: 1–11 DOI: 10.1061/(ASCE)WR.1943-5452.0000737.

Poulin A, Brissette F, Leconte R, Arsenault R, Malo J-S. 2011. Uncertainty of hydrological modelling in climate change impact studies in a Canadian, snow-dominated river basin. *Journal of Hydrology* **409** (3–4): 626–636 DOI: 10.1016/j.jhydrol.2011.08.057

Pour S, Harun S, Shahid S. 2014. Genetic Programming for the Downscaling of Extreme Rainfall Events on the East Coast of Peninsular Malaysia. *Atmosphere* **5**: 914–936 DOI: 10.3390/atmos5040914

Prudhomme C, Davies H. 2008a. Assessing uncertainties in climate change impact analyses on the river flow regimes in the UK. Part 2: future climate. *Climatic Change* **93** (1–2): 197–222 DOI: 10.1007/s10584-008-9461-6

Prudhomme C, Davies H. 2008b. Assessing Uncertainties in Climate Change Impact Analyses on The River Flow Regimes in The UK. Part 1: Baseline Climate. *Climatic Change* **93**: 177–195 DOI: 10.1007/s10584-008-9464-3

Qin H, Sun AC, Liu J, Zheng C. 2012. System dynamics analysis of water supply and demand in the North China Plain. *Water Policy* **14** (2): 214 DOI: 10.2166/wp.2011.106

Quick MC, Pipes A. 1977. U.B.C. WATERSHED MODEL / Le modèle du bassin versant U.C.B. *Hydrological Sciences Bulletin* **22:1**: 153–162 DOI: 10.1080/02626667709491701

Racherla PN, Shindell DT, Faluvegi GS. 2012. The added value to global model projections of climate change by dynamical downscaling: A case study over the

continental U.S. using the GISS-ModelE2 and WRF models. *Journal of Geophysical Research: Atmospheres* **117**: D20118 DOI: 10.1029/2012JD018091

Rajasekaram V, McBean GA, Simonovic SP. 2010. A systems dynamic modelling approach to assessing elements of a weather forecasting system. *Atmosphere-Ocean* **48** (1): 1–9 DOI: 10.3137/AO931.2010

Raje D, Mujumdar PP. 2009. A conditional random field-based downscaling method for assessment of climate change impact on multisite daily precipitation in the Mahanadi basin. *Water Resources Research* **45** (10): W10404 DOI: 10.1029/2008WR007487

Raje D, Mujumdar PP. 2010. Reservoir performance under uncertainty in hydrologic impacts of climate change. *Advances in Water Resources* **33** (3): 312–326 DOI: 10.1016/j.advwatres.2009.12.008

Refsgaard JC. 1997. Parameterisation, calibration and validation of distributed hydrological models. *Journal of Hydrology* **198** (1–4): 69–97 DOI: 10.1016/S0022-1694(96)03329-X

Rupp DE, Abatzoglou JT, Hegewisch KC, Mote PW. 2013. Evaluation of CMIP5 20 th century climate simulations for the Pacific Northwest USA. *Journal of Geophysical Research: Atmospheres* **118** (19): 10,884-10,906 DOI: 10.1002/jgrd.50843

Salvi K, Ghosh S, Ganguly AR. 2015. Credibility of statistical downscaling under nonstationary climate. *Climate Dynamics* **46** (5): 1991–2023 DOI: 10.1007/s00382-015-2688-9

Salvi K, Kannan S, Ghosh S. 2013. High-resolution multisite daily rainfall projections in India with statistical downscaling for climate change impacts assessment. *Journal of Geophysical Research: Atmospheres* **118** (9): 3557–3578 DOI: 10.1002/jgrd.50280

Schmid M, Wickler F, Maloney KO, Mitchell R, Fenske N, Mayr A. 2013. Boosted Beta Regression. *PLoS ONE* **8** (4) DOI: 10.1371/journal.pone.0061623

Schnorbus M, Bennett A, Werner A, Berland A. 2011. Hydrologic Impacts of Climate Change in the Peace , Campbell and Columbia Watersheds , British Columbia , Canada Available at: https://pacificclimate.org/sites/default/files/publications/Schnorbus.HydroModelling.FinalReport2.Apr2011.pdf

Schoof JT, Pryor SC. 2001. Downscaling temperature and precipitation: A comparison of regression-based methods and artificial neural networks. *International Journal of Climatology* **21**: 773–790 DOI: 10.1002/joc.655

Seiller G, Anctil F. 2014. Climate change impacts on the hydrologic regime of a Canadian river: Comparing uncertainties arising from climate natural variability and lumped hydrological model structures. *Hydrology and Earth System Sciences* **18** (6): 2033–2047 DOI: 10.5194/hess-18-2033-2014

Sharif M, Burn DH. 2006. Simulating climate change scenarios using an improved K-nearest neighbor model. *Journal of Hydrology* **325**: 179–196 DOI: 10.1016/j.jhydrol.2005.10.015

Sharifi A, Kalin L, Tajrishy M. 2013. System Dynamics Approach for Hydropower Generation Assessment in Developing Watersheds: Case Study of Karkheh River Basin, Iran. *Journal of Hydrologic Engineering* **18** (8): 1007–1017 DOI: 10.1061/(ASCE)HE.1943-5584.0000711

Sharma A, O'Neill R. 2002. A nonparametric approach for representing interannual dependence in monthly streamflow sequences. *Water Resources Research* **38(7)** (7) DOI: 10.1029/2001WR000953

Shastri H, Paul S, Ghosh S, Karmakar S. 2015. Impacts of urbanization on Indian summer monsoon rainfall extremes. *Journal of Geophysical Research Atmospheres* **120**: 495–516 DOI: 10.1002/2014JD022061

Sheil D, Murdiyarso D. 2009. How forests attract rain: an examination of a new hypothesis. *Bio Science* **59** (4): 341–347 DOI: 10.1525/bio.2009.59.4.12

Shepard D. 1968. A two-dimensional interpolation function for irregularly-spaced data. In *23rd ACM National Conference*517–524. DOI: 10.1145/800186.810616

Simas AB, Barreto-Souza W, Rocha A V. 2010. Improved Estimators for A General Class of Beta Regression Models. *Computational Statistics and Data Analysis* **54**: 348–366 DOI: 10.1016/j.csda.2009.08.017

Simonovic SP. 1992. Reservoir systems analysis: closing gap between theory and practice. *Journal of Water Resources Planning and Management* **118** (3): 262–280 DOI: 10.1061/(ASCE)0733-9496(1992)118:3(262)

Simonovic SP. 2008. Engineering Literature Review: Water Resources - Infrastructure Impacts, Vulnerabilities and Design Considerations for Future Climate Change.In Adapting to Climate Change, Canada's First National Engineering Vulnerability Assessment of Public Infrastructu DOI: 10.1017/CBO9781107415324.004

Simonovic SP. 2009. *Managing Water Resources: Methods and Tools for a Systems Approach*. Available at: https://www.amazon.ca/Managing-Water-Resources-Methods-Approach/dp/1844075540

Simonovic SP, Fahmy H. 1999. A new modeling approach for water resources policy analysis. *Water Resources Research* **35** (1): 295–304 DOI: 10.1029/1998WR900023

Simonovic SP, Li L. 2003. Methodology for Assessment of Climate Change Impacts on Large-Scale Flood Protection System. *Journal of Water Resources Planning and Management* **129** (October): 361–371 DOI: 10.1061/(ASCE)0733-9496(2003)129:5(361)

Simonovic SP, Fahmy H, El-Shorbagy A. 1997. The Use of Object-Oriented Modeling for Water Resources Planning in Egypt. *Water Resources Management* **11** (4): 243–261 DOI: 10.1023/A:1007988424353

Srivastav RK, Simonovic SP. 2014. Multi-site, Multivariate Weather Generator Using Maximum Entropy Bootstrap. *Climate Dynamics* DOI: 10.1007/s00382-014-2157-x

Stahl K, Moore RD, Shea JM, Hutchinson D, Cannon AJ. 2008. Coupled modelling of glacier and streamflow response to future climate scenarios. *Water Resources Research* **44** (2): 1–13 DOI: 10.1029/2007WR005956

Stern RD, Coe R. 1984. A Model fitting Analysis of Daily Rainfall Data. *Journal of the Royal Statistical Society* **147** (1): 1–34

Stewart IT, Cayan DR, Dettinger MD. 2004. Changes in Snowmelt Runoff Timing in Western North America under a 'Business As Usual' Climate Change Scenario. *Climatic Change* **62**: 217–232

Von Storch H, Zorita E, Cubasch U. 1993. Downscaling of global climate change estimates to regional scales: an application to Iberian rainfall in wintertime. *Journal of Climate* **6**: 1161–1171 DOI: 10.1175/1520-0442(1993)006<1161:DOGCCE>2.0.CO;2

Teegavarapu RS V., Simonovic SP. 2014. Simulation of Multiple Hydropower Reservoir Operations Using System Dynamics Approach. *Water Resources Management* **28** (7): 1937–1958 DOI: 10.1007/s11269-014-0586-2

Tripathi S, Srinivas V V., Nanjundiah RS. 2006. Downscaling of precipitation for climate change scenarios: A support vector machine approach. *Journal of Hydrology* **330** (3–4): 621–640 DOI: 10.1016/j.jhydrol.2006.04.030

Vensim. 2014. *Vensim Reference Manual*. Ventana Systems Inc.: MA, USA.

Vrac M, Paillard D, Naveau P. 2007. Non-linear statistical downscaling of present and LGM precipitation and temperatures over Europe. *Climate of the Past* **3** (4): 669–682 DOI: 10.5194/cpd-3-899-2007

Vuuren DP van, Edmonds J, Kainuma M, Riahi K, Thomson A, Hibbard K, Hurtt GC, Kram T, Krey V, Lamarque JF, et al. 2011. The representative concentration pathways: An overview. *Climatic Change* **109** (1): 5–31 DOI: 10.1007/s10584-011-0148-z

Warren FJ, Lemmen DS. 2014. Canada in a Changing Climate :Sector Perspectives on Impacts and Adaptation; Government of Canada, Ottawa, ON, 286p.

Wei S, Yang H, Song J, Abbaspour KC, Xu Z. 2012. System dynamics simulation model for assessing socio-economic impacts of different levels of environmental flow allocation in the Weihe River Basin, China. *European Journal of Operational Research* **221** (1): 248–262 DOI: 10.1016/j.ejor.2012.03.014

Werner AT. 2011. BCSD Downscaled Transient Climate Projections for Eight Select GCMs over British Columbia, Canada. Hydrologic Modelling Project Final Report (Part I) Available at: http://scholar.google.com/scholar?hl=en&btnG=Search&q=intitle:BCSD+Downscaled+Transient+Climate+Projections+for+Eight+Select+GCMs+over+British+Columbia,+Canada#0%5Cnhttp://scholar.google.com/scholar?hl=en&btnG=Search&q=intitle:BCSD+downscaled+transient+cl

Werner AT, Cannon AJ. 2015. Hydrologic Extremes – An Intercomparison of Multiple Gridded Statistical Downscaling Methods. *Hydrology and Earth System Sciences Discussions* **12**: 6179–6239 DOI: 10.5194/hessd-12-6179-2015

Wetterhall F, Halldin S, Xu CY. 2005. Statistical precipitation downscaling in central Sweden with the analogue method. *Journal of Hydrology* **306**: 174–190 DOI: 10.1016/j.jhydrol.2004.09.008

Wilby R., Dawson C., Barrow E. 2002. SDSM — a decision support tool for the assessment of regional climate change impacts. *Environmental Modelling & Software* **17** (2): 147–159 DOI: 10.1016/S1364-8152(01)00060-3

Wilby RL. 2005. Uncertainty in water resource model parameters used for climate change impact assessment. *Hydrological Processes* **19**: 3201–3219 DOI: 10.1002/hyp.5819

Wilby RL, Harris I. 2006. A Framework for Assessing Uncertainties in Climate Change Impacts: Low-Flow Scenarios for The River Thames, UK. *Water Resources*

Research **42**: W02419 DOI: 10.1029/2005WR004065

Wilby RL, Wigley TML. 1997. Downscaling general circulation model output: a review of methods and limitations. *Progress in Physical Geography* **21(4)**: 530–548 DOI: 10.1177/030913339702100403

Wilby RL, Charles SP, Zorita E, Timbal B, Whetton P, Mearns LO. 2004. Guidelines for use of climate scenarios developed from statistical downscaling methods Available at: http://www.ipcc-data.org/guidelines/dgm_no2_v1_09_2004.pdf

Wilby RL, Hay LE, Leavesley GH. 1999. A Comparison of Downscaled and Raw GCM Output: Implications for Climate Change Scenarios in The San Juan River Basin, Colorado. *Journal of Hydrology* **225**: 67–91 DOI: 10.1016/S0022-1694(99)00136-5

Wilby RL, Whitehead PG, Wade AJ, Butterfield D, Davis RJ, Watts G. 2006. Integrated Modelling of Climate Change Impacts on Water Resources and Quality in A Lowland Catchment: River Kennet, UK. *Journal of Hydrology* **330**: 204–220 DOI: 10.1016/j.jhydrol.2006.04.033

Wilks DS. 1999. Multisite downscaling of daily precipitation with a stochastic weather generator. *Climate Research* **11**: 125–136 DOI: 10.3354/cr011125

Wilks DS, Wilby RL. 1999. The weather generation game: a review of stochastic weather models. *Progress in Physical Geography* **23** (3): 329–357 DOI: 10.1191/030913399666525256

Winz I, Brierley G, Trowsdale S. 2009. The Use of System Dynamics Simulation in Water Resources Management. *Water Resources Management* **23** (7): 1301–1323 DOI: 10.1007/s11269-008-9328-7

Wood AW, Leung LR, Sridhar V, Lettenmaier DP. 2004. Hydrologic Implications of Dynamical and Statistical Approaches to Downscaling Climate Model Outputs. *Climatic Change* **62**: 189–216 DOI: 10.1023/B:CLIM.0000013685.99609.9e

Wood AW, Maurer EP, Kumar A, Lettenmaier DP. 2002. Long-Range Experimental

Hydrologic Forecasting for The Eastern United States. *Journal of Geophysical Research : Atmospheres* **107**: 1–15 DOI: 10.1029/2001JD000659

World Climate Research Programme. 2009. ETCCDI/CRD climate change indices: definitions of the 27 core indices Available at: http://etccdi.pacificclimate.org/list_27_indices.shtml [Accessed 4 September 2015]

Yang C-C, Chang L-C, Ho C-C. 2008. Application of System Dynamics with Impact Analysis to Solve the Problem of Water Shortages in Taiwan. *Water Resources Management* **22** (11): 1561–1577 DOI: 10.1007/s11269-008-9243-y

Yeh W. 1985. Reservoir Management and Operations Models ’. *Water Resource Reasearch* **21** (12): 1797–1818

Young KC. 1994. A multivariate chain model for simulating climatic parameters from daily data. *Journal of Applied Meteorology* **33** (6): 661–671 DOI: 10.1175/1520-0450(1994)033<0661:AMCMFS>2.0.CO;2

Zwiers F, Schnorbus MA, Maruszeczka GD. 2011. Hydrologic impacts of climate change on BC water resources: summary report for the Campbell, Columbia and Peace river watersheds: 1–24 Available at: http://pacificclimate.org/news/2011/new-publication-hydrologic-impacts-climate-change-bc-water-resources-summary-report

Appendices

Appendix A: ANUSPLIN and NCEP/NCAR data set details

ANUSPLIN Data: ANUSPLIN data sets have been developed by Dr. Michael Hutchinson of The Australian National University using thin plate spline smoothing algorithm. Thin plate smoothing splines is a generalization of standard multi-variate linear regression (Hutchinson and de Hoog, 1985). In this spline algorithm, the parametric model is substituted by a suitably smooth non-parametric function. The degree of complexity or the degree of smoothness of the fitted function is usually calculated from the data by optimizing a measure of predictive error of the fitted surface specified by the generalized cross validation (GCV) (Carven and Wahba, 1979). A brief overview of the basic theory and applications to spatial interpolation of climate data is given in Hutchinson and Xu (2013).

These datasets are very useful in climate studies or hydrology because climate station data are rarely available in remote forest locations of Canada. ANUSPLIN data set contains daily maximum and minimum temperature and total precipitation data with a grid spacing of 10 km. Grids were interpolated from daily Environment Canada climate station observations utilizing thin plate smoothing spline surface fitting method. Daily ANUSPLIN dataset is available from 1950 to 2013. For ANUSPLIN data access please follow the link: http://open.canada.ca/data/en/dataset/d432cb3d-8266-4487-b894-06224a4dfd5b.

NCEP/NCAR data: In 1991, The National Centers for Environmental Prediction (NECP) and National Centre for Atmospheric Research (NCAR) cooperated in Climate Data Assimilation System (CDAS) project (denoted “reanalysis”) to produce a 40-year record of global analyses of atmospheric variables to support research and climate communities (Kalnay *et al.*, 1996). The main objective of this project was to use a state-of-the-art analysis/forecast system and simulated climate data using historical dataset from 1948 to present. The NCEP/NCAR Reanalysis data set is globally gridded data set which describes the state of the Earth's atmosphere. These data sets are available in 6-hourly, daily and monthly and have approximately 2.5° x 2.5° spatial resolution. Data is available in 17 different pressure levels and 28 sigma levels. There are large numbers of climate variables (e.g., precipitation, temperature, relative humidity, u-wind, v-wind etc.) are available in several heights and pressure levels. In NCEP/NCAR website, climate variables are divided into seven different groups based on level or properties: (1) pressure level; (2) surface; (3) surface fluxes; (4) other fluxes; (5) tropopause; (6) derived data and (7) spectral coefficient. NCEP/NCAR data set distributed in Netcdf and GRIB files. These data sets are freely available from NOAA Earth System Research Laboratory website (https://www.esrl.noaa.gov/psd/data/reanalysis/reanalysis.shtml).

Appendix B: RAVEN and hydrologic model details

RAVEN is a hydrological modeling framework, a software package for hydrologic modeling(Craig and Snowdon, 2010). RAVEN uses a "generic discretization approach" where a river basin subdivided into multiple subbasins and act as hydrological response units (HRUs) (Figure B.1). Within HRU, flow distributed vertically and redistributed laterally through routing. Each HRU consists of a single combination of vegetation cover, land use/land type, terrain type, stratified aquifer and a defined soil profile.

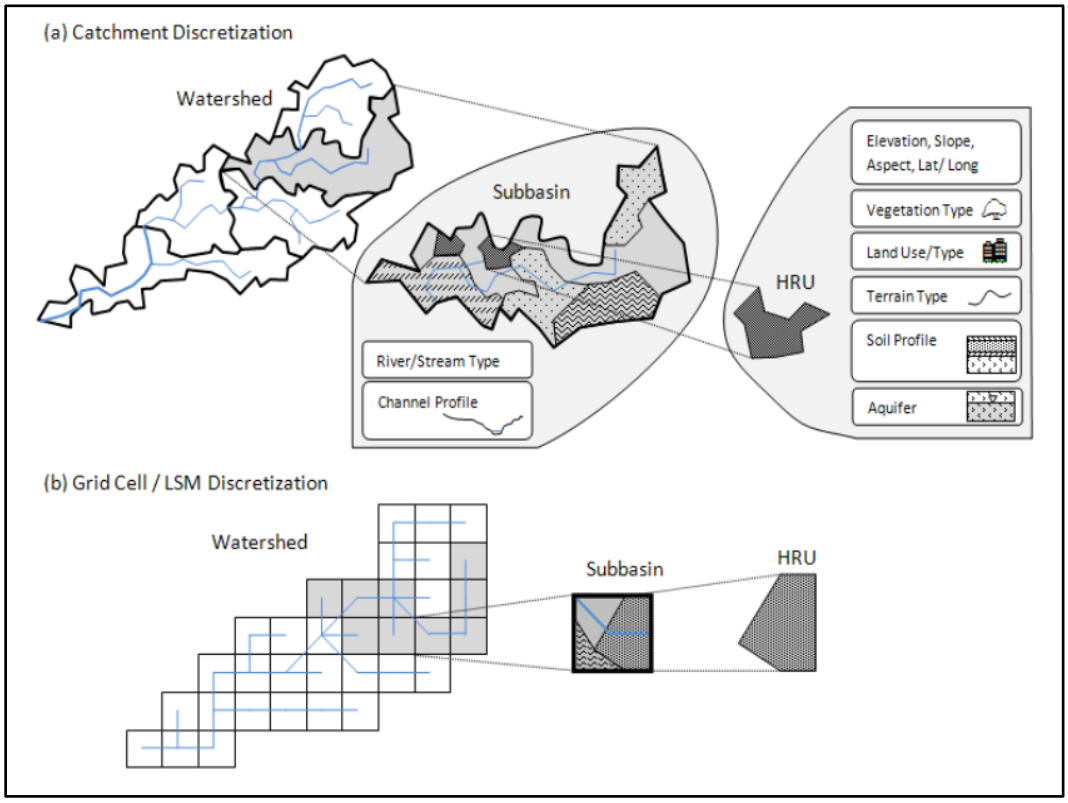

Figure B.1 Land surface partitioning in Raven (after Craig and Snowdon, 2010)

Each HRU is defined by a finite number of storage components i.e. snowpack, soil, canopy, in which energy and water stored. Given a set of user specified hydrologic process (e.g. precipitation, snowmelt, evaporation etc.) data, RAVEN solves the resultant

zero and one-dimensional energy and water balance problem for a single HRU. Each HRU has defined geometric properties (latitude, longitude, area, and parent sub-basin), subterranean soil profile and topography (slope, aspect). In RAVEN modeler have flexibility to determine the degree of model complexity. For example, a watershed can be treated as a single giant HRU where precipitation and temperature data is needed for streamflow simulation. In other side, RAVEN could be integration of thousands of HRUs with multiple storage components and forced (e.g. longwave radiation, wind velocity, air pressure etc.) measured hourly basis.

The simulation of RAVEN is fundamentally straight forward. It starts with some initial conditions of a watershed and moves forward with time. With respect to time the model starts simulate the distribution of energy, mass and water within and in between HRUs in response to physical forcing (i.e. precipitation, laterally routing of water and energy downstream to the catchment outlet). The entire system simulates based on one time steps specified by users. RAVEN has large user-customized subroutines which help to emulate a number of existing hydrological models. RAVEN has achieved near perfect emulation of UBC watershed model (used in this study) and HBV model (Bergstrom, 1995) used by Environment Canada.

To run this RAVEN, five input files are needed, which contain information regarding hydrological processes of a watershed and features of HRUs. The details about input files are given below:

- modelname.rvi: It is a primary input file. It contains information regarding numerical algorithm options (e.g. simulation duration, start time, time step,

routing method, etc.) and model structure (primarily, representation of soil column).

- modelname.rvh – It is a HRU definition file. This file specifies details about HRU properties and connects between HRUs and subbasins.
- modelname.rvt- This file is a time series/forcing function file. This file specifically describes temperature, precipitation, and other environmental forcing functions in the basin.
- modelname.rvp- This file is a class parameter file which contains information about user specified model parameters (e.g. vegetation class, land use, aquifer class, soil profile for each HRU).
- modelname.rvc - This is an initial condition file for all HRUs in a basin. This file holds information about user-specified initial conditions for all state variables in all HRUs and subbasins.

More details about RAVEN and how to run this model are given in "Raven: User's and Developer's Manual" prepared by Craig and Snowdon(2010). For our study we used UBC watershed model calibrated by BC Hydro. Therefore, all input files are provided, we only had to change the "modelname.rvt" according to our data. The details about input files used for this study given below:

modelname.rvi:

```
:FileType rvi ASCII Raven 1.0
# DataType         Raven Input File
#
:Application      GreenKenue
:Version          3.4.19
:WrittenBy        gjost
:CreationDate     Tue, Aug 12, 2014 11:44 AM
#
#------------------------------------------------------------------------
# Converted from UBCWM WAT file
```

```
:SourceFile  C:\Users\Sohom Mondal\Desktop\RavenSCA\RavenSCA\Raven\SCA2010_100.wat
#
:RunName              BR_2066-2095_CanESM2_rcp26
:StartDate          2066-01-01 00:00:00
:Duration           43800 00:00:00
:TimeStep            24:00:00
:Method             ORDERED_SERIES
:Interpolation      FROM_FILE SCA2010_100_GaugeWeights.txt
:Routing            NONE
:CatchmentRoute     DUMP
:Evaporation        MONTHLY_FACTOR
:OW_Evaporation     MONTHLY_FACTOR
:SWRadiationMethod  UBC
:SWCanopyCorrect    UBC
:LWRadiationMethod  UBC
:WindspeedMethod    UBC
:RainSnowFraction   UBC
:PotentialMeltMethod UBC
:OroTempCorrect     UBC
:OroPrecipCorrect   UBC_2
:CloudCoverMethod   UBC
:SnapshotHydrograph
:PrecipIceptFract   USER_SPECIFIED
:MonthlyInterpolationMethod    LINEAR_21
:SoilModel          SOIL_MULTILAYER 5
:DebugMode          no
:EndPause           no
:WriteEnsimFormat   no
#-----------------------------------------------------------------------
# Soil Layer Alias Definitions
#
:Alias TOP_SOIL      SOIL[0]
:Alias INT_SOIL      SOIL[1]
:Alias SHALLOW_GW    SOIL[2]
:Alias DEEP_GW       SOIL[3]
:Alias INT_SOIL2     SOIL[4]
#-----------------------------------------------------------------------
# Hydrologic process order for UBCWM Emulation
#
:HydrologicProcesses
:SnowAlbedoEvolve  UBC
:SnowBalance       UBC
:Precipitation
:GlacialMelt       UBC
:Infiltration      INF_UBC        TOP_SOIL
:SoilEvaporation   SOILEVAP_UBC
:Flush             PONDED_WATER   SURFACE_WATER
:-->Conditional    HRU_TYPE       IS_NOT GLACIER
:Flush             PONDED_WATER   GLACIER
:-->Conditional    HRU_TYPE       IS GLACIER
:Flush             SURFACE_WATER  INT_SOIL
:-->Conditional    HRU_TYPE       IS_NOT GLACIER
:Percolation       PERC_LINEAR    INT_SOIL INT_SOIL2
:Baseflow          LINEAR_STORAGE INT_SOIL2
:Baseflow          LINEAR_STORAGE SHALLOW_GW
:Baseflow          LINEAR_STORAGE DEEP_GW
```

```
:GlacierRelease    LINEAR_STORAGE
:EndHydrologicProcesses
#-------------------------------------------------------------
# HRU Groups
# - one for each elevation band
# - required for UBCWM emulation:
#   - because UBCWM aggregates the TOP_SOIL state variable over each band
# NOTE: only required for strict UBCWM emulation
#
:DefineHRUGroups Band1, Band2, Band3, Band4, Band5, Band6, Band7, Band8, Band9
:AggregatedVariable TOP_SOIL Band1
:AggregatedVariable TOP_SOIL Band2
:AggregatedVariable TOP_SOIL Band3
:AggregatedVariable TOP_SOIL Band4
:AggregatedVariable TOP_SOIL Band5
:AggregatedVariable TOP_SOIL Band6
:AggregatedVariable TOP_SOIL Band7
:AggregatedVariable TOP_SOIL Band8
:AggregatedVariable TOP_SOIL Band9
```

modelname.rvh

```
:FileType rvh ASCII Raven 1.0
# DataType         Raven HRU file
:Application       GreenKenue
:Version           3.4.19
:WrittenBy         gjost
:CreationDate      Tue, Aug 12, 2014 11:44 AM
#-------------------------------------------------------------------------
# Converted from UBCWM WAT file
:SourceFile  SCA2010_100.wat
#-------------------------------------------------------------
# Sub basins
#    WATfile mapping:
#       (hardcoded except for NAME)
:SubBasins
 :Attributes, ID,   NAME, DOWNSTREAM_ID, PROFILE, REACH_LENGTH, GAUGED
 :Units,      none, none, none,          none,    km,           none
  1,          SCA2010_100,   -1,         NONE,    _AUTO,        1
:EndSubBasins

#-------------------------------------------------------------
# Sub basin properties
#    WATfile mapping:
#       1  -log(P0FRTK/(1+P0FRTK))  N0FASR
:SubBasinProperties
 :Parameters, RES_CONSTANT, NUM_RESERVOIRS
 :Units,      1/d,          none
              1,            1.31681,      2
:EndSubBasinProperties
#-------------------------------------------------------------
# Hydrologic Response Units
#    WATfile mapping:
```

```
:HRUs
 :Attributes, ID, AREA, ELEVATION, LATITUDE, LONGITUDE, BASIN_ID, LAND_USE_CLASS, VEG_CLASS, SOIL_PROFILE, AQUIFER_PROFILE, TERRAIN_CLASS, SLOPE, ASPECT
 :Units, none, km2, m, deg, deg, none, none, none, none, none, none, ratio, deg
        1,  22.7358,  256.9, 49.75, -100,  1,  OPEN_1,
FOREST,  DEFAULT_P,  DEFAULT_AQ, DEFAULT_T,  0,  0
        2,  85.5298,  256.9, 49.75, -100,  1,  OPEN_1,
FOREST,  DEFAULT_P,  DEFAULT_AQ, DEFAULT_T,  0,  180
        3,  36.4745,  256.9, 49.75, -100,  1,  FOREST_1,
FOREST,  DEFAULT_P,  DEFAULT_AQ, DEFAULT_T,  0,  142.2
        6,  26.2009,  455.2, 49.75, -100,  1,  OPEN_2,
FOREST,  DEFAULT_P,  DEFAULT_AQ, DEFAULT_T,  0,  0
        7,  46.5794,  455.2, 49.75, -100,  1,  OPEN_2,
FOREST,  DEFAULT_P,  DEFAULT_AQ, DEFAULT_T,  0,  180
        8,  67.5597,  455.2, 49.75, -100,  1,  FOREST_2,
FOREST,  DEFAULT_P,  DEFAULT_AQ, DEFAULT_T,  0,  115.2
        11,  24.4882,  653.5, 49.75, -100,  1,  OPEN_3,
FOREST,  DEFAULT_P,  DEFAULT_AQ, DEFAULT_T,  0,  0
        12,  43.5345,  653.5, 49.75, -100,  1,  OPEN_3,
FOREST,  DEFAULT_P,  DEFAULT_AQ, DEFAULT_T,  0,  180
        13,  70.3473,  653.5, 49.75, -100,  1,  FOREST_3,
FOREST,  DEFAULT_P,  DEFAULT_AQ, DEFAULT_T,  0,  115.2
        16,  26.2023,  839.7, 49.75, -100,  1,  OPEN_4,
FOREST,  DEFAULT_P,  DEFAULT_AQ, DEFAULT_T,  0,  0
        17,  44.6147,  839.7, 49.75, -100,  1,  OPEN_4,
FOREST,  DEFAULT_P,  DEFAULT_AQ, DEFAULT_T,  0,  180
        18,  60.8131,  839.7, 49.75, -100,  1,  FOREST_4,
FOREST,  DEFAULT_P,  DEFAULT_AQ, DEFAULT_T,  0,  113.4
        21,  24.9199,  989.3, 49.75, -100,  1,  OPEN_5,
FOREST,  DEFAULT_P,  DEFAULT_AQ, DEFAULT_T,  0,  0
        22,  44.3021,  989.3, 49.75, -100,  1,  OPEN_5,
FOREST,  DEFAULT_P,  DEFAULT_AQ, DEFAULT_T,  0,  180
        23,  40.168,  989.3,  49.75,  -100,  1,  FOREST_5,  FOREST,
DEFAULT_P,  DEFAULT_AQ,  DEFAULT_T,  0,  115.2
        24,  0.1125,  989.3,  49.75,  -100,  1,  GLACIER,  FOREST,
GLACIER,  DEFAULT_AQ,  DEFAULT_T,  0,  0
        25,  0.0375,  989.3,  49.75,  -100,  1,  GLACIER,  FOREST,
GLACIER,  DEFAULT_AQ,  DEFAULT_T,  0,  180
        26,  37.7402,  1125.7,  49.75,  -100,  1,  OPEN_6,
FOREST,  DEFAULT_P,  DEFAULT_AQ, DEFAULT_T,  0,  0
        27,  67.0937,  1125.7,  49.75,  -100,  1,  OPEN_6,
FOREST,  DEFAULT_P,  DEFAULT_AQ, DEFAULT_T,  0,  180
        28,  35.506,  1125.7,  49.75,  -100,  1,  FOREST_6,  FOREST,
DEFAULT_P,  DEFAULT_AQ,  DEFAULT_T,  0,  115.2
        29,  0.0759,  1125.7,  49.75,  -100,  1,  GLACIER,  FOREST,
GLACIER,  DEFAULT_AQ,  DEFAULT_T,  0,  0
        30,  0.0341,  1125.7,  49.75,  -100,  1,  GLACIER,  FOREST,
GLACIER,  DEFAULT_AQ,  DEFAULT_T,  0,  180
        31,  50.6053,  1286.7,  49.75,  -100,  1,  OPEN_7,
FOREST,  DEFAULT_P,  DEFAULT_AQ, DEFAULT_T,  0,  0
        32,  89.965,  1286.7,  49.75,  -100,  1,  OPEN_7,  FOREST,
DEFAULT_P,  DEFAULT_AQ,  DEFAULT_T,  0,  180
        33,  19.4596,  1286.7,  49.75,  -100,  1,  FOREST_7,
FOREST,  DEFAULT_P,  DEFAULT_AQ, DEFAULT_T,  0,  115.2
```

```
        34,     0.2132,  1286.7,  49.75,  -100,    1,      GLACIER,      FOREST,
GLACIER,      DEFAULT_AQ,  DEFAULT_T,  0,      0
        35,     0.0468,  1286.7,  49.75,  -100,    1,      GLACIER,      FOREST,
GLACIER,      DEFAULT_AQ,  DEFAULT_T,  0,      180
        36,     54.1244,         1477.1,  49.75,  -100,    1,      OPEN_8,
FOREST,       DEFAULT_P,   DEFAULT_AQ,  DEFAULT_T,  0,      0
        37,     96.2212,         1477.1,  49.75,  -100,    1,      OPEN_8,
FOREST,       DEFAULT_P,   DEFAULT_AQ,  DEFAULT_T,  0,      180
        38,     5.03431,         1477.1,  49.75,  -100,    1,      FOREST_8,
FOREST,       DEFAULT_P,   DEFAULT_AQ,  DEFAULT_T,  0,      115.2
        39,     0.748,   1477.1,  49.75,  -100,    1,      GLACIER,      FOREST,
GLACIER,      DEFAULT_AQ,  DEFAULT_T,  0,      0
        40,     0.132,   1477.1,  49.75,  -100,    1,      GLACIER,      FOREST,
GLACIER,      DEFAULT_AQ,  DEFAULT_T,  0,      180
        41,     23.8486,         1720.7,  49.75,  -100,    1,      OPEN_9,
FOREST,       DEFAULT_P,   DEFAULT_AQ,  DEFAULT_T,  0,      0
        42,     44.2903,         1720.7,  49.75,  -100,    1,      OPEN_9,
FOREST,       DEFAULT_P,   DEFAULT_AQ,  DEFAULT_T,  0,      180
        43,     0.301136,        1720.7,  49.75,  -100,    1,      FOREST_9,
FOREST,       DEFAULT_P,   DEFAULT_AQ,  DEFAULT_T,  0,      117
        44,     2.3035,  1720.7,  49.75,  -100,    1,      GLACIER,      FOREST,
GLACIER,      DEFAULT_AQ,  DEFAULT_T,  0,      0
        45,     0.4065,  1720.7,  49.75,  -100,    1,      GLACIER,      FOREST,
GLACIER,      DEFAULT_AQ,  DEFAULT_T,  0,      180
:EndHRUs

#------------------------------------------------------------
# HRU Groups
# - one for each elevation band
# - required because UBCWM aggregates the TOP_SOIL state variable over each band
# # - also implemented for land class types for reporting.
# NOTE: only required for strict UBCWM emulation
#
#------------------------------------------------------------
# Elevation Bands
#
:HRUGroup Band1
 1, 2, 3
:EndHRUGroup
:HRUGroup Band2
 6, 7, 8
:EndHRUGroup
:HRUGroup Band3
 11, 12, 13
:EndHRUGroup
:HRUGroup Band4
 16, 17, 18
:EndHRUGroup
:HRUGroup Band5
 21, 22, 23, 24, 25
:EndHRUGroup
:HRUGroup Band6
 26, 27, 28, 29, 30
:EndHRUGroup
:HRUGroup Band7
 31, 32, 33, 34, 35
```

```
:EndHRUGroup
:HRUGroup Band8
 36, 37, 38, 39, 40
:EndHRUGroup
:HRUGroup Band9
 41, 42, 43, 44, 45
:EndHRUGroup
#-------------------------------------------------------
# Land Classes
:HRUGroup Open_N
 1, 6, 11, 16, 21, 26, 31, 36, 41
:EndHRUGroup
:HRUGroup Open_S
 2, 7, 12, 17, 22, 27, 32, 37, 42
:EndHRUGroup
:HRUGroup Forest
 3, 8, 13, 18, 23, 28, 33, 38, 43
:EndHRUGroup
:HRUGroup Glacier
 24, 25, 29, 30, 34, 35, 39, 40, 44, 45
:EndHRUGroup
```

modelname.rvt:

```
:FileType rvt ASCII Raven 1.0
# DataType         Raven Met Station File
:Application       GreenKenue
:Version           3.4.19
:WrittenBy         gjost
:CreationDate      Tue, Aug 12, 2014 11:44 AM
# Converted from UBCWM WAT file
:SourceFile  SCA2010_100.wat
:Gauge SCAComp
:Latitude 49.75  #
:Longitude -100  #
:Elevation 1283.06  # C0ELPT
:RainCorrection 1.23189  # 1+P0RREP
:SnowCorrection 1.78912  # 1+P0SREP
:CloudTempRanges 8 14  # A0FOGY A0SUNY
:MonthlyEvapFactor 0.2, 0.2, 0.2, 0.2, 0.246, 0.258, 0.232, 0.218, 0.2, 0.2, 0.2, 0.2,  #
V0EMOF(12) * A0EDDF
:EnsimTimeSeries futmodel.tb0
:EndGauge
```

modelname.rvp

```
:FileType rvp ASCII Raven 1.0
# DataType         Raven Parameters file
:Application       GreenKenue
:Version           3.4.19
:WrittenBy         gjost
:CreationDate      Tue, Aug 12, 2014 11:44 AM
#-------------------------------------------------------------------------
# Converted from UBCWM WAT file
:SourceFile  SCA2010_100.wat
#-------------------------------------------------------------------------
# Orographic Corrections
```

```
:AdiabaticLapseRate   4.5    # A0TLZZ
:WetAdiabaticLapse    5.14635 5    # A0TLZP A0PPTP
:ReferenceMaxTemperatureRange    20    # A0TERM(1)
:UBCTempLapseRates    9.76867 0.17731 6.4 2 9.60412 0.180804    # A0TLXM A0TLNM
A0TLXH A0TLNH P0TEDL P0TEDU
:UBCPrecipLapseRates  256.9 522.648 1088.02 8.26314 5.09852 12.1289 0    # C0ELEM(1)
E0LMID  E0LHI P0GRADL P0GRADM P0GRADU A0STAB
:UBCEvapLapseRates    0.9    # A0PELA
:UBCExposureFactor    0.15    # F0ERGY
:UBCCloudPenetration  0.25    # P0CAST
:UBCLWForestFactor    0.76    # P0BLUE*P0LWVF
:UBCNorthSWCorr       0.4 0.4 0.4 0.7 0.9 1 0.9 0.7 0.4 0.4 0.4 0.4    # V0NOTH
:UBCSouthSWCorr       1 1 1 1 1 1 1 1 1 1 1 1    # V0SOTH
#-----------------------------------------------------------------------
# Global snow parameterss
:RainSnowTransition 1.5 1    # (A0FORM+P0TASR)/2  A0FORM-P0TASR
:UBCSnowParams        0.201606 0.95 0.9 0.65 15 3500    # P0ALBMIN P0ALBMAX
P0ALBREC P0ALBASE P0ALBSNW P0ALBMLX
:IrreducibleSnowSaturation    0.05    # A0WEHO (= A0WEHF)
:UBCGroundwaterSplit    0.59267    # P0DZSH
#-------------------------------------------------------------
# Soil classes
#    WATfile mapping:
#       (hardcoded)
:SoilClasses
 :Attributes, SAND, CLAY, ORGANIC
 :Units,      frac, frac, frac
  TOPSOIL,   1, 0, 0
  INT_SOIL,  1, 0, 0
  GWU_SOIL,  1, 0, 0
  GWL_SOIL,  1, 0, 0
:EndSoilClasses
#-------------------------------------------------------------
# Soil parameters
#    WATfile mapping:
#       0.5   P0PERC   P0EGEN   P0AGEN
:SoilParameterList
 :Parameters, POROSITY, MAX_PERC_RATE, UBC_EVAP_SOIL_DEF,
UBC_INFIL_SOIL_DEF
 :Units,      none,     mm_per_d,     mm,              mm
  [DEFAULT], 0.5, 22.7411, 100, 100
:EndSoilParameterList
#-------------------------------------------------------------
# Soil parameters
#    WATfile mapping:
#       0.0                  0.0
#       -ln(P0IRTK/(1+P0IRTK))   -ln(P0IRTK/(1+P0IRTK))
#       -ln(P0UGTK/(1+P0UGTK))   0.0
#       -ln(P0DZTK/(1+P0DZTK))   0.0
:SoilParameterList
 :Parameters, BASEFLOW_COEFF, PERC_COEFF
 :Units,      1/d,            1/d
  [DEFAULT],   0,   0
  INT_SOIL,   1.20393,  0.708193
  GWU_SOIL,   0.0795053,  0
  GWL_SOIL,   0.0116554,  0
```

```
            :EndSoilParameterList
#------------------------------------------------------------
# Soil profiles
#    WATfile mapping:
#       (hardcoded)
# name, layers, {soilClass, thickness} x layers
#
:SoilProfiles
  LAKE, 0
  GLACIER, 0
  DEFAULT_P, 5, TOPSOIL,10.0, INT_SOIL,10.0, GWU_SOIL,10.0, GWL_SOIL,10.0, INT_SOIL,10.0
:EndSoilProfiles
#------------------------------------------------------------
# Vegetation classes
#    WATfile mapping:
#       (hardcoded)
# - these parameters are required but have no affect in UBCWM emulation mode
#
:VegetationClasses
 :Attributes,   MAX_HT, MAX_LAI, MAX_LEAF_COND
 :Units,        m,      none,    mm_per_s
  FOREST,      25,     6.0,     5.3
:EndVegetationClasses
#------------------------------------------------------------
# Vegetation parameters
#    WATfile mapping:
#       (1-POPINT)   (1-POPINT)   P0PINX
:VegetationParameterList
 :Parameters,  TFRAIN, TFSNOW, MAX_INTERCEPT_RATE
 :Units,       frac,   frac,   mm/d
  FOREST,     0.88,   0.88,   10
:EndVegetationParameterList
#------------------------------------------------------------
# LandUse classes
#    WATfile mapping:
#       {OpenN,OpenS,Forest,GlacierN,GlacierS}Band#   C0IMPA   (C0CANY if forest, otherwise 0)
:LandUseClasses
 :Attributes, IMPERM, FOREST_COV
 :Units,      frac,   frac
            OPEN_1, 0.58804,   0
          FOREST_1, 0.58804,   1
            OPEN_2, 0.46901,   0
          FOREST_2, 0.46901,   1
            OPEN_3, 0.0902974,   0
          FOREST_3, 0.0902974,   1
            OPEN_4, 0.102789,   0
          FOREST_4, 0.102789,   1
            OPEN_5, 0.00965001,   0
          FOREST_5, 0.00965001,   1
           GLACIER, 0.00965001,   0
            OPEN_6, 0.346535,   0
          FOREST_6, 0.346535,   1
            OPEN_7, 0.144307,   0
          FOREST_7, 0.144307,   1
            OPEN_8, 0.122393,   0
          FOREST_8, 0.122393,   1
```

```
            OPEN_9, 0.195882,   0
           FOREST_9, 0.195882,   1
:EndLandUseClasses
#-------------------------------------------------------------
# LandUse parameters
#    WATfile mapping:
#       [DEFAULT]  -ln(P0CLDG/(1+P0CLDG)   A0PEFO   -ln(P0GLTK/(1+P0GLTK)  S0PATS
#              (or 10000 if P0CLDG <= 0)
:LandUseParameterList
 :Parameters, CC_DECAY_COEFF, FOREST_PET_CORR, GLAC_STORAGE_COEFF,
SNOW_PATCH_LIMIT
 :Units,      1/d,          none,          1/d,          mm
   [DEFAULT], 0.0953102,          1,          1.17942,          200
:EndLandUseParameterList
#-------------------------------------------------------------
# Terrain classes
#    WATfile mapping:
#       (hardcoded)
# - these parameters required but have no affect in UBCWM emulation mode
:TerrainClasses
 :Attributes, NAME, HILLSLOPE_LEN, DRAINAGE_DENS
 :Units,      none, none,          m/m
        DEFAULT_T, 100,          1.0
:EndTerrainClasses
```

modelname.rvc

```
:FileType rvc ASCII Raven 1.0
# DataType         Raven Initial Conditions file
#
:Application       GreenKenue
:Version           3.4.19
:WrittenBy         gjost
:CreationDate      Tue, Aug 12, 2014 11:44 AM
#
#-------------------------------------------------------------------------
# Converted from UBCWM WAT file
:SourceFile  C:\Users\Sohom Mondal\Desktop\RavenSCA\RavenSCA\Raven\SCA2010_100.wat
#-------------------------------------------------------------
# Initial basin conditions
#    WATfile mapping:
#       1  O0GWUZ+O0GWDZ
:BasinInitialConditions
 :Attributes, ID,   Q
 :Units,      none, m3/s
   1, 17
:EndBasinInitialConditions
#-------------------------------------------------------------
# Soil moisture content - for each HRU
#    WATfile mapping:
#       5000-S0SOIL
:InitialConditions SOIL[0]
```

```
 5000, 5000, 5000, 5000, 5000, 5000, 5000, 5000, 5000, 5000, 5000, 5000, 5000, 5000, 5000, 5000, 5000,
5000, 5000, 5000, 5000, 5000, 5000, 5000, 5000, 5000, 5000, 5000, 5000, 5000, 5000, 5000, 5000, 5000,
5000, 5000, 5000,
:EndInitialConditions

#---------------------------------------------------------
# Initial Upper groundwater storage - for each HRU
#    WATfile mapping:
#       O0GWUZ*86.4/(total watershed area, in km2)/(BASEFLOW_COEFF for GWU_SOIL)
:InitialConditions SOIL[2]
 10.022, 10.022, 10.022, 10.022, 10.022, 10.022, 10.022, 10.022, 10.022, 10.022, 10.022, 10.022, 10.022,
10.022, 10.022, 10.022, 10.022, 10.022, 10.022, 10.022, 10.022, 10.022, 10.022, 10.022, 10.022, 10.022,
10.022, 10.022, 10.022, 10.022, 10.022, 10.022, 10.022, 10.022, 10.022, 10.022, 10.022,
:EndInitialConditions
#---------------------------------------------------------
# Initial Lower groundwater storage - for each HRU
#    WATfile mapping:
#       O0GWDZ*86.4/(total watershed area, in km2)/(BASEFLOW_COEFF for GWL_SOIL)
:InitialConditions SOIL[3]
 37.2889, 37.2889, 37.2889, 37.2889, 37.2889, 37.2889, 37.2889, 37.2889, 37.2889, 37.2889, 37.2889,
37.2889, 37.2889, 37.2889, 37.2889, 37.2889, 37.2889, 37.2889, 37.2889, 37.2889, 37.2889, 37.2889,
37.2889, 37.2889, 37.2889, 37.2889, 37.2889, 37.2889, 37.2889, 37.2889, 37.2889, 37.2889, 37.2889,
37.2889, 37.2889, 37.2889, 37.2889,
:EndInitialConditions
#---------------------------------------------------------
# Snow water equivalent - for each HRU
#    WATfile mapping:
#    oneof {S0SWEON,S0SWEOS,S0SWEF,0,0} for
{OpenNorth,OpenSouth,Forest,GlacierNorth,GlacierSouth}
:InitialConditions SNOW
 0, 0, 0, 0, 0, 0, 0, 0, 0, 0, 0, 0, 0, 0, 0, 0, 0, 0, 0, 0, 0, 0, 0, 0, 0, 0, 0, 0, 0, 0, 0, 0, 0, 0, 0, 0, 0,
:EndInitialConditions
#---------------------------------------------------------
# Snow albedo - for each HRU
#    WATfile mapping:
#    oneof {ALBOPNN,ALBOPNS,ALBFOR,ALBOPNN,ALBOPNS} for
{OpenNorth,OpenSouth,Forest,GlacierNorth,GlacierSouth}
:InitialConditions SNOW_ALBEDO
 0.3, 0.3, 0.65, 0.3, 0.3, 0.65, 0.3, 0.3, 0.65, 0.3, 0.3, 0.65, 0.3, 0.3, 0.65, 0.3, 0.3, 0.3, 0.3, 0.65, 0.3, 0.3,
0.3, 0.3, 0.65, 0.3, 0.3, 0.3, 0.3, 0.65, 0.3, 0.3, 0.3, 0.3, 0.65, 0.3, 0.3,
:EndInitialConditions
#---------------------------------------------------------
# Snow snowmelt - for each HRU
#    WATfile mapping:
#    oneof {S0MEOSN,S0MEOSS,S0MEFS,S0MEOSN,S0MEOSS} for
{OpenNorth,OpenSouth,Forest,GlacierNorth,GlacierSouth}
:InitialConditions CUM_SNOWMELT
 0, 0, 0, 0, 0, 0, 0, 0, 0, 0, 0, 0, 0, 0, 0, 0, 0, 0, 0, 0, 0, 0, 0, 0, 0, 0, 0, 0, 0, 0, 0, 0, 0, 0, 0, 0, 0,
:EndInitialConditions
#---------------------------------------------------------
# Snow liquid - for each HRU
#    WATfile mapping:
#     oneof
#    {0.05*(S0SWEON-S0WEDON),0.05*(S0SWEOS-S0WEDOS),0.05*(S0SWEF-
S0WEDF),0.05*(S0SWEON-S0WEDON),0.05*(S0SWEOS-S0WEDOS)}
#     for
```

```
#       {OpenNorth,OpenSouth,Forest,GlacierNorth,GlacierSouth}
:InitialConditions SNOW_LIQ
 0, 0, 0, 0, 0, 0, 0, 0, 0, 0, 0, 0, 0, 0, 0, 0, 0, 0, 0, 0, 0, 0, 0, 0, 0, 0, 0, 0, 0, 0, 0, 0, 0, 0, 0, 0, 0, 0, 0,
:EndInitialConditions
```

To run the RAVEN user need to download executable **Raven.exe** from here: http://www.civil.uwaterloo.ca/jrcraig/Raven/Downloads.html and unzip to a local drive. The unzip folder should has "Raven.exe", "model.rvc", "model.rvh", "model.rvi","model.rvp", "model.rvt", "model.wat" and "model.tb0" file. The "model.tb0" needs to be update with user specified precipitation and temperature data and run the "Raven.exe" file from command window or simply click on it. By default RAVEN will generate a hydrograph file, watershed diagnostic file, a complete state of the system simulation file and an error file. Error file contains errors and warnings for a particular run. The "model.tb0" looks like:

```
#################
:ColumnMetaData
:ColumnName MAX_TEMPERATURE MIN_TEMPERATURE PRECIP
:ColumnUnits DegC DegC mm
:ColumnType float float float
:EndColumnMetaData
:StartTime      2036-01-01 00:00:00
:DeltaT         24:00:00
:EndHeader
Max Temp Min Temp PRECIP
11              5.9         1.3
11              -3.9          0
11              -0.88       1.5

5.9             1.50        0.029
```

Appendix C: Reservoirs inflow, storage, release and power details for far future time period (2066-2065)

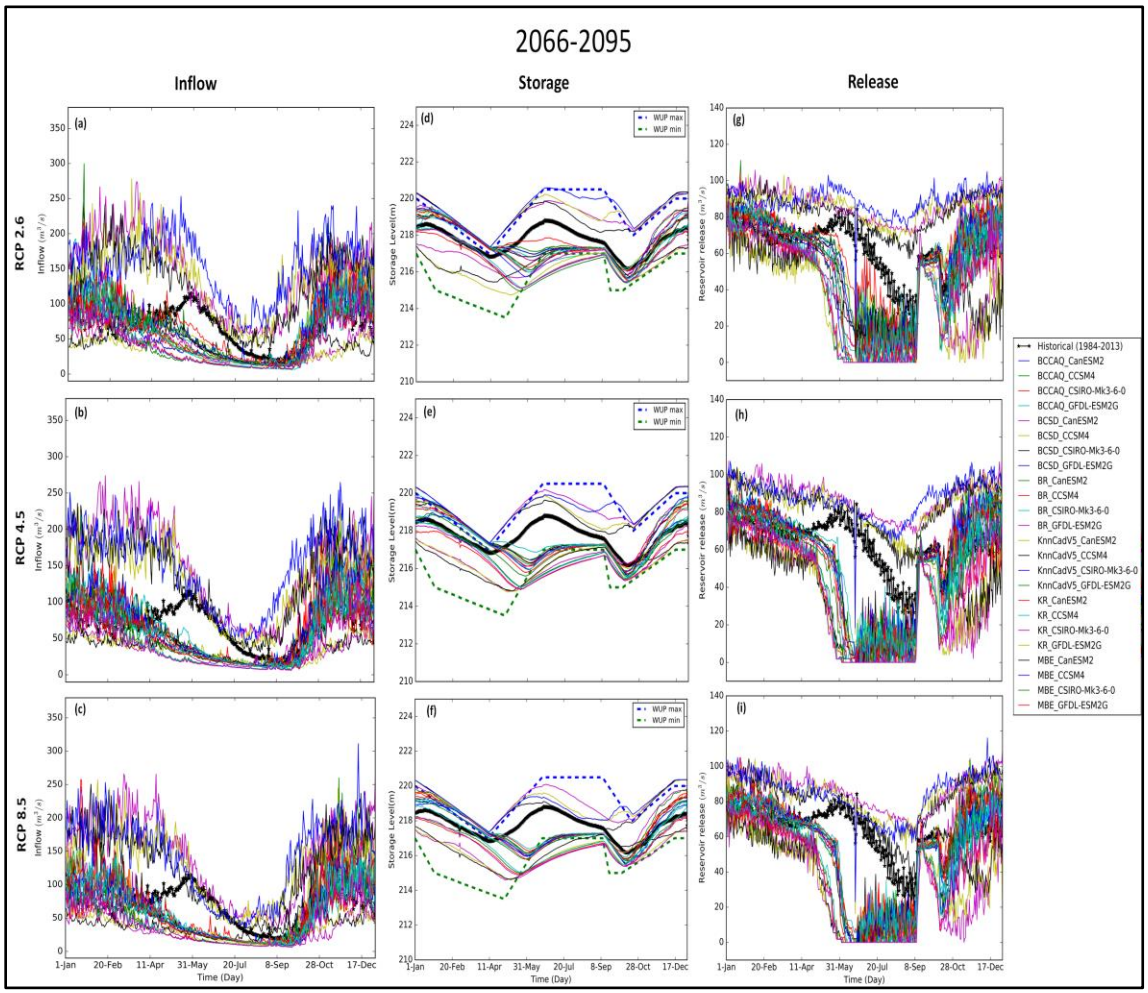

Figure C.1 Projected mean daily simulated inflow (m^3/s) (a-c), storage level (m) (d-f) and release (m^3/s) (g-i) for near future (2066-2095) with historical (1984-2013) observed inflow (m^3/s), storage level (m) and release (m^3/s) from Strathcona Dam, BC, Canada for different emission scenarios

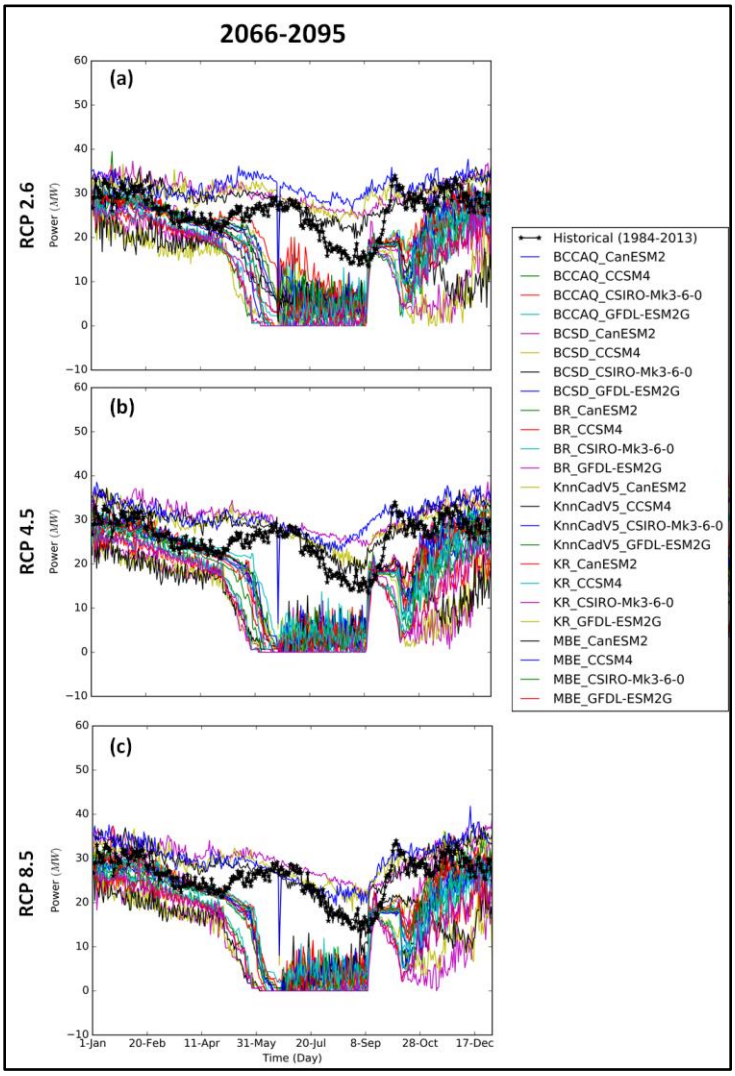

Figure C.2 Projected mean daily power production (megawatt) for near future (2066-2095) with historical (1984-2013) power production (megawatt) from Strathcona Dam, BC, Canada for different emission scenarios

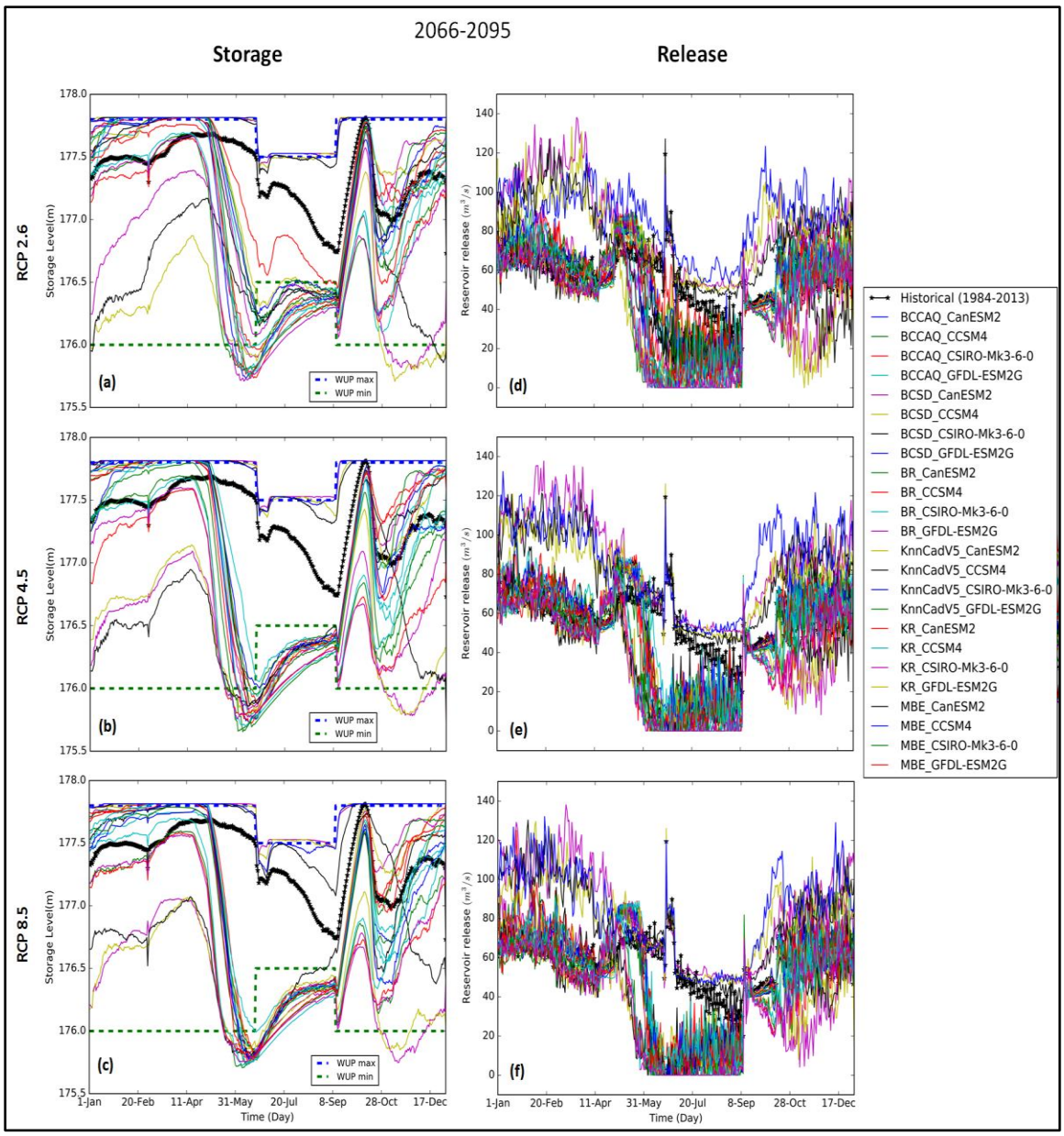

Figure C.3 Projected mean daily simulated storage level (m) (a-c) and release (m^3/s) (d-f) for near future (2066-2095) with historical (1984-2013) observed storage level (m) and release (m^3/s) from Ladore Dam, BC, Canada for different emission scenarios

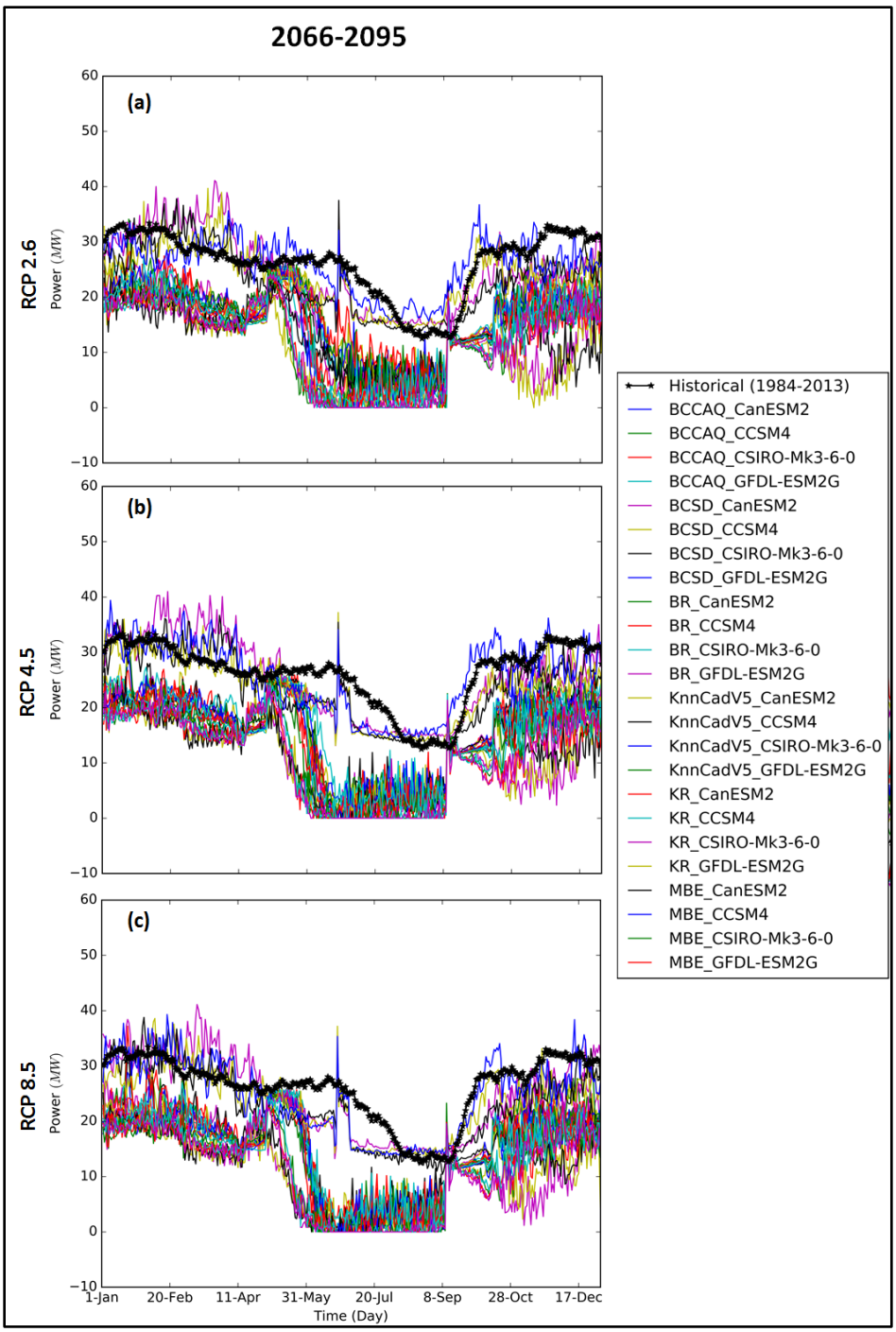

Figure C.4 Projected mean daily power production (megawatt) for near future (2066-2095) with historical (1984-2013) power production (megawatt) from Ladore Dam, BC, Canada for different emission scenarios

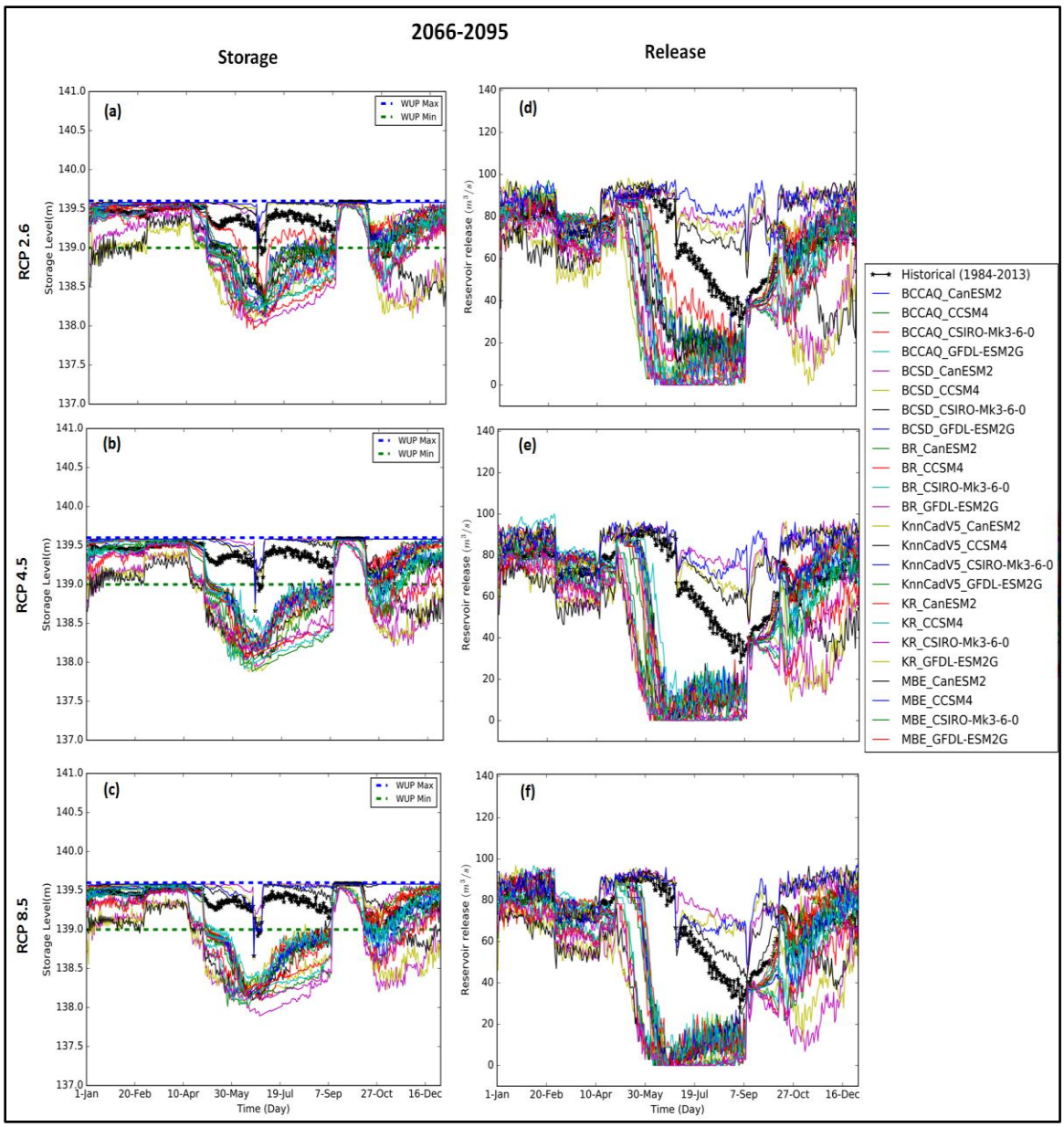

Figure C.5 Projected mean daily simulated storage level (m) (a-c) and release (m^3/s) (d-f) for near future (2066-2095) with historical (1984-2013) observed storage level (m) and release (m^3/s) from John Hart Dam, BC, Canada for different emission scenarios

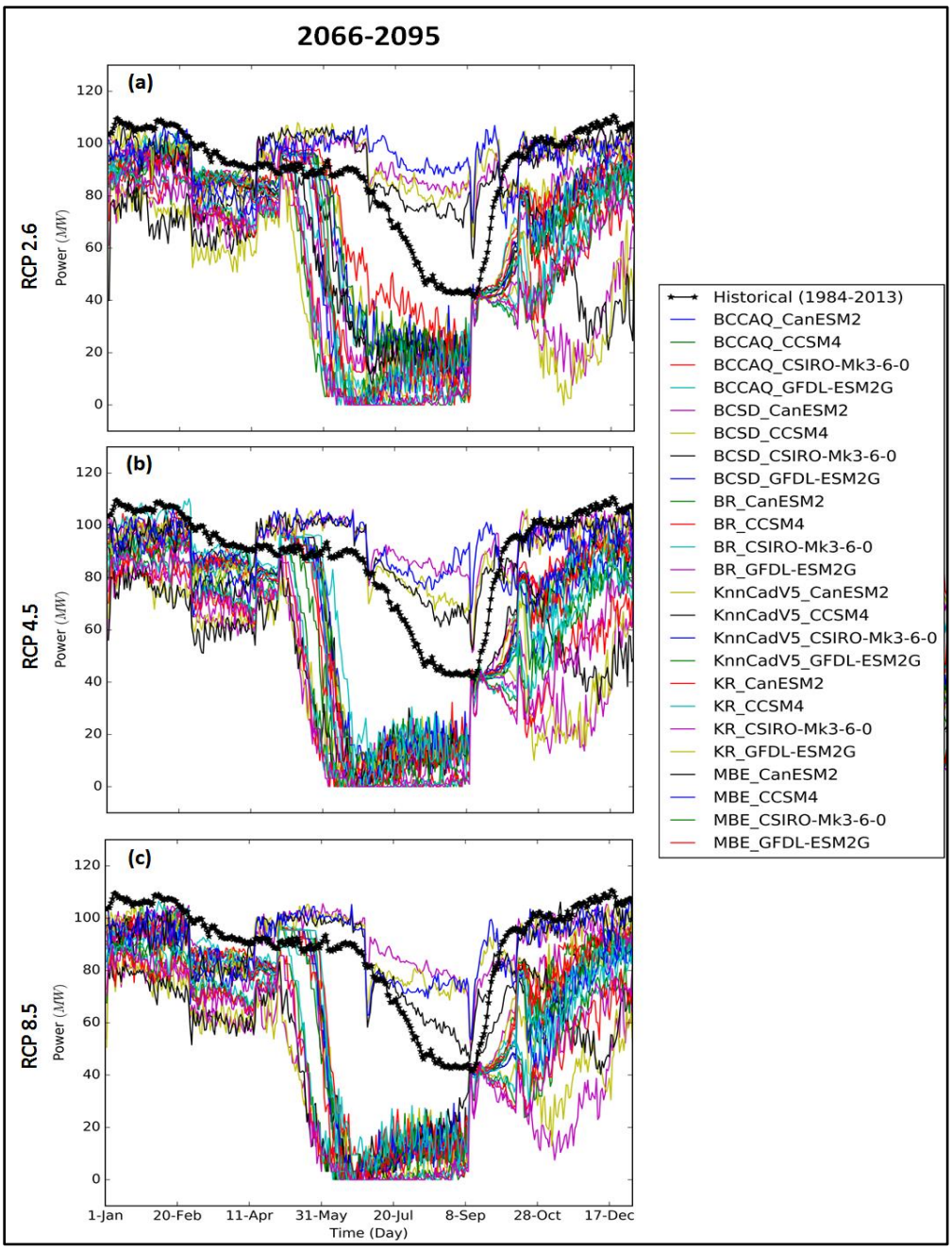

Figure C.6 Projected mean daily power production (megawatt) for near future (2066-2095) with historical (1984-2013) power production (megawatt) from John Hart Dam, BC, Canada for different emission scenarios

Appendix D: Beta Regression Model Code and Installation Details

The beta regression model developed in MATLAB environment. For this model we have three function files (CRAT.m, betalik.m and betareg_main.m) and an Input-Output file (Input and output file for Downscaling Beta Regression.m). "betalik.m" is link function file where "betareg_main.m" is regression function file. CART.m processes the input data using PCA and CART. To run this model all four files should be in a same folder with an input file (.csv) contains future climate variables. The .csv file structure should look like:

Variable	Tasmax	Tasmax	Tasmax	Tasmin	Tasmin	Tasmin
Station	ELK	ERC	WOL	ELK	ERC	WOL
Year Month Day						
1990 01 01	xx	xx	xx	xx	xx	xx
1990 01 02	xx	xx	xx	xx	xx	xx

Apart from that user need historical observed precipitation file and predictor variables (Tmax,Tmin, hus, mslp,u-wind and v-wind) file similar format as shown above. Keep all of these files in a same folder and run the "Input and output file for Downscaling Beta Regression.m" file in MATLAB. It will simulate the future precipitation data in a catchment scale. The details MATLAB codes are given below:

Input and output file for Downscaling Beta Regression.m

```
clc
clear
[x header]=xlsread('Training Predictor NCEP data 1960-1990.csv');
y=xlsread('Training_Predictand Anusplin Precipitation 1960-1990.csv');
k=dir('*tmaxtminhuspsluava*.csv');
for i=1:length(k)
z=xlsread(k(i).name);
Simulated_Precipitation=Beta_Regression(x,y,z);
```

```
expression = ('\_');
splitStr=regexp(k(i).name,expression,'split');
filename=num2str(cell2mat(strcat('Simulated_Pr_BR','_',splitStr(2),'_',splitStr(3),'_',splitStr(4),'_',splitStr(5
),'_',splitStr(6))));
col_header={'Year', 'Month', 'Day', header{2,4:13}};
xlswrite(filename,Simulated_Precipitation,'Sheet1','A2');     %Write data
xlswrite(filename,col_header,'Sheet1','A1');     %Write column header
end
```

betalik.m

```
function y = betalik(vP, mX, vy)
k = length(vP);
eta = mX*vP(1:k-1);
mu = exp(eta) ./ (1+exp(eta));
phi = vP(k);
y = -sum( gammaln(phi) - gammaln(mu*phi)- gammaln(abs(1-mu)*phi) + ((mu*phi-1) .* log(vy)) + ( (1-
mu)*phi-1 ) .* log(1-vy) );
```

betareg_main.m

```
function [vP, muhat]= betareg(vy, mX)
format short g;
n = length(vy);
p = size(mX,2);
if(max(vy) >= 1 || min(vy) <= 0)
   error(sprintf('\n\nERROR: DATA OUT OF RANGE (0,1)!\n\n'));
end
if(p >= n)
    error(sprintf('\n\nERROR: NUMBER OF COVARIATES CANNOT EXCEED NUMBER OF
OBSERVATIONS!\n\n'));
end
ynew = log( vy ./ (1-vy) );
if(p > 1)
    betaols = (mX \ ynew);
elseif(p==1)
    betaols = (mean(ynew));
end
olsfittednew = mX*betaols;
olsfitted = exp(olsfittednew) ./ (1 + exp(olsfittednew));
olserrorvar = sum((ynew-olsfittednew).^2)/(n-p);
ybar = mean(vy);
yvar = var(vy);
% starting values
vps = [betaols;(mean(((olsfitted .* (1-olsfitted))./olserrorvar)-1))];
vP = fminsearch(@(vP) betalik(vP, mX, vy), abs(vps));
etahat = mX*vP(1:p);
muhat = exp(etahat ) ./ (1+exp(etahat));
phihat = vP(p+1);
end
```

CRAT.m

```
function [Simulated_Precipitation] = Beta_Regression(x,y,z)
%x=Training period Predictor Variables e.g. tasmax, tasmin,psl,mslp,ua,va
%y=Training period Predictand Variable e.g. Precipitation
%z=Testing period Predictor Variables (data points where regression value
%will be calculated)
% Length of Tranning predictor data and predictand should be same
if length(x)~=length(y);
   disp('Input Matrix length should be same for Predictor and Predictand ')
end
% Matrix dimension should be same for training period and testing period predictors
if size(x,2)~=size(z,2)
   disp('Training and Testing period predictors dimension is not same')
end
Traning_Predictor=x(:,4:end);
Tranning_Predictand=y(:,4:end);
Testing_Predictor=z(:,4:end);
Testing_Predictor_Date=z(:,1:3);
% Kmeans clustering for rainfall state
rand('state',0);
% Three clusters has taken for clustering, do cluster validation before
% choose the no of clusters
k=3;
[IDX,C,sumd,D]= kmeans(Tranning_Predictand,k); % IDX is the rainfall state for observed data
% Normaization of the Predictor variable (1960-1990)
[Z,mu,sigma] = zscore(Traning_Predictor);
%PCA
[pc,score1,latent1] = princomp(Z);
Var=(cumsum((latent1)./sum(latent1))*100);
% Find the variance which is less or equal to 98%
Ln_var_explained=length(find(Var<=98));
%Buliding classification Tree
T=classregtree(score1(2:end,1:Ln_var_explained),IDX(1:end-1,:));
Temp_val=zscore(Testing_Predictor)*pc;
Rain_state_Prediction_Traning_Period=T(Temp_val(:,1:Ln_var_explained));
% Vector Space of observed data pr on the basis of rainfall state tranning
% period
Observed_data_pr_Rainfall_state=[Tranning_Predictand IDX];
observed_pr_data_state_1=(Observed_data_pr_Rainfall_state(Observed_data_pr_Rainfall_state(:,end)==1,
1:end-1));
% Scaling the data in range (0,1)
Pr_tranning_1=bsxfun(@times,(bsxfun(@minus, observed_pr_data_state_1,
min(observed_pr_data_state_1))), (1./(max(observed_pr_data_state_1)-min(observed_pr_data_state_1))));
Tranning_Predictand_state1=((Pr_tranning_1*(length(Pr_tranning_1)-1))+0.5)/length(Pr_tranning_1);
observed_pr_data_state_2=(Observed_data_pr_Rainfall_state(Observed_data_pr_Rainfall_state(:,end)==2,
1:end-1));
% Scaling the data in range (0,1)
Pr_tranning_2=bsxfun(@times,(bsxfun(@minus, observed_pr_data_state_2,
min(observed_pr_data_state_2))), (1./(max(observed_pr_data_state_2)-min(observed_pr_data_state_2))));
Tranning_Predictand_state2=((Pr_tranning_2*(length(Pr_tranning_2)-1))+0.5)/length(Pr_tranning_2);
observed_pr_data_state_3=(Observed_data_pr_Rainfall_state(Observed_data_pr_Rainfall_state(:,end)==3,
1:end-1));
% Scaling the data in range (0,1)
```

```
Pr_tranning_3=bsxfun(@times,(bsxfun(@minus, observed_pr_data_state_3,
min(observed_pr_data_state_3))), (1./(max(observed_pr_data_state_3)-min(observed_pr_data_state_3))));
Tranning_Predictand_state3=((Pr_tranning_3*(length(Pr_tranning_3)-1))+0.5)/length(Pr_tranning_3);
%Vector Space of observed data predictor(Temp) on the basis of rainfall
%state tranning period
Observed_data_predictor_Rainfall_state=[score1(:,1:Ln_var_explained) IDX];
Observed_predictor_data_state_1=(Observed_data_predictor_Rainfall_state(Observed_data_predictor_Rai
nfall_state(:,end)==1, 1:end-1));
Observed_predictor_data_state_2=(Observed_data_predictor_Rainfall_state(Observed_data_predictor_Rai
nfall_state(:,end)==2, 1:end-1));
Observed_predictor_data_state_3=(Observed_data_predictor_Rainfall_state(Observed_data_predictor_Rai
nfall_state(:,end)==3, 1:end-1));
%Vector Space of testing data(Predictor:Temp)on the basis of rainfall state
Testdata_predictor_Rainfall_state=[Testing_Predictor_Date Temp_val(:,1:Ln_var_explained)
Rain_state_Prediction_Traning_Period];
Testdata_state_1= Testdata_predictor_Rainfall_state(Testdata_predictor_Rainfall_state(:,end)==1, 1:end-
1);
Testdata_state_2= Testdata_predictor_Rainfall_state(1<Testdata_predictor_Rainfall_state(:,end) &
Testdata_predictor_Rainfall_state(:,end)<=2, 1:end-1);
Testdata_state_3= Testdata_predictor_Rainfall_state(Testdata_predictor_Rainfall_state(:,end)>2, 1:end-1);
for i=1:10
 %Bulid regression for state I
mX1=[ones(length(Observed_predictor_data_state_1),1) Observed_predictor_data_state_1];
vy1=Tranning_Predictand_state1(:,i);
vP1=betareg_main(vy1,mX1);
%Bulid regression for state II
mX2=[ones(length(Observed_predictor_data_state_2),1) Observed_predictor_data_state_2];
vy2=Tranning_Predictand_state2(:,i);
vP2=betareg_main(vy2,mX2);
%Bulid regression for state III
mX3=[ones(length(Observed_predictor_data_state_3),1) Observed_predictor_data_state_3];;
vy3=Tranning_Predictand_state3(:,i);
vP3=betareg_main(vy3,mX3);
% Calculate the precipitation for Testin period or Validation period
Predicted_Rain_State1=[ones(length(Testdata_state_1),1) Testdata_state_1(:,4:8)]*vP1(2:end);
Predicted_Rain_State2=[ones(length(Testdata_state_2),1) (Testdata_state_2(:,4:8))]*vP2(2:end);
Predicted_Rain_State3=[ones(length(Testdata_state_3),1) (Testdata_state_3(:,4:8))]*vP3(2:end);
Rain(:,i)=[Predicted_Rain_State1;Predicted_Rain_State2;Predicted_Rain_State3];
Rain(Rain<0)=0;
end
% Arrange the Date for Validation or Testing period
Date=[datenum(Testdata_state_1(:,1:3));datenum(Testdata_state_2(:,1:3));datenum(Testdata_state_3(:,1:3)
)];
%combine the data (simulated precipiation with date)
Predcited_Precipitation=[Date Rain];
%sort the data based date
Precipitation=sortrows(Predcited_Precipitation,1);
% Final bind of simulated precipitation data with time
Simulated_Precipitation=[Testing_Predictor_Date Precipitation(:,2:end)];
end
```

Appendix E: Code for flow frequency analysis

For Campbell River flow frequency analysis we used GEV distribution. To do so we used "ismev" package from **R** in python environment. For this analysis, flow information generated by UBCWM is used as input to the code. The details of the code are given below:

```
"""
Created on Thu May 26 14:51:54 2016
@author: Sohom Mondal & Patrick A. Breach
"""

from scipy.stats import genextreme as gev
import os
import pandas as pd
import numpy as np
import matplotlib.pyplot as plt
import rpy2.robjects as R
from rpy2.robjects.packages import importr
import glob
os.chdir('E:/RCP 26/New folder')
files=glob.glob('*rcp26*')
ismev = importr('ismev')
result = {}
Tr = np.array(np.arange(2, 301), dtype=np.float32)
hist=pd.read_excel('E:/Data and Code/Hydrological Modeling/CampbellData-ForSohom -1984-2013.xlsx',index_col=0,usecols=[3,4])
df_hist=hist.resample('A').max().sort_index(axis=1)
x1 = R.FloatVector(df_hist.values)
a1, b1, c1 = list(ismev.gev_fit(x1)[6])
result1 = gev.isf(Tr**-1, c1, a1, b1)
k=pd.DataFrame.from_dict(result1)
for i, fl in enumerate(files):
    df = pd.read_csv(fl, index_col=0,usecols=[1,4],parse_dates=True)
    df = df.resample('A').max().sort_index(axis=1)
    for col in df.columns:
        x = R.FloatVector(df[col].values)
        a, b, c = list(ismev.gev_fit(x)[6])
        result[i] = gev.isf(Tr**-1, c, a, b)
k1=pd.DataFrame.from_dict(result)
fig, ax = plt.subplots(3)
line=ax[0].plot(k1)
l,=ax[0].plot(k,'r--',linewidth=5,label="Historical (1984-2013)")
ax[0].legend(handles=[l],fontsize=10,frameon=False,loc=2)
#ax[0].set_ylabel('Streamflow Q ($m^3$/s)',fontsize=10)
ax[0].set_ylim([0,7000])
ax[0].set_title("RCP 2.6",position=(0.5, 0.8),fontsize=10)

files1=glob.glob('*rcp45*')
result2 = {}
for i, fl in enumerate(files1):
```

```
    df = pd.read_csv(fl, index_col=0,usecols=[1,4],parse_dates=True)
    df = df.resample('A').max().sort_index(axis=1)
    for col in df.columns:
        x = R.FloatVector(df[col].values)
        a, b, c = list(ismev.gev_fit(x)[6])
        result2[i] = gev.isf(Tr**-1, c, a, b)
k2=pd.DataFrame.from_dict(result2)
line1=ax[1].plot(k2)
l1,=ax[1].plot(k,'r--',linewidth=5,label="Historical (1984-2013)")
ax[1].legend(handles=[l1],fontsize=10,frameon=False,loc=2)
#ax[1].set_ylabel('Streamflow Q ($m^3$/s)',fontsize=10)
ax[1].set_ylim([0,7000])
ax[1].set_title("RCP 4.5",position=(0.5, 0.8),fontsize=10)

files2=glob.glob('*rcp85*')
result3 = {}
for i, fl in enumerate(files2):
    df = pd.read_csv(fl, index_col=0,usecols=[1,4],parse_dates=True)
    df = df.resample('A').max().sort_index(axis=1)
    for col in df.columns:
        x = R.FloatVector(df[col].values)
        a, b, c = list(ismev.gev_fit(x)[6])
        result3[i] = gev.isf(Tr**-1, c, a, b)
k3=pd.DataFrame.from_dict(result3)
line2=ax[2].plot(k3)
l2,=ax[2].plot(k,'r--',linewidth=5,label="Historical (1984-2013)")
ax[2].legend(handles=[l2],fontsize=10,frameon=False,loc=2)
#ax[2].set_ylabel('Streamflow Q ($m^3$/s)',fontsize=10)
plt.xlabel('Retrun period, T (years)')
ax[2].set_ylim([0,7000])
ax[2].set_title("RCP 8.5",position=(0.5, 0.8),fontsize=10)
#fig.savefig('2066-2095 flow frequency.tiff', dpi=700)
m1=k1.mean(axis=1)
m2=k2.mean(axis=1)
m3=k3.mean(axis=1)
m=k.mean(axis=1)
```

Curriculum Vitae

Name: Sohom Mandal

Post-secondary Education and Degrees:
Bidhan Chandra Krishi Viswavidyalaya
Mohanpur, Nadia, West Bengal, India
2006-2010 Bachelor of Technology.

Indian Institute of Technology Bombay
Powai, Mumbai, India
2010-2012 Master of Technology.

Honours and Awards:
Graduate Research Scholarship
University of Western Ontario
2013-2017

Related Work Experience
Teaching Assistant
The University of Western Ontario
2013-2016

Publications:

1. Sohom Mandal, Roshan K. Srivastava and Slobodan Simonovic (2015), "Use of beta regression for statistical downscaling of precipitation in the Campbell river basin, British Columbia, Canada" Journal of Hydrology, 538, 49-62. doi:10.1016/j.jhydrol.2016.04.009

2. Sohom Mandal, Patrick Breach and Slobodan Simonovic (2016), "Uncertainty in precipitation projection under changing climate conditions: A regional case study", American Journal of Climate Change, 5, 116-132. doi:10.4236/ajcc.2016.51012.

3. Sohom Mandal and Slobodan Simonovic (2017), "Assessment of future streamflow under changing climate condition: comparison of various sources of uncertainty". Hydrological Processes (In Press). doi: 10.1002/hyp.11174